UNIVERSIDADE DE LISBOA

FACULDADE DE FARMÁCIA

DEPARTAMENTO DE MICROBIOLOGIA E IMUNOLOGIA

ENGINEERING NEW STRATEGIES TO IMPROVE PHARMACOKINETICS OF THERAPEUTIC PROTEINS

CÁTIA SOFIA DE CARVALHO CANTANTE

Doutoramento em Farmácia

Especialidade em Biotecnologia Farmacêutica

2014

UNIVERSIDADE DE LISBOA

FACULDADE DE FARMÁCIA

ENGINEERING NEW STRATEGIES TO IMPROVE PHARMACOKINETICS OF THERAPEUTIC PROTEINS

CÁTIA SOFIA DE CARVALHO CANTANTE

Tese orientada pelo Professor Doutor João Gonçalves e Doutor Frederico Aires-da-Silva, especialmente elaborada para a obtenção do grau de doutor em Farmácia (Biotecnologia Farmacêutica)

Lisboa

2014

Cátia Sofia de Carvalho Cantante was financially supported by a PhD fellowship (SFRH/BD/48598/2008) from Fundação para a Ciência e a Tecnologia (FCT), Lisbon, Portugal.

De acordo com o disposto no ponto 1 do artigo nº 45 do Regulamento de Estudos Pós-Graduados da Universidade de Lisboa, deliberação nº 4624/2012, publicado em Diário da República – Série nº 65 – 30 Março de 2012, a autora desta dissertação declara que participou na concepção e execução do trabalho experimental, interpretação dos resultados obtidos e redação dos manuscritos.

The research work described in the present Thesis was performed from April 2009 until May 2014, under the supervision of Professor João Gonçalves (PhD) and Frederico Aires-da-Silva (PhD), mainly at the URIA/CPM of the Faculdade de Farmácia da Universidade de Lisboa, Lisbon, Portugal. This project was also performed in collaboration with the Pharmacokinetics, and Metabolism and Genetics group from iMed.UL, Faculdade de Farmácia, ITN (Instituto Superior Técnico), Faculdade de Medicina Veterinária, IMM (Faculdade de Medicina) da Universidade de Lisboa, Lisbon, Portugal; with CQFB/REQUIMTE, Faculdade de Ciências e Tecnologia, Universidade Nova de Lisboa, Caparica, Portugal; and with TechnoAntibodies (TechnoPhage S.A.), Lisbon, Portugal.

The results described in this thesis were included in manuscripts already published or in preparation, in peer-reviewed journals, and in posters in international and national scientific meetings:

Morais, M., Cantante, C., Gano, L., Santos, I., Lourenço, S., Santos, C., Fontes, C., Aires da Silva, F., Gonçalves, J., Correia, J.D. (2014) Biodistribution of a ^{67}Ga-labeled anti-TNF VHH single-domain antibody containing a bacterial albumin-binding domain (Zag). *Nucl. Med. Biol.* pii: S0969-8051(14)00012-22

Cantante, C., Lourenço, S., Morais, M., Leandro, J., Gano, L., Silva, N., Leandro, P., Fontes, C., Correia, J.D.G., Aires-da-Silva, F., Gonçalves, J. (2014) Albumin-binding domain (Zag) from *Streptococcus zooepidemicus* as a strategy to improve half-life of therapeutic proteins. Submitted to Journal of Biological Chemistry

Cantante, C., Lourenço, S., Oliveira, S., Leandro, J., Morais, M., Gano, L., Silva, N., Leandro, P., Fontes, C., Correia, J.D.G., Aires-da-Silva, F., Gonçalves, J. (2014) Albumin-binding domain (ProtH) from *Streptococcus pyogenes*, a new approach to increase half-life of therapeutic proteins. Submitted to Journal of Biological Chemistry

Cantante C., Lourenço S., Leandro J., Morais M., Oliveira S., Gano L., Fontes C., Correia J., Leandro P., Silva F., Gonçalves J. "Albumin-binding domains Zag and ProtH improve pharmacokinetics and affect biodistribution of an anti-TNF VHH". 5th PEGS Europe, Protein & Antibody Engineering Summit, Lisbon, Portugal, 4-8th November, 2013

Correia J., Morais M., Gano L., Santos I., Cantante C., Lourenço S., Santos C., Fontes C., Silva F., Gonçalves J. "Pharmacokinetic properties of a 67Ga-labeledanti-TNF VHH single domain antibody containing a bacterial albumin-binding domain (Zag)". 2nd International Workshop on Innovative Personalized Radioimmunotherapy, Pharmacy Faculty, Nantes, France, 9-12th July, 2013

Cantante C., Lourenço S., Leandro J., Morais M., Gano L., Fontes C., Correia J., Leandro P., Silva F., Gonçalves J. "Albumin-binding domain from Streptococcus pyogenes protein H increases half-life and affect blood clearance of anti-TNF VHH". 5th Postgraduate iMed.UL students meeting, Faculty of Pharmacy-University of Lisbon, Lisbon, Portugal, 18th July, 2013

Cantante C.,Lourenço S., Leandro J., Morais M., Gano L., Fontes C., Correia J.,Leandro P., Silva F., Gonçalves J. "Albumin-binding domain from Streptococcus pyogenes protein H increases half-life and affect blood clearance of anti-TNF VHH". 4th PEGS Europe, Protein & Antibody Engineering Summit, Vienna, Austria, 6-8th November, 2012

Cantante C.,Lourenço S., Morais M., Gano L., Santos C., Fontes C., Correia J.,Silva F., Gonçalves J. "Albumin-binding domain (Zag) from Streptococcus zooepidemicus increases half-life and affect blood clearance of anti-TNF VHH". 8th PEGS Summit Boston, Protein & Antibody Engineering Summit, Boston, USA, 30th April- 4th May, 2012

ABSTRACT

Recombinant antibody formats and therapeutic proteins have found increasing applications as therapeutics, e.g. for the treatment of cancer or inflammatory diseases. While whole antibodies have an exceptionally long half-life, small antibody formats and small molecular weight therapeutic proteins often suffer from rapid elimination from circulation. Usually, this involves frequent administration and repeated infusions with the drug application intravenous or subcutaneously, using a slow adsorption into the blood stream. These limitations of small size protein drugs have led to the development and implementation of several half-life extension strategies to prolong circulation of these molecules and thus improve their administration, pharmacokinetic and pharmacodynamic properties. Over the recent years, plasma protein binding has been shown to be an effective approach to improve pharmacokinetic properties of short half-life molecules. Within this context, in order to improve the half-life of therapeutic proteins we have investigated new strategies based on protein fusions with two albumin-binding domains (ABDs) from streptococcal cell surface proteins. These two ABDs were the Zag and protein H (ProtH) derived from *Streptococcus zooepidemicus and Streptococcus pyogenes,* respectively. To validate our ABDs half-life strategy and as a proof-of-concept, the Zag and ProtH domains were fused with an anti-TNFα VHH single-domain antibody. Our results showed that Zag and ProtH ABDs alone and fused to the anti-TNFα VHH could be stably produced *in vitro*, present nanomolar binding to human, rat and mouse albumins, quantified by ELISA, and for VHH-Zag, using surface plasmon resonance (SPR). VHH, VHH-Zag and VHH-ProtH proteins presented high thermal properties, and human and mouse serum stabilities as well. Moreover, the fusion of the ABDs with the anti-TNFα VHH did not affect the efficacy of the therapeutic molecule against TNFα. Furthermore and importantly, fusion with Zag and ProtH domains strongly increases the half-life and stability of the anti-TNFα VHH. Comparing with the VHH (terminal half-life of 47 min), VHH-Zag (terminal half-life of ~31 h) and VHH-ProtH (terminal half-life of ~21 h) presented prolonged circulation times of 39-fold and 26-fold, respectively. Therefore, after injection, the residence in mouse serum presented higher time extensions until 72 h for VHH-Zag and 48 h for VHH-ProtH (*versus* 2 h exhibited by VHH). The biodistribution profile of

VHH-Zag was determined with technetium 99 m (^{99m}Tc) and gallium 67 (^{67}Ga)-radiolabelling. The prolonged circulation time with both radionuclides lead to a reduction of the ^{99m}Tc-VHH-Zag in kidneys and an increase of the presence of the fusion anti-TNFα VHH in blood and other organs, e.g. liver, intestine, muscle and lungs. The biodistribution profile of VHH-ProtH was evaluated with ^{99m}Tc, presenting a similar organ distribution that the observed for the nanobody alone. Accordingly, ^{99m}Tc-VHH-ProtH is retained in kidneys and showed a trend to accumulate within highly perfused organs like and intestine.

Though, Zag and ProtH unmodified ABDs preserved the albumin-binding ability and thermal stability of the fusions with the recombinant antibody, these domains present very different amino acid sequences and unit organization. Whereas, Zag ABD presents one domain with 52 aa, ProtH ABD possess three C repeats (C1C2C3) that were tested in ELISA assays to evaluate the binding of each unit alone (C1, C2 and C3) or several combinations of these repeats (C1C2, C2C3 and C1C2C3), to human serum albumin. The results obtained showed that C1 repeat is a key unit for the albumin-binding, presenting the highest HSA binding with similar values that those observed with the three repeats. The predicted *in silico* of the three-dimensional structure of ProtH showed an α-helical conformation. Nuclear magnetic resonance (NMR) assignments show that Zag domain presents a three-α-helix three-dimensional structure. Circular dichroism (CD) measurements confirmed the α-helical conformation of these motifs and also indicate that the conformation of both ABDs is maintained in the presence of HSA.

In summary, the results presented on this Thesis strongly demonstrate that Zag and ProtH ABDs are promising strategies to increase the half-life of therapeutic proteins. Both ABDs will be certainly an alternative to the recent most used PEGylation or N-glycosilation approaches to improve therapeutic applications of recombinant proteins. Furthermore, Zag and ProtH can be engineered and be used on therapeutic applications as protein scaffolds.

Keywords: Albumin-binding domain (ABD), biodistribution, half-life, pharmacokinetics, streptococcal protein H, streptococcal protein ZAG, therapeutic proteins.

RESUMO

Nos últimos anos, os formatos de anticorpos recombinantes e as proteínas terapêuticas têm sido desenvolvidos e utilizados para diversas aplicações terapêuticas, como por exemplo, para o tratamento de cancro e doenças inflamatórias, entre outras. Enquanto que os anticorpos no seu formato natural, ou imunoglobulinas, possuem um tempo de semi-vida excepcionalmente longo, os pequenos derivados de anticorpos e as proteínas terapêuticas são, geralmente, rapidamente eliminadas da circulação sanguínea. Para aplicações terapêuticas esta característica faz com que, frequentemente, seja necessário recorrer-se a uma administração frequente e a infusões repetidas com uma aplicação intravenosa ou subcutânea, utilizando uma adsorção lenta destes medicamentos biológicos na corrente sanguínea. Estas limitações, inúmeras vezes relacionadas com o reduzido tamanho destas moléculas, têm resultado no desenvolvimento e implementação de diversas estratégias de extenção do tempo de semi-vida, para prolongar a sua presença na circulação sanguínea. Desta forma, é possível melhorar o seu modo de administração e as suas propriedades farmacocinéticas e farmacodinâmicas, sem afectar a sua eficácia terapêutica.

Actualmente, algumas das estratégias mais utilizadas pela indústria farmacêutica para aumentar o tempo de circulação deste tipo de moléculas terapêuticas, como a PEGilação e a glicosilação, apresentam várias desvantagens. Entre as mesmas encontram-se os elevados custos na produção, o facto de o processo de conjugação nem sempre produzir moléculas com iguais propriedades terapêuticas e de não serem métodos que permitam uma reprodutividade das características da molécula terapêutica, na sua produção. Para evitar estes problemas, existe uma necessidade de desenvolvimento de metodologias alternativas para o mesmo fim.

Deste modo, neste projecto científico desenvolvemos novas estratégias para melhorar o tempo de semi-vida de proteínas terapêuticas, utilizando dois domínios de ligação à albumina, provenientes de proteínas da superfície celular de estreptococos (proteína ZAG e a proteína H). A proteína ZAG é uma proteína da superfície membranar de *Streptococcus zooepidemicus*, que apresenta um domínio de ligação à albumina (Zag) constituído por 52 aminoácidos. Esta proteína também possuí uma região de ligação às imunoglobulinas. Assim como a proteína ZAG, a proteína H, proveniente da superfície celular de *Streptococcos*

pyogenes, também apresenta um domínio de ligação à albumina (ProtH), constituído por três unidades denominadas repetições C (C1C2C3) e uma região de ligação às imunoglobulinas. Pensa-se que estas proteínas possam ser factores de virulência bacterianos e que possam funcionar como mecanismo de escape das bactérias à vigilância do sistema imunitário, camuflando estes microorganismos com proteínas plasmáticas do hospedeiro.

Uma vez que a albumina é das proteínas plasmáticas mais abundantes e apresenta um tempo de semi-vida muito elevado (~19 dias em humanos), o objectivo deste trabalho científico foi utilizar a capacidade natural de ligação à albumina destes domínios para, em fusão com um proteína terapêutica, melhorar o desempenho farmacocinético destas moléculas, aumentando assim o seu tempo de semi-vida em circulação. Deste modo, os domínios de ligação à albumina (ABDs, do inglês *albumin-binding domains*) Zag e ProtH foram testados utilizando, como prova-do-conceito, um anticorpo recombinante (VHH, designado também por *nanobody*) desenvolvido pela empresa de biotecnologia belga Ablynx contra o TNFα (factor de necrose tumoral alfa), para o tratamento da artrite reumatóide. Este *nanobody* foi desenvolvido para bloquear a interacção entre o TNFα e o seu receptor, prevenindo assim o desencadeamento da resposta inflamatória responsável pela formação das junções artritícas, nos doentes com artrite reumatóide. Este tipo de moléculas têm sido sido extensivamente estudadas ao longo dos últimos anos para o tratamento da artrite reumatóide e encontram-se em ensaios clínicos de fase II, com o nome de ATN-103 (actualmente Ozoralizumab).

Os resultados obtidos mostraram que ambos os ABDs sozinhos ou em fusão com o VHH podem ser estavelmente produzidos em bactérias, preservando as suas propriedades naturais de ligação à albumina, com uma ligação às albuminas humana, de rato e de ratinho na ordem do nanomolar e apresentando também elevadas estabilidades térmica e no soro humano e de ratinho. Adicionalmente, a fusão destes domínios com o VHH não afectou a ligação ao TNFα nem a eficácia terapêutica do *nanobody*. A fusão dos domínios Zag e ProtH com a molécula terapêutica aumentaram eficazmente o tempo de semi-vida da mesma. Comparando com o anticorpo recombinante não-modificado (tempo de semi-vida terminal de 47 min), o VHH-Zag (tempo de semi-vida terminal de ~31 h) e o VHH-ProtH (tempo de semi-vida terminal de ~21 h) apresentaram aumentos de 39 e de 26 vezes, respectivamente, no tempo de circulação plasmática em murganhos. Após injecção, observou-se a presença no sangue de ratinho até às 72 h para o VHH-Zag e até às 48 h para o VHH-ProtH, comparando com o curto tempo apresentado para o VHH de apenas 2 h.

O perfil de biodistribuição do VHH-Zag foi avaliado utilizando a marcação com os radioisótopos tecnécio 99 m (^{99m}Tc) e gálio 67 (^{67}Ga). Nos estudos feitos com os dois radioisótopos, verificou-se que a extensão do tempo de circulação do VHH-Zag também influenciou o perfil de biodistribuição, conduzindo a uma redução da presença do anticorpo nos rins e um aumento da quantidade de proteína no sangue e nos orgãos mais irrigados, como o fígado, intestino, músculos e pulmões. O perfil de biodistribuição do VHH-ProtH foi determinado, usando apenas a marcação com o radioisótopo ^{99m}Tc. Deste modo, o ^{99m}Tc-VHH-ProtH mostrou um perfil de biodistribuição diferente do ^{99m}Tc-VHH-Zag, mas semelhante ao do ^{99m}Tc-VHH, ou seja, com uma retenção mais acentuada nos rins e uma menor presença no sangue. O ^{99m}Tc-VHH-ProtH também mostrou uma tendência para se acumular em orgão altamente perfundidos, como o intestino. Contudo, embora o ^{99m}Tc-VHH-Zag e o ^{99m}Tc-VHH-ProtH apresentem um perfil de biodistribuição diferente, ambos revelaram um elevado tempo de semi-vida, comparando com o *nanobody* não-modificado.

Deste modo, o nosso objectivo de desenvolver estes domínios como estratégias para aumentar o tempo de semi-vida de proteínas foi alcançado. Após se determinar que os ABDs Zag e ProtH em fusão com o anticorpo mantinham a sua capacidade de ligação à albumina, fomos investigar se estes domínios não-modificados mantinham as mesmas propriedades. Para atingir este objectivo, as proteínas Zag e ProtH foram clonadas num vector de expressão bacteriano, expressas em *E. coli* e, posteriormente purificadas. Seguidamente, verificamos que os domínios de ligação à albumina Zag e ProtH não-modificados preservam as propriedades de ligação às albuminas humana, de rato e de ratinho observadas anteriormente, assim como também mantêm a estabilidade térmica observada quando se encontram em fusão com o VHH.

Estas proteínas possuem uma sequência de aminoácidos e organização de domínios muito diferentes. Enquanto que o domínio Zag é composto por uma única unidade de 52 aminoácidos, o domínio ProtH é constituído por três unidades, denominadas de sequências repetidas C ou repetições C (C1C2C3). Estas unidades apresentam, entre si uma elevada homologia entre as suas sequências aminoacídicas. Para avaliar a ligação que cada uma destas unidades à albumina, várias combinações destes domínios (C1, C2, C3, C1C2, C2C3, C1C2C3) foram expressas em bactéria e purificadas. De todas as combinações, a unidade C1 tem uma elevada ligação à albumina humana semelhante à ligação observada com os três domínios juntos, mostrando assim que esta unidade apresenta um papel muito importante para a ligação à albumina de todo o domínio. De todas as repetições C, a C1 também é a que apresenta uma maior estabilidade térmica. A previsão *in silico* da estrutura tridimensional do

ABD ProtH revelou uma possível conformação de alfa-hélix. Os resultados de resonância magnética nuclear (RMN) mostraram que o ABD Zag possui uma estrutura tridimensional de tri-α-hélix. Os dados de dicroismo circular confirmam os resultados referidos anteriormente e indicam que, em ambos os domínios, a ligação à albumina não altera a conformação de nenhuma destas proteínas, mantendo a sua conformação helical.

Como perspectivas futuras, seria interessante determinar a estrutura tridimensional do domínio ProtH e investigar por RMN ou cristalografia de raio-X as interacções entre a albumina e estas proteínas. Assim será possível determinar o local de ligação à albumina de cada um destes domínios.

Em conclusão, estes resultados demonstram que os domínios de ligação à albumina Zag e ProtH podem ser utilizados como estratégias promissoras, para o aumento do tempo de semi-vida de proteínas terapêuticas, como alteranativa às metodologias mais utilizadas actualmente pela indústria farmacêutica. Outra potencial aplicação para estas proteínas será a seu desenvolvimento como *scaffolds* terapêuticos para o tratamento de inúmeras doenças, como por exemplo, a artrite reumatóide.

Palavras-chave: Biodistribuição, domínio de ligação à albumina (ABD), farmacocinética, proteína H de estreptococos, proteínas terapêuticas, proteína ZAG de estreptococos, tempo de semi-vida.

ACKNOWLEDGMENTS (AGRADECIMENTOS)

Em primeiro lugar, gostaria de agradecer ao Professor Doutor João Gonçalves, orientador desta tese. Agradeço-lhe por me ter proposto começar a trabalhar neste projecto há mais de 6 anos atrás e por me ter incutido o entusiasmo e curiosidade para desenvolver este trabalho e ter permitido que fosse muitos vezes além do que era possível fazer no laboratório. Muito obrigada por ter acreditado nas minha capacidades, por me ter acompanhado neste caminho nem sempre fácil, por ter possibilitado a realização deste trabalho e pela amizade, ajuda e apoio ao longo destes anos.

Quero agradecer também ao Doutor Frederico Aires-da-Silva (TechnoPhage e FMV-UL), co-orientador desta tese. Obrigada também por me teres proposto este projecto e me teres acolhido nos primeiros anos deste trabalho e me teres ensinado muito sobre anticorpos, engenharia de proteínas, farmacocinética entre outras coisas. Agradeço-te também pela tua constante disponibilidade e por sempre me teres acompanhado, apoiado e ajudado ao longo destes anos. Muito obrigada pela tua amizade e por teres sempre uma palavra de força nas piores alturas. E por sempre incentivares o pensamento criativo e o ir mais além do que o que está acessível. Obrigada pela grande ajuda na correcção da tese e dos artigos.

Obrigada a todos os meus colegas de laboratório que me acompanharam neste precurso. Muitos deles já não estão no laboratório, mas além de colegas muitos tornaram-se amigos. À Catarina Santos (dos anticorpos) que sempre me acompanhou até agora e me ajudou na parte das proteínas, ensaios com HIV e colaborou comigo em muitos projectos que nos foram propondo. À Soraia que também me ajudou em vários ensaios com anticorpos e também colaborou comigo em partes do trabalho. À Ana por me ter dado uma ajuda enorme com a parte da produção de proteínas e clonagens difíceis, que começou no laboratório do Professor Doutor Carlos Fontes (FMV-UL) e continou na nossa companhia. Ao Vasco pela ajuda com os protocolos, até horas muito tardias, de expressão e purifcação de proteínas para NMR. À Catarina (ACS), ao Luís, ao Pedro, à Lídia, ao André, e à Catarina Milho (do laboratório da Professora Doutora Madalena Pimentel) obrigada pela ajuda e companheirismo sempre que

precisava de alguma coisa, nem que que fosse para discutir ideias ou fazer uma pausa estratégica no fim do dia e pelo vossa amizade. À Sofia Romano e ao Galber pela ajuda, companhia e amizade. À Rita e Acil, por muitas vezes discutirem comigo problemas com os anticorpos, me fazerem companhia fora de horas e me fazerem rir ao fim de um dia complicado. À Inês, Paula, Mariana e Sylvie, obrigada por me terem acompanhado e pela vossa disponibilidade. Obrigada a todos pelo convívio (muitas vezes até altas horas a fazer experiências no laboratório) e pelo excelente ambiente de trabalho que ajudou a superar tantos dias difíceis.

Quero agradecer também à TechnoPhage/TechnoAntibodies pela colaboração neste projecto, por me ter acolhido nos primeiros anos deste trabalho e ter possibilitado a realização de várias experiências. À equipa do laboratório, quero agradecer à Sara e à Soraia pela vossa colaboração em parte do trabalho experimental (e companhia no PEGS Boston 2012, juntamente com a Catarina Santos). Quero também agradecer à Clara, à Filipa, à Sofia Fernandes, à Daniela e à Sara Maia por todo o apoio, ajuda e amizade. Quero também agradecer ao Dr. Miguel Garcia e à Dra. Sofia Corte-Real pela oportunidade de poder trabalhar na empresa, pela colaboração ao longo destes anos e por terem possibilitado a realização de parte do trabalho experimental deste projecto.

Muito obrigada ao Professor Doutor João Correia, Dra. Lurdes Gano e Dr. Maurício Morais (ITN-UL) pela colaboração em parte deste projecto nos ensaios de biodistribuição e farmacocinética em ratinhos e por toda a ajuda, amizade, discussão de ideias, disponibilidade ao longo deste projecto e pelas correcções dos artigos e posters.

Muito obrigada ao Professor Doutor Carlos Fontes (FMV-UL) pela enorme ajuda com as proteínas e me ter acolhido 6 meses no seu laboratório. Agradeço também à Joana, Teresa, Lena, Shabir e Inês pela amizade, por me terem acompanhado e ajudado e pela vossa disponibilidade e excelente ambiente de laboratório. Agradeço também ao Jorge pela amizade e ajuda, por me ter apresentado tantas pessoas interessantes e por me continuar a acompanhar na investigação científica.

Muito obrigada à Professora Doutora Paula Leandro (FFUL) pela colaboração em parte deste projecto nos ensaios SEC e em especial ao Dr. João Leandro por todo o trabalho experimental com a optimização dos ensaios, pela amizade, por toda a ajuda e disponibilidade ao longo deste projecto e nas correcções dos artigos e posters. Agradeço também à Mariana pela ajuda com a parte prática, disponibilidade e amizade.

Muito obrigada ao Professor Doutor Eurico Cabrita e Dr. Ângelo Figueiredo (CQFB/ REQUIMTE-UNL) pela colaboração em parte deste projecto nos ensaios de NMR, cristalografia e toda a parte estrutural. Quero agradecer todo o vosso trabalho, paciência, amizade e disponibilidade nestes últimos anos. Obrigada também pela ajuda nas correcções de artigos e por me terem dado a conhecer a RMN e ensinado muitas coisas sobre biologia estrutural de proteínas.

Muito obrigada ao Professor Doutor Miguel Castanho (IMM-UL) pela colaboração em parte deste projecto nos ensaios de CD e em especial à Dra. Diana Gaspar por todo o trabalho experimental com o CD, pela amizade, disponibilidade, ajuda e pelas correcções dos artigos.

Muito obrigada ao Professor Doutor Nuno Silva (FFUL) pela enorme ajuda no tratamento dos dados de farmacocinética e biodistribuição. Obrigada por toda a disponibilidade e por me ter ensinado muitos conceitos nesta área. Agradeço também pela correcção dos artigos e pela discussão de ideias.

Agradeço também ao Professor Doutor Bruno Sepodes pela ajuda nos primeiros ensaios de farmacocinética que foram feitos no início do projecto.

Quero fazer um agradecimento especial à Professora Doutora Madalena Pimentel, ao Professor Doutor Carlos São-José e à Dra. Catarina Baptista por toda amizade, disponibilidade e ajuda ao longo destes últimos anos.

Também quero agradecer ao Dr. Pedro Borrego pela ajuda com o GraphPad Prism e pela amizade. Muito obrigada ao Dr. Pedro Borralho, Dr. Rui Castro pela ajuda, disponibilidade e companheirismo. Quero também agradecer aos restantes colegas do CPM André, Duarte, Pedro, Pedro, Miguel, Maria, Francisco e Adriano pela vossa amizade e companheirismo.

Também quero agradecer aos meus amigos que me acompanharam, me apoiaram e me fizeram companhia tantas vezes quando eu estava mesmo a precisar de uma pausa para carregar baterias. Obrigada pela vossa amizade ao longo de todos estes anos!

Quero fazer um agradecimento muito especial ao Telmo pelo apoio nos bons e mau momentos, pela força, ajuda, compreensão e paciência ao longo destes anos.

Quero também fazer um agradecimento muito especial aos meus pais por sempre terem acreditado em mim e me terem dado a oportunidade de poder ser o queria quando fosse grande. Muito obrigada pelo vosso apoio incondicional, pela força e por estarem sempre do meu lado com uma palavra de incentivo.

ABBREVIATIONS

General

Aa	Amino acid
Ab	Antibody
ABD	Albumin-binding domain
ADCC	Antibody-dependent cell-mediated cytotoxicity
ADME	Adsorption, distribution, metabolism and excretion
Ag	Antigen
CDC	Complement-dependent cytotoxicity
CDR	Complementary determining regions
CH	Constant heavy chain
DNA	Deoxyribonucleic acid
Fab	Fragment antigen binding
Fc	Fragment crystallizable
FDA	Food and Drug Administration
HA	Hemagglutinin tag
HER2	Human epidermal growth factor receptor 2 (also known as ErbB-2)
His	Histidine tag
HSE	Hydroxyethyl starch
Ig	Immunoglobulin
IgBD	Immunoglobulin-binding domain
IgG	Immunoglobulin G
$\mathbf{K_{aff}/K_D}$	Affinity constant
$\mathbf{K_{off}}$	Dissociation constant
$\mathbf{K_{on}}$	Association constant
mAb	Monoclonal antibody
mPEG	Methoxy polyethylene glycol
MW	Molecular weight
MHC	Major histocompatibility complex

PEG	Polyethylene glycol
PD	Pharmacodynamic
PSA	Polysialic acid
PK	Pharmacokinetic
RA	Rheumatoid arthritis
scDb	Single-chain diabody
scFv	Single-chain variable fragment
sdAb	Single-domain antibody
SpA	Staphylococcal protein A
SpG	Streptococcal protein G
TNF_{α}	Tumor necrosis factor α
VH	Variable heavy chain
VHH	Camel variable heavy chain
VL	Variable light chain
VNAR	Shark heavy chain antibody

Reagents and Techniques

ABTS	2,2'-azino-bis(3ethylbenzothiazoline-6-sulphonic acid)
CD	Circular dichroism
ELISA	Enzyme-linked immunosorbent assay
HSA	Human serum albumin
HRP	Horseradish peroxidase
IPTG	Isopropyl-beta-D-thiogalactopyranoside
LB	Luria broth medium
MSA	Mouse serum albumin
NMR	Nuclear magnetic resonance
PBS	Phosphate buffer saline
PCR	Polymerase chain reaction
RSA	Rat serum albumin
SDS-PAGE	Sodium dodecyl sulfate polyacrylamide gel electrophoresis

SEC	Size exclusion chromatography
SPR	Surface plasmon resonance

Amino acids

A	Alanine	**L**	Leucine
R	Arginine	**K**	Lysine
N	Asparagine	**M**	Methionine
D	Aspartic acid	**F**	Phenylanine
C	Cysteine	**P**	Proline
Q	Glutamine	**S**	Serine
E	Glutamic acid	**T**	Threonine
G	Glycine	**W**	Tryptophan
H	Histidine	**Y**	Tyrosine
I	Isoleucine	**V**	Valine

TABLE OF CONTENTS

Figures

Tables

INTRODUCTION

I - Therapeutic Proteins

At the end of 2011, approximately 200 biologics were approved for therapeutic applications and more than 600 are in different stages of clinical development as drug molecules (Walsh, 2010; Kontermann, 2011).

Besides monoclonal antibodies (mAbs) and vaccines, which account for more than two-thirds of these products, hormones, growth factors, cytokines, fusion proteins, coagulation factors, enzymes and other proteins are enumerated. With the exception of antibodies and Fc fusion proteins, many of these proteins possess a molecular mass below 50 kDa and for that reason, are rapidly cleared from circulation, presenting short terminal half-lives in the range of minutes to a few hours (Fig. 1). In order to maintain a therapeutically effective concentration over a prolonged period of time, infusions or frequent administrations are performed, or the drug is applied loco-regional or subcutaneously, using a slow adsorption into the blood stream. Half-life extension strategies have therefore become increasingly important to improve the pharmacokinetic (PK) and pharmacodynamic (PD) properties of therapeutic proteins, but also for reasons of compliance (Kontermann, 2012).

Several half-life extension strategies are already used in approved drugs, including PEGylation, hyperglycosylation, binding to human serum albumin and fusion to an immunoglobulin G (IgG) Fc region. However, there is a strong need for new strategies, not only to further improve the pharmacokinetic properties of these molecules, but also to facilitate production and application of these half-life extended drugs. These strategies include those that increase the hydrodynamic radius of the drug, thus aiming at reducing the renal clearance and also strategies that implement recycling by neonatal Fc receptor (FcRn), which is responsible for the extraordinary long half-life of IgG molecules and serum albumin. In the past 5 to 10 years, half-life extension strategies experienced a rapid growth in the establishment of novel approaches, including the application of novel hydrophilic polymers,

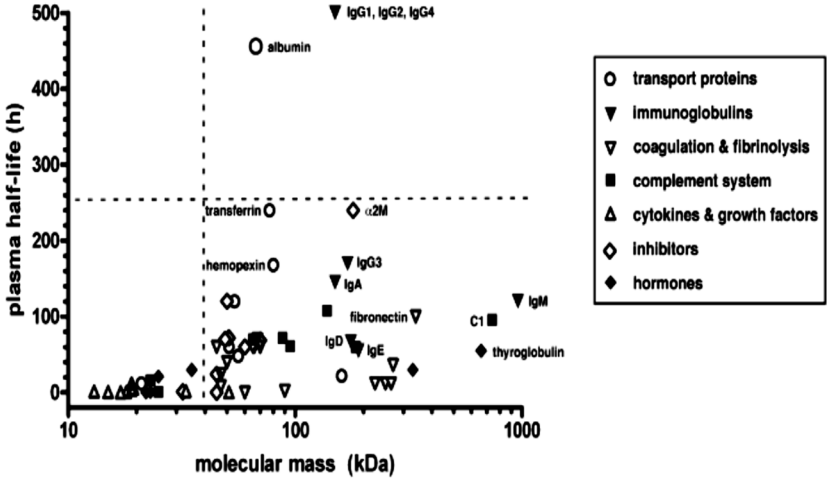

Fig. 1 - The molecular mass and half-life of plasma proteins. Proteins are allocated according to their function (Kontermann, 2012).

the generation of recombinant PEG mimic polypeptide chains and the development of several albumin-binding molecules. Furthermore, the half-life of IgG molecules was altered by engineering of the Fc region, which opens new opportunities for the development of next-generation antibody and protein drugs (Kontermann, 2012).

I.1 - Engineered antibody fragments and therapeutic proteins

As one of the most important defences against disease, antibodies are produced by the immune system in response to substances (antigens) that appear to be foreign to the human body. In vertebrates, there are five different classes of antibodies known as IgD, IgA, IgM, IgE and IgG, which differ in their function from the immune system. IgGs are the most abundant immunoglobulins in the blood and the dominant format of therapeutic antibodies (Aires da Silva *et al.*, 2008). These typical antibodies are usually 'Y' shaped molecules and are bivalent molecules composed of two identical heavy (H) and two light (L) chains with a molecular mass of approximately 150 kDa (Fig. 2). Monovalent derivates thereof include Fab fragments, which are linked via a flexible region (hinge) to a constant fragment (Fc) region, single-chain Fv (scFv) and single variable domains from human IgGs (domain antibodies, dAbs) or camelid (VHH) and shark (VNARs) single-domain antibodies (sdAbs) (Holliger and Hudson, 2005). These antibody formats are small in size (11-50kDa) and do not possess an Fc region, thus they are not capable of exerting Fc-mediated effector functions. The small size and less complex structure of these molecules compared with IgG facilitate production, e.g. in bacterial expression systems (Kontermann, 2009). In addition, small bivalent derivates (e.g. diabodies) have been generated with the lack of constant domains. Bivalent diabodies are composed of the V_L and V_H domain connected by a short linker of approximately 5 amino acid residues, leading to the formation of a homodimeric protein. Recombinant antibody fragments also include several bispecific formats, e.g. minibodies, Fab_2, as well as multimeric formats (Fig. 2) (Holliger and Hudson, 2005).

In comparison with whole antibodies, small antibody fragments such as Fab or scFv exhibit better pharmacokinetics for tissue penetration and also provide full binding specificity because the antigen-binding surface is unaltered. Indeed, the first clinical trials of scFv fragments are likely to be as multivalent reagents, because they exhibit high functional affinity and have been very successful in preclinical studies (Holliger and Hudson, 2005; Hudson and Souriau, 2003). Small size antibody fragments are monovalent and often present fast off-rates and poor retention time on the target (Hudson and Souriau, 2003). Therefore, Fab and scFv fragments have been engineered into multimeric conjugates to increase

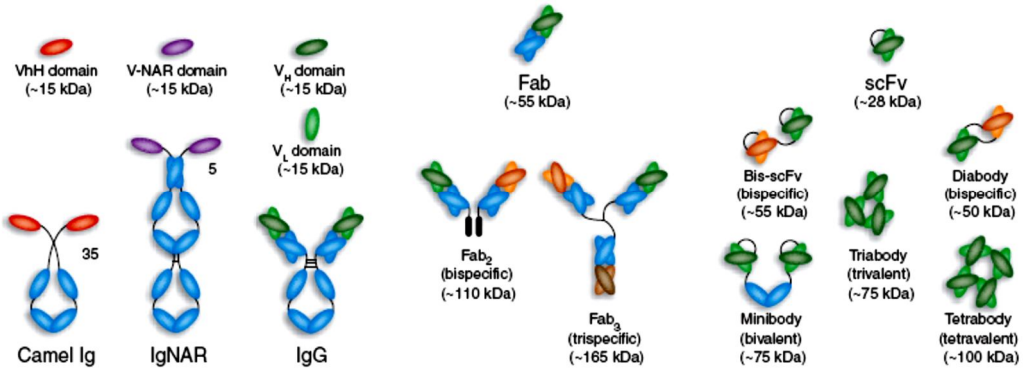

Fig. 2 - Schematic representation of different antibody formats. A variety of antibody fragments are depicted, including Fab, scFv, single-domain V_H, VHH and VNAR and multimeric formats, such as minibodies, bis-scFv, diabodies, triabodies, tetrabodies and chemically conjugated Fab multimers (sizes given in kDa are approximate) (Holliger and Hudson, 2005).

functional affinity through the use of either chemical or genetic cross-links. Various methods have been devised to genetically encode multimeric scFvs, of which the most successful design was the simple reduction of scFv linker length to direct the formation of bivalent dimers (diabodies), triabodies or tetrabodies (Holliger and Hudson, 2005). In general, several multivalent antibody conjugates are generated to be monospecific. However, some strategies have also been applied to produce bispecific multimers. These bispecific antibodies have two different binding specificities fused together in a single molecule. Because of dual specificity, they can bind to two adjacent epitopes on a single antigen, thereby improving avidity. Antibody engineering has also been applied to the development of bifunctional antibodies. In contrast to bispecific antibody derivates, bifunctional molecules combine the antigen-binding site of an antibody with a biological function encoded by a linked or fused partner (Hudson and Souriau, 2003). These include radionuclides, cytokines, toxins, enzymes, peptides and proteins. Recently, ibritumomab or Zevalin® (Biogen Idec) (Vose *et al.*, 2007), tositumomab or Bexxar® (GlaxoSmithKline) (Macklis, 2006), both applied to the treatment of Non-

Hodgkin lymphoma, and gemtuzumab or Mylotarg® (Wyeth) (Larson *et al.*, 2002) with therapeutic use against acute myeloid leukemia, are three examples of FDA-approved bifunctional antibodies designed to specifically deliver cytotoxic drugs into cancer cells.

To escape immunosurveillance, many pathogenic viruses have evolved narrow cavities (canyons) in their surface antigens, which bind their target receptors but are poorly accessible to intact antibodies and are thus largely immunosilent. This antibody response is caused by the limited diversity of complementarity-determining region (CDR) loop lengths, which constrains the displayed antigen-binding surfaces to mostly flat or concave topologies (Arndt *et al.*, 2004). Interestingly, the camelids (camels and llamas) and cartilaginous fish (wobbegong and nurse sharks), have evolved high-affinity single V-domains mounted on an Fc-equivalent constant domain framework as an integral and crucial component of their immune system (Klooster *et al.*, 2007; Stretsov and Nuttal, 2005). In addition to these conventional antibodies, camelids and sharks also produce unusual antibodies composed only of heavy chains. These peculiar heavy chain antibodies (hcAbs) lack light chains (and, in the case of camelid antibodies, also the C_H1-domain). Therefore, the antigen binding site of hcAbs is formed only by a single domain that is linked directly via a hinge region to the Fc-domain. The variable domain is designed VHH for camelid and VNAR for shark single-domain antibodies (Fig. 3). The CDR3 region of these antibodies possesses the extraordinary capacity to form long finger-like extensions that can extend into cavities on antigen, e.g. the active site crevice of enzymes. The CDR3 can form convex extensions that occupy the cleft for the substrate and is often much longer than that of conventional V_H domains. The extended CDR3 is usually stabilized by an additional disulfide bond connecting the CDR3 to the adjacent CDR1 loop

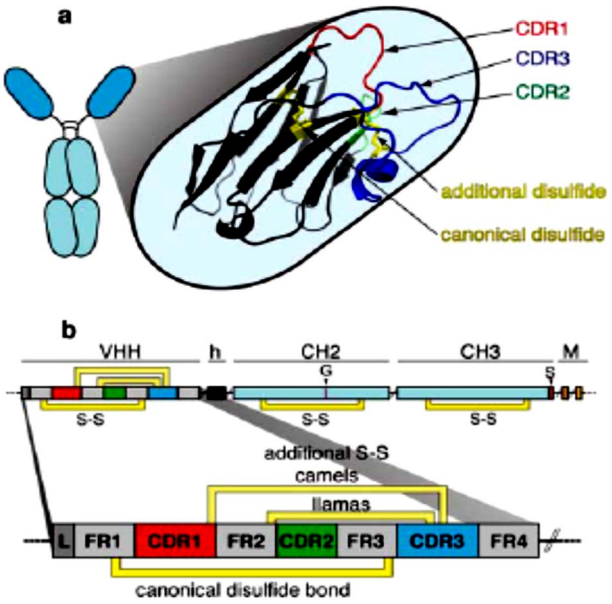

Fig. 3 - Schematic diagram of the VHH domain of a camelid heavy chain antibody. **a** The three CDRs of the antigen-binding paratope are depicted as colored loops: CDR1 *red*, CDR2 *green*, and CDR3 *blue*. **b** The canonical disulphide bond connecting framework regions 1 and 3 (FR1 and FR3) in the two *β*-sheets of the immunoglobulin domain is indicated in *yellow*. Many camelid antibodies contain an additional disulfide bond (S–S) connecting the CDR3 with the end of the CDR1 (camels) or the beginning of the CDR2 (llamas). *h* Hinge, *M* transmembrane domain of membrane isoform, *G* glycosylation site, *S* stop codon of secretory isoform (Wesolowski *et al.*, 2009).

(common in camel and shark sdAbs) or to the CDR2 loop (common in llama sdAbs). The interface of conventional V_H and V_L domains is stabilized by hydrophobic interactions, the corresponding residues in llama antibodies are replaced by hydrophilic residues. In shark sdAbs, the CDR2 loop is replaced by two shorter less variable loops (Wesolowski *et al.*, 2009).

In general, camelid VHH and shark VNAR domains are soluble and can be produced as stable *in vitro* targeting reagents for sensitive diagnostic platforms and nanosensors. Compared to monoclonal antibodies, VHH domains have also demonstrated improved penetration against cryptic (immuno-evasive) target antigens (Holliger and Hudson, 2005). However, for *in vivo* administration, humanization (or deimmunization) may be crucial to reduce immunogenicity, although llama VHH domains have been claimed to be only minimally immunogenic (Cortez-Retamozo *et al.*, 2004). As it is frequently observed with display technologies, favourable properties (such as good expression, stability and solubility) are co-selected with binding activity of VHH molecules (Holliger and Hudson, 2005).

I.2 - Scaffolds

Antibody size dependence of epitope accessibility can be highly non-linear and some protein surface-exposed structures can be completely obstructed for full size antibodies (Chen *et al.*, 2010; Chen *et al.*, 2009). Therefore, a large amount of work has been aimed at developing novel scaffolds of much smaller size. The term “scaffold” reflects the use of a protein framework that can carry altered amino acids or insertions giving protein variants with entirely novel functions, typically new binding specificities. Such scaffolds are stable, soluble and easy to format, manufacture and express in microbial cell cultures. High stability independent of disulfide bonds is a clear advantage, facilitating high yields in bacterial expression and enabling intracellular applications. There are presently approximately 50 suggested protein scaffolds reported and these have intensely reviewed over the last years (Dimitrov, 2009; Dimitrov and Marks, 2009; Chen *et al.*, 2008; Honegger, 2008; Kolmar and Skerra, 2008; Saerens *et al.*, 2008; Skerra, 2007). Examples of several non-immunoglobulin scaffolds are illustrated in Fig. 4 and Table 1.

Table 1: Non-immunoglobulin scaffolds for generation of new affinity ligands (adapted from Grönwall and Ståhl, 2009).

Name	Scaffold	Residue/S-S-bonds	Secondary structure	Randomization	Selection method	Reference/Company
Adnectin	Fibronectin	94/-	β-Sandwich	2-3 lopps	Phage display mRNAdisplay; yeast-two-hybrid	Koide *et al*., 1998; Xu *et al*., 2002, **Adnexus Therapeutics**
Affibody	Protein A	58/-	α_3	13 aa on 2α-helices	Phage display	Nord *et al*., 1997, **Affibody AB**
Anticalin	Lipocalin (BBP)	160-180/2 S-S	β-Barrel	4 loops (16 aa)	Phage display	Beste *et al*., 1999, **Prieris Proteolab**
Aptamer	TrxA	108/1 S-S	α/β	20 aa loop insert	Phage display yeast-two-hybrid	Borghouts *et al*., 2005, **Aptanomics**
Avimer	A-domain	*n* x~40/3 S-S+ Ca^{2+}	Oligomeric, ~4loops	21 aa loop insert	Phage display	Silverman *et al*., 2005, **Amgen**
Darpin	Ankyrin repeat	67+ *n* x 33/-	α_2/β_2	7 aa on β-turn and 1 α-helix (of every repeat)	Ribosome display	Binz *et al*., 2004, **Molecular Partners**
Kunitz domain	APPI	58/3 S-S	α/β	1-2 loops	Phage display	Dennis and Lazarus, 1994; Williams and Baird, 2003, **Dyax**
PDZ-domain	Ras-binding AF-6	~100/-	α_3/β_3	Entire domain by PCR mutagenesis	Phage display	Schneider *et al*., 1999; Ferrer *et al*., 2005, **BioTech Studio LLC**

Affibodies are small antibody mimetics (~6 kDa), robust 3-helix proteins, designed based on the Z domain of staphylococcal protein A that were developed for targeted therapy of several diseases, e.g. cancer and inflammatory diseases (Jonsson *et al.*, 2009; Tolmachev *et al.*, 2007). Affibody® molecules can also be used for protein purification (Nord *et al.*, 2001), enzyme inhibition ("Phusion Hot Start High-Fidelity DNA Polymerase", Finnzymes), research reagents for protein capture and detection (Lundberg *et al.*, 2007; Renberg *et al.*, 2007) and diagnostic imaging (Orlova *et al.*, 2006).

An ABD-fused tumor-targeting construct was derived from a HER2-specific Affibody molecule, which belongs to a class of small protein A-derived antibody mimetics, originally developed for imaging purposes. The original affibody presented a rapid kinetics ideal for imaging, but the uptake in kidneys was very high, which was incompatible with radionuclide therapy that would be a logical extension of the successful tumour targeting obtained. Therefore, Nilsson and co-workers decided to convert the imaging tracer to a candidate for targeted radiotherapy by fusion to ABD (Tolmachev *et al.*, 2007). The albumin association did not compromise the tumour targeting properties. Compared with the non-fused Affibody molecule, kidney uptake was decreased 25-fold and the tumour uptake increased three to five-fold. This combined with retained high specificity for the tumour, allowed for successful radioimmunotherapy using the beta-emitting nuclide ^{177}Lu. Treatment of mice bearing HER2-overexpressing microxenografts completely prevented tumour formation, in contrast to radioactivity coupled to an ABD-fused construct against an irrelevant antigen (Tolmachev *et al.*, 2007). The HER2-specific Affibody ABY-025 is in clinical development for tumour diagnosis (Gebauer and Skerra, 2009; Baum *et al.*, 2010).

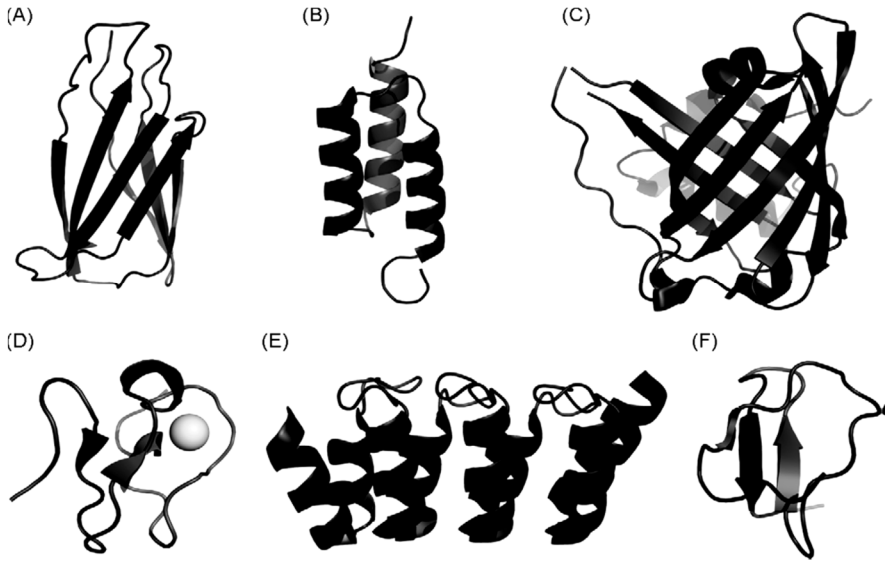

Fig. 4 - Representative illustrations of a selection of scaffold proteins applied for generation of novel affinity proteins. (A) Adnectin, derived from 10th fibronectin type III domain (PDB ID: 1TTG). (B) Affibody, derived from Z-domain of protein A (PDB ID: 1Q2N). (C) Anticalin, derived from the bilin-binding protein, here a digoxigenin binding anticalin is illustrated (PDB ID: 1LKE). (D) Avimer, designed from a consensus human A-domain here an A-domain is represented by the LDL receptor ligand-binding module 5 stabilized by a Ca2+ ion (PDB ID: 1AJJ). (E) Darpin, designed from a consensus ankyrin repeat domain, here a HER2-binding darpin with two repeat modules is illustrated (PDB ID: 2JAB). (F) Kunitz domain, derived from the protease inhibitor domain of the amyloid beta protein precursor (PDB ID: 1AJJ). Images were generated using PyMOL software (Grönwall and Ståhl, 2009).

I.3 - Pharmacokinetics of therapeutic proteins

The basic paradigm of clinical pharmacology is the fact that drug effects, desired as well as undesired, are function of drug concentrations within different organs and tissues in the human body. Thus, drug concentrations are the driving force for the spectrum of drug responses observed in a drug-treated patient (Meibohm, 2012). Pharmacokinetics is the study and characterization of the time course of drug adsorption, distribution, metabolism and excretion (ADME), and provides a quantitative analysis of how living systems handle xenobiotics and biodrugs (Mahmood, 2009). The pharmacokinetic properties, especially their distribution, metabolism and excretion, are influenced by several factors including size, shape, charge, hydrophilicity, interaction with other molecules and cells, and sensitivity to proteolytic degradation (Tang *et al.*, 2004). Similar to conventional small molecule drugs, protein therapeutics is characterized by well-defined properties that form the basis for the design of therapeutic dosing regimens as well as drug delivery strategies. The distribution volume of proteins is determined largely by their molecular weight, physicochemical properties (e.g., charge, lipophilicity), protein binding, and their dependency on active

transport processes (Meibohm, 2012). Since most therapeutic proteins have high molecular weight and are thus large in size, their apparent volume of distribution is usually small and limited the volume of the plasma or the extracellular space, predominantly because of their limited mobility secondary to impaired passage through biomembranes (Zito, 1997). In contrast, to small molecular drugs, protein transport from vascular space into the interstitial space of tissues is largely mediated by convection rather than diffusion, following the unidirectional fluid flux from the vascular space through paracellular pores into the interstitial tissue space. The subsequent removal from the tissues is accomplished by lymph drainage back into the systemic circulation (Flessner *et al.*, 1997). Another, but much less prominent pathway for the movement of protein molecules from the vascular to the interstitial space is transcellular migration via endocytosis (Reddy *et al.*, 2006).

Engineering antibodies or proteins for therapy must generally exhibit high affinity, discriminating specificity, minimal immunogenicity and low cross-reactivity. Normally, these factors can be addressed by making relatively small changes to the primary protein structure of the molecule. In addition to this, a major consideration in protein engineering is developing one that exhibits optimal pharmacokinetics: appropriate dosing leading to optimal bioavailability, uptake, distribution and clearance in targeted and non-targeted tissues, which will lead to optimal pharmacodynamics (Constantinou *et al.*, 2010; Beckman *et al.*, 2007; Batra *et al.*, 2002). Therapeutic administration requires a balance between prolonged retention at the target site and slow clearance, which can lead to liver accumulation and high radiation exposure of other tissues (Holliger and Hudson, 2005).

Systematic *in vivo* studies have provided striking confirmation that size is an important parameter in pharmacokinetics and biodistribution of therapeutic proteins. Large IgG molecules specific for tumour surface molecules have been found to penetrate solid tumours only slowly, are non-uniform in their final distribution and have high serum levels and associated toxicities. Conversely, small scFv fragments (30 kDa) are cleared extremely rapidly and have poor tumour retention because of their monovalent binding properties. Some biodistribution studies (Kenanova *et al.*, 2005; Robinson *et al.*, 2005) have independently confirmed that diabodies, because of their small size, are rapidly eliminated through the kidneys, thereby limiting the exposure to the bone marrow, which is most often the dose-limiting organ with intact radiolabeled mAbs.

However, small size antibodies have to be administered by infusion or repeated intravenous bolus injections in order to maintain a therapeutically effective dose over a prolonged period of time, or are restricted to loco-regional treatment. Their rapid elimination

is mainly due to renal filtration and degradation, because the kidney generally filters out molecules below 50-60 kDa (Tang *et al.*, 2004). This has led to the development of half-life extension strategies to prolong circulation of these recombinant antibodies in the blood and thus improve administration and pharmacodynamic properties. With an increasing number of small antibody molecules and antibody mimetics developed for clinical applications, strategies to improve pharmacokinetics, especially half-life extension, have become increasingly important, not only with respect to therapeutic efficacy but also regarding the costs of therapy as well as convenience for patients, and compliance (Mahmood and Green, 2005; van de Weert *et al.*, 2005; Tang *et al.*, 2004).

II – Renal clearance and FcRn-mediated recycling

As mentioned in the previous section, due to their small size, some protein therapeutics have to be administered as infusion or repeated intravenous (i.v.) or subcutaneous (s.c.) bolus injections in order to maintain a therapeutically effective dose over a long period of time, or are restricted to loco-regional treatment. A comparison of the half-lives of plasma proteins reveals the threshold for rapid excretion to be in the range of approximately 40-50 kDa, demonstrating that the size of the molecules is one of the determining factors (Fig. 1). The glomerular filtration barrier is formed by the fenestrated endothelium, the glomerular basement membrane (GBM) and the slit diaphragm located between the podocyte foot processes (Tryggvason and Wartiovaara, 2005). The fenestrae between the glomerular endothelial cells presents diameters between 50-100 nm, consequently, allowing free diffusion of molecules. It was suggested that the slit diaphragm represents the ultimate macromolecular barrier, forming an isoporous, zipper-like filter structure with numerous small, 4-5 nm diameter pores and a lower number of 8-10 nm diameter pores (Haraldsoon and Sörensson, 2004; Wartiovaara *et al.*, 2004; Rodewald and Karnovsky, 1974). In addition to size, the charge of a protein contributes to renal filtration. It has been suggested that the proteoglycans of the endothelial cells and the GBM contribute to an anionic barrier, which partially prevents the passage of plasma macromolecules (Tryggvason and Wartiovaara, 2005). Therefore, the size of a therapeutic protein, that is, its hydrodynamic radius, and also its physicochemical properties, that is, charge, represent starting points in order to improve half-life. Interestingly, of all the plasma proteins, two kinds of molecules, serum albumin and IgGs, exhibit an extraordinary long half-life in humans. Thus, human serum albumin (HSA) has a half-life of 19 days and immunoglobulins (IgG1, IgG2 and IgG4) have half-lives in the

range of 3 to 4 weeks, exceeding those of the other plasma proteins (Lobo *et al.*, 2004; Peters, 1996). In humans, IgG molecules present half-lives in the range of 1 to 4 weeks depending on the subclass (IgG1, IgG2, IgG4 = 12–21 days, IgG3 = 7–8 days) and possibly also the allotype (Kontermann, 2009). The half-lives of the other Ig classes are shorter (IgM = 5–6 days, IgA = 6 days, IgD = 3 days, IgE = 2 days). The half-lives of therapeutic IgGs can differ dramatically and differences can also be seen between different forms of antibodies. The approved fully human, humanized, and chimeric antibodies possess half-lives in the range of 1–3 weeks. In contrast, murine IgGs are much more rapidly cleared from the circulation, with half-lives of approximately 2–3 days (Lobo *et al.*, 2004; Ternant and Paintaud, 2005). These long half-lives, which clearly set albumin and IgG apart from the other plasma proteins (Fig. 1) are caused by a recycling process mediated by the neonatal Fc receptor (Roopenian and Akilesh, 2007; Anderson *et al.*, 2006; Lencer and Blumberg, 2005). FcRn, expressed, for example, by endothelial cells, is capable of binding albumin and IgGs in a pH-dependent manner. The kinetics of IgG and albumin recycling is illustrated in Fig. 5. Thus, after cellular uptake of plasma proteins through macropinocytosis, albumin and IgG will bind to FcRn in the acidic environment of the endosomes. This binding diverges from albumin and IgG from degradation in the lysosomal compartment and redirects them to the plasma membrane, where they are released back into the blood plasma because of the neutral pH (Section III.2). This offers additional opportunities to extend or modulate the half-life proteins, for example, through fusion to albumin or to Fc region of IgG (Kontermann, 2009).

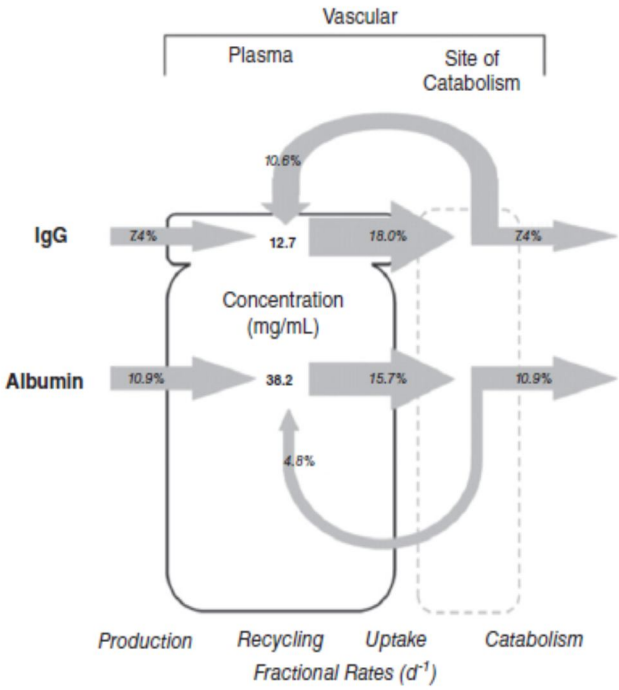

Fig. 5 - Effect of FcRn-mediated recycling on IgG and albumin turnover in humans expressed as fractional rates. Shown are homeostatic plasma concentrations (12.1 and 38.2 mg mL^{-1}), fractional catabolic rates (7.4 and 10.9%/day), the FcRn-mediated fractional recycling rates (10.6 and 4.8%/day), and the fractional production rates (7.4 and 10.9%/day). The figure is to scale: areas for plasma amount and arrow widths for rates (Meibohm, 2012).

III – Half-life extension strategies

With an increasing number of therapeutic proteins approved and developed, including various alternative antibody formats, many of them presenting a short plasma half-life, serum half-life extension of small therapeutic proteins has become an established method to increase potency and improve patient compliance by allowing for fewer administrations (Frejd, 2012). There is no strict correlation between molecular mass and half-life though, factors other than size also influences half-life. Studies of the half-lives of various recombinant antibody fragments in animals also revealed rapid elimination from the circulation (Holliger and Hudson, 2005). In mice, scFv fragments have a terminal half-life of approximately 10–30 minutes, and molecules with a size similar to Fab fragments, such as diabodies, single-chain diabodies and tandem scFvs, have a half-life of 5–6 hours. In comparison, the half-life of IgGs in mice is in the range of 4–5 days. From these and other studies it is evident that small-sized antibody molecules that also lack an Fc region are indeed rapidly cleared from the circulation. This is especially a concern for therapeutic applications such as cancer and chronic inflammatory diseases, where long-lasting activity is desirable (Kontermann, 2009).

Strategies to extend the half-lives of recombinant antibodies and other proteins can be divided into those that (i) rely on increasing the size and thus the hydrodynamic volume; and (ii) in addition implement recycling by the FcRn, the receptor responsible for the long half-lives of IgGs and albumin (Fig. 6 and Table 2) (Kontermann, 2009). These strategies comprise a variety of different approaches including chemical coupling of polymers and carbohydrates, post-translational modifications such as *N*-glycosylation, and fusion to recombinant polymer mimetics. Additionally, conjugation, binding or fusion to an Fc region or serum albumin, respectively, results not only in an increase size but also incorporates FcRn-mediated recycling (Table 2). More recently, nanoparticulate formulations have also been developed to improve the half-life and biodistribution of therapeutic proteins, for example, through encapsulation into liposomes or polymeric capsules (Pisal *et al.*, 2010).

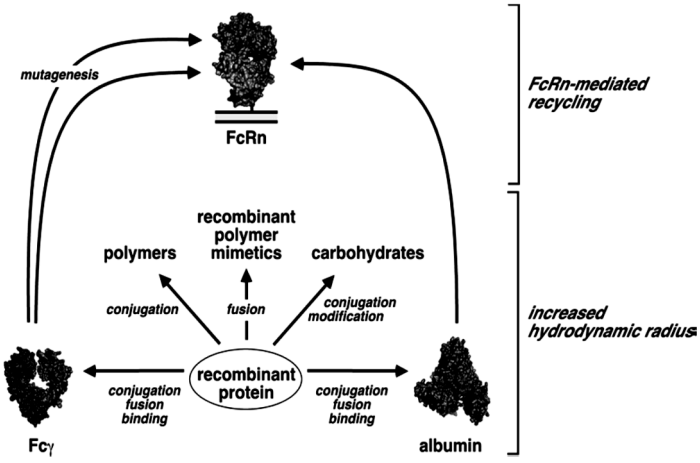

Fig. 6 - Strategies to improve half-lives of therapeutic proteins (Kontermann, 2009).

Table 2: Recombinant antibody and antibody/albumin complexes (adapted from Kontermann, 2012).

Strategy	Modification	Effect on hydrodynamic radius	Effect on fcRn-mediated recycling	Effect on half-life
PEGylation	Chemical conjugation methoxy polyethylene glycol (mPEG)	Increased	None	Prolonged depending on PEG size and structure
Polysialylation	Chemical conjugation or attached by post-translational modification of polysialic acid	Increased (plus change in pI)	None	Prolonged depending on extent of polysialylation
HESylation	Chemical conjugation of hydroxyethyl starch (HES)	Increased	None	Prolonged depending on HES size and structure
Recombinant PEG mimetics	Genetic fusion of flexible, hydrophilic amino acid chains	Increased	None	Prolonged depending on size and composition
***N*-glycosylation**	Post-translational attachment of *N*-glycans	Increased	None	Moderately prolonged
***O*-glycosylation**	Post-translational attachment of *O*-glycans	Increased	None	Moderately prolonged
Fc fusion	Genetic fusion of IgG Fc region	Increased	Utilized	Prolonged
Engineering Fc	Mutations introduced into the Fc region of IgGs or Fc fusion proteins	Unaltered	Utilized or diminished (depending on mutations)	Prolonged or reduced
IgG binding	Genetic fusion or conjugation to IgG-binding moieties	Increased upon binding to IgG	Utilized or diminished (depending on binding site)	Prolonged
Albumin fusion	Genetic fusion to serum albumin	Increased	Utilized	Prolonged
Albumin binding	Genetic fusion or conjugation to albumin-binding moieties (peptides, protein domains, antibody fragments, antibody mimetic scaffolds, small chemicals, fatty acids, etc.)	Increased after binding to albumin	Utilized	Prolonged
Albumin coupling	Chemical conjugation to cysteine 34	Increased	Utilized	Prolonged
Nanoparticles	Encapsulation into or conjugation to nanoparticles (e.g., liposomes, polymeric capsules)	Strongly increased by the size of the nanoparticles (50-200nm)	None	Prolonged (slow release)

III.1 – Strategies to increase the hydrodynamic radius

The primary approach in improving the half-life of a protein therapeutic is to reduce the renal clearance rate, for example, by increasing the size above the renal cut-off. This can be

achieved by several ways including chemical and post-translational modifications as well as genetic engineering (Table 2).

These strategies comprise a variety of different methods, including di- or multimerization, chemical coupling of polymers or carbohydrates, post-translational modifications such as *N*-glycosylation, and fusion to polymer mimetics. Another obvious approach to increase the size of therapeutic proteins is the fusion to another proteins moiety, for example, a plasma protein. Mainly, fusion to immunoglobulin Fc region or serum albumin has been used to extend the half-life of peptides and proteins (Schulte, 2009). Because albumin and Fc containing proteins utilize recycling by the FcRn, these strategies are described below (Section III.2).

Another approach to increase the hydrodynamic volume of small molecular weight drugs is the incorporation or encapsulation of these molecules into liposomal carrier systems. In addition to liposomes, various other nanoparticulate carrier systems have been used to improve pharmacokinetic and pharmacodynamics properties of proteins. The carrier systems combine several advantages. Because of their large size in the range of 50 to 200 nm, the half-life is strongly increased (Hartung and Bendas, 2012; Landfester *et al.*, 2012). Furthermore, nanoparticulate formulations influence biodistribution, for instance, accumulation in tumours through an enhanced permeability and retention in the tumour tissue (Peer *et al.*, 2007). Additionally, they are also capable of protecting the protein drug from degradation, for example, through plasma proteases, and can act as a slow release formulation, namely, as a drug depot in the body (Hartung and Bendas, 2012; Landfester *et al*, 2012).

Several studies showed that PEGylation and glycosylation are the most efficient and relevant strategies for therapeutic use of recombinant antibodies (Jevsevar *et al.*, 2010; Solá and Griebenow, 2010; Kontermann, 2009).

III.1.1 - PEGylation

PEGylation, that is, the chemical conjugation of polyethylene glycol (PEG), mainly of its methoxy derivative, methoxy polyethylene glycol (mPEG), was established more than two decades ago (Jevsevar *et al.*, 2010). Conjugation of one or more PEG chains to a protein is an established and approved method to prolong the half-life of a protein, and various PEGylated molecules are in clinical use (Duncan, 2006; Harris and Chess, 2003). In 1990, the first PEGylated protein drug was approved by the FDA (Fishburn, 2008; Harris and Chess, 2003) and since then eight more PEGylated protein drugs have been approved, including enzymes,

interferon-α2b, G-CSF, hGH, erythropoietin and a Fab fragment (Gaberc-Porekar *et al.*, 2008; Veronese and Mero, 2008).

PEG molecules are amphiphilic, chemically inert polymers of ethylene oxide, composed by ethylene oxide units connected in a linear or branched configuration and a varying length. In the approved drugs, one or several PEG chains of 5 to 40 kDa are conjugated. The dipole nature of the oxygen atom makes PEG highly hydrophilic. A monomer unit can bind two to three water molecules, thus PEG can bind water up to its own molecular mass, occupying a large hydrodynamic volume. Therefore, the molecular mass of PEGylated proteins is drastically increased through the binding of water molecules, reflected by a strong increase of the hydrodynamic radius. Different coupling methods have been established, comprising random and site-directed approaches. The PEGylation strategy, that is, the site of PEGylation as well as the number and size of the attached PEG chains, has to be carefully chosen in order to avoid a reduction or abrogation of the activity of the therapeutic protein (Knop *et al.*, 2010; Fishburn, 2008). Ideally, a single PEG chain is conjugated in a site-directed manner, for example, over the use of existing or genetically introduce cysteine residues. This is exemplified by Cimzia (certolizumab pegol), a bacterially produced anti-TNF Fab' fragment, where a 40 kDa PEG chain is attached to the free cysteine at the C-terminus of the heavy chain, that is opposite the antigen-binding. Certolizumab pegol was the first PEGylated antibody fragment that was approved for clinical use. The antibody was approved to reduce signs and symptoms of Crohn's disease and maintain clinical response in adult patients from moderately to severely active disease which have had an inadequate response to conventional therapy, and is also in development for the treatment of rheumatoid arthritis and psoriasis. The terminal half-life was determined to be approximately 14 days (Melmed *et al.*, 2008; Rutgeerts *et al*, 2008). In general, this strategy is considered to be safe and well tolerated (Veronese and Mero, 2008). Although in animals, the occurrence of renal tubular vacuolization has been observed due to accumulation of the non-degradable PEG chains in the kidney.

PEGylation also influences polarity, structure and surface properties leading to altered physicochemical properties (solubility, stability), immunogenicity, cellular uptake, elimination and tissue localization (Hamidi *et al.*, 2006). Thus, besides improved circulation half-lives, the advantages of PEGylation include reduced immunogenicity, improved solubility, enhanced proteolytic resistance, improved bioavailability, and reduced toxicity. PEGylation was successfully applied to prolong the half-lives of a variety of antibodies and antibody fragments including IgG and scFv molecules by coupling one or more PEG chains

with different sizes. However, several studies also showed that PEGylation can affect antigen binding and bioactivity (Veronese and Mero, 2008).

Recently, alternative strategies to PEGylation have been established. For example, it was noted that the polypeptide backbone, resembles, at least in part, the structure of PEG. This has led to the generation of long polypeptide chains of hydrophilic and flexible structure, which can be genetically fused to recombinant proteins (Schellenberger *et al.*, 2009; Schlapschy *et al.*, 2007). Thus, chemical conjugation and additional purification steps are avoided. Besides, the fused polypeptide chains are biodegradable and have also been shown to be immunologically inert. *In vivo* studies established that this recombinant PEG mimetics behave in a similar manner to PEG that is they result in a drastic increase of the hydrodynamic radius and extension of the half-life (Kontermann, 2012).

III.1.2 - *N*- and *O*-glycosylation

As an alternative, carbohydrate chains can be attached to therapeutic proteins. Because this process takes place naturally, for example, by post-translational modifications in mammalian cells, therapeutic proteins have been genetically modified to contain additional *N*- or *O*-glycosylation (Solá and Griebenow, 2010; Li and d'Anjou, 2009; Sinclair and Elliott, 2005). Human antibodies are glycoproteins with varying degrees of glycoslyation depending on the isotype. All IgG isotypes possess a single *N*-glycosylation site in the C_H2 domain (amino acid Asn297). IgG3 was *N*-glycosylated at the C_H3 domain. Often ignored is the observation that 20–25% of the immunoglobulins also exhibit *N*-glycosylation of the variable domains, either of the variable heavy or light chains, or even both variable domains, which in some cases has been reported to be associated with a pathophysiological role of the antibodies (Batra *et al.*, 2002). IgG-Fc glycosylation has been shown to influence Fc-mediated effector functions of antibodies, especially antibody-dependent cell-mediated cytotoxicity (ADCC) and complement-dependent cytotoxicity (CDC), but as well as other properties such as thermal stability and pharmacokinetics. In addition to the modulation of the composition of existing glycans, the introduction of new *N*-glycans was applied to increase the hydrodynamic radius and thus the plasma half-life of recombinant proteins (Solá and Griebenow, 2010; Jefferis, 2005).

Several studies emphasize that the introduction of (additional) *N*-glycosylation sites into a protein leads to only a moderate increase in plasma half-lives. Nevertheless, it can improve administration and efficacy of therapeutic proteins. For example, Stork and co-workers

introduced 3–9 *N*-glycosylation sites in the linker regions as well as a C-terminal extension of a bispecific single-chain diabody (scDb) molecule. Expression in HEK293 cells resulted in heterogeneous populations of glycosylated molecules possessing an increased hydrodynamic radius. In mice, the circulation time was prolonged, resulting in an approximately 3-fold increased area under the plasma concentration-time curve from 0 to 24 hours (AUC24) compared with non-glycosylated scDb (Stork *et al.*, 2008).

III.1.3 – Polysialylation, HESylation and other strategies

Carbohydrates have also been chemically conjugated to therapeutic proteins in a similar way to the PEGylation approach. For example, polysialic acid (PSA) has been investigated as an alternative to PEG (Gregoriadis *et al.*, 2005; Gregoriadis *et al.*, 2000). PSA is found on the surface of several cells including mammalian cells, thus is a biocompatible and biodegradable natural polymer. Colominic acid, a linear polymer of α-(2,8)- linked *N*-acetylneuraminic acid, was used for polysialylation of various proteins including asparaginase, insulin and antibody fragment and was shown to be capable of prolonging their half-lives (Constantinou *et al.*, 2008).

Another carbohydrate structure, which has been established for half-life extension of therapeutic proteins, is hydroxyethyl starch (HES). HES is a modified, branched amylopectin, isolated from waxy maize starch, composed of glucose units linked by α-1,4- and α-1,6-glycosidic bonds. HES is an approved plasma volume expander with a proven safety record. Because of its close similarity to glycogen, HES is not immunogenic (Agreda-Vásquez *et al.*, 2008; Brecher *et al.*, 1997). The size and structure of HES and thereby its stability can be adjusted by acidic hydrolysis and by chemical hydroxyethylation at positions 2, 3, and 6 of the glucose unit. The HESylation technology was pioneered by the company Fresenius and Kabi to improve the pharmacokinetic and pharmacodynamic properties of therapeutic proteins. For example, it was successfully applied to produce improved derivatives of erythropoietin by chemical coupling of 60 kDa HES (Hey *et al.*, 2012).

Another interesting approach is the fusion of recombinant polypeptides in the strategy used by Schellenberger and colleagues to extend the half-life of peptides or proteins. Their work showed that genetic fusion of an unstructured recombinant polypeptide of 864 amino acids, called XTEN, to exenatide peptide, for treating type 2 diabetes, should increase exenatide half-life in humans from 2.4 h to a projected time to 139 h. XTEN lacks hydrophobic amino acid residues that often contribute to immunogenicity and complicate manufacture. Based on

XTEN fusions to exenatide, glucagon, GFP (Green Fluorescent Protein) and human growth hormone, XTEN can provide an effective means for extending half-life of therapeutic proteins, and the recombinant nature of XTEN provides several advantages over traditional PEGylation (Schellenberger *et al.*, 2009).

III.2 – Strategies implementing FcRn-mediated recycling

IgG molecules and serum albumin possesses extraordinary long half-lives in humans. The half-life of IgG1 is in the range of 21-23 days and that of human serum albumin is 19 days (Kontermann, 2009). No other soluble serum protein is known to exhibit these long half-lives. In both cases, pH-dependent binding to FcRn after endosomal uptake into endothelial cells is responsible for recycling into the bloodstream (Lencer and Blumberg, 2005). The neonatal Fc receptor also known as Brambell receptor, is an MHC class I-related receptor consisting of a heavy chain, which is non-covalently associated with β2-microglobulin (B2M) light chain. The domain III of albumin is responsible for FcRn binding and the long serum half-life. *In vitro* mutagenesis and binding studies showed that the conserved H166 residue of the human FcRn heavy chain, located opposite to the FcRn-IgG interaction site, plays a critical role in the pH-dependent FcRn-albumin interaction (Andersen *et al.*, 2006; Chaudhury *et al.*, 2006) (Fig. 7).

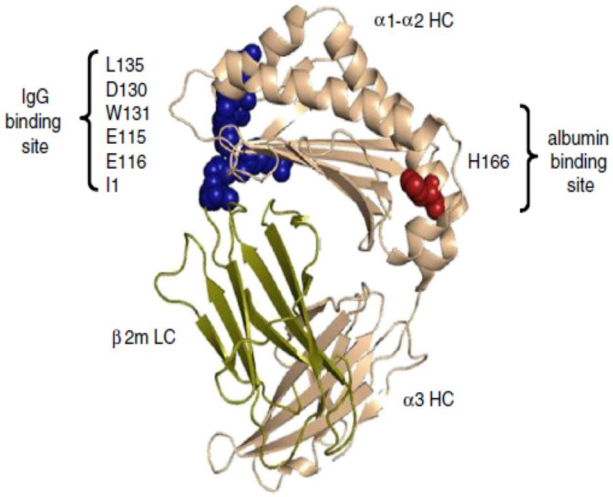

Fig. 7 - The crystal structure of FcRn and its ligands binding sites. The crystal structure of a truncated recombinant soluble FcRn with the HC (α1, α2 and α3) shown in cream and the β2m subunit in green. The amino acid residues essential for IgG binding (E115, E116, D130, W131, E133 and L135 of the FcRn HC and I1 of β2m) are highlighted by blue spheres while H166, which is crucial for albumin binding is indicated by red spheres (Sleep *et al.*, 2013).

FcRn is also involved in transplacental transport of maternal IgG to the fetus and in antigen presentation (Roopenian and Akilesh, 2007). The FcRn-mediated recycling mechanism of albumin is illustrated in Fig. 8. Briefly, following pinocytosis, plasma proteins move to acidic endosomal compartments where IgG and albumin bind FcRn with high affinity at distinct binding sites. When FcRn is saturated, unbound plasma proteins or excess ligands are destined for degradation in lysosomes, while bound complex is diverted to the cell membrane

where IgG and albumin dissociate from FcRn at physiologic pH, providing longer survival to the two proteins. Unbound receptor is either recycled back to endosome for another round of recycling or degraded in the lysosome (Kim, 2012). Concerning binding stoichiometry, one or two molecules of FcRn can bind one IgG molecule. Under equilibrium conditions, two molecules of FcRn bind one IgG (2:1 stoichiometry), whereas alterations of the carbohydrate moieties on FcRn can result in 1:1 binding stoichiometry under nonequilibrium conditions (Sánchez *et al.*, 1999). IgG and albumin bind to FcRn independently and noncooperatively. Unlike FcRn-IgG binding, albumin binds FcRn with a 1:1 stoichiometry, and a large positive charge in entropy upon binding suggests a hydrophobic interaction (Chaudhury *et al.*, 2006).

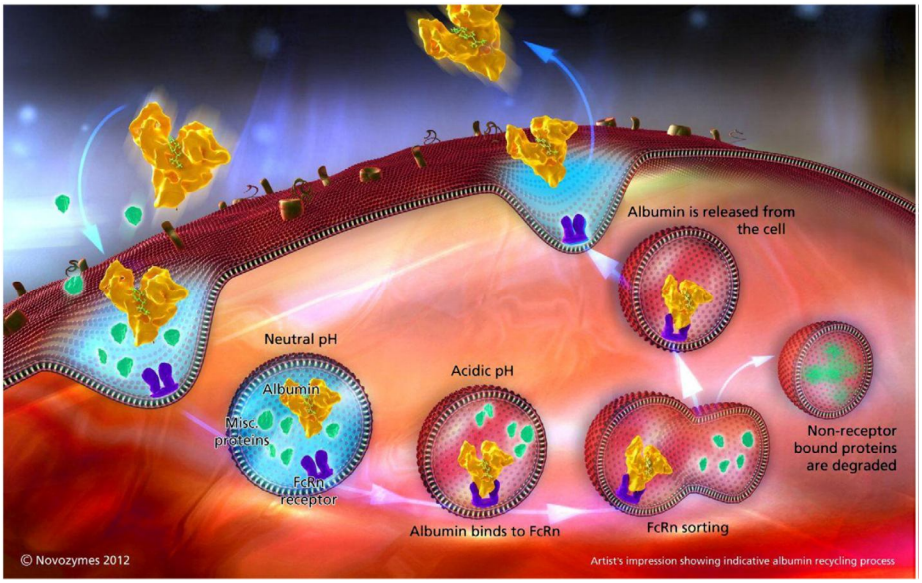

Fig. 8 - FcRn mediated, pH-dependent, albumin recycling. Extracellular albumin (gold heart-shaped protein) with drug attached (green molecule) is pinocytosed along with a range of other plasma constituents at neutral pH (blue shading). Upon acidification of the vesicle (red shading) albumin binds to the integral FcRn membrane protein (purple molecule). Non-FcRn interacting proteins and plasma constituents are sorted to the lysosome for degradation while vesicles containing functional albumin–FcRn complexes are recycled back to the plasma membrane cell surface where they are exposed to neutral pH of the plasma and the albumin is released back into the circulation (Sleep *et al.*, 2013).

Since the Fc region of IgG has been involved in pH-depending binding to FcRn (Martin *et al.*, 2001), protein engineering of the Fc region can improve the half-life of therapeutic antibodies with enhanced binding of FcRn at acidic pH. Another approach is via fusion to the Fc region of IgG molecule to recombinant antibody fragments, and these fusion proteins exhibit affinities similar to whole antibodies, but because of their smaller size are able to penetrate more easily into tissues (Kontermann, 2009; Holliger and Hudson, 2005).

III.2.1 - Half-life extension by binding to albumin

In contrast with antibodies, albumin is also present at high concentration in the interstitial compartment and has a larger volume of distribution. Proteins that take advantage of albumin to increase their half-life will therefore have a different tissue distribution profile than Fv-fused proteins (Frejd, 2012). However, some applications (e.g. of cytokines, growth factors, receptor-neutralizing antibodies, bispecific antibodies) may require monovalent interaction and the lack of Fc-mediated effector functions (ADCC, CDC) (Müller and Kontermann, 2007). In these cases, fusion to albumin or albumin-binding domain (ABD) offers an alternative.

The strategy of binding antibody fragments or peptides to albumin is meanwhile being extensively explored for the design of a new generation of albumin-binding antibodies and therapeutically active peptides. Three strategies can be distinguished: (i) bivalent antibodies that binds the desired antigen or peptide derivatives are constructed, which additionally comprise the heavy or light chains of antibodies as an albumin-binding domain; (ii) the fc region is substituted by albumin and two antigen-binding regions (Fab regions) are fused to albumin; (iii) an albumin-binding domain or peptide with high affinity in the nano to fentomolar range to albumin is bound to Fab regions, other antibody formats or therapeutic peptides (Elsadek and Kratz, 2012).

III.2.1.1 - Human serum albumin

Human serum albumin (HSA) provides colloidal osmotic pressure in plasma and buffering capacity in the blood, and serves as a transport and depot protein for numerous endogenous and exogenous compounds (Fanali *et al.*, 2012; Fasano *et al.*, 2005). The protein binding results in an increased solubility in plasma, decreased toxicity, and/or protection against oxidation or the bound compounds (Kragh-Hansen *et al.*, 2002). HSA (~ 600 µM, 585 aa, MW ~67.000) is the most abundant plasma protein, with a normal concentration of approximately 34–54 g/L and with an average plasma volume of 2.5-3.0 L for a 70 kg person, the average intravascular albumin mass is 113-126 g (~120 g). Human albumin is one of the few non-glycosylated plasma proteins and it is synthesized predominantly in the liver. Hepatocytes do not contain a large pool of stored intracellular albumin, rather the protein is rapidly secreted from the cell resulting in approximately 13-14 g of albumin entering the intravascular space every day, equivalent to 3.7%/day of the total albumin mass of 360 g for a 70 kg person (Sleep *et al.*, 2013). Human serum albumin is a α-helical protein monomer

composed of three structurally homologous domains (I, II, III), each being further divided into two subdomains (A, B), connected by random coil (Fig. 9). Albumin is a major carrier protein for a variety of small molecules such as ions, fatty acids, hormones, bilirubins, and drugs (Fasano *et al.*, 2005; Ghuman *et al.*, 2005; Sugio *et al.*, 1999). The modular structure organization of HSA provides a variety of ligand binding sites, illustrated in Fig. 9. Also, several sites with acyl chain binding activity have been identified in this molecule (Bhattacharya *et al.*, 2000). In humans, albumin has a half-life of approximately 19-20 days, while in mice the half-life is approximately 1.07-1.6 days and 1.9 days in rats (Schmidt *et al.*, 2013; Peters, 1996; Stevens *et al.*, 1992; Peters, 1985; Beeken *et al.*, 1962).

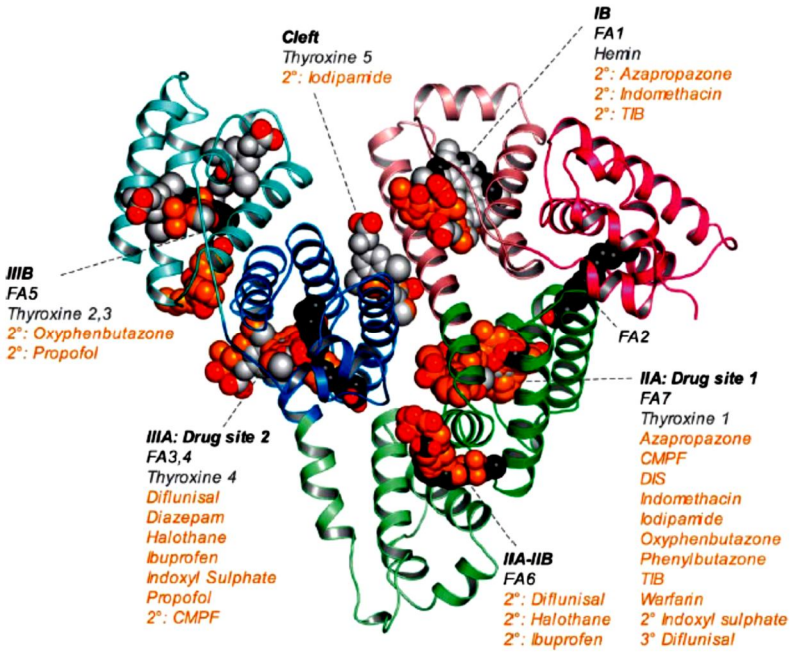

Fig. 9 - Summary of the ligand binding capacity of HSA as defined by crystallographic studies. Ligands are depicted in space-filling representation; oxygen atoms are coloured red; all other atoms in fatty acids (myristic acid), other endogenous ligands (hemin, thyroxin) and drugs are coloured dark-grey, light grey and orange, respectively (Ghuman *et al.*, 2005).

HSA abundance makes it an important factor in the pharmacokinetic behaviour of many drugs, affecting their efficacy and rate of delivery (Fasano *et al.*, 2005). Over the past decades, albumin has played an increased role as a drug carrier for therapeutic and diagnosis agents. Albumin also represents a valuable biomarker for several pathological conditions including cancer, rheumatoid arthritis, ischemia, post-menopausal obesity, severe acute graft-*versus*-host disease, and diseases that need monitoring of the glycemic control (Fanali *et al.*, 2012). The first evidence demonstrating that tumours are able to trap plasma proteins and use their degradation products for proliferation appeared in the middle of the 20th century (Babson and Winnick, 1954). The high HSA turnover in tumours has been explained by the fact that albumin represents the main energy and nutrition source for the tumour growth, with liver having an active metabolic role (Kratz, 2008). In the later stages of disease, malnutrition and inflammation supress HSA synthesis (Yeun and Kaysen, 1998; Ballmer *et al.*, 1994). The

reduced HSA concentration in blood seems to be due to the production of cytokines, such as interleukin-6, which modulate the production of HSA by hepatocytes (Barber *et al*., 1999). Alternatively, the tumour necrosis factor α may increase the permeability of the microvasculature, thus allowing an increased transcapillary passage of HSA. The presence of micrometastatic tumour cells in the liver may indicate that the Kupfer cells produce a variety of cytokines, which may modulate HSA synthesis by hepatocytes (McMillan et al., 2001; Barber *et al*., 1999). As a consequence there is a slight or no hypoalbuminemia in the early stages of cancer, but as the disease progresses HSA levels drop significantly, serving as a good indicator of cancer prognosis (Gupta and Lis, 2010; Sun *et al*., 2009; McMillan *et al*., 2001; Barber *et al*., 1999).

Patients with active rheumatoid arthritis frequently develop hypoalbuminemia, primarily by high HSA uptake at sites of inflammation (Kratz, 2008; Niwa *et al*., 1990; Ballantyne *et al*., 1971; Wilkinson *et al*., 1965). The metabolism of synovial cells is highly up-regulated, and the HSA uptake is probably a relevant source covering their high demand for nitrogen and energy. The permeability of the blood-joint barrier for HSA in rheumatoid arthritis patients is markedly increased (Kratz, 2008) Remarkably, using preclinical models it has been demonstrated that serum albumin accumulates in the arthritis paws of mice suffering from collagen-induced arthritis (Wunder *et al*., 2003). Since the anti-rheumatic drug methotrexate bound serum albumin has shown promising activity in the collagen-induced murine arthritis model, HSA may represent an attractive drug carrier to target drugs to inflamed joints of patients with rheumatoid arthritis (Kratz, 2008).

III.2.1.2 - Fusion to albumin

Direct fusion to the whole albumin has been applied to a variety of proteins, including interferons, interleukin 2 (IL-2), insulin, human growth hormone, and antibody fragments. Merrimack Pharmaceuticals, Inc. has developed an albumin fusion protein, using the scFv format for targeting HER2 and HER3. The bispecific format of MM-111 could be an optimal approach of inhibiting the enhancement of cell proliferation of HER3 in HER2-overexpressing tumours. This molecule entered clinical development for PhaseI/II in June 2009 and is currently in clinical trials with patients with tumours that over-express HER2 in a phase I study and restricted for breast cancer patients, in phase II (Elsadek and Kratz, 2012). Müller and co-workers generated bispecific anti-CD3 x anti-CEA antibody albumin fusion proteins by fusing either a bispecific single-chain diabody or a bispecific tandem scFv to the

N-terminus of HSA, or two different scFvs, one at the N-terminus and one at the C-terminus. All three constructs possessed a molecular mass of approximately 120 kDa, and showed similarly prolonged circulation after intravenous injection into mice, with terminal half-lives increased 4- to 5-fold compared with scDb and tandem scFv (taFv) molecules (MW ~55.000) and AUC_{24} values increased approximately 10-fold. However, differences were observed in the ability to activate peripheral blood mononuclear cells (PBMCs) in a target cell-dependent manner, where effector and targets have to come into close contact. Here the scDb-HSA fusion protein was superior to the taFv-HSA and the scFv-HSA-scFv fusion proteins, but was still less active than the parental scDb molecule (Müller *et al.*, 2007). Reduced bioactivity was also observed for other albumin fusion proteins, e.g. albuferon alpha, albuferon beta, and albuleukin, presumably caused by fusing the large albumin moiety to a comparably small therapeutic protein component. Nevertheless, these proteins displayed improved therapeutic efficacy, demonstrating that fusion of a therapeutic protein to albumin improves both pharmacokinetics and pharmacodynamics (Kontermann, 2009).

III.2.1.3 - Fusion to bacterial albumin-binding domains

Depending on the nature of the therapeutic protein, its fusion or coupling to serum albumin can complicate the manufacturing process, especially if the protein as such is produced recombinantly in, for example, *Escherichia coli*. Pre-clinical development can also be affected by the fact that human serum albumin does not always cross-react with the neonatal receptor of other species, murine FcRn, for example, binds very weakly to HSA (Andersen *et al.*, 2011).

As an alternative to direct fusion to albumin, several molecules have been exploited as albumin-binding moieties, employing reversible, non-covalent interaction with serum albumin. These albumin-binding moieties comprise small synthetic chemicals, peptides, antibodies or antibody fragments, as well as naturally occurring albumin-binding domains, and several reports show that binding derivates of albumin-binding domain from streptococcal protein G can be used to increase the plasma half-life of a fusion protein partner (Fig. 10) (Kontermann, 2009).

Pathogenic Gram-positive bacteria express cell wall-associated proteins that interact in several ways with the extracellular environment. These proteins are involved in host escape mechanisms of the bacteria, as virulence factors (Patti *et al.*, 1994) and might become useful as components in vaccines against these bacteria (Ji *et al.*, 1994; Mamo *et al.*, 1994).

Curiously, some of these bacterial proteins present binding to plasma proteins as albumin, IgG or fibrinogen. Examples of these surface proteins are the streptococcal surface proteins G (Sjöbring *et al.*, 1989) and G-related proteins MAG (Jonsson *et al.*, 1994), MIG and ZAG (Jonsson *et al.*[b], 1995), H (Ákesson *et al.*, 1994; Frick *et al.*, 1994; Nilsson *et al*, 2008) , M (M1, M5, M12) (Ákesson *et al.*, 1994; Sandin *et al.*, 2006; Retnoningrum and Cleary, 1994), PAB (de Château *et al.*, 1996; de Château and Björck, 1994) and FAI (Talay *et al.*, 1996). This section will be focused in the well-studied streptococcal albumin-binding domains (ABDs) from proteins G and PAB, and the ABDs from ZAG (and ZAG-related MIG and MAG proteins), and finally the albumin-binding domain from Protein H.

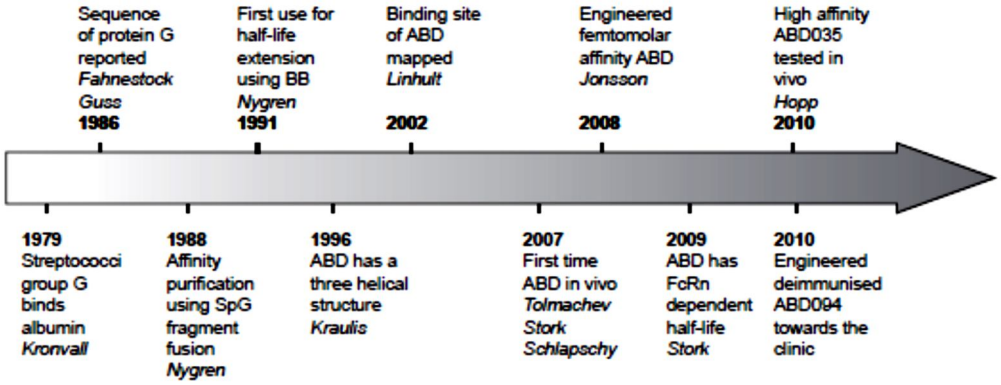

Fig. 10 - Historical outline of the development of using ABD for half-life extension (Frejd, 2012).

III.2.1.3.1 - Protein G

Many streptococcal strains are known to bind the most abundant plasma proteins, namely, immunoglobulin G and albumin. Based on the specific albumin binding activity expressed on the cell surface, Widebäck *et al.* grouped the streptococcal albumin receptors into five different types (**a-e**) (Widebäck *et al.*, 1983). The type **a** receptors are expressed on human group G strains, and the best studied bacterial albumin-binding domains are from protein G of strain G148. As shown in Fig. 11, protein G is a bi-functional receptor with different parts responsible for the IgG and albumin binding. More precisely, three Ig-binding domains and three serum albumin-binding domains (Sjölander *et al.*, 1997; Sjöbring *et al.*, 1991; Sjöbring *et al.*, 1988; Åkerström *et al.*, 1987; Björck *et al.*, 1987).

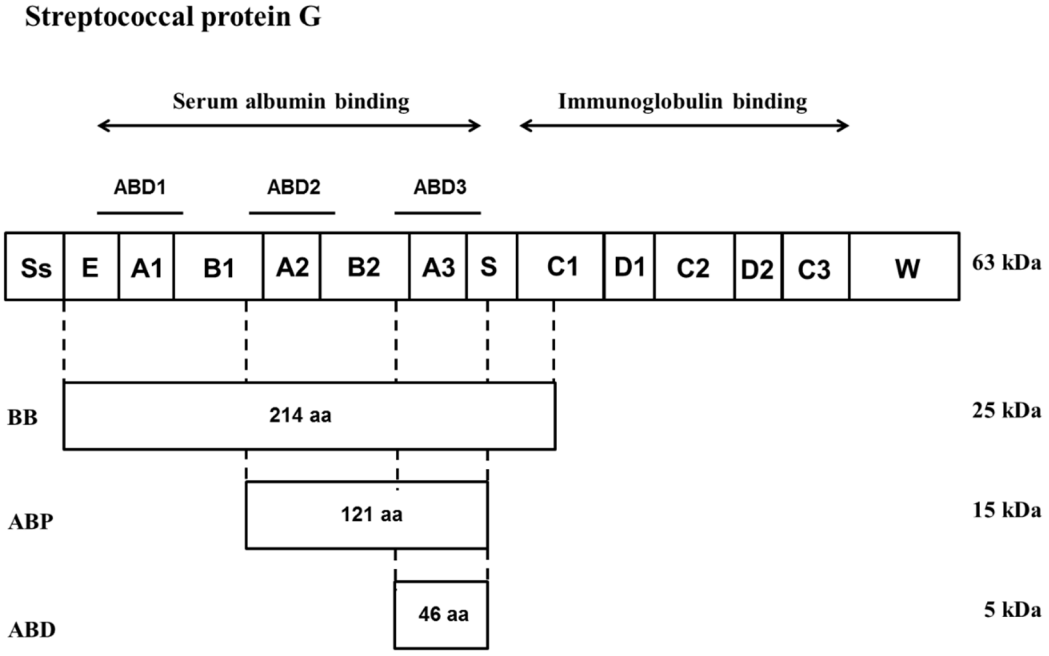

Fig. 11 - An overview of the streptococcal protein G (SpG). The IgG and albumin-binding parts are separated. Both parts consist of three homologous domains. Nomenclature according to Ståhl and Nygren (1999) (adapted from Linhult *et al.*, 2002).

Pioneering approaches from the 1990s included fusion to larger albumin binding fragments, BA or BABA (BB), derived from SpG (Fig. 11). In 1991, Nygren and co-workers reported on the use of BB to extend the half-life of a soluble form of CD4 (Nygren *et al.*, 1991). CD4 is an important component of the infection mechanism of HIV being a target receptor for the virus envelope protein gp120. By providing an excess of half-life extended CD4, the authors reasoned that the infectious action of viral gp120 would be diluted or even blocked. A fusion construct containing an N-terminal BB followed by two domains of the extracellular part of CD4 (E1 and E2) followed by a C-terminal BB region was produced and shown to bind recombinant gp120. In a kinetics study in mice, the BB-stabilized CD4 was compared with an IgG1 Fc-stabilized CD4 or CD4 or BB alone. It turned out that the half-life of the BB-stabilized protein or BB alone ($t_{1/2}$ 15-24h) was similar or slightly better than the Fc-stabilized counterpart, and much longer than CD4 alone. The long half-life of BB was confirmed in monkeys, where it had a half-life of 16 days. As the SpG derivates are of bacterial origin, Nygren and co-workers suggested the use of a much smaller but still albumin binding part of the receptor (<6 kDa, denoted ABD) to minimize potential recognition by the immune system (Nygren *et al.*, 1991). ABD was initially used as an affinity tag (Nilsson *et al.*, 1997), and later used as an affinity handle fused to antibody fragments such as Fv or Fab, to facilitate capture in a sandwich ELISA format (König and Skerra, 1998).

Nevertheless, protein G has the well-studied ABD used in fusion with therapeutic proteins for half-life extension and structural studies, including the resolution of its three-dimensional structure and mutagenesis studies to reveal residues involved in interaction with albumin from different species (Linhult *et al.*, 2002; Kraulis *et al.*, 1996). Protein G ABD is composed by 46 amino acid residues, forming a left-handed three-helix bundle. The domain on its own is chemically and thermally stable and it is independent from disulfide bonds, crosslinks, bound ligands or metal ions. An affinity of approximately 1–4nM for human serum albumin was determined by various methods. Residues involved in binding were localized mainly in helix 2 and 3 by mutational analysis and chemical shift perturbation (Johannson *et al.*, 2002; Linhult *et al.*, 2002).

Several *in vivo* studies, have demonstrated the applicability of fusion to the ABD from protein G to improve the plasma half-lives of small antibody molecules (e.g. Fab fragments, bispecific antibody derivatives) and various antibody mimetics. One application consisted of the fusion of the ABD to the C-terminus of the light chain of an anti-HER2 Fab increased the terminal half-life in mice from approximately 2 to 20.9 hours (Schlapschy *et al.*, 2007). Similar results were described for a single-chain diabody-ABD fusion protein (scDb-ABD), which extended the half-life from 5.6 hours to 27.6 hours after a single intravenous injection into mice (Nilsson and Tolmachev, 2007). Stork and colleagues extended the plasma of a single-chain diabody against carcinoembryonic antigen (CEA) and CD3 capable of retargeting T cells to CEA-expressing tumour various strategies were applied including PEGylation, N-glycosilation and fusion to an albumin-binding domain from streptococcal protein G. Furthermore, prolonged circulation time results were shown in an increased accumulation in CEA^+ tumours, which were most pronounced for scDb-ABD and PEGylated scDb. Interestingly, tumour accumulation of the scDb-ABD fusion protein was approximately 2-fold higher compared to PEGylated scDb, although both molecules exhibit similar plasma half-lives and similar affinities for CEA. Comparing half-lives in FcRn wild-type and FcRn heavy chain knockout mice, the contribution of FcRn to the long plasma half-life of scDb-ABD was confirmed, while no differences were observed for PEGylated scDb. Compared to scDb, a reduced cytotoxic activity was observed for scDb-ABD, which was further reduced in the presence of albumin (Stork *et al.*, 2009). The protein G ABD was also applied to prolong the half-life of Affibody molecules, derived from the Z domain of protein A (Tolmachev *et al.*, 2007) and to investigate the impact of a very high affinity binding to serum albumin, using an affinity maturated variant of ABD with femtomolar affinity binding to HSA (Jonsson *et al.*, 2008).

As illustrated in Fig. 12, at least 16 protein G-related albumin-binding (GA) modules or domains with relatively high sequence identity have been identified in six proteins and four bacterial species (Johansson *et al.*, 2002). The most well-conserved region in this sequences so far identified is the C-terminal part of the second helix and the flexible region between helices 2 and 3 (residues 32 to 39) (Johansson *et al*., 1997).

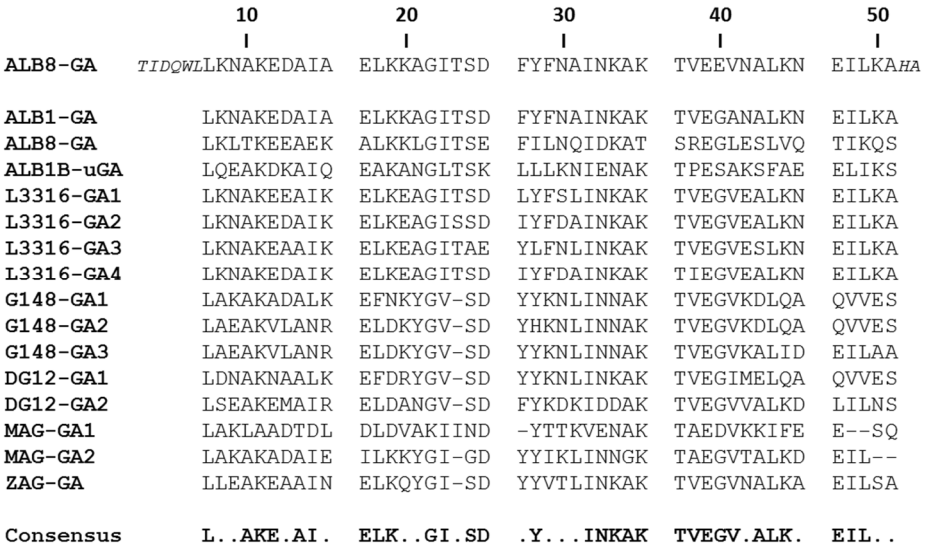

Fig. 12 – **Peptide sequence alignment of 16 different GA modules from six proteins and four bacterial species**. The consensus sequence is shown at the bottom. Conserved amino acids have been shaded. The GA module of protein PAB (de Château and Björck, 1994) under study in this work is at the top (ALB8-GA) followed by the second HSA-binding domain (ALB8-uGA) of protein PAB (de Château *et al*., 1996). The conserved, mobile, and folded sequence originally defined as the GA module comprises 45 amino acid residues, whereas the material studied here contains eight additional residues (in italics). Preparation of this 53 amino acid fragment (residues 213 to 265 of the intact protein), as well as preparation of NMR samples, has been described previously (de Château and Björck, 1994; Johansson *et al.*, 1995). ALB1-GA is from another isolated of *P. magnus* expressing protein PAB (de Château and Björck, 1994) and ALB1B- uGA is from protein urPAB (de Château and Björck, 1996). L3316-GA1-4 originate from a protein L-like molecule (Murphy *et al.*, 1994), G148-GA1-3 from streptococcal protein G (Guss *et al.*, 1986), DG12-GA1-2 a bovine *Streptococcus dysgalactiae* isolate (Sjöbring, 1992), MAG-GA1-2 from protein MAG of S. dysgalactiae (Jonsson *et al*., 1994) and finally, ZAG-GA from protein ZAG of *Streptococcus zooepidemicus* isolate (Jonsson *et al.*[b], 1995) (adapted from Johansson *et al.*, 1997).

III.2.1.3.2 - PAB streptococcal cell-surface protein

Protein PAB, a surface molecule from the anaerobic human commensal and pathogen *Peptostreptococcus magnus*, was found containing a domain of 45 amino acid residues showing high affinity for HSA. The sequence analysis of this domain revealed homologies both to the HSA-binding domain of protein G and to the framework regions of protein L, suggesting that this mosaic protein has emerged as the result of interspecies exchange of an

HSA-binding protein module (de Château and Björck, 1994, de Château *et al.*, 1996). This domain has been subject to module shuffling between bacterial species, and was subsequently named the GA module (de Château and Björck, 1994). Such shuffling of modules seems to be a persistent activity among this group of genes, and when a consensus sequence of 15 nucleotides (called "recer" sequence) flanking the different modules in the *P. magnus* family of surface proteins was identified, a model for the shuffling was proposed (de Château and Björck, 1996). Recer sequences were also identified in Ig-binding domains, and promote interdomain in frame recombination and act as structureless flexibility-promoting spacer sequences in the corresponding protein (de Château *et al.*, 1996). The albumin-binding protein G of group G streptococcal strain G148 carries three GA modules in the N-terminal part of the protein showing up to 60% identity to the shuffled module of protein PAB, indicating that protein G might be the source of the GA modules in protein PAB. Analysis of gene encoding protein PAB revealed that the HSA binding domain had been transferred from the protein G gene by action of a conjugational plasmid from a third bacterial species, *Enterococcus faecalis* (de Château *et al.*, 1996; de Château *et al.*, 1994). This protein contains two GA modules (Johansson *et al.*, 1997; de Château *et al.*, 1996), and nuclear magnetic resonance (NMR) and circular dichroism (CD) analyses to determine the stability, secondary structure, and global fold of this module, identify a three-helix-bundle structure with a left-handed folding topology (Johansson *et al.*, 1995). The X-ray structures at 2.7 Å resolution and in the presence of fatty acid at 2.5 Å resolution, shows how GA module forms a complex with HSA (Lejon *et al.*, 2004; Lejon *et al.*, 2008). The GA module binds to HSA at a site in domain II of the albumin molecule close to a cleft bounded by helices 2 and 3 in domain IIA, helices 7 and 8 in domain IIB, and the loop region before helix 7 in IIB (Fig. 13). In the GA module, residues from the second helix and the two loops surrounding it are involved in binding. The GA helices pack outside the cleft at an angle of ~60º against HSA helix 3 in domain IIA. Although this arrangement is almost identical to the orientation reported for the all α-helical

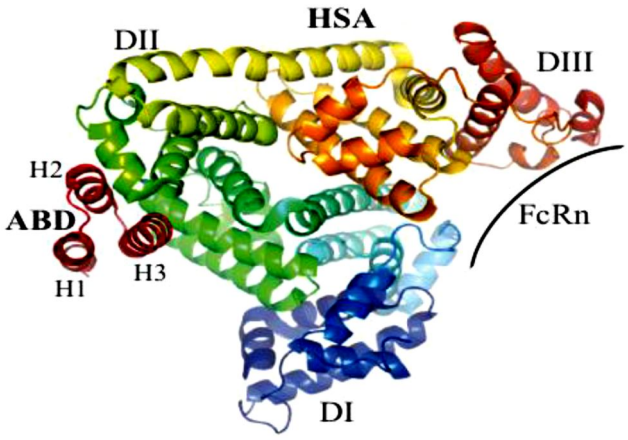

Fig. 13 - Structure of the complex formed by SpG ABD and HSA. The albumin-binding domains recognize a site located in domain II of HSA that does not overlap with the binding site for the FcRn, which plays an important role in albumin homeostasis. The picture was generated from PDB-file 1TF0 (Nilvebrant and Sober, 2013).

affibody-Z_{SpA} complex (Högbom *et al.*, 2003), the respective binding sites on the Z domain and the GA module do not overlap. The three-helix bundle Z domain of protein A and the GA module share a striking similarity in their overall structure. Even so, it is helix 1 of the Z domain that packs against the affibody helices, not the second and third as in the HSA-GA case (Lejon *et al.*, 2004). Residues Phe27, Tyr28 and Glu47 were confirmed as necessary residues for binding HSA and for conferring species specificity (Cramer *et al.*, 2007; Lejon *et al.*, 2004). The presence of fatty acid in the HSA-GA binding interface might influence complex formation. The binding of fatty acid causes the side chain of Lys212 to be pushed aside slightly into a position that allows it to form a hydrogen bond to GA (Lejon *et al.*, 2004; Lejon *et al.*, 2008). A previous study present the crystal structure at 1.4 Å resolution of GA module and compare it with crystal structure of the GA-albumin complex. The study of the interaction of this domain in various crystal forms indicates that no crystal would have been formed without making the relevant protein-protein interactions. The analysis of GA dimer interactions between chain A and chain B shows that there is one main interface involving 11 residues from chain A and another 11 different residues in chain B. Cramer and co-workers show more than one protein-binding surface on the GA in solution and that there are three residues (Trp5, Val38, Asn42) participating in protein-protein interactions on the dimer interface between GA module (Cramer *et al.*, 2007).

III.2.1.3.3 - MAG and MIG streptococcal cell-surface proteins

Jonsson and co-workers cloned and sequenced two genes encoding IgG-binding proteins from *Streptococcus dysgalactiae* strains isolated from cases of bovine mastitis. These proteins, called MIG and MAG, were highly homologous in their IgG-binding domains as well as to protein G from group G streptococci. Protein MIG contained five IgG-binding domains, while protein MAG only presents one such domain. Interestingly, both proteins MIG and MAG have one albumin-binding domain and also bound the proteinase-complexed form of the plasma proteinase inhibitor α_2-macroglobulin (α_2-M). These findings suggest that both proteins are tri-funtional with a similar structural organization (Jonsson *et al.*, 1994; Jonsson and Müller, 1994). The protein MAG, a plasma protein receptor from *S. dysgalactiae* strain 8215, has an albumin-binding domain (50 amino acids) in the center of the molecule with homology to the albumin-binding domains of protein G. The IgG binding domain located in the C-terminal part of the molecule shows high homology to streptococcal type III Fc receptor. The alpha 2 M-binding domain is located in the N terminus of the molecule and

is composed of a unique amino acid sequence (Jonsson *et al.*, 1994). In protein MAG the ABD is flanked by an upstream located region which binds α_2M and a downstream located region that binds IgG (Fig. 14). The albumin receptors of *S. dysgalactiea* belong to albumin receptors of type **c** and present a broader binding profile than protein G. This is reflected for example by the binding of type **c** receptors to serum albumins from cow, goat and sheep, which are not reactive with protein G (Falkenberg *et al.*, 1992).

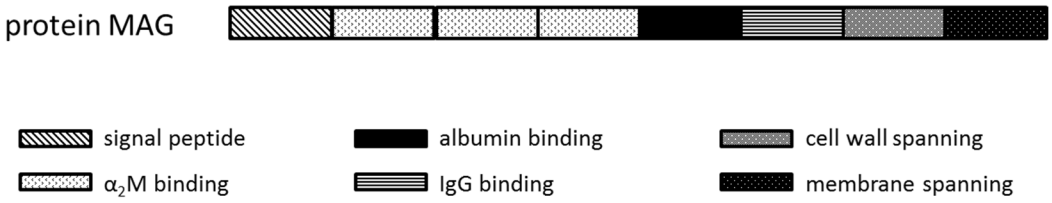

Fig. 14 - Schematic presentation of protein MAG. The different functional domains are indicated by boxes (adapted from Jonsson *et al.*, 1994)

III.2.1.3.4 - ZAG streptococcal cell-surface protein

Like other streptococcal species, *Streptococcus zooepidemicus* specifically binds through cell surface components, a number of host-derived proteins such as immunoglobulin G (IgG) (Myhre and Kronvall, 1980; Kronvall *et al.*, 1979), serum albumin (Widebäck *et al.*, 1983), fibronectin, collagen (Mamo *et al.*, 1987) and α_2-macroglobulin (α_2M) (Müller *et al.*, 1985). These host-parasite recognition components might be of importance as virulence factors by acting as adhesins, antiopsonins or host mimicry factors (Jonsson *et al.*, 1995).

The ability to bind IgG from several species and of different subclasses has led to the classification of bacterial IgG-binding proteins in six different Fc receptor types. According to this classification, the IgG receptors from *S. zooepidemicus* are distinct from the well-studied type I and type III Fc receptors, staphylococcal protein A and streptococcal protein G, respectively. The cloning and sequencing of the *zag* gene revealed that the protein ZAG from *S. zooepidemicus* Z5 has many similarities to the type III Fc receptors from group C and G streptococci. The IgG-binding domains from ZAG are homologous to the IgG-binding domains in protein G, as well to the corresponding domains in proteins MIG and MAG from *S. dysgalactiae* (Jonsson *et al.*, 1995).

Protein ZAG shows an albumin-binding profile similar to those of protein G (Nygren *et al.*, 1990; Nygren *et al.*, 1988) and the albumin-binding DG12 protein from a bovine group G streptococcus (Sjöbring, 1992). Protein ZAG and MAG also present what can be considered monomeric forms of the repetitive albumin-binding domains in protein G and DG12.

Alignment of the albumin-binding domain of ZAG with the corresponding domains of other streptococcal proteins also reveals a close evolutionary relationship. In the N-terminus, ZAG protein presents a 52 amino acid sequence ABD with binding to human, rat, mouse, horse and dog serum albumin. Downstream from this region there are two 70-amino-acid repeats homologous to the IgG-binding domains of type III Fc receptors (Fig. 15) (Jonsson *et al.*, 1995).

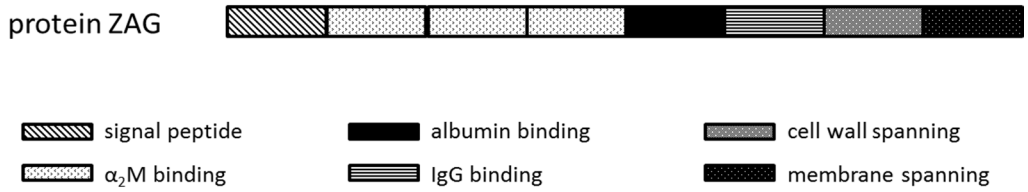

Fig. 15 - Schematic presentation of protein ZAG. The different functional domains are indicated by boxes (adapted from Jonsson *et al.*, 1995)

These proteins also found to interact with the plasma proteinase inhibitor α_2M through a unique amino acid sequence that competes for the same or nearby binding site(s), as do proteins MIG and MAG (Jonsson *et al.*, 1995). Pairwise amino acid sequence alignment of various functional domains of proteins MIG, MAG, ZAG and protein G shows a high homology in the signal sequence, followed by a region of low homology, representing the α_2M-binding domains in proteins MIG, MAG and ZAG and by the functionally undefined region E in protein G (Jonsson *et al.*, 1995; Olsson *et al.*, 1990). The importance of proteins MIG, MAG and ZAG in infection and host defense is not known, but Valentin-Weigand and colleagues (Valentin-Weigand *et al.*, 1995) have published interesting data showing that the binding of the proteinase-complexed α_2M to animal group C streptococci inhibits phagocytosis *in vitro*. This finding indicates that this type of proteins have functional similarities to the streptococcal M proteins (Jonsson *et al.*, 1995).

III.2.1.3.5 - Protein H

Protein H, is a multidomain protein present on the cell surface of some strains of *Streptococcus pyogenes* (Frick *et al.*, 1994). This protein is identified in clinical isolates of the M1 serotype (Podbielski *et al.*, 1993) and has affinity for the constant (IgGFc) region of immunoglobulin (Ig) G and serum albumin (Åkesson *et al.*, 1990; Frick *et al.*, 1994). The M protein family comprises a large group of surface proteins in *S. pyogenes*, which contribute to the potential pathogenicity of these clinically significant bacteria. This family includes the M proteins and proteins with affinity for IgG and/or IgA (Fischetti, 1989), and can be divided

into two major classes, A and C, according to the type of repeat found (O'Toole *et al.*, 1992). M proteins are regarded as major virulence determinants due to their anti-phagocytic properties, whereas the role for IgG Fc-binding bacterial proteins in pathogenicity and virulence remains unclear (Frick *et al.*, 1995). The protein H, like protein G (Björck *et al.*, 1987) and other streptococcal surface proteins, presents different binding sites for albumin and immunoglobulin G (Fig. 16). Protein H albumin-binding domain (ProtH) is closer to the bacterial cell wall and IgG-binding further towards the N-terminal. No homology was detected when the IgGFc-binding repeats where compared with the same regions of protein G, but the albumin-binding regions of protein G and H were shown to have evolved convergently. The albumin-binding region was mapped to three repeats (C1-C3) in the C-terminal half of protein H (Frick *et al.*, 1994). The C repeats are quite similar in various M proteins, and the protein H albumin-binding repeats have a high homology with the C repeats of protein M1, and also present a similarity of 94-95% among the three repeats (Åkensson *et al.*, 1994). In the C-terminal of protein H was also identified a D domain which attaches protein H to the bacterial cell wall. The D domain has a hydrophobic transmembrane region and contributes to the three-dimensional structure of the albumin-binding C-repeats rather than being directly involved in the interaction with albumin (Frick *et al.*, 1994). In protein G, albumin-binding is in the N-terminal half and IgGFc binding in the C-terminus of the molecule (Åkerström *et al.*, 1987). Competitive binding experiments demonstrated that protein G and H bound to the same or closely located sites in albumin, which has previously been mapped for protein G to disulfide loops 6-8 (Falkenberg *et al.*, 1992).

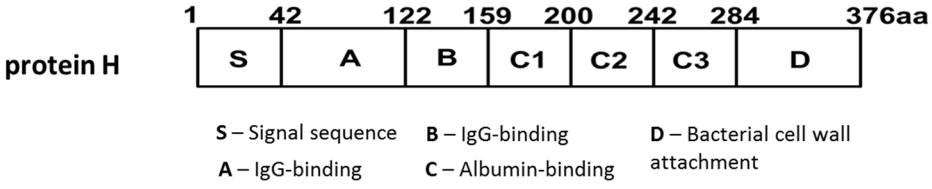

Fig. 16 - Schematic presentation of protein H. The different functional domains are indicated by boxes (adapted from Frick *et al.*, 1994)

S. pyogenes is an exclusive human pathogen that can cause a variety of complications ranging from mild and superficial infections, such as pharyngitis and impetigo, to invasive and life-threatening conditions, including necrotizing fasciitis and streptococcal toxic shock syndrome (Cunningham, 2000). Serious sequelae following *S. pyogenes* infections are rheumatic fever and glomerulonephritis. In order to survive in human blood, *S. pyogenes* has

evolved a number of defense mechanisms, that including anti-phagocytic M and M-like proteins, and some serotypes secrete a protein (protein SIC) that binds to and inactivates many antibacterial peptides (Frick *et al.*, 2003). For instance, protein H and M1 protein released from the bacterial cell wall by polymorphonuclear neutrophils-derived proteases, bind beta-2 glycoprotein I (β_2GPI), a human heparin binding plasma protein with antibacterial activities, and inhibit the activity of β_2GPI-derived antibacterial-peptides, as an immune defense system mechanism (Nilsson *et al.*, 2008). Therefore, Protein H was shown to inhibit complement activation at the bacterial surface, suggesting that Ig-binding could contribute to resistance to phagocytosis, and is possible that the release of complement-activating IgG-protein H complexes from the bacterial surface could be involve in the development of severe complications associated with *S. pyogenes* infections (Berge *et al.*, 1997; Kihlberg *et al.*, 1999). Frick and colleagues proposed a role for protein H in the dissemination of streptococci from their initial site of colonization, through the formation of virulent aggregates, suggesting that induction of expression may be important in establishing an invasive infection (Frick *et al.*, 2000). Furthermore, another study suggests that the expression of surface virulence factors like protein H, M and M-related proteins may not be essential for the invasion but are important for the survival once the organism disseminate and colonize organs (Smith *et al.*, 2003). These findings may provide a partial explanation of the continued emergence of virulent *S. pyogenes* isolates, but the role of protein H as a virulence factor in response to biological pressures in an infected host still needs further investigation.

III.2.1.4 - Fusion to albumin-binding peptides

Albumin-binding peptides (ABP) represent an alternative to the use of bacterial ABDs, having the advantage of being smaller in size. Dennis and co-workers at Genentech, Inc. published pioneering work on the attachment of albumin-binding single-chain antibodies in which they discovered a peptide comprising 18 amino acids (Ac-RLIEDICLPRWGCLWEDD-NH_2) with high binding affinity for human serum albumin (K_D ~0.5 µM). A related sequence (QRLMEDICLPRWGCLWEDDF) comprising 20 amino acids was then fused with a single-chain antibody D3H44 Fab directed against the tissue factor and showed a similar affinity for HSA, and when injected in mice or rabbits, extended the plasma half-life 26-fold to 10.4 h and 37-fold to 34.2 h in rabbits, which corresponds to 25-43% of the half-life in these animals (Dennis *et al.*, 2002). As a consequence, the same authors performed a study comparing the tumour uptake, tumour penetration as well as biodistribution

of Herceptin® (trastuzumab), of a Fab4D5 directed against HER2 and of Ab.Fab4D5 that additionally had the ABP. Their results showed that unlike Fab4D5, AB.Fab4D5 did not accumulate in kidneys, suggesting that association with albumin leads to an altered route of clearance and metabolism, and both Fab and ABP fusion molecule showed deep tumor penetration, that was more pronounced for the albumin-binding conjugate, due to the much smaller size of these molecules (Dennis *et al.*, 2007).

III.2.1.5 - Fusion to albumin-binding antibody fragments and other strategies

Complexation with albumin can also be achieved through the use of bispecific antibody molecules binding with one arm to the target antigen and with the other arm to albumin. For example, the pharmacokinetics of nanobodies, which are derived from variable domains (VHH) of camelid heavy chain antibodies, were improved by fusion with an anti-albumin nanobody. VHH-based Ablynx technology for treatment of rheumatoid arthritis and cancer is described in Section V.

A similar strategy was applied to dAbs, which are derived from human V_H and V_L domains with a size of only 11–13 kDa (Holt *et al.*, 2003). Domantis Ltd (acquired in 2007 by GlaxoSmithKline) has developed a further strategy of binding biological molecules such as peptides, cytokines or receptors to albumin, using albumin fragments high affinity for albumin. Albumin-binding dAbs were selected using phage display from large synthetic dAb libraries. One of these molecules (dAbm16), which binds to mouse serum albumin (MSA), showed a 51-fold increase in the terminal half-life (from 42 minutes for a control dAb to 24 hours) in mice. Similar improvements were observed for dAbs binding to rat serum albumin (RSA): a high-affinity binding dAb (13 nM) had the same half-life in rats as RSA (53 hours), while a low-affinity binder (1 mM) exhibited a reduced half-life of 43 hours, demonstrating a correlation between the strength of albumin binding and the half-life. The anti-MSA dAbm16 was further used as a fusion partner for the human form of IL-1 receptor antagonist (IL-1ra), a potent inhibitor of Il-1 signalling approved for the treatment of rheumatoid arthritis. The half-life of the fusion protein was 4.3 hours, compared with 2 minutes for IL-1ra. The fact that the fusion protein is much more rapidly cleared than dAbm16 alone indicates that additional mechanisms contribute to clearance of the fusion protein. In a collagen-induced arthritis model, improved efficacy was observed for the dAbm16-IL-1ra fusion protein compared with IL-1ra, demonstrating that improved pharmacokinetics translates into improved pharmacodynamics (Holt *et al.*, 2008). In a more recent application, Walker and co-workers

fused an albumin-binding dAb (DOM7 h-14) to Interferon-α2b (IFN-α2b) and compared its pharmacokinetics and efficacy to IFN-α2b alone and Albinterferon-α2b (HSA-IFN-α2b). This comparison is of special interest because Novartis have discontinued the regulatory approval of Albinterferon-α2b. IFN-α2b-DOM7 h-14 showed a longer half-life than HSA-IFN-α2b in rats (22.6 h vs. 14.2h). More importantly, the antiviral activity of the albumin-binding IFN-α2b-DOM7 h-14 was approximately 6-fold greater than HSA-IFN-α2b in a molar comparison and the superiority of IFN-α2b-DOM7 h-14 over HSA-IFN-α2b was confirmed *in vivo* in a human melanoma xenograft model (Walker *et al*., 2010).

Recently, a novel class of albumin-binding derivatives were isolated using DNA-encoded chemical libraries, capable of forming kinetically stable complexes with both HSA and MSA, with promising results for half-life extension of small molecules. Dumelin and co-workers used 428-d-Lys as a portable albumin binder that shown to improve the *in vivo* circulatory time of agents of pharmaceutical interest by more than 100-fold. 428-d Lys derivatives of fluorescein and of metal ion–DTPA (diethylene triamine pentaacetic acid) complexes exhibited promising *in vivo* properties and are likely to represent superior blood-pool contrast agents for clinical applications by increasing the measurement time, reducing the extravasation, and thereby increasing the contrast (Dumelin *et al.*, 2008).

The Albumod™ technology is an example of Affibody® technology that makes use of the high affinity of ABDs for HSA and extends the half-life of conjugated biopharmaceuticals. As a consequence, the resulting albumin drug complex essentially acquires pharmacokinetic properties similar to endogenous albumin and bound cytokines, single-chain antibodies or drugs containing the ABD have a significant increased plasma half-life. As an example, Affibody bound the granulocyte colony-stimulating factor (G-CSF), a peptide growth factor that stimulates the bone marrow to produce granulocytes and stem cells, to their ABD. The conjugate of G-CSF and ABD forms a stable complex with albumin and increased the plasma half-life by a factor of 10, compared to G-CSF alone, in rats. Recently, the company Algeta exclusively licensed two Albumod™ antibodies labelled with the alpha particle emitter thorium-227 for therapeutic targeting HER2 or PDGFRβ expressing tumors (Elsadek and Kratz, 2012).

A recent interesting development of ABD is to add a new binding specificity to the ABD-molecules while retaining the native albumin binding capacity. Based on their previous mutational analysis of the albumin binding epitope of ABD (Linhult *et al*., 2002), Hober and colleagues randomized 11 amino acid residues that should not interfere with albumin binding (Alm *et al*., 2010). AS scaffold, an in house ABD* that was stabilized to withstand alkaline

conditions by replacement of four asparagines in the structure (Gülich *et al.*, 2000) was chosen. The library was displayed on bacteriophage and subjected to selections. The initial aim was to isolate a dual affinity purification handle for fusion proteins, and the protein A derivate, domain Z was chosen as target. Initial binders were characterized and a lead binder could be successfully affinity-purified both on HSA sepharose and from crude lysate on the commercially available MabSelect Sure matrix containing a modified domain Z and used for purification of monoclonal antibodies (Alm *et al.*, 2010). Next, the group investigated the approach for creating dual ABD binders intended for therapeutic applications. Using the same library, binders were selected against human TNFα (Nilvebrant *et al.*, 2011). First generation binders were identified, but although several were bispecific, a relatively high affinity for TNFα seemed to limit the affinity for albumin and vice-versa. Thus, a new affinity maturation library was designed and a bacterial-based cell display system was used for isolation of improved binders. As cell display enables the use of fluorescence-activated cell sorting (FACS), selections could be performed against both targets simultaneously by labelling TNFα and HSA with different fluorophores and indeed, bispecific binders with high affinity against both target could now be isolated. Therefore, ABD can be used not only as a fusion domain for extending the plasma half-life of proteins, but can also be used as a target-binding domain itself, with intrinsic long half-life.

III.2.2 – Fusion to Ig-binding domains

Besides the several IgBDs mentioned before in streptococcal cell surface proteins with albumin-binding domains (see section III.2.1.3), the most well-studied IgBD from *Staphylococcus aureus* protein A (SpA), was applied as a scaffold to create the Affibody® molecules (see section II.2) (Tolmachev *et al.*, 2007).

Non-covalent interaction with serum IgG might represents a feasible alternative to binding serum albumin, as a strategy to extend half-life of therapeutic proteins. IgBDs have a length of 50-60 amino-acid residues and form either a three-α-helix bundle or a compact structure composed of a four-stranded β-sheet and one-α-helix (Tashiro and Montelione, 1995). The primary binding site on IgG is located at the C_H2-C_H3 interface of the heavy chain (Deisenhofer, 1981). Though, most of the bacterial IgDBs from proteins A, G and L are also capable of binding to different regions of the Fab fragment (Tashiro and Montelione, 1995). In a recent study, the domain B of SpA was fused with the C-terminus of a single-chain diabody (scDbCEACD3) to extend the circulation time of the recombinant antibody. The

fusion protein retained full antigen-binding activity and was capable to simultaneously bind to IgG. The result was a prolonged half-life (11.8 h) compared with the unmodified scDb (1.3 h), although it did not reach the half-life seen for IgG, which might be due to competition for binding to FcRn (Unverdorben *et al.*, 2012). Recently, an extended serum half-life was also shown for a fusion protein (ZZ-PE38) comprising two Z domains and a *Pseudomonas* exotoxin A (ETA) fragment (Mazor *et al.*, 2007). This fusion protein was used to produce a large IgG-toxin immunoconjugate by complexation with a chimeric anti-HER2 monoclonal antibody *in vitro*. After i.v. injection into mice, the half-life was extended to 4 h for the antibody-ZZ-PE38 complex, compared with 18 min for an scFv-ETA molecule. Another study from Kontermann and colleagues compare the half-lives the same antibody fragment (scDBCEACD3) and a scFv, both fused with various IgBDs from SpA, SpG and *Finelgoldia* (formely *Peptostreptococcus*) protein L (PpL). Thus, binding to V_H domains belonging to the V_H3 family was shown for the domain D of SpA, and this site is structurally distinguished from its Fc binding site (Graille *et al.*, 2000). Domain C4 from PpL is capable of binding to certain subgroups of Vκ light chain domains (Graille *et al.*, 2002; Åkerström and Björck, 1989) and domain C3 of SpG has been shown to bind also to the C_H1 domain of IgG molecules (Derrick and Wigley, 1994). Their results demonstrate that the half-lives in mice are prolonged to various extents depending on the applied IgDBs. The longest terminal half-lives were seen for the fusion proteins containing the C3 of SpG (scDB-SpG_{C3} $t_{1/2}$ = 23.3 h and scFv-C3 $t_{1/2}$ = 20.8 h) and domains B (scDB-SpA_B $t_{1/2}$ = 11.8 h and scFv-SpA_B = 4.4 h) and D (scDB-SpA_D $t_{1/2}$ = 9.0 h and scFv-SpA_D = 4.9 h) of SpA (Hutt *et al.*, 2011). These findings make these domains, especially the SpG_{C3}, promising modules for half-life extension of small-sized therapeutics.

IV - Anti-TNFα VHH as study model

The application of albumin-binding antibodies has already reached clinical phase II studies for the treatment of rheumatoid arthritis (Elsadek and Kratz, 2012). The company Ablynx has developed a unique technique in which so-called camelid antibodies, targeting important acute and chronic diseases across a broad range of therapeutic areas including haematology, neurology, inflammation, pulmonary diseases and oncology.

In this project we used a single-domain antibody (VHH) against rheumatoid arthritis from Ablynx (Silence *et al.* Patent US2007/0077249 A1), as a proof of concept, to validate the efficacy of two albumin-binding domains from cell surface proteins ZAG (Zag ABD) and

protein H (ProtH ABD) in the improvement of the pharmacokinetic properties of small therapeutic proteins.

IV.1 - Rheumatoid arthritis

Rheumatoid arthritis (RA) name was introduced in the 1850s, but classification criteria were only developed in 1956 (Ropes *et al*., 1959; Storey *et al*., 1994; Arnett *et al*., 1988). RA is one of the most frequent chronic inflammatory joint diseases as it affects about 0.5-1% of the world's population. It is characterized by joint pain, swelling and stiffness due to joint inflammation and damage, causes disability and lost working capacity, and may cause premature death (Caporali *et al*., 2009). Before the advent of biological drugs, RA was treated with non-steroidal anti-inflammatory drugs (NSAIDs), corticosteroids and disease-modifying anti-rheumatic drugs (DMARDs), which methotrexate (MTX) is currently the most widely used, alone or in combination with other DMARDs. Other frequently used DMARDs include sulphasalazine, hydroxychloroquine and leflunomide (O'Dell, 2004; Atzeni *et al*., 2013).

RA has emerged as a prototypic immune-mediated inflammatory disease and is common focus of clinical studies of tumour necrosis factor antagonists. This is a chronic disease in which inflammation of the synovial tissue results in articular cartilage and bone destruction. Parallel advances in research on the pathogenesis of RA and cytokine biology converged on TNFα and interleukin-1 as key factors in inflammation and matrix destruction (Arend and Dayer, 1990; Saxne *et al*., 1988). The concept arose that elevated concentrations of TNFα at the sites of inflammation were driving disease pathology, and the removal of excess TNFα from sites of inflammation became a therapeutic goal (Knight *et al*., 1993; Brennan *et al*., 1989). TNFα plays a role in lymphoid tissue development and have a homeostatic role in host defense against some bacterial infections and initiates the defense response to local injury. At low concentrations in tissues, is thought that TNFα has beneficial effects, such as the augmentation of host defense mechanisms against infections. At high concentrations, TNFα can lead to excess inflammation and organ injury (Tracey *et al*., 2008).

TNFα biology presents a network of ligands, receptors and signaling pathways with several layers of complexity. Many immune and non-immune cells types can produce TNFα including macrophages, T cells, mast cells, granulocytes, natural killer (NK) cells, fibroblasts, neurons, keratinocytes and smooth muscle cells. First, TNFα is released from cells as a soluble cytokine (sTNF, a homotrimer of 17 kDa monomers) after being enzymatically cleaved from its cell-surface-bound precursor (tmTNF, a homotrimer of 26 kDa monomers)

by TNFα-converting enzyme (TACE). TNFα acts via two distinct receptors – TNF receptor 1 (TNFR1) (p55, CD120a) and TNFR2 (p75, CD120b) – on a wide variety of cell types to mediate their biologic functions. Although, its affinity for TNFR2 is five times higher than its affinity for TNFR1. Both TNFR1 and TNFR2 are membrane glycoproteins that specifically bind TNFα and lymphotoxin α3 (LTα3), but they differ in their cellular expression profiles, affinities for ligands, cytoplasmic tail structures and signaling mechanisms. TNFR1 is constitutively expressed on virtually all cell types except erythrocytes, whereas TNFR2 is generally inducible and is preferentially expressed on endothelial and hematopoietic cells (Atzeni *et al*., 2013; Tracey *et al*., 2008).

The biology of TNFα has been extensively studied, particularly with regard to its many activities when expressed at high concentrations in the context of inflammation and disease. TNFα is a pleiotropic cytokine, in that it mediates a wide variety of biologic activities. Some activities of TNFα are common to several diseases, such as those that modulate cell recruitment, cell proliferation, cell death and immune regulation (Schottelius *et al*., 2004; Feldmann, 2002). Other biologic activities of TNFα may be restricted to certain diseases, such as matrix degradation and osteoclastogenesis in RA or granuloma formation in Crohn's disease. TNFα also plays an important role in the regulation of a cascade of pathogenic events in psoriasis and other diseases, exemplified by the rapid induction of cytokines, such as IL-1 and IL-6, and the induction of acute-phase proteins, such as C-reactive protein (CRP) (Feldmann, 2002).

In patients with RA, the synovial membrane lining the joint space becomes inflamed as a consequence of increased vascularity and influx of inflammatory cells. Similar histopathology is seen in murine collagen-induced arthritis, for which TNFα was observed within the intimal lining layer and synovial sublining at all stages of disease (Mussener *et al*., 1997). The staining of TNFα was particularly intense at the invasive front, the cartilage-pannus junction (Choy and Panayi, 2001). The hypothesis that TNFα drives much of the pathophysiology in a rheumatoid joint is supported by studies of TNFα overexpression or TNFα neutralization in animal models of RA (Klareskog and McDevitt, 1999; Butler *et al*., 1997). Many of the TNFα neutralization studies in mouse models of RA demonstrated amelioration of clinical disease similar to that seen in studies of TNFα antagonists in patients with RA, showing apparent differences in the impact on bone erosion. For instance, TNFα blockade in human TNFα-transgenic mice suppressed joint destruction more than synovial inflammation (Zwerina *et al*., 2004). Other studies of TNFα blockade in rat models of arthritis have also demonstrated significant suppression of cartilage and bone erosion (Bendele *et al*., 2000).

Understanding the role of TNFα in the pathogenesis of RA has been important to the development of drugs capable of controlling its clinical signs and symptoms, and halting its radiographic progression. Today, there are 5 registered TNF blockers in the United States and the European Union: Enebrel® (etanercept), Remicade® (infliximab), Humira® (adalimumab), Simponi® (golimumab) and Cimzia® (certolizumab) (www.fda.gov; www.ema.europa.eu). Pathophysiological role of cytokines and other mediators, and their inhibitors are illustrated in Fig. 17, that also describe the mechanism of TNF inhibition of etanercept, infliximab and adalimumab. All agents except etanercept are anti-TNF mAbs or fragments thereof. Infliximab, adalimumab and golimumab are full-length bivalent IgG mAbs, whereas certolizumab is a monovalent Fab antibody fragment covalently linked to polyethylene glycol. Infliximab is a chimeric protein containing ~25% mouse-derived amino acids comprising the V_H and V_L domains and ~75% human-derived amino acids comprising the C_H1 and Fc constant regions. Certolizumab is a humanized protein containing amino acid sequences in the CDR regions derived from a mouse anti-TNF mAb and inserted into human

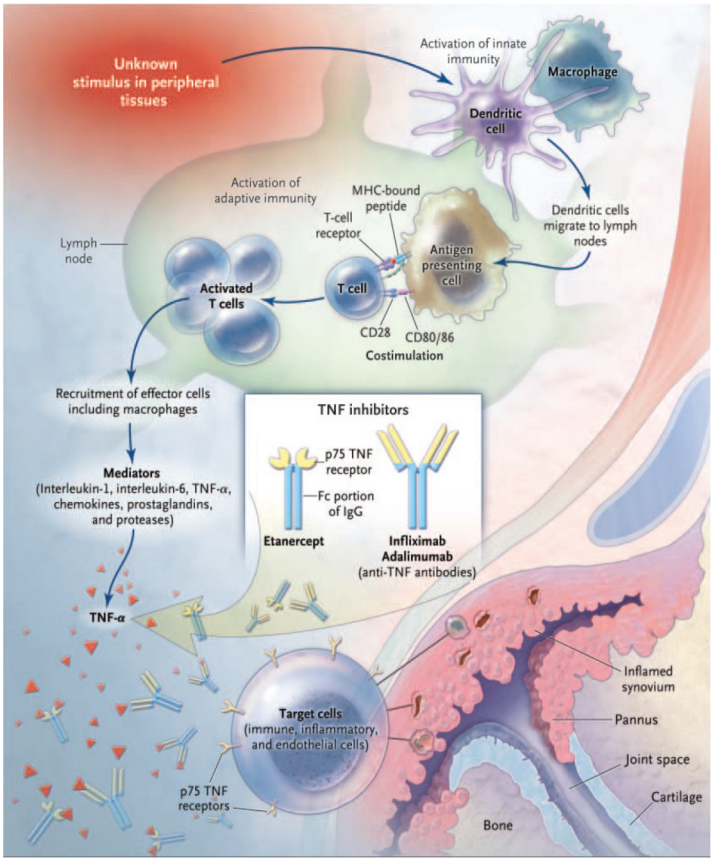

Fig. 17 - Pathophysiological role of cytokines, other mediators and their inhibitors in RA. In the current model of the pathogenesis of RA, an infective agent or other stimulus binds to receptors on dendritic cells, activating the innate immune system. Dendritic cells migrate into lymph nodes, presenting antigen to T cells, which are activated by the dual signal of antigen presentation and costimulation through CD28. Activated T cells proliferate and migrate into the joint. In the synovial tissue, T cells produce interferon-γ and other proinflammatory cytokines that stimulate macrophages and fibroblasts as well as chondrocytes, osteoclasts, and B cells. Activated macrophages and fibroblasts release a variety of cytokines, including TNFα. TNFα is a central component in the cascade of cytokines, stimulating the production of additional inflammatory mediators and the further recruitment of immune and inflammatory cells into the joint. Infliximab and adalimumab are monoclonal anti-TNFα antibodies that bind to TNFα with high affinity and prevent it from binding to its receptors. Etanercept is a fusion protein consisting of two p75 TNF receptors that are linked to the Fc portion of human IgG1. It also binds to TNF-α and prevents it from interacting with its receptors on cell surfaces (Scott *et al.*, 2006).

V_H and V_L domains frameworks. Adalimumab and golimumab are fully human mAbs. The TNFα-antagonist mAbs also differ in their IgG isotypes, the Fc regions of which govern effector functions, like complement fixation and Fc receptor-mediated biologic activities. Infliximab, adalimumab and golimumab are IgG1 antibodies, which are capable of complement fixation and Fc-receptor binding. Certolizumab is a Fab fragment of an IgG1 mAb and lacks effector functions because it has no Fc region. The hinge of certolizumab is modified and covalently linked to two crosslinked chains of a 20 kDa PEG to enhance solubility and half-life *in vivo* (Tracey *et al.*, 2008; Weir *et al.*, 2006).

Tumour necrosis factor inhibitors and other biological agents have heralded a so-called therapeutic revolution, transforming the outlook for patients with rheumatoid arthritis (Scott *et al.*, 2010).

IV.2 - Ablynx VHH technology for treating rheumatoid arthritis and cancer

Ablynx camelid antibodies comprise heavy-chain antibody fragments containing a single variable domain (VHH) and two constant domains (C_H2 and C_H3). The VHH domains combine high target specificity and affinity for their antigen target with low viscosity as compared to single-chain antibodies and ease of manufacturing in humanized variants in camels and llamas or meanwhile in eukaryocytes such as bacteria or yeasts (Muyldermans, 2013; Freken *et al.*, 2000; Freken *et al.*, 1998), forming the basis of a new generation of therapeutic antibodies which Ablynx has named nanobodies.

Using such camelid antibodies, murine trivalent antibodies were constructed with one molecule that bind human serum albumin and the other, two molecules target murine or human TNFα (Coppieters *et al.*, 2006). In a collagen-induced arthritis model, a trivalent bispecific antibody MT1-MT1-AR1 (MT1 = anti-mouse TNFα nanobody, AR1 = albumin-binding nanobody) demonstrated a convincing proof of concept (Fig. 18), and its efficacy exceeded that of the clinically used anti-TNFα antibody Enebrel® (Coppieters *et al.*, 2006). Additionally, the binding affinity of the MT1-MT1-AR1 for albumin significantly prolonged its serum half-life and promoted its targeting to inflamed joints, as evaluated by ^{99m}Tc labeling and camera imaging, in comparison to the bivalent anti-TNFα nanobody MT1-MT1 (Fig. 18b). Since albumin is known to accumulate in the inflamed joints in the collagen-induced arthritis (Wunder *et al.*, 2003) as well as the clinically used Nanocoll®, an albumin ^{99m}Tc-labeled microparticle, this very likely explains the excellent therapeutic efficacy observed *in vivo* (Elsadek and Kratz, 2012). In parallel development, Ablynx had developed

an analogous trivalent antibody TR2-TR2-AR1 (MW ~45 kDa) that was directed against human TNFα. This trivalent molecule, named ATN-103, was developed for clinical evaluation, and in phase I studies showed good tolerability. Subsequently, AT-103 (now named Ozoralizumab) was licensed to Pfizer who have completed the recruitment of two phase II studies in 48 patients in Japan and the USA, with subcutaneous administration of Ozoralizumab every 4 weeks for 16 weeks in patients with rheumatoid arthritis, and have an open label extension of phase II study in 260 patients with rheumatoid arthritis ongoing to ensure long term safety of the novel albumin-binding nanobody (Kratz and Elsadek, 2012).

Ozorolizumab addressed an extremely large market (US$ 16.9 billion for all TNFα inhibitors in 2008) and could have substantial advantages over three conventional and only partially humanized antibodies Remicade®, Enebrel® and Humira®, due to ease of manufacturing and reduced cost. This molecule also presents a better efficacy due to an albumin-mediated targeting to inflamed joints and a reduction of side effects compared to the currently approved antibodies. That can include serious and sometimes fatal blood disorders, serious infections, lymphoma and solid tissue cancers, reports of serious liver injury, reactivation of hepatitis B, reactivation of tuberculosis, drug-induced lupus, and demyelinating central nervous system disorders (Elsadek and Kratz, 2012).

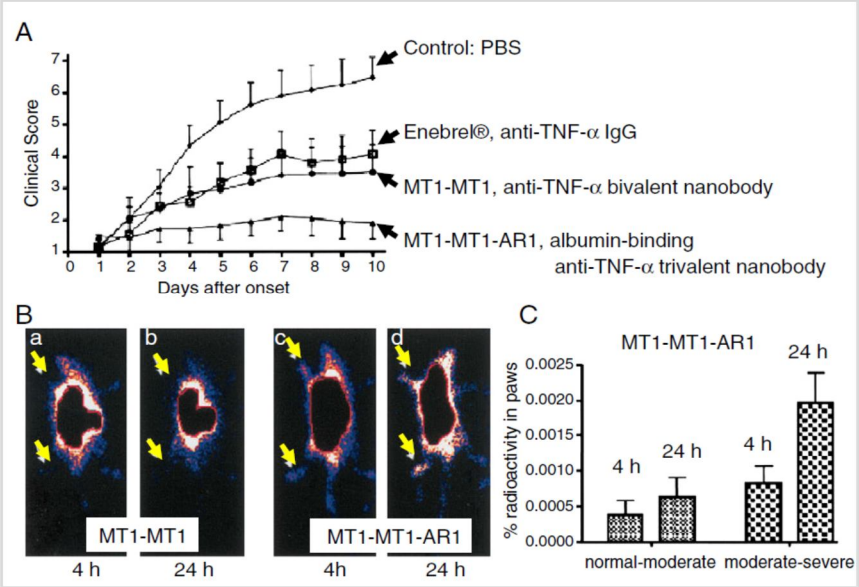

Fig. 18 - Therapeutic effects of Enebrel® (100 μg), the anti-TNF-α bivalent antibody MT1-MT1 (100 μg) and the anti-TNF-α trivalent antibody MT1-MT1-AR1 (100 μg) containing the albumin-binding domain AR1 in the collagen-induced arthritis model (9 mice per group). BOTTOM: Scintigraphic images comparing 99mTc-labeled MT1-MT1 and MT1-MT1-AR1 after 4 h and 24 h (left) and accumulation of MT1-MT1-AR1 in the inflamed paws after 4 h and 24 h (right) (Elsadek and Kratz, 2012).

The advent of Ablynx nanobody technology using albumin-binding nanobodies has also been successfully explored for tumour targeting (Cortez-Retamozo *et al.*, 2002: Cortez-Retamozo *et al.*, 2004; Tijink *et al.*, 2008). For example, to improve the pharmacokinetic properties of an anti-EGFR nanobody, a trivalent, bispecific nanobody construct was developed, which binds with two

arms to EGFR and with one arm to mouse serum albumin (Roovers *et al.*, 2007). These nanobodies, due to its small size of only 15 kDa, are rapidly cleared from the circulation through the kidney, with a half-life of approximately 1.5 hours in mice. The trivalent fusion protein (molecular mass 50 kDa) exhibited an increased half-life of 44 hours in mice and improved tumour uptake (Tijink *et al.*, 2008). Interestingly, faster and deeper tumour penetration was described for this bi-functional nanobody molecule compared with the anti-EGFR antibody cetuximab.

OBJECTIVES

Recombinant antibody fragments and single-domain antibodies are a promising class of biopharmaceuticals with very high potential in future therapeutic applications. However, owing to their low molecular weight (< 60kDa) they usually have short half-life's ranging from a few minutes to a few hours. Consequently, high doses and repeated administration are necessary to maintain their therapeutic activity. As a result, there is a pressing need to identify and develop new strategies to enhance the *in vivo* circulating half-life of these molecules. Over the recent years, plasma protein binding has been shown as an effective approach to improve pharmacokinetic properties. Within this context, the aim of this research project is to explore the albumin binding approach to enhance the circulating half-life of small protein-based fusion biodrugs.

To achieve this goal, we will develop and compare two strategies based on protein fusions with albumin-binding domains (ABDs) from streptococcal cell surface proteins. These two new ABDs will be the Zag and protein H (ProtH) derived from *Streptococcus zooepidemicus and Streptococcus pyogenes,* respectively. To validate our ABDs half-life strategy and as a proof-of-concept, the Zag and ProtH domains will be fused with an anti-TNFα VHH single-domain antibody. This anti-TNFα VHH is a well-studied molecule with promising results for treatment of rheumatoid arthritis that is being developed by the Belgium Company Ablynx (Silence *et al*. Patent US2007/0077249 A1).

Therefore, the goals defined to be achieved are the following:

1) Construction and engineering of Zag and ProtH ABDs fusions with the anti-TNFα VHH;

2) Optimize the expression and purification conditions of Zag, ProtH, VHH and the fusion recombinant proteins, VHH-Zag and VHH-ProtH;

3) Characterization of the fusion proteins properties: albumin and human TNFα bindings, thermal stability and human and mouse serum stability;

4) Evaluate the efficacy of the fusion proteins;

5) Determine and compare the pharmacokinetics and biodistribution of both strategies;

6) Study and characterization of the ProtH and Zag ABDs three-dimensional structure.

ALBUMIN-BINDING DOMAIN (ZAG) FROM STREPTOCOCCUS ZOOEPIDEMICUS AS A STRATEGY TO IMPROVE HALF-LIFE OF THERAPEUTIC PROTEINS

Brief Introduction

Streptococcal albumin-binding domains have been successfully explored as fusion proteins to improve the pharmacokinetic properties of therapeutic proteins (Kontermann, 2012).

ZAG is a protein G-related cell-surface protein from *S. zooepidemicus*, with an Ig-binding region located in the C-terminus and an ABD composed by 52 amino acids (Jonsson *et al.*, 1994).

In this study we fused protein ZAG ABD (Zag) with a nanobody against TNFα from Ablynx, used as a proof of concept to validate our strategy to increase half-life of therapeutic proteins. Firstly, we intend to optimize the production of the recombinant proteins (VHH and VHH-ProtH) in *E.coli*, an easy way to obtain high amounts of protein with lower costs. Then we characterize the antigen and albumin binding of the Zag fusion protein and compare the therapeutic efficacy of the VHH-Zag with the unmodified antibody. We also evaluate the thermal stability and *in vitro* and *in vivo* serum stabilities of the both proteins. Finally, we determine the initial and terminal half-lives of VHH and VHH-Zag and the organ biodistribution profiles of both proteins, using ^{99m}Tc radiolabelling.

Albumin-binding domain (Zag) from *Streptococcus zooepidemicus* as a strategy to improve the half-life of therapeutic proteins

Cátia Cantante[1,2], Sara Lourenço[3], Maurício Morais[4], João Leandro[5], Lurdes Gano[4], Nuno Silva[5], Paula Leandro[5], Mónica Serrano[6], Adriano O. Henriques[6], Carlos Fontes[6], João D. G. Correia[4], Frederico Aires-da-Silva[3,7] and João Gonçalves[1,2]

[1] CPM-URIA, Faculdade de Farmácia, Universidade de Lisboa, 1649-003 Lisbon, Portugal
[2] Instituto de Medicina Molecular, Faculdade de Medicina, Universidade de Lisboa,1649-028 Lisbon, Portugal
[3] Technophage, SA, 1649-028 Lisbon, Portugal
[4] Centro de Ciências e Tecnologias Nucleares, Instituto Superior Técnico, Universidade de Lisboa, 2695-066 Bobadela LRS, Portugal
[5] iMed.UL, Faculdade de Farmácia, Universidade de Lisboa, 1649-003 Lisbon, Portugal
[6] Instituto de Tecnologia Química e Biológica (ITQB), Universidade Nova de Lisboa, 2780-157 Oeiras, Portugal
[7]Faculdade de Medicina Veterinária, CIISA, Universidade de Lisboa,1300-477 Lisbon, Portugal

Keywords: albumin-binding domain, half-life, nanobody, pharmacokinetics, TNFα, ZAG cell surface protein.

Background: Half-life extension is a key feature to improve pharmacokinetics of therapeutic low molecular weight proteins and peptides.

Results: Fusion of streptococcal Zag albumin-binding domain (ABD) to a single-domain antibody (nanobody) resulted in an improvement in pharmacokinetic properties leading to a significant increase in circulation time *in vivo.*

Conclusions: The Zag ABD fusion can be successfully applied to improve the pharmacokinetics of short half-life therapeutic molecules.

Significance: This work demonstrates the potential of a new approach to increase the half-life of therapeutic proteins by using the ZAG albumin-binding domain from *Streptococcus zooepidemicus.*

ABSTRACT

Recombinant antibody fragments and single-domain antibodies are a promising class of biopharmaceuticals with very high potential in future therapeutic applications. However, due to their small size are rapidly cleared from circulation. Plasma protein binding can be an effective approach to improve pharmacokinetic properties of short half-life molecules. Aimed at improving the pharmacokinetic properties of therapeutic proteins, we propose herein a bacterial albumin-binding domain (Zag) derived from *Streptococcus zooepidemicus.* To validate our approach and as a proof of concept, the Zag ABD was fused with an anti-TNFα VHH single-domain antibody. Our results shown that the VHH-Zag fusion recombinant protein could be stably expressed in the soluble format in *Escherichia coli* and, specifically

recognize TNFα and serum albumins (human, rat and mouse). Moreover, data also demonstrated that VHH activity against the therapeutic target was not affected when fused with Zag ABD. Importantly, Zag ABD strongly increased the half-life of the VHH in 39-fold (47 min for VHH *versus* 31 hours for VHH-Zag) and the residence in mouse serum (2 hours for VHH *versus* 72 hours for VHH-Zag). The prolonged circulation time also lead to a reduction of the VHH-Zag in kidneys and an increase of the presence of the fusion VHH in blood and other organs, e.g. liver, intestine, muscle and lungs. These findings demonstrate that the Zag ABD fusion strategy is a promising approach to increase the half-life of therapeutic proteins, without affecting their therapeutic efficacy.

INTRODUCTION

Recombinant antibody fragments and single-domain antibodies have been under investigation and development with promising results for clinical applications. However, owing to their low molecular weight (< 60kDa) they usually have short half-life's ranging from a few minutes to a few hours. Consequently, high doses and repeated administration are necessary to maintain their therapeutic activity[1]. Within this context, in the past decade several efforts have been undertaken towards the development and implementation of half-life extension strategies to prolong the circulation time of these molecules and consequently improve their pharmacokinetic properties and therapeutic potential[2]. Some of these strategies have focused on increasing hydrodynamic volume, e.g. PEGylation and glycosylation[1,2]. For instance, PEGylation has been successfully applied to prolong the half-life of several recombinant antibodies and antibody fragments for clinical use[3]. Although this approach is an industry-established method, several studies also indicate that PEGylation can lead to reduce antigen binding and bioactivity[2,4]. As an alternative, other half-life extension approaches are based on implementing FcRn-mediated recycling, responsible for the long half-life of the human plasma proteins albumin (~19 days) and immunoglobulin G (~21 days)[1,2]. These new strategies to improve pharmacokinetic disposition of small therapeutic proteins are focused on fusion to the Fc region, on binding to or fusion with long-circulating serum plasma proteins such as albumin, or on fusion with albumin-binding domains and peptides, or immunoglobulin-binding domains[1,2,5]. Dennis and colleagues developed a strategy based on the fusion of an albumin-binding peptide, using peptide phage display to develop peptides with high affinity to albumin. One of the selected albumin-binding peptides was added to a Fab antibody fragment, by recombinant fusion, with an increase in half-life of 26-fold to

10.4 h in mice[6]. Moreover, fusion to the albumin-binding domain 3 (ABD3) from protein G of *Streptococcus* strain G148 has been extensively studied and several *in vivo* studies have demonstrated significant improvement of the plasma half-life and pharmacokinetic properties of therapeutic proteins[1,5-8]. Jonsson and co-workers have described a plasma protein receptor, a protein-G related cell surface protein from *Streptococcus zooepidemicus*, termed protein ZAG, a 45 kDa protein that binds α_2-macroglobulin, serum albumin and immunoglobulin G (IgG). The IgG-binding domains from ZAG are homologous to the IgG-binding domains in protein G and to the corresponding domains in proteins MIG and MAG from *Streptococcus dysgalactiae*[9]. Protein ZAG shows an albumin-binding profile similar to those of protein G[10] and the albumin-binding DG12 protein from a bovine group G streptococcus[11]. In the N-terminus, ZAG protein presents a 52 amino acid sequence (Zag ABD) with binding to human, rat, mouse, horse and dog serum albumin. Downstream from this region there are two 70-amino-acid repeats homologous to the IgG-binding domains of type III Fc receptors[9].

In the present study, we used the Zag ABD as a new approach for extension of the circulation time of therapeutic proteins. To validate our strategy and as a proof-of-concept, the Zag ABD was fused with an anti-TNFα VHH single-domain antibody. The fusion protein showed specific binding to serum albumin and compared with the parental VHH nanobody, exhibited a strong increase of serum half-life in mice to approximately 39-fold. These results demonstrate, for the first time, the ability of this new streptococcal ABD to improve pharmacokinetic disposition of therapeutic proteins.

EXPERIMENTAL PROCEDURES

Materials – Human serum albumin (HSA) (catalog no. A3782), rat serum albumin (RSA) (catalog no. A6272), mouse serum albumin (MSA) (catalog no. A3139), human (catalog no. H4522) and mouse serum (catalog no. H5905), and pT7-FLAG2 expression vector were purchased from Sigma-Aldrich (USA). HRP-conjugated anti-His-tag, HRP-conjugated anti-HA-tag, anti-HA affinity matrix, 2,2'-Azino-di-[3-ethylbenzthiazoline sulfonate (6)] diammonium salt (ABTS), tetrazolium salt WST-1 and cOmplete EDTA-free protease inhibitors cocktail were acquired from Roche (Germany). Recombinant human TNFα and Amicon centrifugal filter units were purchase from Millipore (USA). PD-10 columns and G25 Sephadex were purchase from GE Healthcare (UK) and Sigma-Aldrich, respectively. Radioactivity measurements were done on a dose calibrator (Aloka Curiemeter, IGC-3, Japan) or on a gamma-counter (Berthold LB 2111, Germany).

Cloning of recombinant proteins – DNA encoding anti-TNFα VHH#3E clone (Silence *et al*. Patent US2007/0077249 A1)[12] was synthesized by Nzytech adding a SfiI restriction site at 5' and 3' ends, respectively, for cloning into the pComb3x plasmid[13]. pComb3X contains a leader peptide sequence ompA (LP) and sequences encoding peptide tags for purification (His_7) and detection (HA). A fragment encoding the LP-VHH-His-HA was amplified by PCR with primers HindIII-LP-SfiI-F (5'-CCC AAG CTT ATG AAA AAG ACA GCT ATC GCG ATT GCA GTG GCA CTG GCT GGT TTC GCT ACC GTG GCC CAG GCG GCC-3') and His-HA-KpnI-R (5'-CGG GGT ACC CCG CTA AGA AGC GTA GTC CGG AAC GTC GTA CGG GTA TGC GCC ATG GTG ATG GTG ATG GTG ATG GTG GCT GCC TCC-3') and subcloned into the expression vector pT7-FLAG2 (Sigma) into the HindIII and KpnI restriction sites. To construct the VHH-Zag fusion protein, a DNA fragment comprising the entire Zag albumin-binding domain of *S. zooepidemicus*[9] was generated by PCR with primers Zag-1 (5'-GAC ATT ACA GGA GCA GCC TTG TTG GAG GCT AAA GAA GCT GCT ATC AAT GAA CTA AAG CAG TAT GGC ATT AGT GAT TAC TAT GTG ACC TTA ATC-3') and Zag-2 (5'-GTA TGG CAT TAG TGA TTA CTA TGT GAC CTT AAT CAA CAA AGC CAA AAC TGT TGA AGG TGT CAA TGC GCT TAA GGC AGA GAT TTT ATC AGC TCT ACC G-3'), adding SpeI and NcoI restriction sites at the fragment 5' and 3' ends, respectively. The resulting PCR fragments were gel-purified, digested with the SpeI and NcoI restriction enzymes and cloned into the appropriately cut pT7-VHH vector. A short GS linker (SGGGGS) was used to link the VHH and Zag ABD. VHH and VHH-Zag constructs were verified by sequencing.

Expression and purification of proteins – VHH and VHH-Zag were expressed in *E. coli* strain BL21(DE3). One liter of LB, containing 100 µg/ml ampicillin was inoculated with 10 ml of overnight culture of bacterial cells transformed with the plasmids pT7-VHH and pT7-VHH-Zag and grown to exponential phase (A_{600} = 0.6-0.9) at 37 ºC. Expression was induced by the addition of 1 mM isopropyl β-D-1-thiogalactopyranoside (IPTG) and growth during 16 h at 18 ºC. Cells were harvested by centrifugation (4000 × *g* for 15 min at 4 ºC) and resuspended in 50 ml equilibration buffer (50 mM HEPES, 1 M NaCl, 5 mM $CaCl_2$, 30 mM imidazole, pH 7.5) supplemented with protease inhibitors. Cells were lysed by sonication. Centrifugation (14000 × *g* for 30 min at 4 ºC) was used to remove cell debris, and the supernatant was filtered through a 0.2 µm syringe filter. The VHH and VHH-Zag were purified using AKTA FPLC System (GE Healthcare) by nickel chelate affinity chromatography with HisTrap HP columns. After a washing step (50 mM HEPES, 1 M NaCl, 5 mM $CaCl_2$, 60 mM imidazole,

pH 7.5) the recombinant antibody fragments were eluted with a linear imidazole gradient from 60 to 300 mM in 50 mM HEPES, 1 M NaCl, 5 mM $CaCl_2$, pH 7.5. Protein fractions were pooled, then desalted and concentrated in 50 mM HEPES, 100 mM NaCl, 5 mM $CaCl_2$, pH 7.5 using Amicon 10K (Millipore). The samples were loaded onto a HiPrep 16/60 Sephacryl S-100 HR gel filtration column (GE Healthcare), fractions were pooled and protein purity was analyzed by SDS-PAGE. Protein concentration was determined spectrophotometrically in Nanodrop ND-1000 at 280 nm and calculated using the calculated ε value of each protein (εVHH = 34380 L mol−1 cm−1; εVHH-Zag = 38850 L mol−1 cm−1).

Size Exclusion Chromatography – Apparent molecular weight of recombinant antibody and formation of antibody/albumin complexes was determined by FPLC-SEC on a HiLoad Superdex 200 HR column (GE Healthcare) with a flow rate of 0.7 ml/min and PBS1x as running buffer at 4 ºC. The following standard proteins were used: apoferritin (443 kDa, R_S 6.1 nm), β-amylase (200 kDa, R_S 5.4 nm), alcohol dehydrogenase (150 kDa, R_S 4.55 nm), bovine serum albumin (67 kDa, R_S 3.55 nm), ovalbumin (45 kDa, R_S 3.05), myoglobin (17.6 kDa, R_S 1.91 nm), ribonuclease A (13.7 kDa, RS 1.64 nm) and cytochrome c (12.4 kDa, R_S 1.77 nm). Blue dextran and L-tyrosine were used to determine the void and total column volume, respectively. Elution volume of the protein standard was used to create a standard curve of Stokes' radius (R_S) *versus* $(-\log K_{av})^{1/2}$ that was used to calculate the Stokes radius of recombinant antibody and antibody/albumin complexes. Complex formation of VHH-Zag with HSA and MSA was analyzed by incubating equimolar amounts of VHH-Zag and albumin (10 μM) in PBS1x at room temperature and subsequent analysis by SEC. SDS-PAGE analysis of collected samples was performed to evaluate albumin binding.

ELISA – Binding properties of VHH and VHH-Zag fusion proteins were determine in 96-well coated with HSA, RSA, MSA (10 μg/well) and human TNFα (200 ng/well) overnight at 4 ºC. After 1 h blocking with 5% soya milk, purified recombinant antibodies and serum samples were titrated in triplicate and incubated for 1 h at room temperature. Human TNFα binding was evaluated in the presence and absence of HSA (1 mg/ml). Detection was performed with HRP-conjugated anti-HA-tag antibody using ABTS substrate. Absorbance was measured at 405 nm in an ELISA reader. GraphPad Prism Software version 5 was used for data analysis.

Affinity measurements – The binding affinities between VHH-Zag and HSA, RSA and MSA were obtained using surface plasmon resonance (SPR) (BIAcore 2000, BIAcore Inc.) Human, rat and mouse albumins were captured on a CM5 chip using amine coupling at ~1000

resonance units. VHH-Zag fusion protein at 0, 10, 50, 100, 200, 300, 400 and 500 nM were injected for 4 min. The bound protein was allowed to dissociate for 10 min before matrix regeneration using 10 mM glycine, pH 1.5. The signal from an injection passing over an uncoupled cell was subtracted from that of an immobilized cell to generate sensograms of the amount of protein bound as function of time. The running buffer, HBS was used for all sample dilutions. BIAcore kinetic evaluation software (version 3.1) was used to determinate K_D from association and dissociation rates using a one-to-one binding model. VHH was used as a control.

Neutralization of TNF-dependent cytolytic activity – In order to measure the anti-TNFα VHH and VHH-Zag blocking effect on TNFα/TNFR (TNF receptor) interaction, a murine aneuploidy fibrosarcoma cell line (L929) was used as a cytotoxic-mediated assay. Briefly, L929 cells were grow to 90% confluence in Dulbecco's modified Eagle's medium supplemented with 10% fetal bovine serum, penicillin (100 units/ml), streptomycin sulfate (10 μg/ml), and L-glutamine (2 mM). Cells were plated in 96-well plates at density of 25,000 cell/well and then incubated overnight. Serial dilutions of anti-TNFα antibody fragments were mixed with a cytotoxic concentration of TNFα (final assay concentration 1 ng/ml) or in absence of this cytokine in order to measure the cell viability. Actinomycin D was added to a final concentration of 1 μg/ml to increase the cell sensitivity. After at least 2 h of incubation at 37 ºC with shaking, the mixture was added to the plated cells. Cells were incubated for 24 h at 37 ºC in an atmosphere of 5% CO_2. Cell viability was determined using the tetrazolium salt WST-1 (10 μg/well) from Roche, after at least 30 min of incubation by measuring the absorbance at 450 nm. GraphPad Prism Software version 5 was used for data analysis.

Protein thermal stability and in vitro serum stability – Melting temperatures of the studied proteins were determined using the Protein Thermal Shift Kit and 7500 Fast Real-Time PCR System (Applied Biosystems) according manufacturer's instructions. Protein samples (5 μg/well) were tested in MicroAmp™ Fast Optical 96-well Reaction Plates and analyzed in quadruplicate using and diluted in 50 mM HEPES, 100 mM NaCl, 5 mM $CaCl_2$, pH 7.5, and Protein Thermal Shift™ Dye 1x. Collected data were analyzed with Protein Thermal Shift Software version 1.1.

To evaluate mouse and human serum stability of recombinant antibodies, VHH and VHH-Zag were incubated at a concentration of 10 μg/ml for up to 4 days and 24 days, respectively, at 37 ºC. The *in vitro* stability of VHH and VHH-Zag in the human and mouse

serum was evaluated by ELISA and Western Blot using HRP-conjugated anti-His-tag antibody as described above.

Pharmacokinetics – Animal care and all pharmacokinetic (PK) studies were conducted according to guidelines for animal care and ethics for animal experiments outlined in the National and European Law. CD-1 mice (Charles River, female, 6-8 weeks, 25-30g weight (n=2) were administered with intravenous injections in the tail vein with 25 µg of VHH and VHH-Zag. Plasma samples were obtained from injected animals at regular intervals of 5, 30, 60, 120, and 360 min, 24, 48 and 72 hours, and fused or unfused recombinant antibody were quantified by ELISA. Briefly, human TNFα was immobilized in 384 well-plates (100 ng/well) overnight at 4 ºC. After 1 h blocking with PIERCE blocking, mouse serum samples were titrated in duplicates and incubated for 1 h at RT. Detection was performed with HRP-conjugated anti-HA antibody using ABTS substrate. Absorbance was measured at 405 nm in an ELISA reader. As described by Stork and co-workers, determined serum concentrations of TNFα-binding proteins were interpolated to the corresponding calibration curves. For comparison, the first time point (5 min) was set to 100%. Pharmacokinetic parameters area under the curve (AUC), $t_{1/2}\alpha$ and $t_{1/2}\beta$ were calculated with Excel, using the first three time points to calculate $t_{1/2}\alpha$ and the last three time points to calculate $t_{1/2}\beta$.

Radiolabelling of $^{99m}Tc(CO)_3$-VHH and $^{99m}Tc(CO)_3$-VHH-Zag proteins – $Na[^{99m}TcO_4]$ was eluted from a $^{99}Mo/^{99m}Tc$ generator. The radioactive precursor *fac*-$[^{99m}Tc(CO)_3(H_2O)_3]^+$ was prepared using a IsoLink® kit (Covidien) and its radiochemical purity checked by RP-HPLC and ITLC-SG. The radiolabeled proteins *fac*-$[^{99m}Tc(CO)_3]$-VHH and *fac*-$[^{99m}Tc(CO)_3]$-VHH-Zag were obtained by reacting the recombinant antibodies with *fac*-$[^{99m}Tc(CO)_3(H_2O)_3]^+$. Briefly, a specific volume of the *fac*-$[^{99m}Tc(CO)_3(H_2O)_3]^+$ solution was added to a nitrogen-purged closed glass vial containing a solution of the His-tag containing proteins VHH or VHH-Zag in order to get a final concentration of 1 mg/ml. The mixture reacted for 3 hours at 37 ºC and the radiochemical purity of *fac*-$[^{99m}Tc(CO)_3]$-VHH and *fac*-$[^{99m}Tc(CO)_3]$-VHH-Zag was checked by ITLC-SG (Varian) analysis every hour using a 5% HCl (6 M) solution in MeOH as eluent. $[^{99m}Tc(CO)_3(H_2O)_3]^+$ and $[TcO_4]^-$ migrate in the front of the solvent (Rf = 1), whereas the radioactive antibodies remain at the origin (Rf = 0). Radioactivity distribution on the ITLC-SG strips was detected by a radioactive scanner (Berthold LB 2723, Germany) equipped with 20 mm diameter NaI(Tl) scintillation crystal. Radioactivity measurements were done on a dose calibrator (Aloka Curiemeter, IGC-3, Japan) or on a gamma-counter (Berthold LB 2111, Germany). Purification of the ^{99m}Tc-radiolabeled

antibodies was performed by gel filtration through Shepadex G-25 or PD-10 column, using 20 nM sodium chloride solution as eluent. After radioactive decay (10 half-lifes), the VHH and VHH-Zag proteins were tested by ELISA to ensure that their binding capacities were unaffected (data not shown).

Partition coefficient – Partition coefficient was evaluated by the "shake-flask" method. The radioactive antibodies were added to a mixture of octanol (1 ml) and 0.1 M PBS1x pH 7.4 (1 m), which has been previously saturated with each other by stirring. This mixture was vortexed and centrifuged (3000 rpm, 10 min) to allow phase separation. Aliquots of both octanol and PBS1x were counted in a γ-counter. The partition coefficient ($P_{o/w}$) was calculated by dividing the counts in the octanol phase by those in the buffer, and the results were expressed as log $P_{o/w}$±SD.

Biodistribution studies of $^{99m}Tc(CO)_3$-VHH and $^{99m}Tc(CO)_3$-VHH-Zag – In vivo evaluation studies of radiolabelled VHH and VHH-Zag were performed in healthy female CD-1 Charles River, 6-8 weeks, 25-30g weight (n=3) mice at 5 min, 30 min, 1 h, 4 h and 24 h. All animal experiments were performed in accordance with the guidelines for animal care and ethics for animal experiments outlined in the National and European Law. Animals were intravenously injected into the tail vein with 100 µl of the radiolabeled compounds (2.6–3.7 GBq). Mice were sacrificed by cervical dislocation at 5 min, 30 min, 1 h, 4 h and 24 h after injection. The dose administered and the radioactivity in the sacrificed animals was measured using a dose calibrator. The difference between the radioactivity in the injected and that in the killed animals was assumed to be due to excretion. Tissues of interest were dissected, rinsed to remove excess blood, weighed, and their radioactivity was measured. The total activity uptake for blood, bone, muscle, was estimated assuming that these organs constitute 6, 10, and 40% of the total body weight, respectively. Blood and urine was also collected at the sacrifice time and analyzed by ITLC.

RESULTS

Expression and purification of VHH and VHH-Zag

The VHH-Zag construct was generated by fusing the Zag ABD from ZAG streptococcal surface protein to the anti-TNFα VHH#3E (Silence *et al*. Patent US2007/0077249 A1)[12] clone, including histidine (His_6) and HA tags in C-terminal (Fig. 1A and 1B). The fusion protein obtained presents 235 amino acid residues with a calculated molecular weight of

~25.2 kDa. The VHH was also constructed as described in the material and methods section and used as control. VHH and VHH-Zag were expressed in *E. coli* BL21 (DE3) and purified by IMAC and gel filtration. SDS-PAGE and Western Blot results showed a single protein band with the expected molecular weights for VHH and VHH-Zag under reducing and non-reducing conditions (Fig. 1C and 1D). After expression and purification of one liter of culture we obtain 20-25 mg of VHH-Zag comparing with 15-20 mg for the VHH.

Binding activity of VHH-Zag against TNFα

After purification, the VHH-Zag binding activity to human TNFα was tested in an ELISA assay as described in the material and methods section. The VHH was used as control and as shown in figures 2A and 2B, both proteins specifically bound to TNFα. Importantly, binding of VHH-Zag to TNFα was not affected by the presence of HSA (without HSA EC_{50} = 0.130 nM; with HSA EC_{50} = 0.118 nM) and was similar with the binding of the parental VHH nanobody (without HSA EC_{50} = 0.100 nM; with HSA EC_{50} = 0.132 nM). Thus, the antigen-binding sites in VHH-Zag are accessible for TNFα binding and the presence of albumin does not interfere with antigen targeting.

Binding activity of VHH-Zag to albumins

In order to determine the *in vitro* relative binding activities of the VHH-Zag fusion protein to human, rat and mouse albumins, an ELISA was performed at neutral (pH 7.0) and acidic environment (pH 6.0) (Material and Methods section). As shown in figures 3A and 3B, the Zag fusion recombinant protein specifically bound to human, rat and mouse albumins. Moreover, binding of VHH-Zag to albumins at pH 6.0 (Table 1) was slightly increased ($EC_{50\ (HSA)}$ = 0.324 nM; $EC_{50\ (RSA)}$ = 0.377 nM; $EC_{50\ (MSA)}$ = 0.175 nM) compared with binding at pH 7.4 ($EC_{50\ (HSA)}$ = 1.074 nM; $EC_{50\ (RSA)}$ = 1.698 nM; $EC_{50\ (MSA)}$ = 4.354 nM) (Fig. 3). After albumin binding confirmation, Biacore analysis was performed to evaluate affinities behavior and parameters of the Zag fusion protein. Affinities of VHH-Zag for human, rat and mouse albumin were in the lower nanomolar range (Fig. 4), showing a higher affinity for HSA and RSA at neutral pH, with K_D of 4.57 nM and K_D of 0.42 nM, respectively, then for MSA, with a K_D of 40.6 nM (Table 2). Affinities were also measured at acid pH and similar results were obtained (data not shown).

Size exclusion chromatography (SEC) analysis was also performed to analyze the interaction between VHH-Zag and human and mouse serum albumin in solution (Fig. 5 and Table 3). VHH-Zag eluted with a predominant peak (65%) corresponding to an apparent molecular mass of 26.4 kDa (R_S 2.59 nm) (Fig. 5A and Table 3). HSA revealed a major peak

(93%) corresponding to the monomeric form with an apparent molecular mass of 68.1 kDa (R_S 3.67 nm) and minor peak (7%) of 163 kDa (Fig. 5B). Incubation of equimolar concentrations of VHH-Zag and HSA shifted the HSA peaks to higher apparent molecular masses, 230.5 kDa (28%) and 101.2 kDa (50%), the later corresponding to a stoichiometry of 1:1 of the complex VHH−Zag/monomeric HSA (R_S 4.16 nm). The unbound VHH-Zag corresponded to ~17%. Similar results were obtained for the MSA. However, MSA showed higher molecular mass forms than the human counterpart (Fig. 5D) and a major peak (40%; monomeric form) with an apparent molecular mass of 64.3 kDa (R_S 3.60 nm). Incubation of MSA with VHH-Zag resulted in the shift of the monomeric MSA to 98.6 kDa (R_S 4.01 nm; 26 %). Unbound VHH-Zag was slighter higher when compared with human albumin (36%).

Thermal stability and in vitro serum stability

The thermal stability of VHH and VHH-Zag was calculated using the Protein Thermal Shift Kit and Protein Thermal Shift Software. The results obtained showed melting temperatures (Tm) of 71.53 to 72.34 ºC for VHH and 69.77 to 70.24 ºC for VHH-Zag (Table 4). These results demonstrate that both proteins have similar Tm and are highly stable. Moreover, these data showed that the fusion of the ZagABD to the anti-TNFα nanobody did not affect its stability. *In vitro* serum stability was analyzed by incubation VHH and VHH-Zag proteins with human and mouse serum at 37 ºC. Samples were incubated during 4 and 24 days in mouse and human serum, respectively. The detection of VHH and VHH-Zag in the collected samples was examined by Western Blot. As shown in figures 7A and 7B, both proteins were detected with the expected molecular weights and no degradation was observed. Moreover, the binding activities were confirmed by ELISA in all the samples and were similar to samples before incubation (Day 0) (data not shown).

Neutralization of TNFα-dependent cytolytic activity by VHH and VHH-Zag

With the aim of measuring the VHH and VHH-Zag blocking effect on TNF-α/TNFR interaction, we have selected a murine aneuploid fibrosarcoma cell line (L929) as a cytotoxic TNFα-mediated assay (material and methods section). As shown in figure 6, both VHH and VHH-Zag inhibited the TNFα-induced cell death of L929 in a dose-dependent manner. Importantly, the inhibitory profiles of VHH and VHH-Zag were almost identical, thus indicating that the fusion with the Zag ABD does not interfere with the activity of the anti-TNFα VHH.

Pharmacokinetic and organ biodistribuition of VHH and VHH-Zag

The pharmacokinetic properties of VHH and VHH-Zag were evaluated in CD-1 mice, after a single i.v. injection (25 µg) into the tail vein. This dose injection was selected according to doses applied in other studies with recombinant antibodies in mice[7,8]. Serum concentrations of VHH and VHH-Zag were determined by ELISA at different time points as described in the material and methods section. Compared with VHH, VHH-Zag showed a highly prolonged residence time in blood and remaining organism (Fig. 8 and Table 5), with the terminal half-life ($t_{1/2}\beta$) increasing from 0.79 h (VHH) to 30.55 h (VHH-Zag), corresponding to a 39-fold increase. Moreover, distribution phase half-life ($t_{1/2}\alpha$) showed a 7-fold increase, from 0.52 h (VHH) to 3.71 h (VHH-Zag). The improvement of pharmacokinetic properties was also demonstrated by comparison of the AUC. For VHH-Zag the $AUC_{(0-24)}$ was increased by a factor of 20 comparing with VHH. To confirm the presence and identity of VHH and VHH-ZAG at each time point, a Western Blot was performed. As illustrated in figure 9, comparing with the unmodified VHH nanobody (residence in serum during 2 h), VHH-Zag can be detected by immunoblot in mouse serum until 72 h after injection.

In order the analyze the biodistribution profile of each molecule, VHH and VHH-Zag were radiolabeled with the "$^{99m}Tc(CO)_3$" core and injected in CD-1 mice. Tissue distribution and *in vivo* stability were monitored over a period of 48 h (Fig. 10 and Tables 6 and 7). For all time points, a total of 84 to 99% of injected activity was recovered. Organ to blood ratio at 24 h (Table 8) showed a very high radioactivity accumulation within the kidney for VHH, with 390 times more concentrated than in the blood. Moreover biodistribution assay also showed a trend for $^{99m}Tc(CO)_3$-VHH accumulation within the highly perfused organs intestine, muscle and liver, respectively with 3 times, 5 times and 11 times more concentrated in these organs than in the blood. For the lung and bone $^{99m}Tc(CO)_3$-VHH also showed a 2-fold increase in concentration when compared to blood. For other organs (spleen, heart, stomach and pancreas), VHH showed a lower concentration when compared to blood. On the contrary, $^{99m}Tc(CO)_3$-VHH-Zag showed only a slight accumulation within the liver and kidney, with approximately 1.5 times more concentrated in these two organs when compared to blood. For the rest of collected organs, no accumulation was observed. When biodistribution results are normalized to organ weight (Fig. 10, Tables 6 and 7), it is evident the higher radioactivity retention of $^{99m}Tc(CO)_3$-VHH in the kidney when compared to $^{99m}Tc(CO)_3$-VHH-Zag. This finding is in agreement with the predominant urinary excretory route of VHH.

DISCUSSION

Herein we have evaluated the ability of the Zag albumin-binding domain (ABD) of streptococcal protein ZAG, a protein-G related surface protein, to extend the circulation half-life of therapeutic proteins. For this purpose and to validate our strategy, the Zag ABD was fused with an anti-TNFα VHH nanobody. Our results, demonstrated that both VHH and VHH-Zag constructs were stably produced in *E. coli*, with high yields of protein of several milligrams per liter of culture. The binding of VHH-Zag fusion protein to human TNFα and human, rat and mouse serum albumin was confirmed by ELISA. Importantly, we demonstrate that the presence of HSA (1 mg/ml) did not affect the binding of VHH-Zag to human TNFα, showing similar values to the unmodified nanobody. These results demonstrate that VHH-Zag is active when exposed to the therapeutic target in the presence of albumin. Moreover, binding of VHH-Zag to human, rat and mouse albumin was not reduced at pH 6.0, showing that VHH-Zag binding to albumin is stable at low pH e.g., found in endosomes. Accordingly, the measured affinities of VHH-Zag for human, rat and mouse albumins at neutral pH, were in the range of nanomolar affinity, with values of 4.57, 0.42 and 40.6 nM, respectively. These affinities values, were similar to those obtained in previous studies, for the streptococcal protein G ABD[7,15,16]. The SEC results, indicate the formation of VHH-Zag/albumin complexes *in vitro* with an increased hydrodynamic radius (4.01 nm *versus* 1.84 nm for the VHH), confirming the albumin binding of VHH-Zag. These findings support the proposal that VHH-Zag uses the albumin binding to achieve extension of the circulation time, probably triggered by the reduced renal clearance and FcRn-mediated recycling mechanism. Accordingly, a previous study using the ABD from protein G in fusion with a single-chain diabody for circulation time extension, confirmed that the long half-life of this therapeutic protein is achieved through the recycling of albumin mediated by the FcRn[17]. Besides the VHH-Zag maintain the albumin binding capacities of the original ABD[9], the TNFα-neutralization assays showed that the Zag fusion did not affect the efficacy of the anti-TNFα VHH. Our results indicate that the TNFα- and albumin-binding abilities of the parental anti-TNFα nanobody were retained in the recombinant molecule VHH-Zag. Furthermore, fusion of Zag with the unmodified VHH did not disturb the high thermal stability of the nanobody (VHH $_{Tm}$ = ~70 ºC *versus* VHH-Zag $_{Tm}$ = ~72 ºC). Serum stability studies also demonstrate the high stability in human and mouse serum of VHH and VHH-Zag proteins (Fig. 7). Regarding the pharmokinetic, when compared to VHH, VHH-Zag showed an extraordinary 39-fold increase of the terminal elimination half-life (47 min *versus* 31 h for the Zag fusion

nanobody). Although VHH-Zag presents a plasma half-life of 31 h, the fusion protein can be detected in mouse serum until 72 h after injection, comparing the short presence of 2 h for VHH (Fig. 9). The half-life of VHH-Zag is slightly higher than the circulation times determined for scDbCEACD3-ABD (27.6 h)[9] and for scDbCEACD3-HSA fusion proteins (25.0 h)[8]. This improvement of half-life probably can be compared with the half-lives of serum albumin, which are 1.07-1.6 days for mouse serum albumin and ~19 days for human serum albumin[18-20]. The organ distribution of $^{99m}Tc(CO)_3$-VHH and $^{99m}Tc(CO)_3$-VHH-Zag (Fig. 10) exhibited a different biodistribution profile in radiolabeled both proteins. $^{99m}Tc(CO)_3$-VHH, was rapidly cleared from the blood and showed high kidney accumulation after 5 min (Fig. 10A and Table 6). $^{99m}Tc(CO)_3$-VHH-Zag had a strongly increased residence in the blood, which led also to increased values in all the other organs (Fig. 10B and Table 7).

A comparable biodistribution profile was recently reported by us using ^{67}Ga as radionuclide[21]. In this study we showed that the Zag domain affected the pharmacokinetic properties of VHH, with impressive differences in blood clearance and total excretion. The biodistribution profile of ^{67}Ga-NOTA-VHH exhibited a rapid clearance from blood and most tissues. On the other hand, ^{67}Ga-NOTA-VHH-Zag presented a slow washout from blood, muscle and bone, and an accumulation in highly irrigated organs such as liver, spleen and lung[21]. Similar results were also described in other study performed by Stork and colleagues[17].

A previous study from Coppieters and co-workers presented similarities results with ours in the TNFα-neutralizating capacities and half-life extension, with bivalent molecules in fusion with AR1, an anti-TNFα VHH targeting murine and human albumin. The trivalent molecules intend to increase the accumulation of the anti-TNFα VHH in the target tissue (inflamed joints) and to prolong its serum half-life (54 min for the unmodified nanobody *versus* 2.2 days for the AR1 fusion protein). Their biodistribution studies demonstrated significantly higher amounts of the bispecific anti-TNFα VHH in fusion with AR1 accumulated in inflamed joints and that this uptake was correlated with the higher clinical scores for the corresponding limbs[22]. Several findings show that large amounts of albumin accumulate and are metabolized in the inflamed joints of rheumatoid arthritis patients[23-26]. Preclinical mouse studies also demonstrated the possibility of albumin behaves as a carrier of therapeutics in rheumatoid arthritis[27-29]. These findings indicate that albumin might be a useful drug-carrier, allowing specific targeting of protein therapeutics to sites of inflammation.

Although Zag ABD has shown considerable improvements in pharmacokinetic properties of the single-domain antibody, concerns with the immunogenicity of these molecules for therapeutic applications may occur. For instance, immunogenicity of the albumin-binding domain of protein G, in the amino acid sequence 254-299, was detected in mice strains[30]. For therapeutic purposes, particularly in small proteins that require administration by repeated injections, it will be necessary reduce or ideally eliminate the immunogenicity. There are several de-immunization strategies that can be applied to reduce the immunogenicity of these ABDs[31-33]. Indeed, we have de-immunization ongoing studies being performed into the Zag ABD. The data already obtained reveals that although there is a slight decrease in Zag affinity, the albumin binding specificity is not affected neither the half-life extension properties.

In conclusion, the present study demonstrates that Zag ABD fusion is a promising strategy for half-life extension of therapeutic proteins. Within this context, we envision that this strategy can be an efficient approach used to improve the pharmacokinetic and pharmacodynamic properties protein or peptides without affecting the efficacy of these molecules. Moreover, due to the accumulation of albumin in inflamed joints, the anti-TNF VHH-Zag fusion approach also has a particular interest for the treatment of rheumatoid arthritis.

REFERENCES

1. Kontermann, R.E. (2009) Strategies to extend plasma half-lives of recombinant antibodies. *Biodrugs* **23,** 93-109

2. Chen, C., Constantinou, A., Deonarain, M. (2011) Modulating antibody pharmacokinetics using hydrophilic polymers. *Expert Opin. Drug. Deliv*. **8**,1221-1236

3. Goel, N., Stephens, S. (2010) "Certolizumab pegol". *MAbs* **2**, 137-147

4. Schlereth, B., Fichtner, I., Lorenczewski, G., Kleindienst, P., Brischwein, K., da Silva, A., Kufer, P., Lutterbuese, R., Junghahn, I., Kasimir-Bauer, S., Wimberger, P., Kimmig, R., Baeuerle, P.A. (2005) Eradication of tumors from a human colon cancer cell line and from ovarian cancer metastases in immunodeficient mice by a single-chain Ep-CAM-/CD3-bispecific antibody construct. *Cancer Res.* **65**, 2882-2889

5. Kontermann, R.E. (2011) Strategies for extended serum half-life of protein. Therapeutics. *Curr. Opin. Biotechnol.* **22**, 1-9

6. Dennis, M.S., Zhang, M., Meng, G., Kadkhodayan, M., Kirchofer, D., Combs, D., Damico, L.A. (2002) Albumin binding as a general strategy for improving the pharmacokinetics of proteins. *J. Biol. Chem.* **277**, 35035-35043

7. Stork, R., Müller, D., Kontermann, R.E. (2007) A novel tri-functional antibody fusion protein with improved pharmacokinetic properties generated by fusing a bispecific single-chain diabody with an albumin-binding domain from streptococcal protein G. *Protein Eng. Des. Sel.* **20**, 569-576

8. Hopp, J., Hornig, N.A., Zettlitz, K., Schwarz, A., Fuß, N., Müller, D., Kontermann, R.E. (2010) The effects of affinity and valency of an albumin-binding domain (ABD) on the half-life of single-chain diabody-ABD fusion protein. *Protein Eng. Des. Sel.* **23**, 827-834

9. Jonsson, H., Lindmark, H., Guss, B. (1995) A Protein G-related cell surface protein in *Streptococcus zooepidemicus*. *Infect. Immun.* **63**, 2968-2975

10. Nygren, P.-Å., Ljungquist, C., Trømborg, H., Nustad, K., Uhlén, M. (1990) Species-dependent binding of serum albumin binding domains of streptococcal protein G. *J. Mol. Recognit.* **1**, 69-74

11. Sjöbring, U. (1992) Isolation and molecular characterization of a novel albumin-binding protein from group G streptococci. *Infect. Immun.* **60**, 3601-3608

12. Silence, K., Lauwereys, M., de Haard, H. (2007) Single domain antibodies directed against tumor necrosis factor-alpha and uses therefor. United States Patent Application Publication, US 2007/007769 A1, Boston, MA

13. Barbas III, C.F., Burton, D.R., Silvermann, G.J. (2001) *Phage Display: A Laboratory Manual*. 1st Ed., Cold Spring Harbor Laboratory Press, Cold Spring Harbor, NY

14. Ameloot, P., Brouckaert, P. (2004) Production and characterization of receptor-specific TNF muteins. *Methods Mol. Med.* **98**, 33-46

15. Linhult, M., Binz, H.K., Uhlén, M., Hober, S. (2002) Mutational analysis of the interaction between albumin-binding domain from streptococcal protein G and human serum albumin. *Protein Sci*. **11**, 206-213

16. Johansson, M.U., Frick, I.-M., Nilsson, H., Kraulis, P.J., Hober, S., Jonasson, O., Linhult, M., Nygren, P.A., Uhlén, M., Björck, L. (2002) Structure, specificity, and mode of interaction for bacterial albumin-binding modules. *J. Biol. Chem.* **277**, 8114-8120

17. Stork, R., Campigna, E., Robert, B., Müller, D., Kontermann, R.E. (2009) Biodistribution of a bispecific single-chain diabody and its half-life extended derivatives. *J. Biol. Chem.* **284**, 25612-25619

18. Dixon, F.J., Maurer, P.H., Deichmiller, M.P. (1953) Half-lives of homologous serum albumins in several species. *Proc. Soc. Exp. Biol. Med.* **83**, 287-288

19. Peters, T., Jr. (1985) Serum albumin. *Adv. Protein Chem.* **37**, 161-245

20. Schmidt, M.M., Townson, S.A., Andreucci, A.J., King, B.M., Schirmer, E.B., Murillo, A.J., Dombrowski, C., Tisdale, A.W., Lowden, P.A., Masci, A.L., Kovalchin, J.T., Erbe, D.V., Wittrup, K.D., Furfine, E.S., Barnes, T.M. (2013) Crystal structure of an HSA/FcRn complex reveals recycling by competitive mimicry of HSA ligands at a pH-dependent hydrophobic interface. *Structure* **21**, 1966-1978

21. Morais, M., Cantante, C., Gano, L., Santos, I., Lourenço, S., Santos, C., Fontes, C., Aires da Silva, F., Gonçalves, J., Correia, J.D. (2014) Biodistribution of a ^{67}Ga-labeled anti-TNF VHH single-domain antibody containing a bacterial albumin-binding domain (Zag). *Nucl. Med. Biol.* pii: S0969-8051(14)00012-22

22. Coppieters, K., Dreier, T., Silence, K., de Haard, H., Lauwereys, M., Casteels, P., Beirnaert, E., Jonckheere, H., Van de Wiele, C., Staelens, L., Hostens, J., Revets, H., Remaut, E., Elewaut, D., Rottiers, P. (2006) Formatted anti-tumor necrosis factor alpha VHH proteins derived from camelids show superior potency and targeting to inflamed joints in a murine model of collagen-induced arthritis. *Arthritis Rheum.* **54**, 1856-1866

23. Neumann, E., Frei, E., Funk, D., Becker, M.D., Schrenk, H.H., Müller-Ladner, U., Fiehn, C. (2010) Native albumin for targeted drug delivery. *Expert. Opin. Drug Deliv.* **7**, 915-925

24. Ballantyne, F.C., Fleck, A., Dick, W.C. (1971) Albumin metabolism in rheumatoid arthritis. *Ann. Rheum. Dis.* **30**, 265-270

25. Wilkinson, P., Jeremy, R., Brooks, F.P., Hollander, J.L. (1965) The mechanism of hypoalbuminemia in rheumatoid arthritis. *Ann. Intern. Med.* **63**, 109-114

26. Levick, J.R. (1981) Permeability of rheumatoid and normal human synovium to specific plasma proteins. *Arthritis Rheum.* **24**, 1550-1560

27. Wunder, A., Müller-Ladner, U., Stelzer, E.H., Funk, J., Neumann, E., Stehle, G., Pap, T., Sinn, H., Gay, S., Fiehn, C. (2003) Albumin-based drug delivery as novel therapeutic approach for rheumatoid arthritis. *J. Immunol.* **170**, 4793-4801

28. Fiehn, C., Müller-Ladner, U., Gay, S., Krienke, S., Freudenberg-Konrad, S., Funk, J., Ho, A.D., Sinn, H., Wunder, A. (2004) Albumin-coupled methotrexate (MTX-HSA) is a new anti-arthritic drug which acts synergistically to MTX. *Rheumatology* **43**, 1097-1105

29. Fiehn, C., Neumann, E., Wunder, A., Krienke, S., Gay, S., Müller-Ladner, U. (2004) Methotrexate (MTX) and albumin coupled with MTX (MTX-HSA) suppress synovial fibroblast invasion and cartilage degradation in vivo. *Ann. Rheum, Dis.* **63**, 884-886

30. Sjölander, A., Nygren, P.-Å., Ståhl, S., Berzins, K., Uhlén, M., Perlmann, P., Andersson, R. (1997) The serum albumin-binding region of streptococcal protein G: a bacterial fusion partner with carrier-related properties. *J. Immunol. Methods* **201**, 115-123

31. De Groot, A.S., Knopp, P.M., Martin, W. (2005) De-immunization of therapeutic proteins by T-cell epitope modification. *Dev. Biol.* **122**, 171-194

32. Baker, M.P., Jones, T.D. (2007) Identification and removal of immunogenicity in therapeutic proteins. *Curr. Opin. Drug. Discov. Devel*. **10**, 219-227

33. Nagata, S., Pastan, I. (2009) Removal of B cell epitopes as a practical approach for reducing the immunogenicity of foreign protein-based therapeutics. *Adv. Drug. Deliv. Rev.* **61**, 977-985

ABBREVIATIONS

ABD, albumin-binding domain; AUC, area under the curve; FcRn, neonatal Fc receptor; HSA, human serum albumin; IgG, immunoglobulin G; PEG, polyethylene glycol; MSA, mouse serum albumin; RSA, rat serum albumin; TNFα, tumour necrosis factor, VHH, camelid single-domain antibody or nanobody; Zag, ABD from streptococcal cell surface ZAG protein.

ACKNOWLEDGMENTS

Fundação para a Ciência e a Tecnologia (FCT), Portugal, is acknowledged for funding (project PTDC/SAU-FAR/115846/2009). C. Cantante e M. Morais thank the FCT for PhD fellowships (SFRH/BD/48598/2008 and SFRH/BD/48066/2008, respectively). We thank Dr. C. Xavier and Prof. V. Cavaliers for a generous gift of p-SCN-Bn-NOTA and fruitful discussions.

FIGURE LEGENDS

Fig. 1: Construction and expression of VHH and VHH-Zag. (A) Schematic representation of the VHH and VHH-Zag constructs including the N-terminal leader peptide (LP), the C-terminal histidine (His_7) and HA tags. (B) Sequence of the wild-type ZAG ABD[9]. (C) SDS-PAGE and (D) Western Blot analysis of the VHH and VHH-Zag purified proteins (3 µg/lane) under reducing (lanes 1 and 2) and non-reducing conditions (lanes 3 and 4). Gels were stained with Coomassie brilliant blue (C) or immunoblotted with an anti-HA-tag antibody (D).

Fig. 2: Binding of VHH and VHH-Zag to human TNFα. ELISA plates were coated with human TNFα (200 ng/well) and binding of VHH and VHH-Zag fusion protein was measured in the presence (A) and absence (B) of HSA (1 mg/ml). Detection was achieved using an HRP-conjugated anti-HA-tag antibody.

Fig. 3: Binding of VHH-Zag to human, rat and mouse albumin. Binding of VHH-Zag fusion protein was evaluated in ELISA at neutral pH - pH 7.4 (A); and acidic pH - pH 6.0 (B). Bound proteins were detected using an HRP-conjugated anti-HA-tag antibody.

Fig. 4: Binding affinity measurements. Representative sensorgrams from Biacore SPR-analysis of VHH-Zag against immobilized HSA, RSA and MSA. Binding curves were fitted in triplicates. VHH was used as control.

Fig. 5: Formation of VHH-Zag/albumin complexes. Size exclusion chromatography analysis of VHH-Zag (A), HSA (B), VHH-Zag/HSA complex (C), MSA (D) and VHH-Zag/MSA complex (E). VHH-Zag was incubated at equimolar concentrations with albumin in PBS1x at room temperature. Peak positions of marker proteins are indicated.

Fig. 6: TNFα-neutralization of VHH and VHH-Zag. Dose-response curves of VHH and VHH-Zag proteins to examine the TNFα-mediated cytoxicity in the presence of 0.5 ng/ml human TNFα, on the TNF-sensitive mouse fibroblast cell line L929.

Fig. 7: *In vitro* stability in human and mouse serum of VHH and VHH-Zag. *In vitro* stability of the recombinant proteins was determined in human serum (A) and mouse serum (B) at 37 ºC, during 24 days and 4 days, respectively. Proteins were detected by Western Blot, using an anti-His-tag antibody.

Fig. 8: Pharmacokinetic properties. Both VHH and VHH-Zag fusion protein were i.v. injected into CD-1 mice (25 µg/animal) and absorbance pharmacokinetic profiles of these proteins were calculated by ELISA. Data were normalized considering maximal concentration at the first time point (5 min).

Fig. 9: *In vivo* stability in mouse serum of VHH and VHH-Zag. *In vivo* stability of VHH-Zag (A) and VHH (B) was evaluated by Western Blot with anti-HA-tag antibody, in the mice serum samples collected during the pharmacokinetic assay.

Fig. 10: Biodistribution $^{99m}Tc(CO)_3$-VHH and $^{99m}Tc(CO)_3$-VHH-Zag. Organ distribution of ^{99m}Tc-VHH (A) and ^{99m}Tc-VHH-Zag (B) proteins in CD-1 mice.

TABLES

Table 1: Binding of VHH-Zag to HSA, RSA and MSA.

Protein	**EC_{50} for HSA (nM)**	**EC_{50} for RSA (nM)**	**EC_{50} for MSA (nM)**
VHH-Zag pH 6.0	0.324 ± 0.06	0.377 ± 0.07	0.175 ± 0.07
VHH-Zag pH 7.4	1.074 ± 0.03	1.698 ± 0.06	4.354 ± 0.08

Table 2: Affinities of VHH-Zag for HSA, RSA and MSA by SPR measurements.

Protein	***K*on ($M^{-1}s^{-1}$)**	***K*off (s^{-1})**	***K*off/Kon**	**K_D**
HSA	$8.68x10^{4}$± 0.42	$3.96x10^{-4}$± 0.07	$4.57x10^{-9}$± 0.22	4.57 ± 0.42 nM
RSA	$1.06x10^{5}$± 0.02	$4.41x10^{-5}$± 0.08	$4.15x10^{-10}$± 0.01	0.42 ± 0.01 nM
MSA	$9.88x10^{4}$± 0.18	$4.26x10^{-3}$± 0.14	$4.06x10^{-8}$± 0.12	40.6 ± 2.1 nM

Table 3: Molecular mass and hydrodynamic radius.

Protein or complex	Length	Calculated M_r[a]	SEC apparent M_r	Stokes' radius (R_S)
	aa	kDa	kDa	nm
VHH	180	19.4	14.9	1.84
VHH-Zag	235	25.2	26.4	2.59
HSA	585	66.5	68.1	3.67
MSA	584	65.9	64.3	3.60
VHH-Zag/HSA	−	91.7	101.2	4.16
VHH-Zag/MSA	−	91.1	98.6	4.01

[a]Calculated based on the amino acid sequence.

Table 4: Thermal stability of VHH and VHH-Zag.

Protein	**Tm B - Mean (°C)**	**Tm B – Median (°C)**	**Tm D - Mean (°C)**	**Tm D - Median (°C)**
VHH	71.53 ± 0.14	71.56 ± 0.14	72.34 ± 0.25	72.43 ± 0.25
VHH-Zag	69.77 ± 0.14	69.87 ± 0.14	70.24 ± 0.23	70.24 ± 0.23

Tm B - Calculated Boltzamnn melting temperature; Tm D - Calculated Derivated melting temperature.

Table 5: Pharmacokinetic parameters of VHH and VHH-Zag.

Protein	$t_{1/2}\alpha$ (h)	$t_{1/2}\beta$ (h)	$AUC_{(0\text{-}24\ h)}$ (%*h)
VHH	0.52 ± 0.25	0.79 ± 0.12	72.75 ± 7.35
VHH-Zag	3.21 ± 0.30	30.55 ± 0.14	1461.15 ± 152,98

Table 6: Biodistribution of ^{99m}Tc VHH (values presented as mean±SD % injected activity/organ weight (g); CV%[a]).

Organ	0.08 h	0.50	1.0	4.0	24	48
Blood	6.02 ± 1.06 ; 18%	1.22 ± 0.47; 39%	0.98 ± 0.30; 30%	0.30 ± 0.02; 8%	0.07 ± 0.05; 67%	0.04 ± 0.01; 14%
Liver	1.94 ± 0.34; 18%	2.22 ± 0.24; 11%	0.58 ± 0.19; 33%	0.51 ± 0.21; 41%	0.35 ± 0.15; 44%	0.45 ± 0.05; 11%
Intestine	1.51 ± 0.15; 10%	0.13 ± 0.01; 10%	0.24 ± 0.06; 24%	0.32 ± 0.10; 30%	0.09 ± 0.05; 55%	0.06 ± 0.02; 31%
Spleen	1.22 ± 0.14; 11%	1.41 ± 0.84; 60%	0.31 ± 0.12; 39%	0.34 ± 0.07; 21%	0.21 ± 0.16; 73%	
Heart	2.24 ± 0.26; 12%	0.46 ± 0.06; 12%	0.36 ± 0.16; 44%	0.19 ± 0.03; 16%	0.06 ± 0.01; 11%	
Lung	6.31 ± 1.81; 29%	4.78 ± 0.98; 20%	0.98 ± 0.12; 12%	0.51 ± 0.04; 9%	0.34 ± 0.26; 77%	
Kidney	107.67 ± 15.39; 14%	116.97 ± 15.27 ; 13%	134.74 ± 12.39; 9%	178.43 ± 34.81; 20%	57.37 ± 5.52; 10%	38.08 ± 15.08; 40%
Muscle	1.55 ± 0.26; 17%	0.42 ± 0.05; 12%	0.32 ± 0.09; 28%	0.08 ± 0.03; 36%	0.03 ± 0.00; 16%	
Bone	1.64 ± 0.23; 14%	0.43 ± 0.04; 10%	0.29 ± 0.05; 18%	0.08 ± 0.02; 20%	0.05 ± 0.00; 8%	
Stomach	0.62 ± 0.24; 38%	0.12 ± 0.03; 28%	0.34 ± 0.17; 50%	0.30 ± 0.15; 51%	0.06 ± 0.03 ; 52%	
Pancreas	1.20 ± 0.13; 11%	0.31 ± 0.09; 28%	0.22 ± 0.07; 32%	0.13 ± 0.04; 27%	0.05 ± 0.00; 6%	

[a]% CV: coefficient of variation %.

Table 7: Biodistribution of ^{99m}Tc VHH-Zag (values presented as mean±SD % injected activity/organ weight (g); CV%[a]).

Organ	0.08 h	0.50 h	1.0 h	4.0 h	24 h	48 h
Blood	33.70; 12%	5.83; 24%	10.17; 28%	6.95; 22%	1.73; 34%	2.07; 33%
Liver	8.56; 17%	7.39; 8%	11.96; 20%	9.44; 69%	2.73; 40%	1.74; 25%
Intestine	0.42; 20%	0.33; 54%	0.77; 12%	2.64; 64%	0.26; 38%	0.32; 59%
Spleen	4.12; 27%	5.49; 19%	12.54; 36%	2.70; 58%	1.82; 61%	
Heart	6.00; 39%	1.82; 23%	1.76; 7%	1.68;27%	0.64; 83%	
Lung	10.64;45%	3.13; 15%	2.43; 52%	1.73; 21%	0.60; 52%	
Kidney	13.50; 13%	28.52; 11%	29.08; 22%	25.17; 27%	8.18; 4%	3.82; 30%
Muscle	1.16; 11%	0.63; 18%	0.68; 14%	0.31; 75%	0.27; 4%	
Bone	2.44; 25%	0.86; 10%	1.17; 12%	0.47; 14%	0.42; 12%	
Stomach	0.28; 41%	0.26; 30%	0.87; 29%	2.10; 81%	0.10 12%	
Pancreas	1.40; 22%	0.61; 13%	0.74; 8%	0.40; 78%	0.24; 45%	

[a]% CV: coefficient of variation %.

Table 8: Organ to blood ratio of ^{99m}Tc-VHH and ^{99m}Tc-VHH-Zag at 24 h time point.

Organ	VHH	VHH-Zag
Liver	11.3	1.82
Intestine	3.42	0.365
Spleen	0.413	0.129
Heart	0.122	0.0342
Lung	1.80	0.0505
Kidney	390	1.37
Muscle	4.77	1.14
Bone	2.09	0.442
Stomach	0.600	0.0514
Pancreas	0.140	0.0189

Figure 1

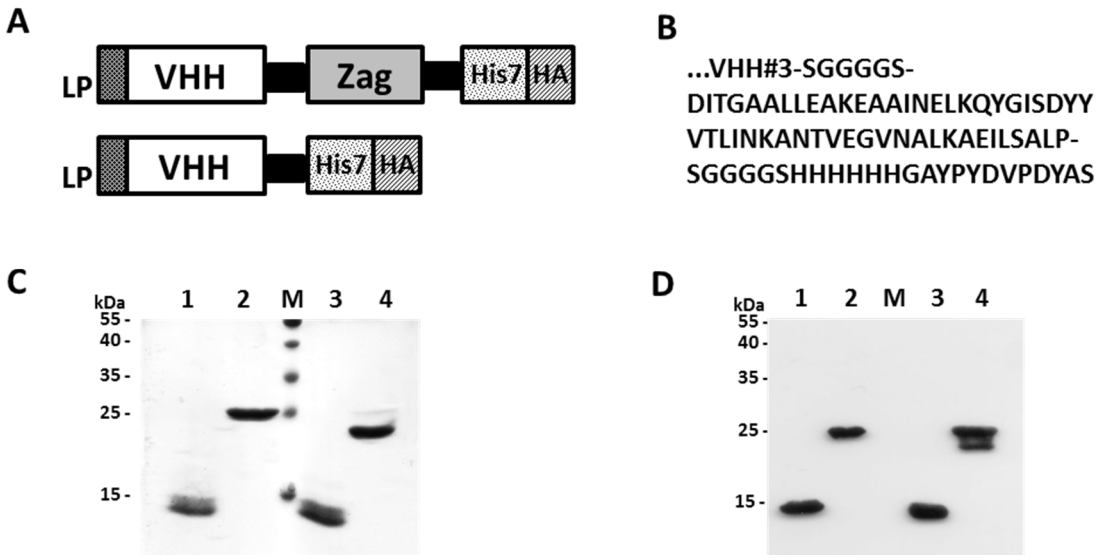
A
LP
VHH
Zag
His7
HA
LP
VHH
His7
HA
B
...VHH#3-SGGGGS-
DITGAALLEAKEAAINELKQYGISDYY
VTLINKANTVEGVNALKAEILSALP-
SGGGGSHHHHHHGAYPYDVPDYAS
C
kDa
1
2
M
3
4
55 -
40 -
35 -
25 -
15 -
D
kDa
1
2
M
3
4
55 -
40 -
35 -
25 -
15 -

Figure 2

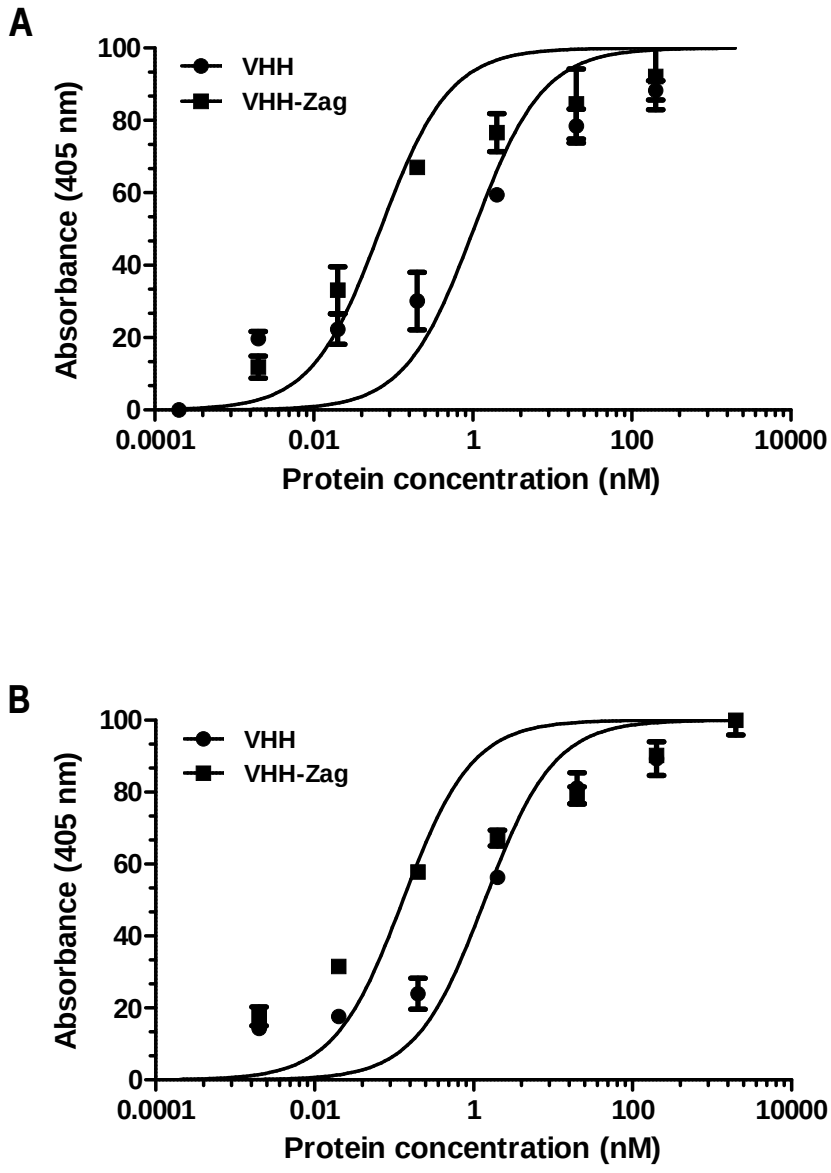
A
VHH
VHH-Zag
Absorbance (405 nm)
Protein concentration (nM)
0
20
40
60
80
100
0.0001
0.01
1
100
10000
B
VHH
VHH-Zag
Absorbance (405 nm)
Protein concentration (nM)
0
20
40
60
80
100
0.0001
0.01
1
100
10000

Figure 3

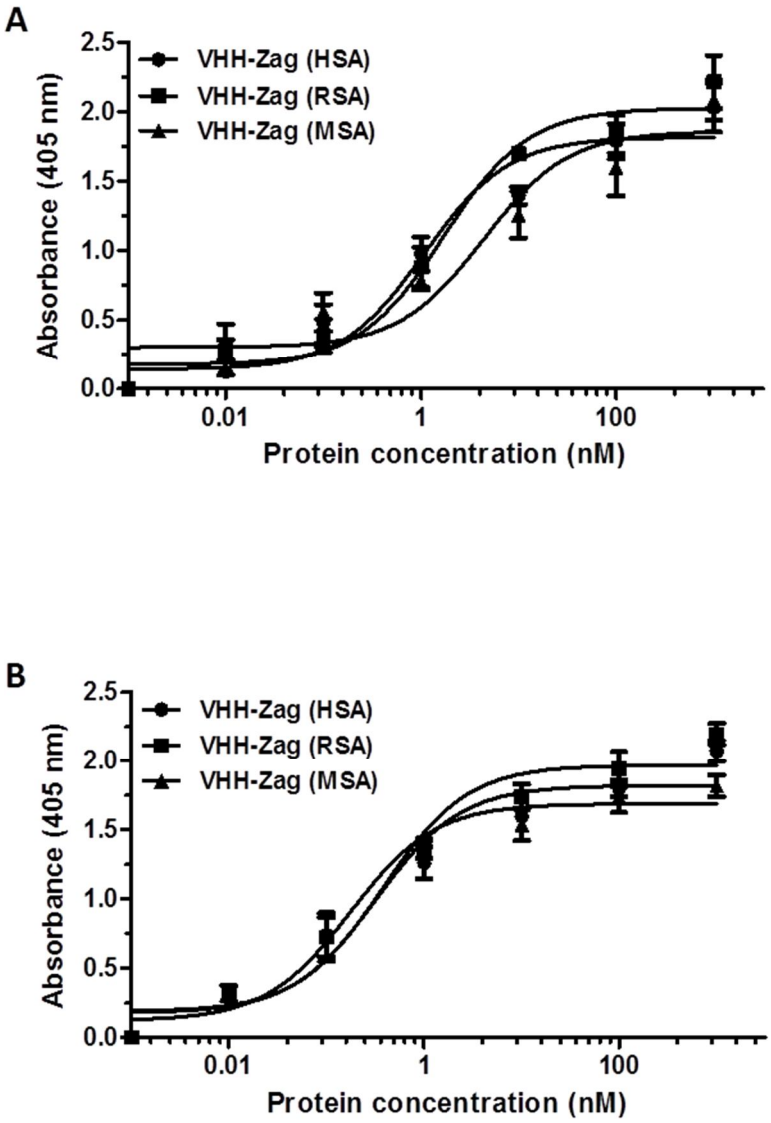
A
VHH-Zag (HSA)
VHH-Zag (RSA)
VHH-Zag (MSA)
Absorbance (405 nm)
2.5
2.0
1.5
1.0
0.5
0.0
0.01
1
100
Protein concentration (nM)
B
VHH-Zag (HSA)
VHH-Zag (RSA)
VHH-Zag (MSA)
Absorbance (405 nm)
2.5
2.0
1.5
1.0
0.5
0.0
0.01
1
100
Protein concentration (nM)

Figure 4

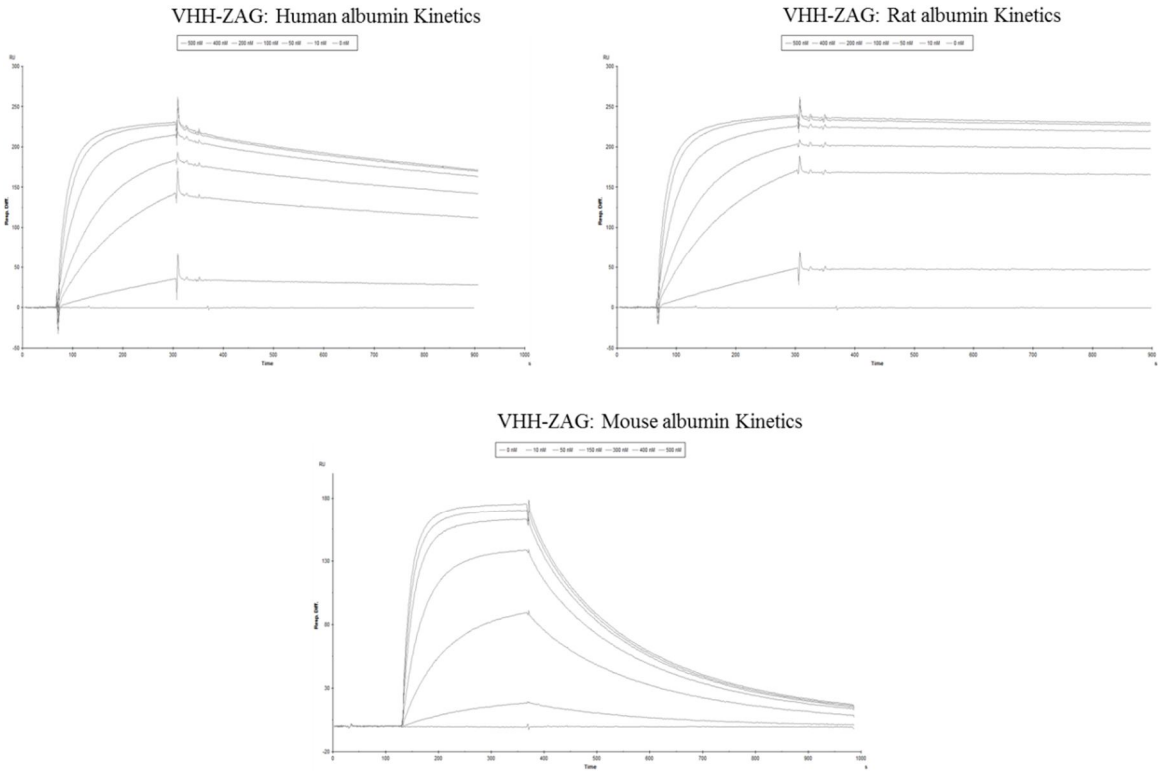
VHH-ZAG: Human albumin Kinetics
VHH-ZAG: Rat albumin Kinetics
VHH-ZAG: Mouse albumin Kinetics

Figure 5

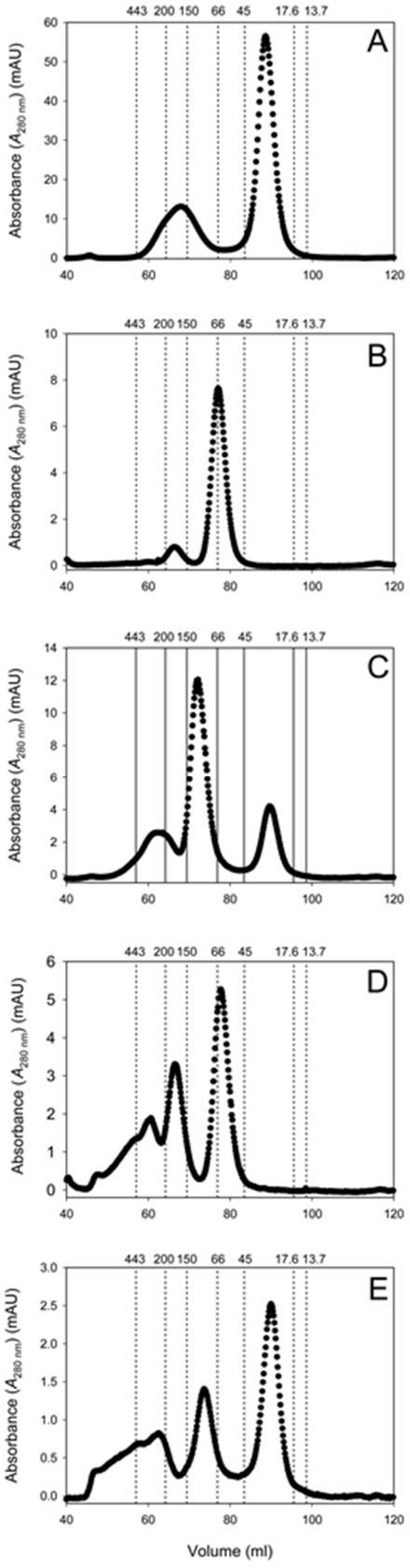
443 200 150 66 45 17.6 13.7
A
B
C
D
E
Absorbance ($A_{280\ nm}$) (mAU)
Volume (ml)

Figure 6

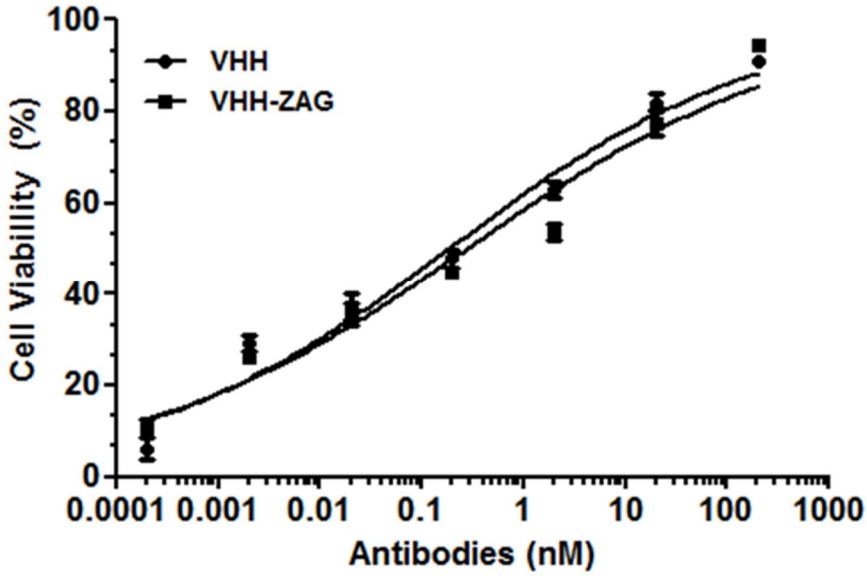
VHH
VHH-ZAG
Cell Viabillity (%)
100
80
60
40
20
0
0.0001
0.001
0.01
0.1
1
10
100
1000
Antibodies (nM)

Figure 7

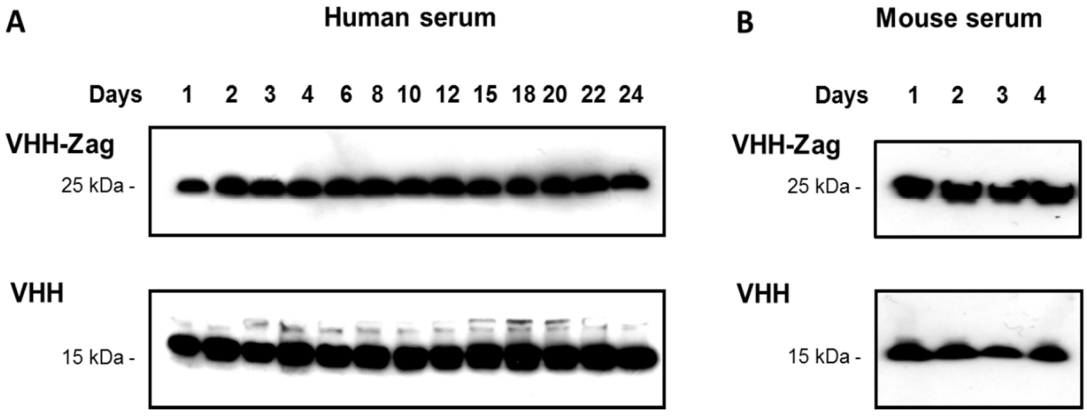
A
Human serum
Days 1 2 3 4 6 8 10 12 15 18 20 22 24
VHH-Zag
25 kDa -
VHH
15 kDa -
B
Mouse serum
Days 1 2 3 4
VHH-Zag
25 kDa -
VHH
15 kDa -

Figure 8

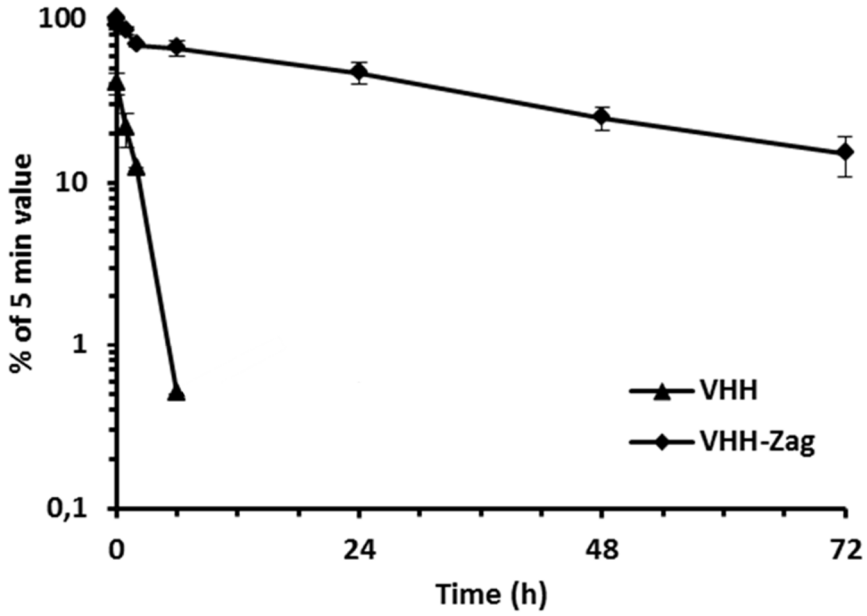

Figure 9

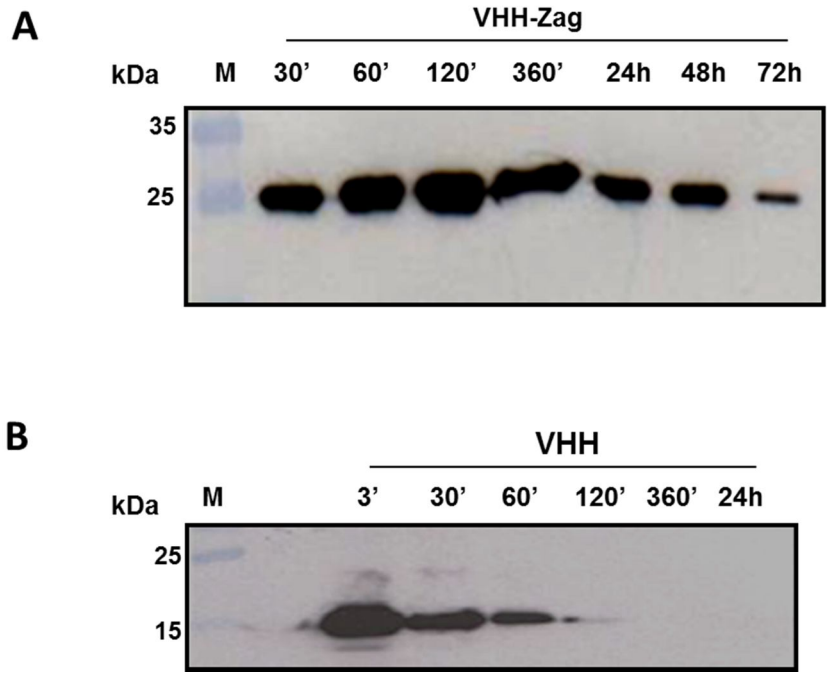
A
VHH-Zag
kDa
M
30’
60’
120’
360’
24h
48h
72h
35
25
B
VHH
kDa
M
3’
30’
60’
120’
360’
24h
25
15

Figure 10

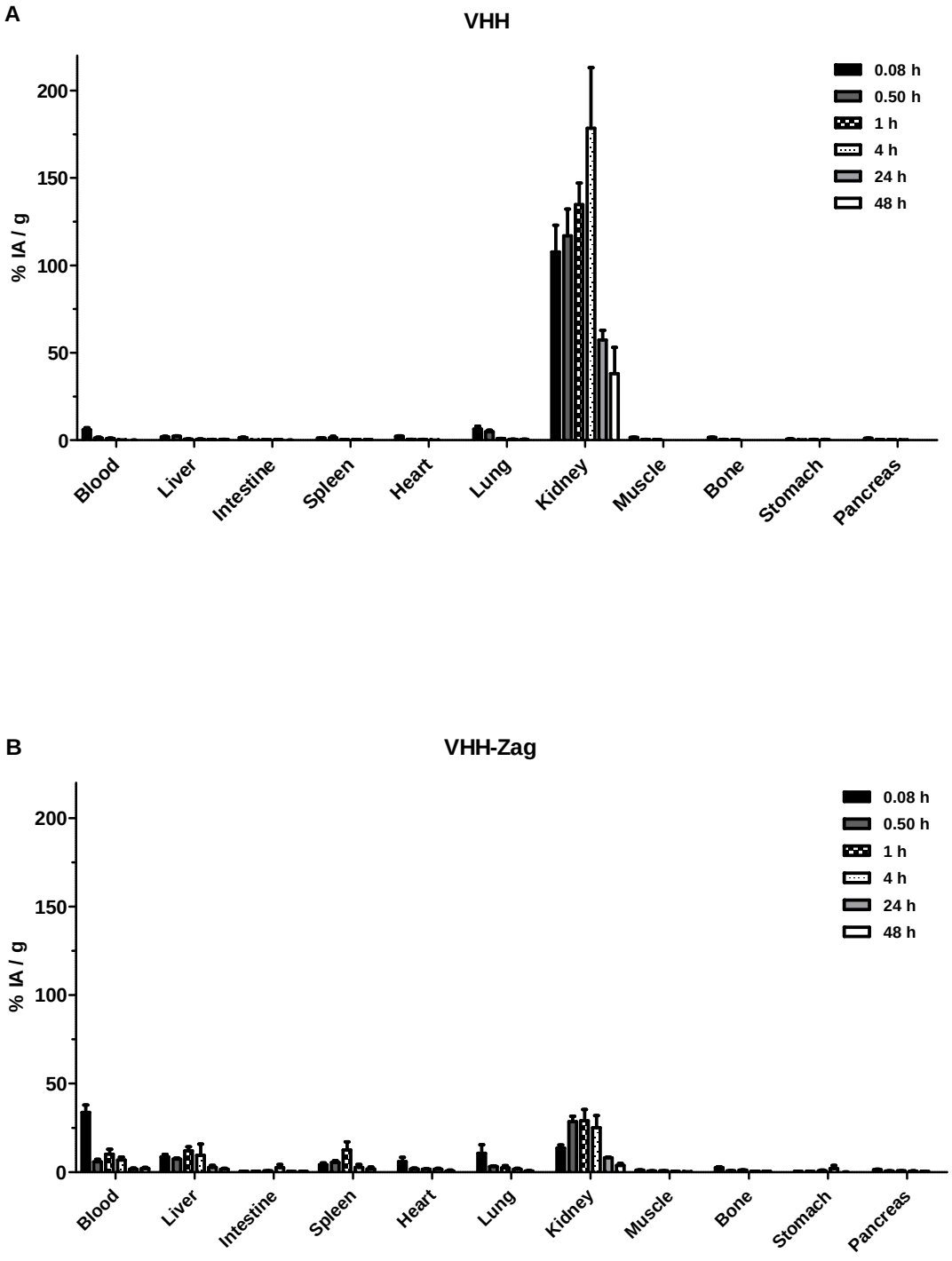
A
VHH
% IA / g
0
50
100
150
200
0.08 h
0.50 h
1 h
4 h
24 h
48 h
Blood
Liver
Intestine
Spleen
Heart
Lung
Kidney
Muscle
Bone
Stomach
Pancreas
B
VHH-Zag
% IA / g
0
50
100
150
200
0.08 h
0.50 h
1 h
4 h
24 h
48 h
Blood
Liver
Intestine
Spleen
Heart
Lung
Kidney
Muscle
Bone
Stomach
Pancreas

BIODISTRIBUTION OF A ^{67}GA-LABELED ANTI-TNF VHH SINGLE-DOMAIN ANTIBODY CONTAINING A BACTERIAL ALBUMIN-BINDING DOMAIN (ZAG)

Brief Introduction

Bacterial albumin-binding domains have been extensively studied and used as fusion proteins to improve the half-life of recombinant antibodies formats or therapeutic proteins (Kontermann, 2011).

ZAG is a cell-surface protein G-related from *S. zooepidemicus*, with an Ig-binding region located in the C-terminus, and an ABD composed by 52 amino acids (Jonsson *et al*., 1994).

In this research work we used ^{67}Ga-radiolabelling to investigate the organ biodistribution of protein ZAG ABD (Zag) fusion with an anti-TNFα VHH from Ablynx, used as a study model to validate our strategy to increase circulation time of therapeutic proteins.

Firstly, we intend to optimize the production of the recombinant proteins (VHH and VHH-Zag) in *E.coli*, an easy way to obtain high amounts of protein with lower costs. Furthermore, we analyze the human serum albumin and TNFα binding of VHH and VHH-Zag proteins, after the conjugation with NOTA and ^{67}GA-NOTA radiolabelling, in order to see if the chemical process could affect the binding properties of the recombinant antibodies. Finally, we evaluate the organ biodistribution profiles of both proteins.

Nuclear Medicine and Biology xxx (2014) xxx–xxx

Contents lists available at ScienceDirect

Nuclear Medicine and Biology

journal homepage: www.elsevier.com/locate/nucmedbio

Biodistribution of a ^{67}Ga-labeled anti-TNF VHH single-domain antibody containing a bacterial albumin-binding domain (Zag)

Maurício Morais [a,1], Cátia Cantante [b,c,1], Lurdes Gano [a], Isabel Santos [a], Sara Lourenço [d], Catarina Santos [b,c], Carlos Fontes [e], Frederico Aires da Silva [d], João Gonçalves [b,c], João D.G. Correia [a,*]

[a] Centro de Ciências e Tecnologias Nucleares, Instituto Superior Técnico, Universidade de Lisboa, Estrada Nacional 10, ao km 139.7, 2695–066 Bobadela LRS, Portugal
[b] CBM–URIA Fac. Farmácia, Universidade de Lisboa, Av. Prof. Gama Pinto, 1649–003 Lisboa, Portugal
[c] IMM, Fac. Med., Universidade de Lisboa, Av. Prof. Egas Moniz 1649–028 Lisboa, Portugal
[d] TechnoPhage S.A., Av. Prof. Egas Moniz, Edifício Egas Moniz Piso 2, 1649–028 Lisboa, Portugal
[e] Fac. Med. Veterinária, Universidade de Lisboa, Av. da Universidade Técnica 1300–477 Lisboa, Portugal

ARTICLE INFO

istory:
l 27 September 2013
l in revised form 3 January 2014
l 10 January 2014
Available online xxxx

Keywords:
Albumin-binding domain
Biodistribution
Gallium-67
Plasma half-life
Single-domain antibodies

ABSTRACT

Introduction: Small domain antibodies (sdAbs) present high potential for both molecular *in vivo* imaging and therapy. Owing to the low molecular weight they are rapidly cleared from blood circulation, and new strategies to extend their half-lifes are needed for therapeutic applications. We have selected a bacterial albumin-binding domain (ABD) from protein Zag to be fused to an anti-tumor necrosis factor (TNF) single variable-domain heavy-chain region antibody (VHH) to delay blood clearance, and evaluated the biodistribution profile of the fusion protein.

Methods: The anti-TNF VHH and the fusion protein VHH-Zag were conjugated to S-2-(4-isothiocyanatobenzyl)-1,4,7-triazacyclononane-1,4,7-triacetic acid (p-SCN-Bn-NOTA). The anti-TNF and albumin-binding properties of the conjugates NOTA-VHH and NOTA-VHH-Zag were assessed by enzyme-linked immunosorbent assay (ELISA). The radioconjugates ^{67}Ga-NOTA-VHH and ^{67}Ga-NOTA-VHH-Zag were obtained by reaction of $^{67}GaCl_3$ with the corresponding conjugates at room temperature. Biodistribution studies were performed in healthy female CD-1 mice.

Results: The immunoreactivity of the VHH-based proteins is preserved upon conjugation to NOTA as well as after radiometallation. The radiochemical purity of the radioconjugates was higher than 95% as determined by ITLC-SG after purification by gel filtration. The biodistribution studies showed that the Zag domain affected the pharmacokinetic properties of VHH, with impressive differences in blood clearance (0.028 ± 0.004 *vs* 1.7 ± 0.8 %I.A./g) and total excretion (97.8 ± 0.6 *vs* 25.5 ± 2.1 %I.A.) for ^{67}Ga-NOTA-VHH and ^{67}Ga-NOTA-VHH-Zag, respectively, at 24 h p.i.

Conclusion: The Zag domain prolonged the circulation time of VHH by reducing the blood clearance of the labeled fusion protein ^{67}Ga-NOTA-VHH-Zag. In this way, the anti-TNF VHH in fusion with the Zag ABD presents a higher therapeutic potential than the unmodified VHH.

1. Introduction

The great majority of therapeutic antibodies marketed are full-length Immunoglobulin G (IgG) molecules that trigger effector functions and present long serum half-life [1]. Indeed, their high molecular weight (~150 kDa) leads to long residence time in blood circulation. Additionally, IgG antibodies diffuse poorly into solid tumors, and clear slowly from the body [1]. Despite their recognized potential for *in vivo* imaging applications, those features lead to poor contrast, which strongly hampers the wide use of antibodies as tracers for target-specific molecular imaging [2,3]. The same holds true for targeted radionuclide therapy of solid tumors using immunoglobulins. Indeed, the long half-life results in irradiation of non-target organs and tissues, and slow extravasation and penetration into the tumor, limiting the radiotherapeutic effect [3,4]. Overall, the drawbacks associated to IgGs, together with the rapid progress in recombinant technologies led to the development of smaller engineered antibodies and proteins, such as single-chain variable fragments (scFvs), sdAbs and affibodies [1–5]. However, due to their lower molecular weight, these proteins present in general significantly shorter half-lifes and very rapid blood clearance, which hampers therapeutic applications, e.g. requiring infusions or repeated injections to maintain a therapeutically effective dose over a prolonged period of time [6]. Aiming to address this issue, several approaches have been proposed to extend plasma half-lifes of therapeutic proteins and, consequently, improve their overall

* Corresponding author. Tel.: +351 21 994 62 33.
E-mail address: jgalamba@itn.pt (J.D.G. Correia).
[1] These authors contributed equally to the article.

0969-8051/$ – see front matter © 2014 Elsevier Inc. All rights reserved.
http://dx.doi.org/10.1016/j.nucmedbio.2014.01.009

Please cite this article as: Morais M., et al, Biodistribution of a ^{67}Ga-labeled anti-TNF VHH single-domain antibody containing a bacterial albumin-binding domain (Zag), Nucl Med Biol (2014), http://dx.doi.org/10.1016/j.nucmedbio.2014.01.009

biological properties. Some of these strategies aim at increasing the hydrodynamic volume of the molecules, thus reducing renal filtration and degradation. Among the various explored approaches, the noncovalent association of a therapeutic protein to plasma proteins, namely to albumin, or fusion of ABDs, peptides or low-molecular-weight albumin binders emerged as quite promising [7–10]. Human serum albumin (HSA) is the most abundant blood plasma protein and is produced in the liver as a monomeric protein of 67 kDa. Albumin presents an extraordinary long circulation half-life of approximately 19 days in humans and 3 days in mice, as a direct result of its size and interaction with the FcRn mediated recycling pathway [8,11]. Furthermore, HSA accumulates in tumors as well as arthritic joints and is a valuable biomarker of many diseases, including cancer, rheumatoid arthritis, and ischemia, among others [11].

ABDs have also been used for improvement of the biological properties of radiolabeled affibodies for systemic radiotherapy, with remarkable reduction of renal accumulation of radioactivity [10,12,13]. More recently, Müller et al. reported a ^{177}Lu-labeled folate conjugate containing an albumin-binding group (4-(*p*-iodophenyl) butyric acid derivative), which presented a significant increase of the tumor-to-kidney ratio of radioactivity compared to the radioconjugate were the albumin-binding group is absent.

We and others have been exploiting bacterial ABDs fused to antibody fragments to prolong the half-life of the resulting fusion proteins [7,8,14,15].

The study presented herein aims at assessing the biodistribution profile of an anti-TNF VHH fused to the Zag ABD (VHH-Zag) isolated from Zag protein, which is a G-related protein from the surface of *Streptococcus zooepidemicus* [16]. To achieve this goal, the fusion protein was conjugated to p-SCN-Bn-NOTA derivative to yield the conjugate NOTA-VHH-Zag, which was labeled with gallium-67 (^{67}Ga). The tissue distribution of the radiolabeled fusion protein (^{67}Ga-NOTA-VHH-Zag) was evaluated in CD-1 mice and the results were compared with those obtained with ^{67}Ga-NOTA-VHH, prepared as control tracer.

2. Materials and methods

SEP-PAK SI cartridges were purchase from Waters. Amicon centrifugal filter (M.W. cut-off = 10 kDa) units and PD-10 columns were purchase from Millipore and GE Healthcare, respectively. Gallium-67 citrate was a gift from the nuclear medicine service of Hospital de Santa Maria (Lisbon, Portugal). Gallium-67 chloride was prepared from Gallium-67 citrate as described in the literature [17]. Diethylenetriaminepentaacetic acid (DTPA) was purchased from Sigma Aldrich. Instant Thin Layer Cromatography (ITLC): Analysis was performed using ITLC-SG Varian and Whatman nº1 strips eluted with the systems:

System A: 2 % HCl 0.5 M in Saline. $^{67}GaCl_3$ migrates in the front of the solvent (Rf = 1), while the radioactive VHH and VHH-Zag stay at the origin (Rf = 0).

System B: 55% MeOH in water. Complex ^{67}Ga-DTPA migrates in the front of the solvent (Rf = 1), $^{67}GaCl_3$ presents some mobility (Rf = 0.4), while the radiolabeled antibody fragments VHH and VHH-Zag stay at the origin (Rf = 0).

Radioactivity distribution on the ITLC strips was detected by a radioactive scanner (Berthold LB 2723, Germany) equipped with 20 mm diameter NaI(Tl) scintillation crystal. Radioactivity measurements were done on a dose calibrator (Aloka Curiemeter, IGC-3, Japan) or on a gamma-counter (Berthold LB 2111, Germany).

2.1. Construction of VHH and VHH-Zag fusion protein

DNA encoding the anti-TNF VHH 3E clone [18] was synthesised by Nzytech adding a *Sfi*I restriction site at 5' and 3' ends, respectively, for cloning into the pComb3x plasmid. pComb3X contains a peptide leader (PL) and sequences encoding peptide tags for purification (6-His) and detection (HA). A fragment encoding the PL-VHH-HIS-HA was generated by PCR and subcloned into the expression vector pT7 (Sigma-Aldrich) into the *Kpn*I and *Hind*III restriction sites. To construct the VHH-Zag fusion, a DNA fragment comprising the entire Zag albumin-binding domain of *Streptococcal* was generated using PCR and adding *Spe*I and *Nco*I restriction sites at the fragment 5' and 3' ends, respectively. The resulting PCR fragments were gel-purified, digested with the *Spe*I and *Nco*I restriction enzymes and cloned into the appropriately cut pT7-PL-VHH-HIS-HA vector. The VHH and VHH-Zag constructs were verified by sequencing.

2.2. Expression and purification of VHH and VHH-Zag

The VHH and VHH fused with the Zag (VHH-Zag) cloned in the pT7 expression vector were expressed in *Escherichia coli* BL21 (DE3) cells. Both VHH and VHH-Zag constructions were confirmed by sequencing. One liter of LB with 100 μg/mL ampicilin was inoculated with 10 mL of overnight culture of transformed BL21 (DE3) and grown to exponential phase (A_{600} = 0,6-0,8) at 37 ºC. Protein expression was induced by addition of 1 mM isopropyl 1-thiol-β-D-galactopyranoside and bacteria were grown 16 h at 18 ºC. Cells were harvested by centrifugation and ressupended in 50 mM HEPES, 1 M NaCl, 5 mM $CaCl_2$, pH 7.5. The pellet was sonicated at 4 ºC during 20 min and centrifuged at 10.000 rpm for 30 min at 4 ºC. Supernatant was purified by immobilized metal affinity chromatography (IMAC), using HP HisTrap columns and the AKTA FPLC system from GE Healthcare [14,15]. After purification, the purity (>95%) of the eluted samples was analyzed by sodium dodecyl sulfate-polyacrylamide gel electrophoresis (SDS-PAGE). The SDS-PAGE analysis of the purified VHH and VHH-Zag samples is presented in Supporting information (Fig. 1S). ExPASy - ProtParam tool was used to estimate the extinction coefficient of VHH and VHH-Zag (ε_{VHH} = 34380 L mol^{-1} cm^{-1}; $\varepsilon_{VHH\text{-}Zag}$ = 38850 L mol^{-1} cm^{-1}).

2.3. Conjugation of p-SCN-Bn-NOTA to VHH and VHH-Zag

The VHH-based antibodies were conjugated to p-SCN-Bn-NOTA as described in the literature [19]. Briefly, VHH or VHH-Zag in 0.05 M sodium carbonate buffer, pH 8.7 (1.5 mL), was added to p-SCN-Bn-NOTA (10-fold molar excess) and incubated for 2 h at room temperature. The coupling reaction was quenched by adjusting the pH to 7.0 – 7.4 using HCl, 1 M. The conjugate was then purified by gel filtration using a HiPrep™ 16/60 Sephacryl™ S-100 High Resolution column purchased from GE Healthcare and 50 mM HEPES, 200 mM NaCl, 5 mM $CaCl_2$, pH 7.5, as eluent. The concentration of NOTA-VHH and NOTA-VHH-Zag was determined at 280 nm using Nanodrop ND-1000 spectrophotometer and the following corrected extinction coefficients: ε_{VHH} = 34380 L mol^{-1} cm^{-1}; $\varepsilon_{VHH\text{-}Zag}$ = 38850 L mol^{-1} cm^{-1} and molecular weights: MW (VHH) = 19.38 kDa; MW(VHH-Zag) = 25.2 kDa .

2.4. Radiolabelling

The pH of a fraction (0.5 mL) of $^{67}GaCl_3$ eluted from a SEP-PAK cartridge was adjusted to 5 by adding sodium acetate up to a 0.26 M concentration. To 150 μL of this solution (20 MBq), NOTA-VHH or NOTA-VHH-Zag (14.3 -16.4 nmol) in 50 μL of acetate buffer (0.1 M, pH = 5) was added and incubated for 5 min at room temperature. The products were purified by gel filtration on a disposable PD10 column. The final solutions were analysed by ITLC: ^{67}Ga-NOTA-VHH, (R_f = 0) using system A and B; ^{67}Ga-NOTA-VHH-Zag (R_f = 0) using system A and B.

Please cite this article as: Morais M., et al, Biodistribution of a ^{67}Ga-labeled anti-TNF VHH single-domain antibody containing a bacterial albumin-binding domain (Zag), Nucl Med Biol (2014), http://dx.doi.org/10.1016/j.nucmedbio.2014.01.009

2.5. ELISA assay

Human serum albumina (HSA), rat serum albumin (RSA), mouse serum albumin (MSA) (10 μg/well) and human TNFα (200 ng/well) were incubated overnight at 4 °C in 96-well plate. The remaining binding sites were blocked with 5% (w/v) soya milk/PBS1x during 1 h. The VHH and VHH-Zag recombinant antibodies conjugated with NOTA and the ^{67}Ga-labelled antibodies (after decay – 10 half-lifes) were incubated for 1 h at room temperature. Detection was performed with HRP-conjugated anti-HA-tag antibody (Roche) using ABTS substrate. Absorbance was measured at 405 nm in an ELISA reader.

2.6. DTPA challenge

Aliquots of ^{67}Ga-NOTA-VHH and ^{67}Ga-NOTA-VHH-Zag were added to an aqueous solution of DTPA (900 μL, 10^{-3} M) in a 1:100 molar ratio, and incubated at 37 °C. The samples were analyzed by ITLC-SG at different time points (2 h, 4 h, 6 h and 24 h) before and after filtration through a disposable PD10 column.

2.7. Biodistribution studies

The *in vivo* biodistribution studies of ^{67}Ga-NOTA-VHH and ^{67}Ga-NOTA-VHH-Zag were performed in groups of 3 healthy female CD-1 mice (Charles River, Spain) weighing approximately 23–25 geach. All animal experiments were performed in accordance with the guidelines for animal care and ethics for animal experiments outlined in the National and European Law. Animals were intravenously injected into the tail vein with 100 μL of the radiolabeled compounds (1.5–3.5 MBq) and were maintained on normal diet ad libitum. At 1 h, 4 h, 24 h post-injection (p.i.) mice were sacrificed by cervical dislocation. The radioactivity administered to the animals was measured using a dose calibrator. The difference between the radioactivity in the injected and that in the killed animals was assumed to be due to total excretion. Tissues of interest were dissected, rinsed to remove excess blood, weighed, and their radioactivity was measured using a gamma counter. Blood and urine was also collected at the sacrifice time and analyzed by ITLC. Biodistribution results were expressed as the percentage of the injected activity per gram of tissue. Statistical analysis of the biodistribution data (t-test) was done with GraphPad Prism and the level of significance was set as 0.05.

3. Results and discussion

In the present study we have evaluated the impact of an albumin-binding domain isolated from the Zag protein, a G-related protein from the surface of *Streptococcus zooepidemicus*, in the biodistribution profile of an anti-TNF VHH. Several *in vivo* studies have demonstrated the interest of fusing the ABD from streptococcal protein G to small recombinant antibody fragments to strongly extend their plasma half-lifes [7]. Results reported by Stork and co-workers also demonstrated enhancement in the blood clearance and changes on the biodistribution pattern of a single-chain diabody (scDb) directed against carcinoembryonic antigen (CEA) and CD3 capable of retargeting T cells to CEA-expressing tumor cells [20].

The VHH and VHH fused with the Zag domain were expressed in *Escherichia coli* BL21 (DE3) cells, purified using IMAC, and analyzed by SDS-PAGE. In previous studies, evaluation of binding by ELISA assays indicated that the Zag fusion protein preserved its binding to human, rat and mouse albumin as well as to TNF. Moreover, the fusion VHH-Zag presented a nanomolar affinity to human, rat and mouse serum albumin (K_d = 0.42 – 40.6 nM) as confirmed by surface plasmon resonance results [14,15].

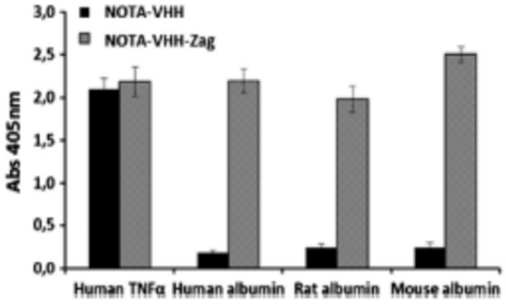

Fig. 1. Binding of the protein conjugates NOTA-VHH and NOTA-VHH-Zag to human, rat and mouse albumin, and human TNFα in ELISA assay.

Biodistribution studies with ^{99m}Tc(CO)$_3$-labelled VHH and VHH-Zag have shown that the Zag ABD fusion strategy affected the blood clearance, renal retention and excretion, as compared to the results obtained with the anti-TNF VHH [14].

The NOTA derivative p-SCN-Bn-NOTA was conjugated to the sdAbs and the resulting conjugates NOTA-VHH and NOTA-VHH-Zag were purified by gel filtration chromatography. The purity (>95%) of the conjugates was also assessed by SDS-PAGE analysis, as described for the precursor antibody fragments. The anti-TNF and the albumin-binding properties of the conjugates were assessed by ELISA (Fig. 1). The results demonstrated that the targeting properties of the antibody fragments were not affect upon conjugation to the chelator.

Radiolabeling of NOTA-VHH and NOTA-VHH-Zag with $^{67}Ga^{3+}$ was fast and efficient at room temperature. For both cases, after 5 minutes reaction, only one species (Rf = 0) was detected by ITLC-SG (Systems A and B) after gel filtration on a disposable PD10 column. Scanning of the column, after purification, in a radiochromatographer has shown negligible radioactivity retention (<5 % of the initial applied radioactivity), suggesting the absence of colloidal species and/or $^{67}GaCl_3$ precursor. Therefore, the species at the application point of the ITLC-SG chromatograms were assigned to ^{67}Ga-NOTA-VHH or ^{67}Ga-NOTA-VHH-Zag (>95% radiochemical purity).

Although we were not able to determine the number of NOTA chelators conjugated to the antibody fragments by Matrix-assisted laser desorption/ionization time-of-flight mass spectrometry (MALDI-TOF-MS), their presence was confirmed by the results of the stability studies of the radioconjugates in the presence of excess DTPA. Indeed, chromatographic analysis (ITLC-SG, systems A and B) of samples collected at different time points (2 h, 4 h, 6 h and 24 h) suggests the presence of only one species (Rf = 0), corresponding to ^{67}Ga-NOTA-VHH or ^{67}Ga-NOTA-VHH-Zag. No unreacted $^{67}GaCl_3$ precursor (System A, Rf = 1; System B, Rf = 0.4) and/or ^{67}Ga-DTPA (System B, Rf = 0.1) were detected. The presence of the latter complex would be explained by the reaction of DTPA with "free", nonspecifically bound, radiometal to the antibody during labeling. Moreover, no significant retention of radioactivity was observed in a

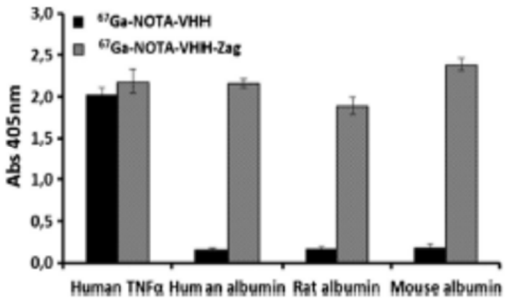

Fig. 2. Binding of ^{67}Ga-NOTA-VHH and ^{67}Ga-NOTA-VHH-Zag proteins to human, rat and mouse albumin, and human TNFα in ELISA.

Please cite this article as: Morais M., et al, Biodistribution of a ^{67}Ga-labeled anti-TNF VHH single-domain antibody containing a bacterial albumin-binding domain (Zag), Nucl Med Biol (2014), http://dx.doi.org/10.1016/j.nucmedbio.2014.01.009

Table 1
Biodistribution of ^{67}Ga-NOTA-VHH and ^{67}Ga-NOTA-VHH-ZAg in CD1- mice ($n = 3$) at 1 h, 4 h and 24 h p.i.

Organ	^{67}Ga-NOTA-VHH			^{67}Ga-NOTA-VHH-Zag		
	% I.A./g ± SD					
	1 h	4 h	24 h	1 h	4 h	24 h
Blood	**0.6 ± 0.2**	**0.16 ± 0.01**	**0.028 ± 0.004**	**8.3 ± 1.3**	**8.0 ± 2.3**	**1.7 ± 0.8**
Liver	**4.0 ± 0.7**	**6.0 ± 0.6**	**0.11 ± 0.01**	**17.6 ± 1.6**	**17.9 ± 3.6**	**20.5 ± 2.7**
Intestine	1.8 ± 0.5	1.4 ± 0.3	0.022 ± 0.005	2.9 ± 0.6	1.9 ± 0.5	1.2 ± 0.6
Spleen	0.26 ± 0.09	2.4 ± 0.3	0.041 ± 0.006	8.7 ± 2.5	11.0 ± 2.0	7.6 ± 1.8
Lung	0.8 ± 0.1	1.8 ± 0.3	0.036 ± 0.001	5.5 ± 0.3	6.6 ± 2.8	1.6 ± 0.4
Kidney	**43.5 ± 3.1**	**17.2 ± 3.0**	**4.8 ± 0.4**	**4.6 ± 1.1**	**6.1 ± 0.5**	**3.7 ± 0.3**
Muscle	0.27 ± 0.03	0.25 ± 0.19	0.010 ± 0.001	2.0 ± 0.5	2.8 ± 0.5	0.55 ± 0.01
Bone	0.26 ± 0.03	1.0 ± 0.2	0.031 ± 0.002	3.1 ± 0.4	1.6 ± 0.3	7.9 ± 1.1
Stomach	0.17 ± 0.07	0.7 ± 0.2	0.013 ± 0.002	0.27 ± 0.01	2.1 ± 0.4	0.4 ± 0.2
Total Excretion (% I.A.)	**71.3 ± 1.6**	**73.0 ± 2.9**	**97.8 ± 0.6**	**4.3 ± 1.5**	**13.6 ± 1.4**	**25.5 ± 2.1**

Radioactivity accumulation in relevant organs and total radioactivity excretion are highlighted in bold characters and numbers.

PD10 column after filtration of the stability samples, which indicates the absence of colloidal species. Therefore, the species detected at Rf = 0 could be ascribed to ^{67}Ga-NOTA-VHH or ^{67}Ga-NOTA-VHH-Zag. These results were further corroborated by the low *in vitro* stability of the radioactive species that resulted from the direct labeling of VHH and VHH-Zag with $^{67}Ga^{3+}$. Indeed, after incubation of those species with excess DTPA (2 h, 37 °C) a significantly high degree of transchelation was observed with formation of a new species corresponding to ^{67}Ga-DTPA.

Brought together, the stability assays clearly demonstrated that the radiolabeling of the antibody fragments with $^{67}Ga^{3+}$ was achieved through NOTA complexation of the radiometal and not through unspecific binding.

The anti-TNF-binding properties of both radiolabeled antibody fragments and the albumin-binding properties of ^{67}Ga-NOTA-VHH-Zag was preserved, as indicated by ELISA assays after radioactive decay of the initial preparation (10 half-lifes) at room temperature (Fig. 2).

The *in vivo* distribution of ^{67}Ga-NOTA-VHH and ^{67}Ga-NOTA-VHH-Zag was evaluated in healthy CD-1 mice to assess the effect of the Zag domain on the pharmacokinetics profile of the radiolabelled VHH. The biodistribution results of both compounds expressed as percentage of injected activity per gram of organ (% I.A./g ± SD) is presented in Table 1. The total radioactivity excretion is also presented as percentage of the total injected activity (% I.A.).

Analysis of the biodistribution results indicated that the introduction of the Zag domain affected dramatically the pharmacokinetic properties of radiolabelled VHH, with remarkable differences in the uptake and elimination rates from major organs as well as on the excretory route. Indeed, the most striking features are the pronounced decrease in blood clearance and in the radioactivity excretion rate from the whole animal. Whereas ^{67}Ga-NOTA-VHH was rapidly cleared from the blood stream (0.6 ± 0.2% I.A./g, 0.16 ± 0.01% I.A./g, 0.028 ± 0.004% I.A./g, at 1 h, 4 h and 24 h respectively) the Zag-containing molecule ^{67}Ga-NOTA-VHH-Zag has a slow blood clearance (8.3 ± 1.3% I.A./g, 8.0 ± 2.3 % I.A./g, 1.7 ± 0.8% I.A./g, at 1 h, 4 h and 24 h respectively). ^{67}Ga-NOTA-VHH has a very rapid total excretion (approximately 70% I.A. at 1 h p.i.), mainly through the urinary pathway. On the contrary, 24 h after administration of ^{67}Ga-NOTA-VHH-Zag only 25.5 ± 2.1% I.A. was eliminated from the animal body.

The biodistribution profile of ^{67}Ga-NOTA-VHH showed a rapid clearance of the radiotracer from most tissues since no relevant radioactivity accumulation in any major organ, except those related with the excretion paths was found. Although there was a small contribution of the hepatobiliar pathway in the elimination of the radiolabelled VHH, most of the activity was rapidly taken by the kidneys and excreted into the urine. However an important amount of activity (4.8 ± 0.4%I.A./g at 24 h p.i.) was retained in this organ which is quite often a biological issue associated to radiolabelled antibody fragments and peptides. In contrast, ^{67}Ga-NOTA-VHH-Zag presented an entirely different tissue distribution. There was a slow washout not only from blood but also from muscle and bone. Moreover, due to the slowest blood clearance, highly irrigated organs such as liver, spleen, lung accumulated relevant sum of activity. The presence of ABD also shifted the excretion pathway from mainly renal to mainly hepato-biliary as indicated by the liver/kidney uptake ratio and the low excretion rate of ^{67}Ga-NOTA-VHH-Zag when compared to ^{67}Ga-NOTA-VHH. This behavior could also be partially assigned to the fact that albumin is biosynthesized in the liver, leading to a high local concentration of this protein and increased accumulation of the ABD-containing radioactive antibody fragment.

Blood samples collected from mice were analyzed by ITLC, at 1 h and 4 h p.i.. The results have shown that both ^{67}Ga-labeled antibody fragments were stable in blood serum, as no metabolites were detected after 4 h p.i. A considerable amount (>50%) of unidentified metabolites was detected by ITLC (Rf > 0) in urine samples after 4 h p.i.

4. Conclusion

In the present study we have determined the biodistribution profile of an anti-TNF antibody fragment in fusion with an ABD from Zag protein. We have shown that the fusion of this ABD can enhance the *in vivo* performance of single-domain antibodies, decreasing the blood clearance, renal retention and excretion, compared to the biodistribution profile of the unmodified antibody fragment. These findings demonstrate that the Zag fusion can be considered as a promising approach to improve the pharmacokinetics of therapeutic proteins and peptides.

Supplementary data to this article can be found online at http://dx.doi.org/10.1016/j.nucmedbio.2014.01.009.

Acknowledgments

Fundação para a Ciência e a Tecnologia (FCT), Portugal, is acknowledged for funding (project PTDC/SAU-FAR/115846/2009). C. Cantante e M. Morais thank the FCT for PhD fellowships (SFRH/BD/48598/2008 and SFRH/BD/48066/2008, respectively). We thank Dr. C. Xavier and Prof. V. Cavaliers for a generous gift of p-SCN-Bn-NOTA and fruitful discussions.

References

[1] Aires da Silva F, Corte-Real S, Goncalves J. Recombinant antibodies as therapeutic agents: pathways for modeling new biodrugs. BioDrugs 2008;22:301–14.
[2] Romer T, Leonhardt H, Rothbauer U. Engineering antibodies and proteins for molecular in vivo imaging. Curr Opin Biotechnol 2011;22:882–7.

Please cite this article as: Morais M., et al, Biodistribution of a ^{67}Ga-labeled anti-TNF VHH single-domain antibody containing a bacterial albumin-binding domain (Zag), Nucl Med Biol (2014), http://dx.doi.org/10.1016/j.nucmedbio.2014.01.009

[3] Goldsmith SJ, Signore A. An overview of the diagnostic and therapeutic use of monoclonal antibodies in medicine. Q J Nucl Med Mol Imaging 2010;54:574–81.
[4] Sharkey RM, Goldenberg DM. Perspectives on cancer therapy with radiolabeled monoclonal antibodies. J Nucl Med 2005;46(Suppl 1):115S–27S.
[5] Vaneycken I, D'Huyvetter M, Hernot S, De Vos J, Xavier C, Devoogdt N, et al. Immuno-imaging using nanobodies. Curr Opin Biotechnol 2011;22:877–81.
[6] Batra SK, Jain M, Wittel UA, Chauhan SC, Colcher D. Pharmacokinetics and biodistribution of genetically engineered antibodies. Curr Opin Biotechnol 2002;13:603–8.
[7] Kontermann RE. Strategies to extend plasma half-lives of recombinant antibodies. BioDrugs 2009;23:93–109.
[8] Kontermann RE. Strategies for extended serum half-life of protein therapeutics. Curr Opin Biotechnol 2011;22:868–76.
[9] Trussel S, Dumelin C, Frey K, Villa A, Buller F, Neri D. New Strategy for the Extension of the Serum Half-Life of Antibody Fragments. Bioconjug Chem 2009;20:2286–92.
[10] Muller C, Struthers H, Winiger C, Zhernosekov K, Schibli R. DOTA Conjugate with an Albumin-Binding Entity Enables the First Folic Acid-Targeted Lu-177-Radionuclide Tumor Therapy in Mice. J Nucl Med 2013;54:124–31.
[11] Fanali G, di Masi A, Trezza V, Marino M, Fasano M, Ascenzi P. Human serum albumin: From bench to bedside. Mol Aspects Med 2012;33:209–90.
[12] Orlova A, Jonsson A, Rosik D, Lundqvist H, Lindborg M, Abrahmsen L, et al. Site-specific radiometal labeling and improved biodistribution using ABY-027, a novel HER2-targeting affibody molecule-albumin-binding domain fusion protein. J Nucl Med 2013;54:961–8.
[13] Tolmachev V, Orlova A, Pehrson R, Galli J, Baastrup B, Andersson K, et al. Radionuclide therapy of HER2-positive microxenografts using a 177Lu-labeled HER2-specific Affibody molecule. Cancer Res 2007;67:2773–82.
[14] Cantante C, Lourenço S, Morais M, Gano L, Santos C, Fontes C, et al. Albumin-binding domain (Zag) from Streptococcus zooepidemicus increases half-life affect blood clearance of anti-TNF VHH. 8th Annual PEGS conference. Boston; 2012.
[15] Cantante C, Lourenço S, Leandro J, Morais M, Gano L, Fontes C, et al. Albumin-binding domain from Streptococcus pyogenes protein H increases half-life and affect blood clearance of anti-TNF VHH. Vienna, Austria: PEGS Europe; 2012.
[16] Jonsson H, Lindmark H, Guss B. A Protein G-Related Cell-Surface Protein in Streptococcus-Zooepidemicus. Infect Immun 1995;63:2968–75.
[17] Scasnar V, Vanlier JE. The Use of Sep-Pak Si Cartridges for the Preparation of Gallium Chloride from the Citrate Solution. Eur J Nucl Med 1993;20:273.
[18] Silence K. USA; 2007/007249 A1.
[19] Xavier C, Vaneycken I, D'huyvetter M, Heemskerk J, Keyaerts M, Vincke C, et al. Synthesis, Preclinical Validation, Dosimetry, and Toxicity of Ga-68-NOTA-Anti-HER2 Nanobodies for iPET Imaging of HER2 Receptor Expression in Cancer. J Nucl Med 2013;54:776–84.
[20] Stork R, Campigna E, Robert B, Muller D, Kontermann RE. Biodistribution of a Bispecific Single-chain Diabody and Its Half-life Extended Derivatives. J Biol Chem 2009;284:25612–9.

ALBUMIN-BINDING DOMAIN (PROTH) FROM STREPTOCOCCUS PYOGENES, A NEW APPROACH TO INCREASE HALF-LIFE OF THERAPEUTIC PROTEINS

Brief Introduction

Streptococcal albumin-binding domains have been successfully investigated as fusion proteins to improve the pharmacokinetics of recombinant antibodies or therapeutic proteins (Kontermann, 2012).

Protein H is a cell surface protein from *S. pyogenes*, with an Ig-binding region located in the N-terminus and an ABD in the C-terminus, composed by three C repeats with a high amino acid sequence homology between them (Frick *et al*., 1995)

In this study we fused protein H ABD (ProtH) with a nanobody against TNFα from Ablynx, used as a study model to validate our strategy to increase half-life. Firstly, we intend to optimize the production of the recombinant proteins (VHH and VHH-ProtH) in *E.coli*, an easy way to obtain high amounts of protein with lower costs. Then we characterize the antigen and albumin binding of the ProtH fusion protein and compare the therapeutic efficacy of the VHH-ProtH with the unmodified antibody. We also evaluate the thermal stability and *in vitro* and *in vivo* serum stabilities of the both proteins. Finally, we determine the initial and terminal half-lives of VHH and VHH-ProtH and the organ biodistribution profiles of both proteins, using ^{99m}Tc radiolabelling.

Albumin-binding domain (ProtH) from *Streptococcus pyogenes,* a new approach to increase half-life of therapeutic proteins

Cátia Cantante[1,2], Sara Lourenço[6], Soraia Oliveira[6], João Leandro[4], Maurício Morais[3], Lurdes Gano[3], Nuno Silva[4], Paula Leandro[4], Carlos Fontes[5], João D. G. Correia[3], Frederico Aires-da-Silva[5,6] and João Gonçalves[1,2]

[1] CPM-URIA, Faculdade de Farmácia, Universidade de Lisboa, 1649-003 Lisbon, Portugal
[2] Instituto de Medicina Molecular, Faculdade de Medicina, Universidade de Lisboa,1649-028 Lisbon, Portugal
[3] Centro de Ciências e Tecnologias Nucleares, Instituto Superior Técnico, Universidade de Lisboa, 2695-066 Bobadela LRS, Portugal
[4] iMed.UL, Faculdade de Farmácia, Universidade de Lisboa, 1649-003 Lisbon, Portugal
[5] Faculdade de Medicina Veterinária, CIISA, Universidade de Lisboa, 1300-477 Lisbon, Portugal
[6] Technophage, SA, 1649-028 Lisbon, Portugal

Keywords: albumin-binding domain, half-life, pharmacokinetics, protein H cell surface protein TNFα, VHH.

Background: Half-life extension is a key feature to improve pharmacokinetics of therapeutic low molecular weight proteins and peptides.

Results: Fusion of streptococcal protein H albumin-binding domain (ABD) – ProtH – to a single-domain antibody (nanobody) resulted in a significant increase in circulation time *in vivo*, improving the pharmacokinetics of the therapeutic molecule.

Conclusions: This strategy can be successfully applied to improve the pharmacokinetics of short half-life therapeutic molecules.

Significance: This work demonstrates the potential of a new approach to increase the half-life of therapeutic proteins by using the ProtH albumin-binding domain from *Streptococcus pyogenes*

ABSTRACT

Recombinant antibody fragments and single-domain antibodies present a great potential as new biodrugs in the treatment of several relevant diseases. However, due to their relatively low-molecular weight (< 60 kDa) they are rapidly cleared from circulation. To solve this problem, plasma protein binding can be an effective approach to improve pharmacokinetic properties of short half-life molecules. Aimed at improving the pharmacokinetic properties of therapeutic proteins, we propose herein a bacterial albumin-binding domain (ProtH) derived from *Streptococcus pyogenes* protein H. To validate our approach and as a proof of concept, the ProtH ABD was fused with an anti-TNFα VHH nanobody. The results obtained show that the ProtH ABD fused to a small therapeutic protein (anti-TNFα VHH) presents a strong binding to mouse, rat and human albumins. Furthermore, the results obtained reveal that the VHH-ProtH antigen-binding sites were still accessible for TNFα binding and the presence of

albumin does not interfere with antigen targeting. Importantly, the VHH fusion with ProtH resulted in a half-life increase of 26-fold in mice (VHH = 47 min *versus* VHH-ProtH = 20.54 h) and a residence until 48 h (*versus* 2 h for the VHH). The biodistribution studies of the radiolabelled ^{99m}Tc-recombinant proteins (VHH and VHH-ProtH) in healthy mice indicated a similar distribution and elimination profile for both proteins, showing high radioactivity accumulation within the highly perfused organs, especially in the kidney. This study demonstrates the great potential of ProtH ABD as a strategy to increase the half-life of therapeutic proteins. Due to the accumulation of albumin in arthritic joints, our results also reveal the special interest of this ABD for the pharmacokinetic improvement of proteins for the treatment of rheumatoid arthritis.

INTRODUCTION

Recombinant antibody fragments and single-domain antibodies represent the fastest growing class of pharmaceutical biotechnology[1]. To date, more than 20 monoclonal antibodies (mAbs) are available for a variety of therapeutic applications[2] and more than 600 are currently in clinical development[3,4]. With the exception of whole antibodies and Fc-fusion proteins, many of these biodrugs present molecular weights below 60 kDa[3]. For instance, anti-TNFα camelid nanobodies (VHH) from Ablynx and domain antibodies (Dab) from Domantis/GSK are in clinical development, showing promising results for the treatment of rheumatoid arthritis[5]. However, due to their small size they have short half-life's and present a rapid clearance from circulation. The limitations of small size protein drugs have led to the development and implementation of several half-life extension strategies to prolong circulation of these molecules and thus improve their administration, pharmacokinetic and pharmacodynamics properties[3,4,6]. Several approaches have been proposed to improve the pharmacokinetics of small proteins based on implementing neonatal Fc receptor (FcRn)-mediated recycling. The long half-lives of albumin (~19 days) and IgG (~21 days) are caused by a recycling process mediated by FcRn, expressed, for example, by endothelial cells[3,4]. The FcRn is capable of binding albumin and IgGs in a pH-dependent manner. Therefore, after cellular uptake of plasma proteins through macropinocytosis, albumin and IgG will bind to FcRn in the acidic environment of the endosomes. This binding diverges albumin and IgG from degradation in the lysosomal compartment and redirects them to the plasma membrane, where they are released back into the blood plasma because of the neutral pH[7-9]. This

mechanism offers other opportunities to extend or modulate the half-life of proteins, for example, through fusion to albumin or albumin fusion moieties, or to Fc region of IgG[3,4].

The streptococcal protein G ABD fusion has been extensively studied, being able to extend the circulation time of recombinant antibodies. Stork and co-workers investigated a recombinant antibody fusion to the protein ABD3 as strategy to prolong circulation time using a bispecific single-chain diabody (scDb) developed for the retargeting of cytotoxic T cells to CEA-expressing tumor cells with successful improvements in half-life extension[10].

Protein H, a molecule expressed at the surface of some strains of *Streptococcus pyogenes*, is found in clinical isolates of the M1 serotype[11] and has affinity for the constant (IgGFc) region of IgG and serum albumin[12]. The role for protein H and other IgG-binding proteins in *S. pyogenes* pathogenicity and virulence is unclear. The protein H, like protein G[13], has separate binding sites for albumin and IgG. The ABD from protein H is located in the N-terminus closer to the bacterial cell wall and IgG-binding region. No homology was detected when the IgGFc-binding repeats were compared with the same regions of protein G, but the albumin-binding regions of protein G and H were shown to have evolved convergently[12]. Competitive binding experiments demonstrated that protein G and H bound to the same or closely located sites in albumin, which has previously been mapped for protein G to disulfide loops 6-8[14].

In the present study, we used the ProtH ABD as a new approach for extension of the circulation time of therapeutic proteins. To validate our strategy and as a proof-of-concept, the ProtH ABD was fused with an anti-TNFα VHH single-domain antibody. The fusion protein showed specific binding to serum albumin and compared with the parental VHH nanobody, exhibited a strong increase of serum half-life in mice to approximately 26-fold. In summary, our results demonstrate for the first time, the ability of this new streptococcal ABD to improve pharmacokinetic disposition of therapeutic proteins.

EXPERIMENTAL PROCEDURES

Materials – Human serum albumin (HSA) (catalog no. A3782), rat serum albumin (RSA) (catalog no. A6272), mouse serum albumin (MSA) (catalog no. A3139), human (catalog no. H4522) and mouse serum (catalog no. H5905), and pT7-FLAG2 expression vector were purchased from Sigma-Aldrich (USA). HRP-conjugated anti-His-tag, HRP-conjugated anti-HA-tag, anti-HA affinity matrix, 2,2'-Azino-di-[3-ethylbenzthiazoline sulfonate (6)] diammonium salt (ABTS), tetrazolium salt WST-1 and cOmplete EDTA-free protease

inhibitors cocktail were acquired from Roche (Germany). Recombinant human TNFα and Amicon centrifugal filter units were purchase from Millipore (USA). PD-10 columns and G25 Sephadex were purchase from GE Healthcare (UK) and Sigma-Aldrich, respectively. Radioactivity measurements were done on a dose calibrator (Aloka Curiemeter, IGC-3, Japan) or on a gamma-counter (Berthold LB 2111, Germany).

Cloning of recombinant proteins – DNA encoding anti-TNF VHH#3E clone (Silence *et al*. Patent US2007/0077249 A1)[15] was synthesized by Nzytech adding a SfiI restriction site at 5' and 3' ends. All the constructs were cloned in pT7-FLAG2 with the leader peptide sequence ompA (LP) from pComb3x plasmid in N-terminal and in histidine and human influenza hemagglutinin (HA) tags in C-terminal[16]. A fragment encoding the LP-VHH-His-HA was generated by PCR with primers HindIII-LP-SfiI-F (5'-CCC AAG CTT ATG AAA AAG ACA GCT ATC GCG ATT GCA GTG GCA CTG GCT GGT TTC GCT ACC GTG GCC CAG GCG GCC-3') and His-HA-KpnI-R (5'-CGG GGT ACC CCG CTA AGA AGC GTA GTC CGG AAC GTC GTA CGG GTA TGC GCC ATG GTG ATG GTG ATG GTG ATG GTG GCT GCC TCC-3') and subcloned into the expression vector pT7-FLAG2 (Sigma) into the HindIII and KpnI restriction sites. To construct the VHH-ProtH fusion protein, a DNA comprising the ProtH albumin-binding domain was amplified by PCR with primers ProtH-F (5'- CCC ACT AGT AAG CAA ATC TCG GAA GCA AGC CG-3') and ProtH-R (5'- CAT GCC ATG CTT CTT TCA GAG CCT TGG CCT CC-3'), adding SpeI and NcoI restriction sites at the fragment 5' and 3' ends, respectively. The resulting PCR fragments were gel-purified, digested with the SpeI and NcoI restriction enzymes and cloned into the appropriately cut pT7-VHH vector. A short GS linker (SGGGGS) was used to link the VHH and VHH-ProtH. The VHH and VHH-ProtH constructs were verified by sequencing.

Expression and purification of proteins – VHH and VHH-ProtH were expressed in *Escherichia coli* strain BL21(DE3). One liter of LB, containing 100 µg/ml ampicillin was inoculated with 10 ml of overnight culture of transformed BL21(DE3) and grown to exponential phase (A_{600} = 0.6-0.9) at 37 ºC. Expression was induced by the addition of 1 mM isopropyl β-D-1-thiogalactopyranoside (IPTG) and growth continued overnight at 18 ºC. Cells were harvested by centrifugation and resuspended in equilibration buffer (50 mM HEPES, 1 M NaCl, 5 mM $CaCl_2$, 30 mM imidazole, pH 7.5) supplemented with protease inhibitors. Cells were lysed by sonication. Centrifugation (14000 × *g* for 1h at 4 ºC) was used to remove cell debris, and the supernatant was filtered through a 0.2 µm syringe filter. The VHH and VHH-ProtH were purified using AKTA FPLC System (GE Healthcare) by nickel chelate

affinity chromatography with HisTrap HP columns. After a washing step (50 mM HEPES, 1 M NaCl, 5 mM $CaCl_2$, 60 mM imidazole, pH 7.5) the recombinant antibody fragments were eluted with a linear imidazole gradient from 60 to 300 mM in 50 mM HEPES, 1 M NaCl, 5 mM $CaCl_2$, pH 7.5. Protein fractions were pooled, then desalted and concentrated in 50 mM HEPES, 100 mM NaCl, 5 mM $CaCl_2$, pH 7.5 using Amicon 10K (Millipore). The samples were loaded onto a HiPrep 16/60 Sephacryl S-100 HR gel filtration column (GE Healthcare), fractions were pooled and concentrated with Amicon 10K. The protein purity was analyzed by reducing and non-reducing SDS-PAGE. Protein concentration was determined spectrophotometrically in Nanodrop ND-1000 at 280 nm and calculated using the calculated ε value of each protein (εVHH = 34380 L mol−1 cm−1; εVHH-ProtH = 34380 L mol−1 cm−1).

ELISA – TNFα (200 ng/well), HSA, RSA and MSA (10 µg/well) were coated in 96-well plates overnight at 4 ºC and the remaining binding sites were blocked with 5% (w/v) soya milk/PBS1x. To evaluate the binding of VHH and VHH-ProtH fusion proteins to TNFα and serum albumin, several dilutions of the purified samples were incubated in triplicates incubated for 1 h at room temperature. To validate the binding of the recombinant proteins to TNFα in presence and absence of albumin, the purified protein samples were incubated with 1 mg/ml of HSA. Detection was performed with HRP-conjugated anti-HA-tag antibody using ABTS substrate. Absorbance was measured at 405 nm in an ELISA reader. GraphPad Prism Software version 5 was used for data analysis.

Size Exclusion Chromatography – Apparent molecular weight of recombinant antibody and formation of antibody/albumin complexes was determined by FPLC–SEC on a HiLoad Superdex 200 HR column (GE Healthcare) with a flow rate of 0.7 ml/min and PBS as running buffer at 4 ºC. The following standard proteins were used: apoferritin (443 kDa, R_S 6.1 nm), β-amylase (200 kDa, R_S 5.4 nm), alcohol dehydrogenase (150 kDa, R_S 4.55 nm), bovine serum albumin (67 kDa, R_S 3.55 nm), ovalbumin (45 kDa, R_S 3.05), myoglobin (17.6 kDa, R_S 1.91 nm), ribonuclease A (13.7 kDa, RS 1.64 nm) and cytochrome c (12.4 kDa, R_S 1.77 nm). Blue dextran and L-tyrosine were used to determine the void and total column volume, respectively. Elution volume of the protein standard was used to create a standard curve of Stokes' radius (R_S) *versus* $(-\log K_{av})^{1/2}$ that was used to calculate the Stokes' radii of recombinant antibody and antibody/albumin complexes. Complex formation of VHH-ProtH with HSA and MSA was analyzed by incubating equimolar amounts of VHH-ProtH and albumin (10 µM), unless otherwise specified, in PBS1x at room temperature and subsequent analysis by SEC. The relative amounts of the oligomeirc forms were calculated by

deconvolution of the obtained chromatograms using the PeakFit software (Systat Software Inc). SDS-PAGE analysis of collected samples was performed to evaluate albumin binding.

Protein thermal stability and in vitro serum stability – Melting temperatures of the studied proteins were determined using the Protein Thermal Shift Kit and 7500 Fast Real-Time PCR System (Applied Biosystems) according manufacturer's instructions. Protein samples (5 µg/well) were tested in MicroAmp^{TM} Fast Optical 96-well Reaction Plates and analyzed in quadruplicate using and diluted in 50mM HEPES, 100 mM NaCl, 5 mM $CaCl_2$, pH 7.5, and Protein Thermal Shift^{TM} Dye 1x. Collected data were analyzed with Protein Thermal Shift Software version 1.1.

To evaluate human and mouse serum stability of recombinant antibodies, VHH and VHH-ProtH were incubated at a concentration of 10 µg/ml for up to 24 days and 4 days, respectively, at 37 ºC. The *in vitro* stability of VHH and VHH-ProtH in the human and mouse serum was evaluated by ELISA and Western Blot using HRP-conjugated anti-His-tag antibody.

Neutralization of TNF-dependent cytolytic activity – In order to measure the anti-TNFα VHH and VHH-ProtH blocking effect on TNF-α/TNFR (TNF receptor) interaction, a murine aneuploidy fibrosarcoma cell line (L929) was used as a cytotoxic-mediated assay[17]. Briefly, L929 cells were grow to 90% confluence in Dulbecco's modified Eagle's medium supplemented with 10% fetal bovine serum, penicillin (100 U/ml), streptomycin sulfate (10 µg/ml), and L-glutamine (2 mg/ml). Cells were plated in 96-well plates at density of 25,000 cell/well and then incubated overnight. Serial dilutions of VHH and VHH-ProtH antibody fragments were mixed with a cytotoxic concentration of TNFα (final assay concentration 1 ng/ml) or in absence of this cytokine in order to measure the cell viability. Actinomycin D was added to a final concentration of 1 µg/ml to increase the cell sensitivity. After at least 2 h of incubation at 37 ºC with shaking, the mixture was added to the plated cells. Cells were incubated for 24 h at 37 ºC in an atmosphere of 5% CO_2. Cell viability was determined using the tetrazolium salt WST-1 (10 µg/well), after at least 30 min of incubation by measuring the absorbance at 450 nm.

Pharmacokinetics – Animal care and all pharmacokinetic (PK) studies were conducted according to guidelines for animal care and ethics for animal experiments outlined in the National and European Law. CD-1 mice (Charles River, female, 6-8 weeks, weight 25-30g) (n=2) were administered with 25 µg of VHH and VHH-ProtH intravenous injections. Plasma

samples were collected from mice at regular intervals of 5, 30, 60, 120, and 360 min, 24, 48 and 72 hours, and fused or unfused antibody were quantified by ELISA. TNFα was immobilized in 384 well-plates (100 ng/well) overnight at 4ºC. After 1 h blocking with 5% soja milk, recombinant antibody fragments were titrated in duplicates and incubated for 1 h at RT. Detection was performed with HRP-conjugated anti-HA antibody using ABTS substrate. Absorbance was measured at 405 nm in an ELISA-reader. As described by Stork and co-workers[10], determined serum concentrations of TNFα-binding proteins were interpolated to the corresponding calibration curves. For comparison, the first time point (5 min) was set to 100%. Pharmacokinetic parameters area under the curve (AUC), $t_{1/2}\alpha$ and $t_{1/2}\beta$ were calculated with Excel, using the first three time points to calculate $t_{1/2}\alpha$ and the last three time points to calculate $t_{1/2}\beta$. To evaluate the residence time of VHH and VHH-ProtH in mouse serum *in vivo*, the serum samples collected during the pharmacokinetic assays were incubated with an anti-HA affinity matrix overnight at 4 ºC. Afterwards, the VHH and VHH-ProtH proteins were detected by Western Blot with an anti-HA-tag antibody.

Radiolabelling of ^{99m}Tc-VHH and ^{99m}Tc-VHH-ProtH proteins – The precursor *fac*-$[^{99m}Tc(CO)_3(H_2O)_3]^+$ was prepared using the Isolink kit (Covidien) and its radiochemical purity checked by RP-HPLC and ITLC. Compounds *fac*-$[^{99m}Tc(CO)_3]$- VHH and *fac*-$[^{99m}Tc(CO)_3]$-VHH-ProtH were obtained by reacting the antibodies with *fac*-$[^{99m}Tc(CO)_3(H_2O)_3]^+$. Briefly, a solution of *fac*-$[^{99m}Tc(CO)_3(H_2O)_3]^+$ was added to an microtube vial containing VHH or VHH-ProtH to get a final concentration of 1 mg/ml. The mixture reacted for 3 hours at 37 ºC and the radiochemical purity of *fac*-$[^{99m}Tc(CO)_3]$-VHH and *fac*-$[^{99m}Tc(CO)_3]$-VHH-ProtH was checked by ITLC analysis every hour. The $[^{99m}Tc(CO)_3(H_2O)_3]^+$ and $[TcO_4]^-$ migrate in the front of the solvent (Rf = 1), while the radioactive small domain antibodies remain at the origin (Rf = 0). Purification of ^{99m}Tc-radiolabeled antibodies was performed by gel filtration through Shepadex G-25 or PD-10 column, using 20 nM sodium chloride solution as eluent. After labeling, VHH and VHH-ProtH proteins were tested in ELISA to ensure that their binding capacities were unaffected (data not shown).

Partition coefficient – Partition coefficient was evaluated by the "shake-flask" method. The radioactive antibodies were added to a mixture of octanol (1 ml) and 0.1 M PBS1x pH 7.4 (1 m), which has been previously saturated with each other by stirring. This mixture was vortexed and centrifuged (3000 rpm, 10 min) to allow phase separation. Aliquots of both octanol and PBS1x were counted in a γ-counter. The partition coefficient ($P_{o/w}$) was

calculated by dividing the counts in the octanol phase by those in the buffer, and the results were expressed as log $P_{o/w}$±SD.

Biodistribution studies of ^{99m}Tc-VHH and ^{99m}Tc-VHH-ProtH proteins – In vivo evaluation studies of the radiolabelled recombinant proteins were performed in healthy female CD-1 mice (Charles River, female, 6-8 weeks, weight 25-30g) (n=3) at 5 min, 30 min, 1, 4 and 24 h and 48 h. All animal experiments were performed in accordance with the guidelines for animal care and ethics for animal experiments outlined in the National and European Law. Animals were intravenously injected into the tail vein with 100 µl of the radiolabeled compounds (2.6–3.7 GBq). Mice were sacrificed by cervical dislocation at different time points after injection (p.i.). The radioactive dose administered (A.I.) and the radioactivity in the sacrificed animals were measured using a dose calibrator. The difference between the radioactivity in the injected and that in the sacrificed animals was assumed to be due to excretion. Tissues of interest were dissected, rinsed to remove excess blood, weighed, and their radioactivity was measured in a gamma counter. The total activity uptake for blood, bone, muscle, was estimated assuming that these organs constitute 6, 10, and 40% of the total body weight, respectively. Blood and urine was also collected at the sacrifice time and analyzed by ITLC.

RESULTS

Expression and purification of VHH and VHH-ProtH

The VHH-ProtH construct was generated by fusing the ProtH ABD from streptococcal surface protein H to the anti-TNFα VHH#3E clone (Silence *et al*. Patent US2007/0077249 A1)[15] , including histidine (His_7) and HA tags in C-terminal (Fig. 1A and B). The VHH-ProtH fusion protein obtained presents 321 amino acid residues with a calculated molecular weight of ~34.7 kDa. The VHH was also constructed as described in the material and methods section and used as control. VHH and VHH-ProtH proteins were expressed in *E. coli* BL21(DE3) and purified by IMAC. SDS-PAGE and Western Blot results showed a protein band for VHH and VHH-ProtH with the expected molecular weights under reducing and non-reducing conditions (Fig. 1C and D). After expression and purification of one liter of culture we could obtain 25-30 mg of VHH-ProtH and 15-20 mg of VHH.

Antigen binding of VHH and VHH-ProtH proteins

After purification, the VHH-ProtH binding activity to human TNFα was tested in an ELISA assay as described in the material and methods section. The VHH was used as control and as shown in figure 2 (A and B), both proteins specifically bound to TNFα. Importantly, binding of VHH-ProtH to TNFα was not affected by the presence of HSA (with HSA EC_{50} = 0.106 nM; without HSA EC_{50} = 0.180 nM;) and was slightly higher than the VHH binding (with HSA EC_{50} = 1.030 nM; without HSA EC_{50} = 1.385 nM). These results reveal that VHH-ProtH antigen binding sites are accessible for TNFα binding and the presence of albumin does not interfere with antigen targeting.

Binding of VHH-ProtH to serum albumins

In order to determine the *in vitro* relative binding activities of the VHH-ProtH fusion protein against human, rat and mouse albumins, an ELISA was performed at neutral (pH 7.4) and acidic environment (pH 6.0). As shown in figures 3A and B, ProtH domain specifically bounds to all albumins. Moreover, binding of the VHH-ProtH fusion protein to albumins at pH 6.0 ($EC_{50\ (HSA)}$ = 53.03 nM; $EC_{50\ (RSA)}$ = 40.76 nM; $EC_{50\ (MSA)}$ = 36.74 nM) was similar with binding at pH 7.4 ($EC_{50\ (HSA)}$ = 39.70 nM; $EC_{50\ (RSA)}$ = 42.88 nM; $EC_{50\ (MSA)}$ = 16.50 nM) (Table 1).

Size exclusion chromatography (SEC) was also used to evaluate interaction between VHH-ProtH and human and mouse serum albumin (Fig. 4 and Table 2). The VHH-ProtH recombinant protein eluted predominantly as a peak that was deconvoluted as a mixture of trimers (97.2 kDa, R_S 4.11, 42%) and dimers (75.6 kDa, R_S 3.79; 37%) (Fig. 4A). Interestingly, neither VHH nor ProtH form oligomers when expressed alone (data not shown). HSA revealed a major peak (93%) corresponding to the monomeric form with an apparent molecular mass of 68.1 kDa (R_S 3.67 nm) and minor peak (7%) of 163 kDa (Fig. 4B). Since unbound VHH-ProtH and human albumin eluted in the same molecular mass range, we incubated HSA with VHH-ProtH in a 1.1 (w/w) ratio. A new peak around 200 kDa appeared and it could be deconvoluted in two peaks corresponding to complexes of HSA and VHH-ProtH: complex I (218 kDa, R_S 5.30 nm; 31%) and complex II (147 kDa, R_S 4.67 nm; 17%). A peak around 76 kDa (32%) corresponded mainly to unbound VHH-ProtH (Fig. 4C, *inset*). The stoichiometry of the complexes is not clear, but at least complex I appear to contain more than one monomer of HSA. Mouse serum albumin demonstrated higher molecular mass forms when compared with the human counterpart (Fig. 4D) and a major peak (40%; monomeric form) with an apparent molecular mass of 64.3 kDa (R_S 3.60 nm). Incubation of

MSA with VHH-ProtH resulted in the shift of the monomeric MSA to a large peak that could be deconvoluted into two peaks (Fig. 4E). The main component was centered at 98.9 kDa (R_S 4.01 nm) and corresponded to ~88% of the total protein. SDS-PAGE analysis (Fig. 4E, *inset*, lane b) reveals that the peak is a complex of MSA and VHH-ProtH. Contrary to the observed with the human albumin, the mouse albumin seems to form a complex with a stoichiometry 1:1 with VHH-ProtH.

Thermal stability and in vitro stability

The thermal stability of VHH and VHH-ProtH was calculated using the Protein Thermal Shift Kit and Protein Thermal Shift Software. Similar melting temperatures (Tm) were obtained for both proteins (VHH: 71.53 to 72.34 ºC; VHH-ProtH: 71.73 to 73.58 ºC) (Table 3). These results demonstrated that both recombinant proteins are highly stable and the ProtH fusion did not affect the stability of the anti-TNFα nanobody. *In vitro* serum stability was analyzed by incubation of VHH and VHH-ProtH proteins with human and mouse serum at 37 ºC. Samples were incubated during 4 and 24 days in mouse and human serum, respectively. The presence of VHH and VHH-ProtH in the collected samples was examined by Western Blot. As shown in figures 6A and 6B, both proteins were detected with the expected molecular weights and no degradation was observed. The binding activities were confirmed by ELISA in all the samples and were similar to samples before incubation (Day 0) (data not shown).

Neutralization of TNFα-dependent cytolytic activity by VHH and VHH-ProtH

In order to measure the VHH and VHH-ProtH blocking effect on TNF-α/TNFR interaction, a murine aneuploid fibrosarcoma cell line (L929) was used as a cytotoxic TNFα-mediated assay (material and methods section). As shown in Fig. 5, both VHH (EC_{50} = 68.29 nM) and VHH-ProtH (EC_{50} = 19.02 nM) inhibited TNFα-induced cell death of L929 in a dose-dependent manner. The data shown that the inhibitory profiles of both recombinant proteins were similar, thus indicating that the fusion with the ProtH ABD does not interfere with the efficacy of the anti-TNFα VHH nanobody.

Pharmacokinetic properties of VHH-ProtH

The pharmacokinetic properties of VHH and VHH-ProtH were evaluated into CD-1 mice, after a single i.v. injection (25 µg) into the tail vein. This dose injection was selected according to doses applied in other studies with recombinant antibodies in mice[10,18]. Serum concentrations of VHH and VHH-ProtH were determined by ELISA at different time points

as described in the material and methods section. When compared with VHH, VHH-ProtH exhibited a highly prolonged residence time in blood and mice (Fig. 7 and Table 4), with the terminal half-life ($t_{1/2}\beta$) increasing from 0.79 h (VHH) to 20.54 h (VHH-ProtH), corresponding to a 26-fold increase. Moreover, distribution phase half-life ($t_{1/2}\alpha$) showed a 7-fold increase, from 0.52 h (VHH) to 3.59 h (VHH-ProtH). The improvement of pharmacokinetic properties was also demonstrated by comparison of the AUC. For VHH-ProtH the $AUC_{(0\text{-}24)}$ was increased by a factor of 21 comparing with VHH. To confirm the presence and identity of VHH and VHH-ProtH at each time point, a Western Blot was performed. As illustrated in figure 8, comparing with the unmodified VHH nanobody (residence in serum during 2 h), VHH-ProtH can be detected in mouse serum until 48 h after injection.

Biodistribution of $^{99m}Tc(CO)_3$-VHH and $^{99m}Tc(CO)_3$-VHH-ProtH

In order the analyze the biodistribution profile of each molecule, VHH and VHH-ProtH were radiolabeled with the "$^{99m}Tc(CO)_3$" core and injected in CD-1 mice. Tissue distributions as well as *in vivo* stability were monitored over a period of 48 h. The biodistribution data of both ^{99m}Tc-recombinant proteins were expressed as percentage of injected activity per gram of organ (% I.A./g ± S.D.) (Fig. 9). For all time points, a total of 85% to 99% of injected activity was recovered. These results clearly indicate similar uptake and elimination rates from major organs for both radiolabeled antibody fragments, $^{99m}Tc(CO)_3$-VHH and $^{99m}Tc(CO)_3$-VHH-ProtH, as well as the same excretory pathway. Most of the activity is rapidly taken by the kidney and excreted through the urinary tract.

Organ to blood ratio (Table 5) showed for both radiolabelled VHH and VHH-ProtH, a similar steady state biodistribution behavior, with a high radioactivity accumulation and retention within the kidney (390 times and 205 times more concentrated than in the blood, respectively, at 24 h p.i.). This high retention is common biological feature of radiolabelled proteins and peptides which is assigned to tubular reabsorption. Consequently, the total radioactivity excretion is not too rapid (70.2 ± 4.3 % I.A. and 62.6 ± 1.1% I.A. at 24 h p.i. for ^{99m}Tc-VHH and ^{99m}Tc-VHH-ProtH, respectively). Moreover biodistribution profile also showed a trend for both antibodies to accumulate within highly perfused organs like liver (11 times and 18 times more concentrated than in the blood, at 24 h p.i. for ^{99m}Tc-VHH and ^{99m}Tc-VHH-ProtH, respectively) and intestine (3 times more concentrated). No important radioactivity accumulation was found for any other organ with a lower concentration when compared to blood, except in the muscle and bone.

Chromatographic analysis of blood samples collected at sacrifice time demonstrated that both radiolabelled proteins are stable in blood serum, as no metabolite was detected. Most of the radioactivity (> 95%) is excreted in the urine as unidentified metabolites that were detected by ITLC after 1 h p.i.

DISCUSSION

Herein, we have evaluated the ability of the ProtH ABD of *S. pyogenes* to extend the circulation half-life of therapeutic proteins. For this purpose and to validate our strategy, the ProtH ABD was fused with an anti-TNFα VHH nanobody.

We have selected this single-domain antibody because VHH proteins are well-studied and natural monomeric antigen binders. Moreover, they can be easily produced and purified, and have high solubility and stability properties[19-22].

Our results, demonstrated that both VHH and VHH-ProtH proteins were stably produced in *E. coli*, with high yields of protein of several milligrams per liter of culture (25-30 mg for the VHH-ProtH and 15-20 mg for the unmodified nanobody).

The binding results obtained demonstrate that the presence of HSA (1 mg/ml) did not affect the binding of VHH-ProtH to human TNFα, showing similar values to the unmodified nanobody.

Moreover and importantly, the ProtH domain was shown to specifically bind to human, mouse and rat albumins. VHH-ProtH presented similar EC_{50} values in the nanomolar range at acidic and neutral pH. These results are according with a previous study that determined a high affinity of the ABD from streptococcal protein H to albumin (K_a = 7.8 nM) by surface plasmon resonanace (SPR)[12]. Other studies also reported albumin binding of the ABD from streptococcal protein G, alone and in fusion with recombinant antibodies, with affinities in the nanomolar range [10,18,23]. We also observed the formation of VHH-ProtH complexes with HSA and MSA *in vitro*, when incubated at different mass ratios. Interestingly, VHH-ProtH forms preferably dimers and trimers in solution with 2-fold increase of radius when comparing with the VHH (4.11/3.79 nm *versu*s 1.84 nm). These findings are supported by the observation that protein H forms temperature-dependent dimers and high molecular mass forms (at temperatures lower than 30 ºC)[12,24-27], probably through the D region and/or the C repeats. The protein H dimers had showed a higher affinity for albumin[12,24]. In this study the binding of VHH-ProtH to HSA or MSA seems to produce complexes in different mass ranges. Binding of VHH-ProtH to HSA produces complexes with high molecular mass, as it

has been seen for protein H binding to IgG[26], whereas binding of VHH-ProtH H to MSA produces complexes that contain fewer subunits of VHH-ProtH.

Furthermore, fusion of ProtH with the nanobody did not affect the high thermal stability of the nanobody (VHH $_{Tm}$ = ~70 ºC *versus* VHH-ProtH $_{Tm}$ = ~72 ºC). Serum stability studies also demonstrate the high stability in human and mouse serum of VHH and VHH-ProtH proteins (Fig. 6). Additionally, the TNF-neutralization assay results indicated a higher inhibition of TNFα activity of VHH-ProtH (EC_{50} = 19.02 nM *versus* EC_{50} = 68.29 nM), which is in accordance with the TNFα binding, showing that at nanomolar level the ProtH ABD fusion improved the efficacy of the anti-TNFα VHH.

Regarding the pharmokinetics, when compared to VHH, VHH-ProtH showed an extraordinary 26-fold increase of the terminal elimination half-life (47 min *versus* 20.5 h for the ProtH fusion nanobody). Moreover, the VHH-ProtH AUC was increased by a factor of 21 and the VHH-ProtH could be detected in the mouse serum until 48 h after injection (Fig. 8).The organ distribution of $^{99m}Tc(CO)_3$-VHH and $^{99m}Tc(CO)_3$-VHH-ProtH (Fig. 9) exhibited similar biodistribution profiles, presenting a kidney retention in both proteins (Fig. 9), common in radiolabelled proteins and peptides which is assigned to tubular reabsorption. Moreover biodistribution profile also showed a trend for both recombinant antibodies to accumulate within highly perfused organs, like the intestine.

Previous studies presented a similar strategy to extend half-life, using the ABD3 from streptococcal protein G in fusion with a bispecific single-chain diabody (scDb) developed for retargeting cytotoxic T cells to CEA-expressing tumor cells[10,18,28]. The terminal half-life of VHH-ProtH is similar of the circulation times determined for scDbCEACD3-ABD (27.6 h)[10] and for the same scDbCEACD3 in fusion with human serum albumin (25,0 h)[29]. This improvement of half-life probably can be compared with the half-lives of serum albumin, which are 1.07-1.6 days for mouse serum albumin and ~19 days for human serum albumin[30-32]. These findings indicate that VHH-ProtH utilizes binding to mouse albumin to achieve an extension in circulation time, most likely caused by reduced renal clearance and FcRn-mediated recycling effects of VHH-ProtH albumin complexes formed *in vivo*. Stork and co-workers, compared the half-life of the scDbCEACD3-ABD in the wild-type and neonatal Fc receptor (FcRn) heavy chain knockout mice and confirmed that the half-life extension of this fusion bispecific single-chain diabody is mediated through recycling by the FcRn[28].

A previous study developed bivalent nanobodies in fusion with AR1, an anti-TNFα VHH targeting murine and human albumin, to increase the accumulation of the single-domain antibody in the target tissue (inflamed joints) and to prolong its serum half-life. Their

biodistribution results demonstrated a significant increase of the bispecific anti-TNFα VHH in fusion with AR1 accumulated in inflamed joints and that this uptake was correlated with the higher clinical scores for the corresponding limbs. The bispecific anti-TNFα VHH in fusion with AR1, also revealed promising results in circulation time extension improvement. Consequently, the fusion with an anti-albumin anti-TNFα VHH substantially increased the half-life of the bivalent molecules targeting human (54 min and 35 min for monovalent VHH *versus* 2.2 days for the AR1 fusion) and mouse TNFα (47 min *versus* 1.9 days for the albumin-binding molecule fusion)[33].

Other studies indicated that high quantities of albumin accumulate and are metabolized in the inflamed joints of patients with active rheumatoid arthritis, which frequently develop hypoalbuminemia[34-37]. Preclinical models have demonstrated the possibility of albumin works as a biocarrier of therapeutic drugs in rheumatoid arthritis[38-40]. This information shows that albumin might be an attractive drug carrier to target biodrugs to inflammed joints of patients with rheumatoid arthritis.

Even though ProtH ABD has shown substantial progresses in pharmacokinetic properties of the nanobody, concerns with the immunogenicity of bacterial molecules for therapeutic applications may occur. For therapeutic use, particularly in small proteins that require administration by repeated injections, it will be necessary reduce or ideally eliminate the immunogenicity, and several de-immunization strategies can be applied to solve the immunogenicity of the ABD[41,42].

In summary, these experiments show that the fusion with ProtH ABD increase the half-life of a nanobody against human TNFα, improving the pharmacokinetic disposition of the parental VHH without affecting its therapeutic efficacy. VHH-ProtH is a promising example of the importance of drug carriers in developing a new generation of targeted therapeutic drugs. Targeting inflamed joints by fusion to ProtH ABD might be an attractive strategy in the treatment of rheumatoid arthritis. Using the properties of albumin as a drug carrier, this strategy to improve pharmacokinetic behavior of therapeutic proteins, can be a promising approach to use as a fusion partner with other molecules for the treatment of several diseases.

REFERENCES

1. Walsh, G. (2005) Biopharmaceuticals: recent approvals and likely directions. *Trends Biotechnol*. **23**, 553-558

2. Deng, R., Jin, F., Prabhu, S., Iyer, S. (2012) Monoclonal antibodies: what are the pharmacokinetic and pharmacodynamics considerations for drug development? *Expert Opin. Drug Metab. Toxicol.* **8**, 141-160

3. Kontermann, R.E. (2009) Strategies to extend plasma half-lives of recombinant antibodies. *Biodrugs* **23,** 93-109

4. Kontermann, R.E. (2011) Strategies for extended serum half-life of protein. *Curr. Opin. Biotechnol.* **22**, 1-9

5. Holliger, P., Hudson, P.J. (2005) Engineered antibody fragments and the rise of single domains. *Nat. Biotechnol*. **23**, 1126-1136

6. Dennis, M.S., Zhang, M., Meng, G., Kadkhodayan, M., Kirchofer, D., Combs, D., Damico, L.A. (2002) Albumin binding as a general strategy for improving the pharmacokinetics of proteins. *J. Biol. Chem.* **277**, 35035-35043

7. Anderson, C.L., Chaudhury, C., Kim, J., Bronson, C.L., Wani, M.A., Mohanty, S. (2006) Perspective - FcRn transports albumin: relevance to immunology and medicine. *Trends Immunol*. **27**, 343-348

8. Roopenian D.C., Akilesh S. (2007) FcRn: the neonatal Fc receptor comes of age. *Nat. Rev. Immunol*. **7**, 715-725

9. Lencer, W.I., Blumberg, R.S. (2005) A passionate kiss, then run: exocytosis and recycling of IgG by FcRn. *Trends Cell Biol*. **15**, 5-9

10. Stork, R., Müller, D., Kontermann, R.E. (2007) A novel tri-functional antibody fusion protein with improved pharmacokinetic properties generated by fusing a bispecific single-chain diabody with an albumin-binding domain from streptococcal protein G. *Protein Eng. Des. Sel.* **20**, 569-576

11. Podbielski , A. (1993) Three different types of organization of vir regulon in group A streptococci. *Mol. Gen. Genet.* **237**, 287-300

12. Frick, I.-M., Ákesson, P., Cooney, J., Sjöbring, U., Schmidt, K.-H., Gomi, H., Hattori, S., Tagawa, C., Kishimoto, F., Björck, L. (1994) Protein H – a surface protein of Streptococcus pyogenes with separate binding sites for IgG and albumin. *Mol. Microbiol.* **12,** 143-151

13. Björck, L., Kastern, W., Lindhal, G., Widebäck, K. (1987) Streptococcal protein G, expressed by streptococci or by *Escherichia coli*, has separate binding sites for human albumin and IgG. *Mol. Immunol*. **24**, 1113-1122

14. Falkenberg, C., Björck, L., Ákesson, P. (1992) Localization of the binding site for streptococcal protein G on human serum albumin. Identification of a 5.5-kDa protein G binding albumin fragment. *Biochemistry*. **31**, 1451-1457

15. Silence, K., Lauwereys, M., Hans de, H. (2007) Single-domain antibodies directed against tumor necrosis factor-alpha and uses therefore. United States Patent Application Publication, US 2007/007769 A1, Boston, MA

16. Barbas III, C.F., Burton, D. R., Silvermann, GJ. (2001) *Phage Display: A Laboratory Manual.* 1st Ed., Cold Spring Harbor Laboratory Press, Cold Spring Harbor, NY

17. Ameloot, P., Brouckaert, P. (2004) Production and characterization of receptor-specific TNF muteins. *Methods Mol. Med.* **98**, 33-46

18. Hopp, J., Hornig, N., A.Zettlitz, K., Schwarz, A., Fuß, N., Müller, D., Kontermann, R.E. (2010) The effects of affinity and valency of an albumin-binding domain (ABD) on the half-life of single-chain diabody-ABD fusion protein. *Protein Eng. Des. Sel.* **23**, 827-834

19. Arbadi-Ghahroudi, M., Tanha, J., MacKenzie, R. (2005) Prokaryotic expression of antibodies. *Cancer Metastasis Rev.* **24**, 501-519

20. Frenken, L.G.J., van der Linden, R.H.J., Herman, P., Bos, J.W., Ruuls, R.C., de Geus, B., Verrips, C.T. (2000) Isolation of antigen specific llama VHH antibody fragments and their high level secretion by *Saccharomyces cerevisiae*. *J. Biotechnol*. **78**, 11-21

21. Frenken, L.G.J., Hessing, J.G., Van den Hondel, C.A., Verrips, C.T. (1998) Recent advances in the large-scale production of antibody fragments using lower eukaryotic microorganisms. *Res. Immunol*. **149**, 589-599

22. Muyldermans, S. (2013) Nanobodies: natural single-domain antibodies. *Annu. Rev. Biochem*. **82**, 775-797

23. Linhult, M., Binz, H.K., Uhlén, M., Hober, S. (2002) Mutational analysis of the interaction between albumin-binding domain from streptococcal protein G and human serum albumin. *Protein Sci*. **11**, 206-213

24. Akerstrom, B., Lindahl, G., Bjorck, L., Lindqvist, A. (1992) Protein Arp and protein H from group A streptococci. Ig binding and dimerization are regulated by temperature. *J. Immunol.* **148**, 3238-3243.

25. Cedervall, T., Akesson, P., Stenberg, L., Herrmann, A., Akerstrom, B. (1995) Allosteric and temperature effects on the plasma protein binding by streptococcal M protein family members. Scandinavian journal of immunology **42,** 433-441

26. Berge, A., Kihlberg, B.M., Sjoholm, A.G., Bjorck, L. (1997) Streptococcal protein H forms soluble complement-activating complexes with IgG, but inhibits complement activation by IgG-coated targets, *J. Biol. Chem*. **272**, 20774-20781

27. Nilsson, B.H.K., Frick, I.-M., Åkesson, P., Forsén, S. Björck, L., Åkerström, B., Wikström, M. (1995) Structure and stability of protein H and the M1 protein from Streptococcus pyogenes. Implications for other surface proteins of Gram-positive bacteria. *Biochemistry* **34**, 13688-13698

28. Stork, R., Campigna, E., Robert, B., Müller, D., Kontermann, R.E. (2009) Biodistribution of a bispecific single-chain diabody and its half-life extended derivatives. *J. Biol. Chem.* **284**, 25612-25619

29. Müller, D., Karle, A., Meissburger, B., Höfig, I., Stork, R., Kontermann, R.E. (2007) Improved pharmacokinetics of recombinant bispecific antibody molecules by fusion to human serum albumin. *J Biol. Chem*. **282**, 12650-12660

30. Dixon, F.J., Maurer, P.H., Deichmiller, M.P. (1953) Half-lives of homologous serum albumins in several species. *Proc. Soc. Exp. Biol. Med.* **83**, 287-288

31. Peters, T, Jr. (1985) Serum albumin. *Adv. Protein Chem.* **37**, 161-245

32. Schmidt, M.M., Townson, S.A., Andreucci, A.J., King, B.M., Schirmer, E.B., Murillo, A.J., Dombrowski, C., Tisdale, A.W., Lowden, P.A., Masci, A.L., Kovalchin, J.T., Erbe, D.V., Wittrup, K.D., Furfine, E.S., Barnes, T.M. (2013) Crystal structure of an HSA/FcRn complex reveals recycling by competitive mimicry of HSA ligands at a pH-dependent hydrophobic interface. *Structure* **21**, 1966-1978

33. Coppieters, K., Dreier, T., Silence, K., de Haard, H., Lauwereys, M., Casteels, P., Beirnaert, E., Jonckheere, H., Van de Wiele, C., Staelens, L., Hostens, J., Revets, H., Remaut, E., Elewaut, D., Rottiers, P. (2006) Formatted anti-tumor necrosis factor alpha VHH proteins derived from camelids show superior potency and targeting to inflamed joints in a murine model of collagen-induced arthritis. *Arthritis Rheum.* **54**, 1856-1866

34. Neumann, E., Frei, E., Funk, D., Becker, M.D., Schrenk, H.H., Müller-Ladner, U., Fiehn, C. (2010) Native albumin for targeted drug delivery. *Expert. Opin. Drug Deliv.* **7**, 915-925

35. Ballantyne, F.C., Fleck, A., Dick, W.C. (1971) Albumin metabolism in rheumatoid arthritis. *Ann. Rheum. Dis.* **30**, 265-270

36. Wilkinson, P., Jeremy, R. Brooks, F.P., Hollander, J.L. (1965) The mechanism of hypoalbuminemia in rheumatoid arthritis. *Ann. Intern. Med.* **63**, 109-114.

37. Levick, J.R. (1981) Permeability of rheumatoid and normal human synovium to specific plasma proteins. *Arthritis Rheum.* **24**, 1550-1560

38. Wunder, A., Müller-Ladner, U., Stelzer, E.H., Funk, J., Neumann, E., Stehle, G., Pap, T., Sinn, H., Gay, S., Fiehn, C. (2003) Albumin-based drug delivery as novel therapeutic approach for rheumatoid arthritis. *J. Immunol.* **170**, 4793-4801

39. Fiehn, C., Müller-Ladner, U., Gay, S., Krienke, S., Freudenberg-Konrad, S., Funk, J., Ho, A.D., Sinn, H., Wunder, A. (2004) Albumin-coupled methotrexate (MTX-HSA) is a new anti-arthritic drug which acts synergistically to MTX. *Rheumatology* **43**, 1097-1105

40. Fiehn, C., Neumann, E., Wunder, A., Krienke, S., Gay, S., Müller-Ladner, U. (2004) Methotrexate (MTX) and albumin coupled with MTX (MTX-HSA) suppress synovial fibroblast invasion and cartilage degradation in vivo. *Ann. Rheum, Dis.* **63**, 884-886

41. Baker, M.P., Jones, T.D. (2007) Identification and removal of immunogenicity in therapeutic proteins. *Curr. Opin. Drug Discov. Devel*. **10**, 219-227

42. Nagata, S., Pastan, I. (2009) Removal of B cell epitopes as a practical approach for reducing the immunogenicity of foreign protein-based therapeutics. *Adv. Drug Deliv. Rev*. **61**, 977-985

ABBREVIATIONS

ABD, albumin-binding domain; AUC, area under the curve; FcRn, neonatal Fc receptor; HSA, human serum albumin; IgG, immunoglobulin G; MSA, mouse serum albumin; PEG, polyethylene glycol; ProtH, ABD from streptococcal cell surface protein H; RSA, rat serum albumin; TNFα, tumour necrosis factor, VHH, camelid single-domain antibody or nanobody.

ACKNOWLEDGMENTS

Fundação para a Ciência e a Tecnologia (FCT), Portugal, is acknowledged for funding (project PTDC/SAU-FAR/115846/2009). C. Cantante e M. Morais thank the FCT for PhD fellowships (SFRH/BD/48598/2008 and SFRH/BD/48066/2008, respectively). We thank Dr. C. Xavier and Prof. V. Cavaliers for a generous gift of p-SCN-Bn-NOTA and fruitful discussions.

.

FIGURE LEGENDS

Fig. 1: Construction and production of VHH and VHH-ProtH. (A) Domain structure of VHH and VHH-ProtH including the N-terminal leader peptide (LP) and the C-terminal histidine (His_7) and HA tags. (B) Sequence of the wild-type ABD. (C) SDS-PAGE and (D) Western Blot analysis of the VHH and VHH-ProtH purified proteins (3 µg/lane) under reducing (lanes 1 and 2) and non-reducing conditions (lanes 3 and 4). Gels were stained with Coomassie brilliant blue (C) or immunoblotted with an anti-HA-tag antibody (D).

Fig. 2: Binding of VHH and VHH-ProtH to human TNFα. ELISA plates were coated with human TNFα (200 ng/well) and binding of VHH and VHH-ProtH fusion protein was measured in the presence (A) and absence (B) of HSA (1 mg/ml). Detection was achieved using an HRP-conjugated anti-HA-tag antibody.

Fig. 3: Binding of VHH-ProtH to human, rat and mouse albumin. Binding of VHH and VHH-ProtH fusion protein was evaluated in ELISA at neutral pH - pH 7.4 (A); and acidic pH - pH 6.0 (B). Bound proteins were detected using an HRP-conjugated anti-HA-tag antibody.

Fig. 4: Formation of VHH-ProtH/albumin complexes. Size exclusion chromatography analysis of VHH-ProtH (A), HSA (B), VHH-ProtH/HSA complex (C), MSA (D) and VHH-ProtH/MSA complex (E). VHH-ProtH was incubated at 1:1 (w/w) with albumins in PBS1x at room temperature. Peak positions of marker proteins are indicated. Chromatograms in C and E were resolved into individual Gaussian peaks by using linear least-squares fit (PeakFit, Systat Software Inc). *Insets* in C and E represent SDS-PAGE analysis of selected fractions. M, molecular weight marker.

Fig. 5: TNFα-neutralization capacities of VHH and VHH-ProtH. Dose-response curves of VHH and VHH-ProtH proteins to examine the TNFα-mediated cytoxicity were calculated in the presence of 0,5 ng/ml human TNFα, on the TNF-sensitive mouse fibroblast cell line L929s.

Fig. 6: *In vitro* stability in human and mouse serum of VHH and VHH-ProtH. In vitro stability of the recombinant proteins was determined in human serum (A) and mouse serum (B) at 37 ºC, during 24 days and 4 days, respectively. Proteins were detected by Western Blot, using an anti-His-tag antibody.

Fig. 7: Pharmacokinetic properties. Both VHH and VHH-ProtH fusion protein were i.v. injected into CD-1 mice (25 µg/animal) and absorbance pharmacokinetic profiles of these proteins were calculated by ELISA, at different time points. Data were normalized considering maximal concentration of protein at the first time point (5 min).

Fig. 8: *In vivo* stability in mouse serum of VHH and VHH-ProtH. In vivo stability of VHH-ProtH (A) and VHH (B) was evaluated by western blot with an anti-HA-tag antibody, in the mice serum samples collected during the pharmacokinetic assay.

Fig. 9: Biodistribution of $^{99m}Tc(CO)_3$-VHH and $^{99m}Tc(CO)_3$-VHH-ProtH. Organ distribution of ^{99m}Tc-VHH (A) and ^{99m}Tc-VHH-ProtH (B) proteins in CD-1 mice.

TABLES

Table 1: Binding of VHH-ProtH to HSA, RSA and MSA.

Protein	**EC_{50} for HSA (nM)**	**EC_{50} for RSA (nM)**	**EC_{50} for MSA (nM)**
VHH-ProtH pH 6.0	53.03 ± 0.02	40.76 ± 0.04	36.74 ± 0.08
VHH-ProtH pH 7.4	39.70 ± 0.03	42.88 ±0.05	16.50 ± 0.07

Table 2: Molecular mass and hydrodynamic radius.

Protein or complex	**Length**	**Calculated M_r[a]**	**SEC apparent M_r**	**Stokes' radius (R_S)**
	aa	*kDa*	*kDa*	*nm*
VHH	180	19.4	14.9	1.84
VHH-ProtH	321	34.7	97.2/75.6	4.11/3.79
HSA	585	66.5	68.1	3.67
MSA	584	65.9	64.3	3.60
VHH-ProtH /HSA	−	101.2	218/147	5.30/4.67
VHH-ProtH /MSA	−	100.6	98.9	4.01

[c]Calculated based on the amino acid sequence.

Table 3: Thermal stability of VHH and VHH-ProtH.

Protein	**Tm B - Mean (°C)**	**Tm B – Median (°C)**	**Tm D - Mean (°C)**	**Tm D - Median (°C)**
VHH	71.53 ± 0.14	71.56 ± 0.14	72.34 ± 0.25	72.43 ± 0.25
VHH-ProtH	71.73 ± 0.08	71.57± 0.08	73.58 ± 0.10	73.70 ± 0.10

Tm B - Calculated Boltzamnn melting temperature; Tm D - Calculated Derivated melting temperature.

Table 4: Pharmacokinetic parameters of VHH and VHH-ProtH.

Protein	**$t_{1/2}\alpha$ (h)**	**$t_{1/2}\beta$ (h)**	**$AUC_{(0\text{-}24\ h)}$ (%*h)**
VHH	0.52 ± 0.25	0.79 ± 0.12	72.75 ± 7.35
VHH-ProtH	3.59 ± 0.24	20.54 ± 0.12	1539.17 ± 92.39

Table 5: Organ to blood ratio of ^{99m}Tc-VHH and ^{99m}Tc VHH-ProtH at 24 h time point

Organ	VHH	VHH-ProtH
Liver	11.3	18.6
Intestine	3.42	3.45
Spleen	0.413	0.456
Heart	0.122	0.121
Lung	1.80	0.375
Kidney	390	205
Muscle	4.77	5.87
Bone	2.09	2.03
Stomach	0.600	0.500
Pancreas	0.140	0.167

Figure 1

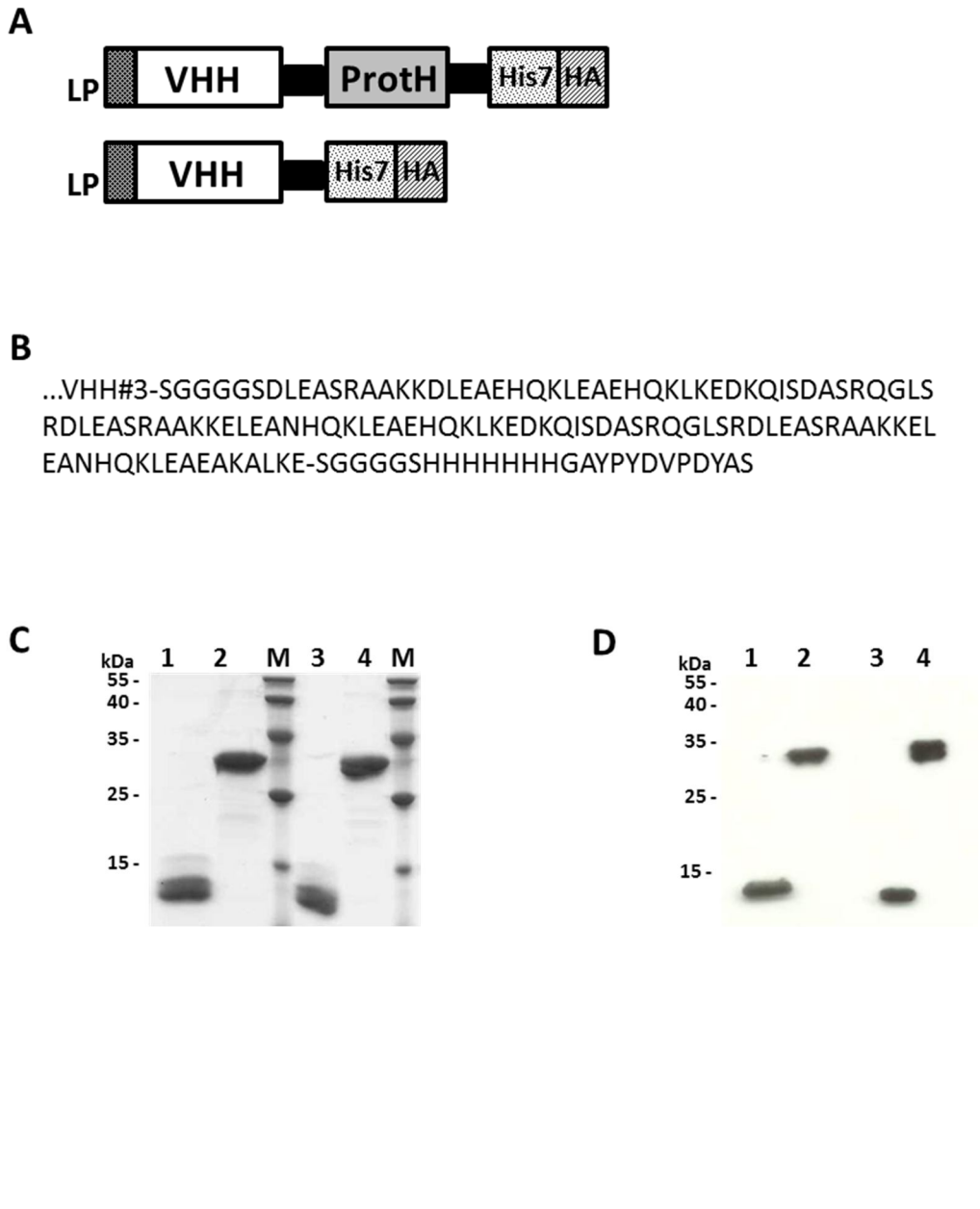
A
LP
VHH
ProtH
His7
HA
LP
VHH
His7
HA
B
...VHH#3-SGGGGSDLEASRAAKKDLEAEHQKLEAEHQKLKEDKQISDASRQGLS
RDLEASRAAKKELEANHQKLEAEHQKLKEDKQISDASRQGLSRDLEASRAAKKEL
EANHQKLEAEAKALKE-SGGGGSHHHHHHHHGAYPYDVPDYAS
C
kDa
1
2
M
3
4
M
55 -
40 -
35 -
25 -
15 -
D
kDa
1
2
3
4
55 -
40 -
35 -
25 -
15 -

Figure 2

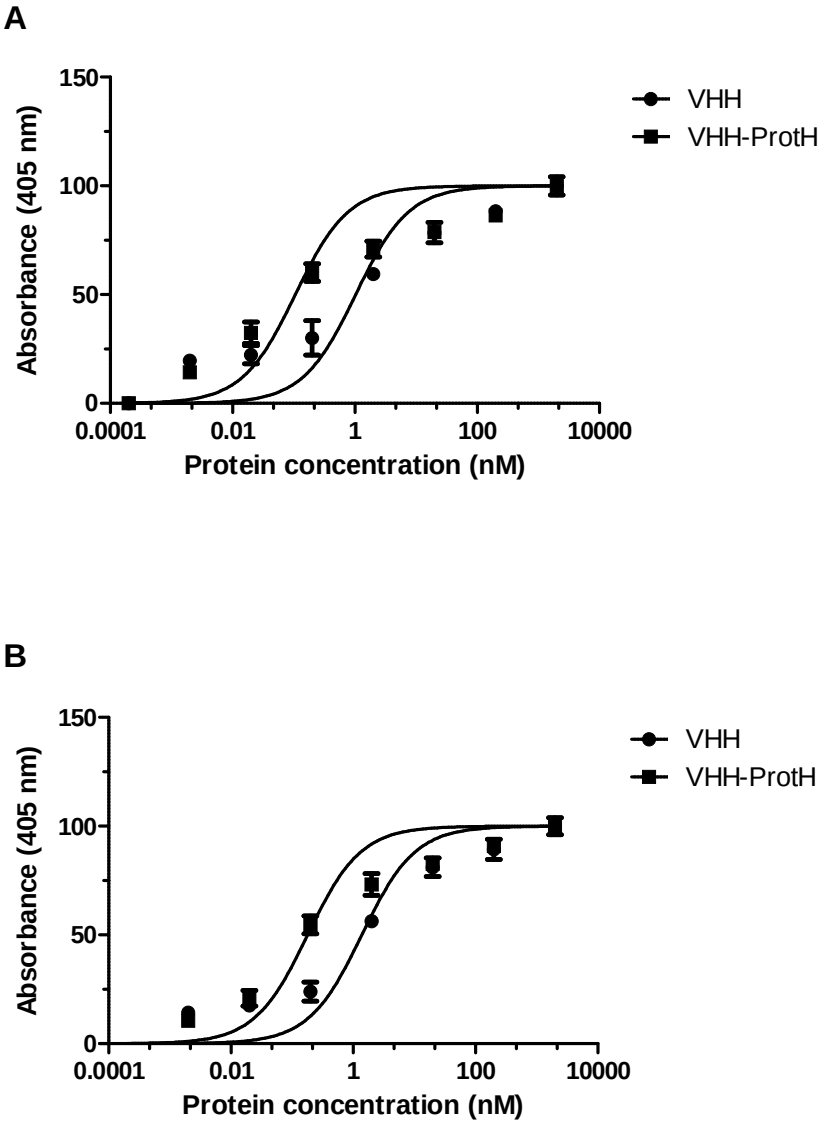
A
150
100
50
0
Absorbance (405 nm)
0.0001
0.01
1
100
10000
Protein concentration (nM)
VHH
VHH-ProtH
B
150
100
50
0
Absorbance (405 nm)
0.0001
0.01
1
100
10000
Protein concentration (nM)
VHH
VHH-ProtH

Figure 3

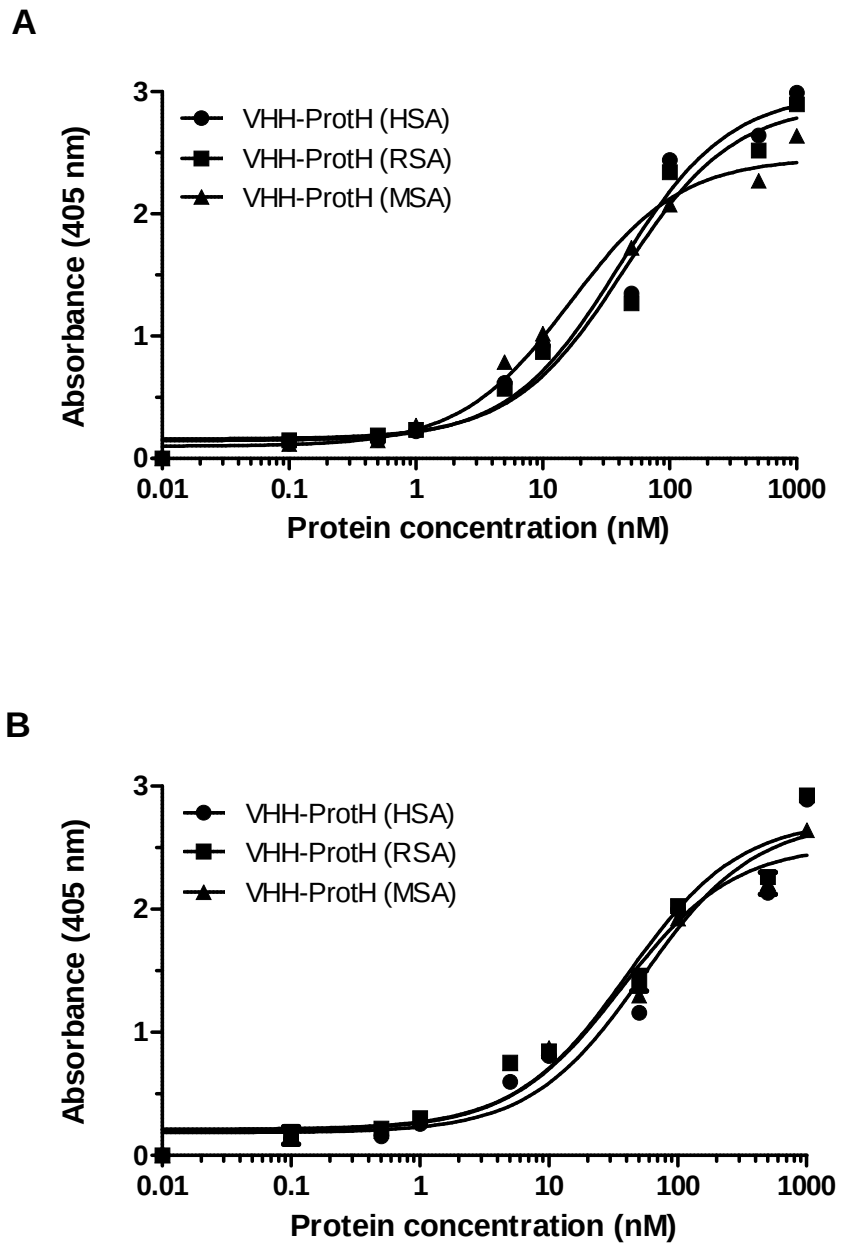
A
Absorbance (405 nm)
VHH-ProtH (HSA)
VHH-ProtH (RSA)
VHH-ProtH (MSA)
Protein concentration (nM)
B
Absorbance (405 nm)
VHH-ProtH (HSA)
VHH-ProtH (RSA)
VHH-ProtH (MSA)
Protein concentration (nM)

Figure 4

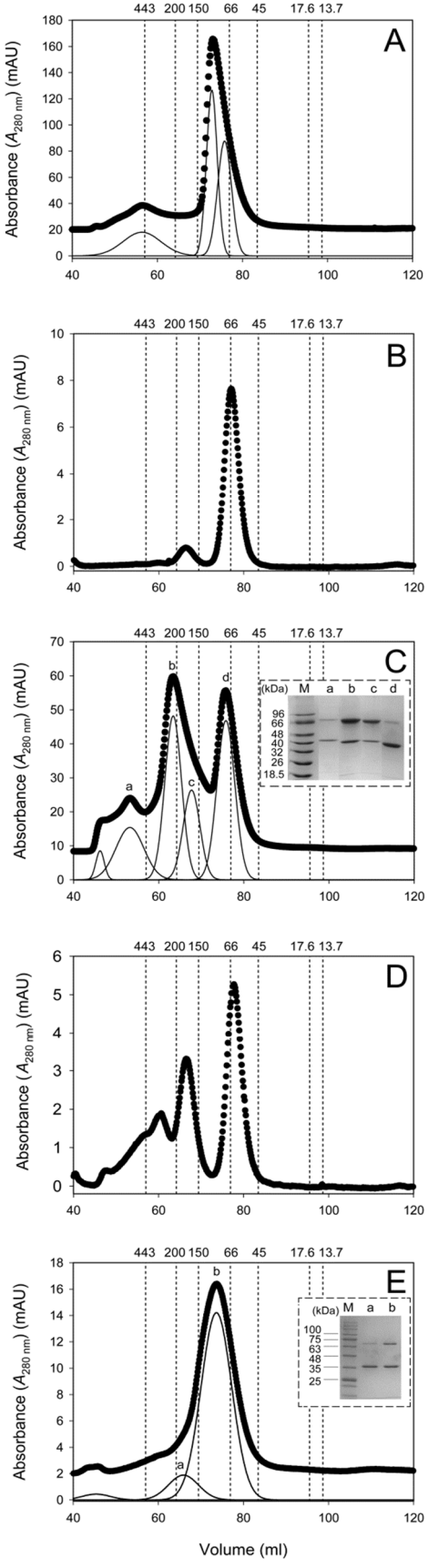
443 200 150 66 45 17.6 13.7
A
B
C
D
E
Absorbance ($A_{280\ nm}$) (mAU)
Volume (ml)
(kDa) M a b c d
96
66
48
40
32
26
18.5
(kDa) M a b
100
75
63
48
35
25

Figure 5

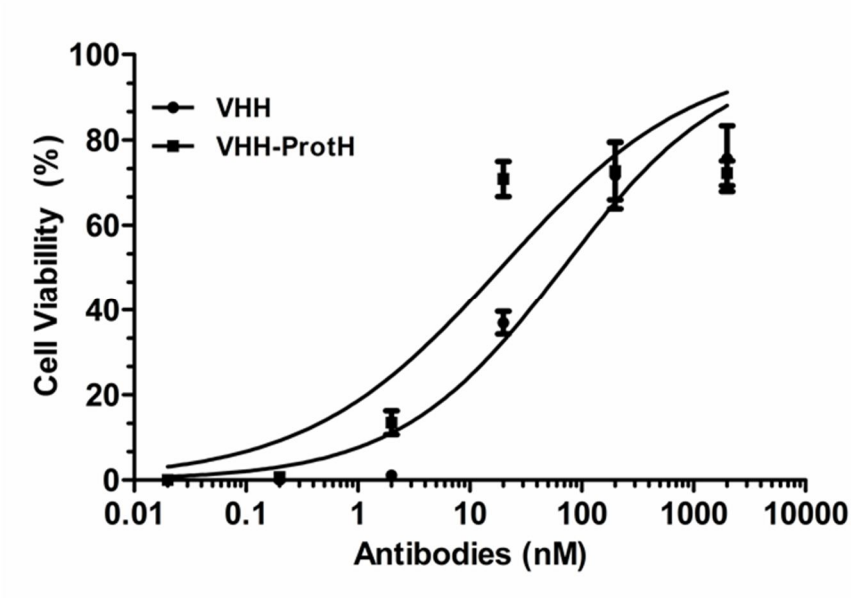
100
80
60
40
20
0
Cell Viabillity (%)
VHH
VHH-ProtH
0.01
0.1
1
10
100
1000
10000
Antibodies (nM)

Figure 6

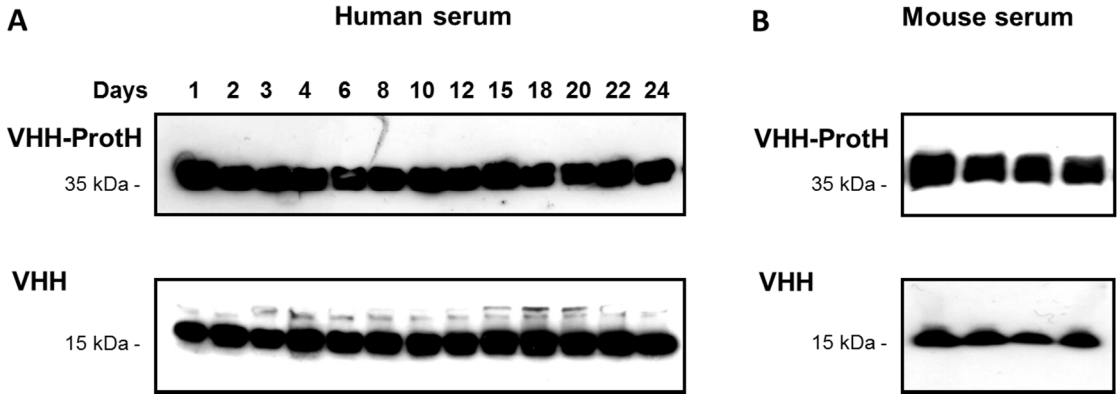
A
Human serum
Days 1 2 3 4 6 8 10 12 15 18 20 22 24
VHH-ProtH
35 kDa -
VHH
15 kDa -
B
Mouse serum
VHH-ProtH
35 kDa -
VHH
15 kDa -

Figure 7

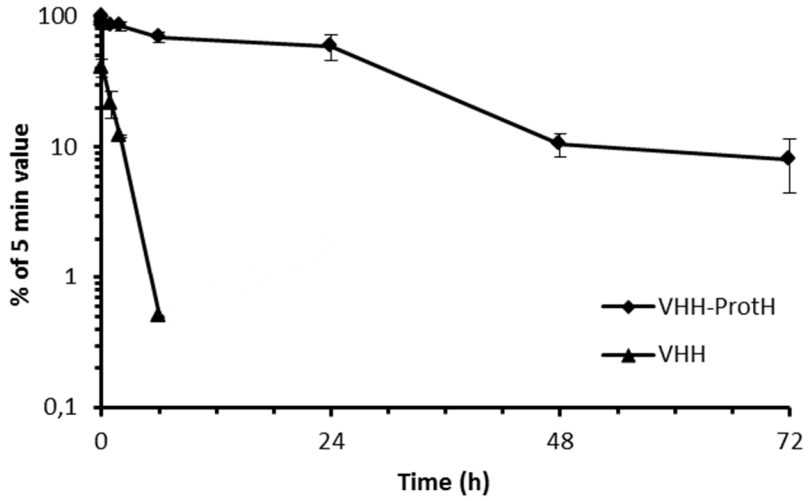

Figure 8

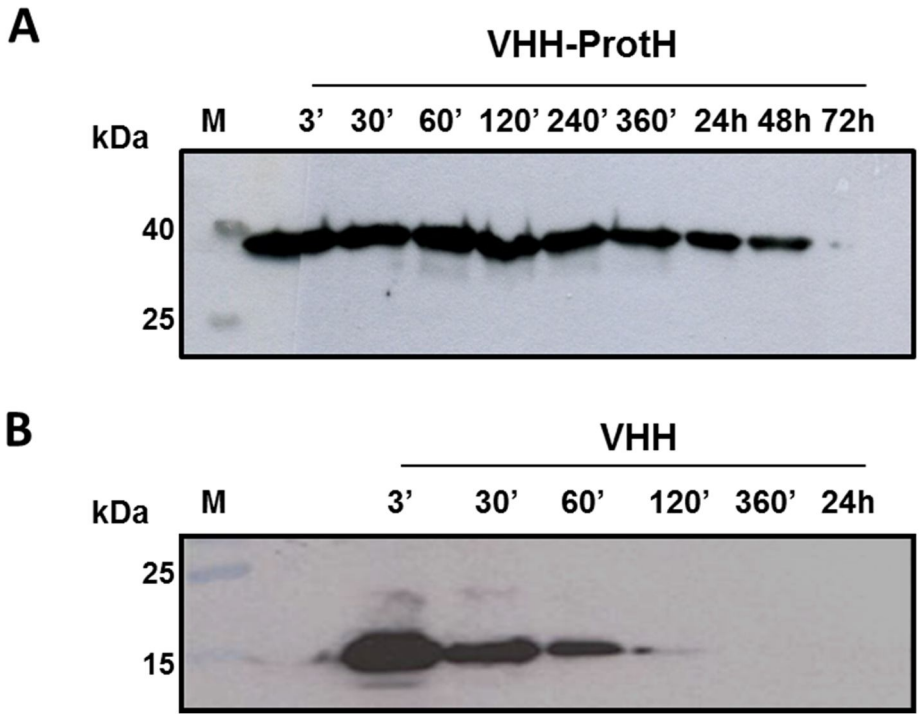
A
VHH-ProtH
M
3’ 30’ 60’ 120’ 240’ 360’ 24h 48h 72h
kDa
40
25
B
VHH
M
3’ 30’ 60’ 120’ 360’ 24h
kDa
25
15

Figure 9

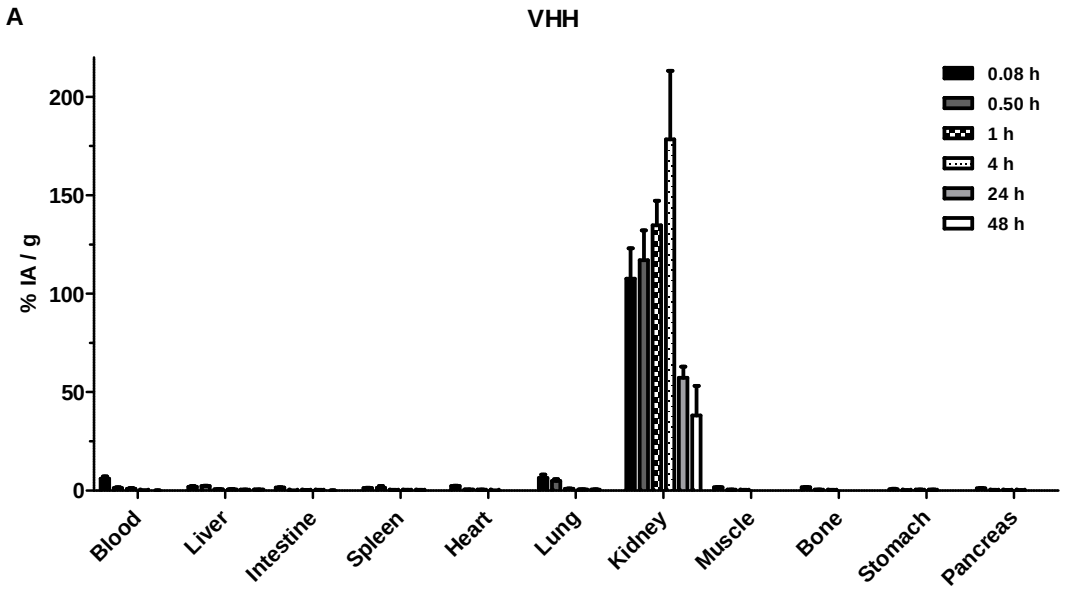
A
VHH
% IA / g
200
150
100
50
0
0.08 h
0.50 h
1 h
4 h
24 h
48 h
Blood
Liver
Intestine
Spleen
Heart
Lung
Kidney
Muscle
Bone
Stomach
Pancreas

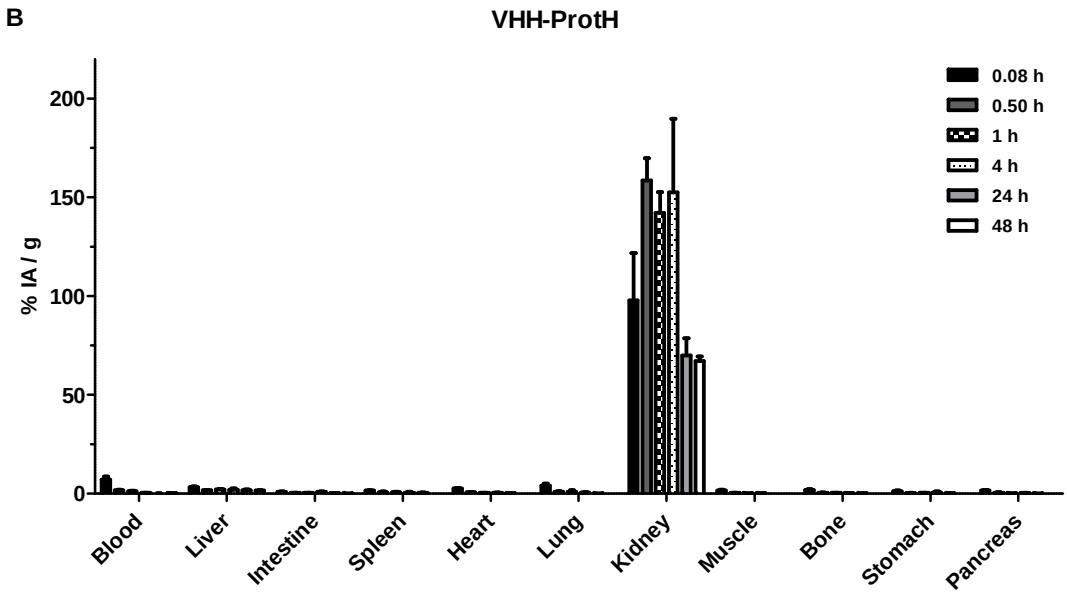
B
VHH-ProtH
% IA / g
200
150
100
50
0
0.08 h
0.50 h
1 h
4 h
24 h
48 h
Blood
Liver
Intestine
Spleen
Heart
Lung
Kidney
Muscle
Bone
Stomach
Pancreas

ALBUMIN-BINDING CHARACTERIZATION AND THREE-DIMENSIONAL STRUCTURE OF ZAG ABD FROM STREPTOCOCCUS ZOOEPIDEMICUS

Brief Introduction

Streptococcal albumin-binding domains have been extensively studied as fusion proteins to improve the pharmacokinetic properties of therapeutic proteins and as protein scaffolds for therapeutic applications (Kontermann, 2012).

ZAG is a cell-surface protein G-related from *S. zooepidemicus*, with an Ig-binding region located in the C-terminus and an ABD composed by 52 amino acids, showing an albumin-binding profile similar to the protein G (Jonsson *et al*., 1994). Protein G albumin-binding domain (SpG) presents a three-α-helix three-dimensional structure (Kraulis *et al*, 1996), and has been successfully explored as a protein scaffold (Fredj, 2012).

In this research work we characterize the protein ZAG ABD (Zag) ability to bind albumin and stability. We also report the circular dichroism (CD) measurements of Zag ABD and Zag/albumin complex conformations, and the assignment of the NMR ^{15}N and ^{13}C backbones resonances of Zag ABD to determine its three-dimensional structure. Firstly, we optimize the production of the Zag ABD in *E.coli*, an easy way to obtain high amounts of protein with lower costs. Then we characterize the albumin binding and stability of the Zag motif. Finally, we investigated the conformation of Zag ABD in the presence and absence of human serum albumin and determined the three-dimensional structure of Zag motif by NMR.

Albumin-binding characterization and three-dimensional structure of Zag ABD from *Streptococcus zooepidemicus*

Cátia Cantante[1,2], Ângelo Figueiredo[3], João Leandro[4], Diana Gaspar[2], Vasco Gonçalves[1,2], Paula Leandro[4], Miguel Castanho[2], Frederico Aires-da-Silva[5,6] Eurico Cabrita[3] and João Gonçalves[1,2]

[1] CPM-URIA, Faculdade de Farmácia, Universidade de Lisboa, 1649-003 Lisbon, Portugal
[2] Instituto de Medicina Molecular, Faculdade de Medicina, Universidade de Lisboa,1649-028 Lisbon, Portugal
[3] CQFB/REQUIMTE, Faculdade de Ciências e Tecnologia, Universidade Nova de Lisboa, 2829-516 Caparica, Portugal
[4] iMed.UL, Faculdade de Farmácia, Universidade de Lisboa, 1649-003 Lisbon, Portugal
[5] Faculdade de Medicina Veterinária, Universidade de Lisboa,1300-477 Lisbon, Portugal
[6] Technophage, SA, 1649-028 Lisbon, Portugal

Keywords: ZAG cell surface protein, albumin-binding domain, serum albumin, three-helix-bundle, protein scaffolds.

Background: Albumin-binding domains (ABD) have been extensively studied and engineered to improve half-life of therapeutic proteins and as protein scaffolds for therapeutic applications.

Results: Streptococcal Zag ABD could be stably produced in bacteria, presenting high binding to human, rat and mouse serum albumins. By NMR spectroscopy we could determine the solution structure of the Zag protein and show that it has a three-alpha helix conformation.

Conclusions: The Zag ABD albumin-binding moiety exhibit albumin-binding properties and a three-dimensional structure similar with other protein G-related proteins.

Significance: This study further establishes Zag albumin-binding domain as a possible scaffold that can be further engineered as a therapeutic protein and as a strategy to improve pharmacokinetics of small therapeutic proteins or peptides.

ABSTRACT

Zag, a protein G-related cell surface protein from *Streptococcus zooepidemicus*, presents a multiple domain structure comprising an albumin-binding domain (ABD), immunoglobulin G (IgG)-binding domains and a α_2-macroglobulin binding site. Streptococcal albumin-binding domains structure and function have been extensively studied in the last years, with promising results for therapeutic applications as scaffolds or used as albumin-binding moieties to improve the pharmacokinetics of small therapeutic proteins. In the present study, we characterize and solved the structure of the Zag ABD from *S. zooepidemicus.* Our results shown that the Zag protein could be stably expressed in the soluble format in *Escherichia coli*, presented high thermal stability properties and specifically recognize mouse, rat and

human albumins. Furthermore, Far-UV circular dichroism analysis of the Zag secondary structure in buffer reveals a high helical content also shows that when the protein is bound to human serum albumin (HSA), the formed complex is also α-helical structured. Importantly, by NMR spectroscopy we could determine the solution structure of the Zag protein and show that it has a three-alpha helix conformation.

Our findings show the great potential of Zag albumin-binding domain as a possible scaffold that can be further engineered as a therapeutic protein and as a strategy to improve pharmacokinetics of small therapeutic proteins.

INTRODUCTION

Since the early 90's, a broad class of three-helix albumin-binding domains have been investigated and described. The protein G albumin-binding domains structure and properties have been extensively studied, and their applications for improving pharmacokinetics of therapeutic antibodies has been well documented[1-4]. Previous work from de Château and Björck with PAB cell surface protein from *Peptosteptococcus magnus*, a mosaic albumin-binding bacterial protein, representing for the first time an example of a shuffled bacterial module[5]. The protein G albumin-binding domain, or other protein G-related albumin-binding modules, as the GA module from PAB protein, showed three-helix bundle architectures[6,7]. Recent studies used molecule based-structure methods to develop new scaffolds for therapeutic applications in several diseases, e.g. cancer and inflammatory diseases[8-10]. Affibody molecules are small (6-7 kDa) high affinity and robust 3-helix proteins, based on a modified immunoglobulin-binding B domain of staphylococcal protein A. Affibody scaffolds are a successful example of the therapeutic potential of these kind of molecules[11-14].

Depending on the bacterial strain, albumin-binding domains (ABDs) and Ig-binding domains (IgBDs) can contain one, two or three repeats of approximate 50-60 amino acid residues[4,5,15,16]. Interestingly, like streptococcal ABDs, IgBDs can also present a three-α-helix bundle and additionally, there were described compact structures composed of a four-stranded β-sheet and one-α-helix[17,18]. At least 16 repeated albumin-binding domains, also known as GA modules, with relatively high sequence identity have been identified in several bacterial species[19]. The interactions between these GA modules with albumin may play an important role in the pathogenesis of these microorganisms. Therefore, pathogenic bacteria may have surface proteins with these domains to allow coating their surfaces with host proteins in mammalian plasma during the infectious process[20].

Jonsson and co-workers described a plasma protein receptor, a protein-G related cell surface protein from *Streptococcus zooepidemicus*, termed protein ZAG, a 45 kDa protein with distinct bind sites for α_2-macroglobulin, serum albumin and immunoglobulin G (IgG). The IgG-binding domains from ZAG are homologous to the IgG-binding domains in protein G and to the corresponding domains in proteins MIG and MAG from *S. dysgalactiae*[4]. Protein ZAG shows an albumin-binding profile similar to those of protein G[21] and the albumin-binding DG12 protein from a bovine group G streptococcus[20]. In the N-terminus, ZAG protein presents a 52 amino acid sequence ABD with binding to human, rat, mouse, horse and dog serum albumin. Downstream from this region there are two amino acid repeats homologous to the IgG-binding domains of type III Fc receptors[4].

In the present study, we characterize and solved the structure of the Zag ABD from *S. zooepidemicus.* For this propose, the Zag/albumin binding activity was characterized by ELISA, SEC and circular dichroism (CD) assays. To solve the Zag ABD structure nuclear magnetic resonance (NMR) ^{15}N and ^{13}C backbone resonances technique was applied.

EXPERIMENTAL PROCEDURES

Materials – Human serum albumin (HSA) (catalog no. A3782), rat serum albumin (RSA) (catalog no. A6272), mouse serum albumin (MSA) (catalog no. A3139) and pT7-FLAG2 expression vector were purchased from Sigma-Aldrich (USA). Antibody HRP-conjugated anti-His-tag, 2,2'-Azino-di-[3-ethylbenzthiazoline sulfonate (6)] diammonium salt (ABTS), and cOmplete EDTA-free protease inhibitors cocktail were acquired from Roche (Germany). HisTrap HP columns and Amicon were purchased from GE Healthcare (UK) and Millipore, respectively.

Construction of pT7-Zag – DNA encoding the Zag albumin-binding domain of *Streptococcus zooepidemicus*[4] was generated by PCR with primers HindIII-Zag-F (5’ -CCC AAG CTT ATG GAC ATT ACA GGA GCA GCC TTG- 3’) and Zag-BglII-R: (5’ -GGA AGA TCT CTA GTG ATG GTG ATG GTG ATG GCT GCC TCC GCC AGA CGG TAG AGC TGA TAA-3’), using the pT7-VHH-Zag vector previously constructed[22], adding HindIII and BglII restriction sites at the fragment 5’ and 3’ ends, respectively and the sequences encoding peptide tag (His_6) for purification and detection. The resulting PCR fragments were gel-purified, digested with the restriction enzymes and cloned into the appropriately cut pT7-FLAG2 vector. A short GS linker (SGGGGS) was used to link the Zag ABD to the His_6-tag. The pT7-Zag construct was verified by sequencing.

Expression and purification of Zag – Zag ABD was expressed in *Escherichia coli* strain BL21(DE3). One liter of LB, containing 100µg/ml ampicillin were inoculated with 10 ml of overnight culture of bacterial cells transformed with the plasmid pT7-Zag and grown to exponential phase (A_{600} = 0.6-0.9) at 37 ºC. Expression was induced by the addition of 1 mM isopropyl β-D-1-thiogalactopyranoside (IPTG) and growth during 16 h at 18 ºC. Cells were harvested by centrifugation (4000 × *g* for 15 min at 4 ºC) and resuspended in 50 ml equilibration buffer (50 mM HEPES, 1 M NaCl, 5 mM $CaCl_2$, 30 mM imidazole, pH 7.5) supplemented with protease inhibitors. Cells were lysed by sonication. Centrifugation (9000 rpm for 30 min at 4 ºC) was used to remove cell debris, and the supernatant was filtered through a 0.2 µm syringe filter. The Zag protein was purified using AKTA FPLC System (GE Healthcare) by nickel chelate affinity chromatography with HisTrap HP columns. After a washing step (50 mM HEPES, 1 M NaCl, 5 mM $CaCl_2$, 60 mM imidazole, pH 7.5) the recombinant antibody fragments were eluted with a linear imidazole gradient from 60 to 300 mM in 50 mM HEPES, 1 M NaCl, 5 mM $CaCl_2$, pH 7.5. Protein fractions were pooled, then desalted and concentrated in 50 mM HEPES, 100 mM NaCl, 5 mM $CaCl_2$, pH 7.5 using Amicon 3K (Millipore). The purity of samples was analyzed by SDS-PAGE. Protein concentration was determined spectrophotometrically at 280 nm.

Protein thermal stability – Melting temperature of the Zag was determined using the Protein Thermal Shift Kit and 7500 Fast Real-Time PCR System (Applied Biosystems, USA) according manufacturer's instructions. Protein samples (5 µg/well) were tested in MicroAmp™ Fast Optical 96-well Reaction Plates and analyzed in quadruplicate using and diluted in 50mM HEPES, 100 mM NaCl, 5 mM $CaCl_2$, pH 7.5, and Protein Thermal Shift™ Dye 1x. Collected data were analyzed with Protein Thermal Shift Software version 1.1.

ELISA – Binding properties of Zag ABD was determine in 96-well coated with HSA, RSA, MSA (10 µg/well) overnight at 4 ºC. After 1 h blocking with 5% soya milk, purified protein samples were titrated in triplicate and incubated for 1 h at room temperature. Detection was performed with HRP-conjugated anti-His-tag antibody using ABTS substrate. Absorbance was measured at 405 nm in an ELISA reader. GraphPad Prism version 5 was used for data analysis.

Size Exclusion Chromatography – Apparent molecular weight of Zag ABD and formation of Zag/albumin complexes was determined by FPLC-SEC on a HiLoad Superdex 200 HR column (GE Healthcare) with a flow rate of 0.7 ml/min and PBS1x as running buffer. The

following standard proteins were used: apoferritin (443 kDa, R_S 6.1 nm), β-amylase (200 kDa, R_S 5.4 nm), alcohol dehydrogenase (150 kDa, R_S 4.55 nm), bovine serum albumin (67 kDa, R_S 3.55 nm), ovalbumin (45 kDa, R_S 3.05), myoglobin (17.6 kDa, R_S 1.91 nm), ribonuclease A (13.7 kDa, RS 1.64 nm) and cytochrome c (12.4 kDa, R_S 1.77 nm). Blue dextran and L-tyrosine were used to determine the void and total column volume, respectively. Elution volume of the protein standard was used to create a standard curve of Stokes' radius (R_S) *versus* $(-\log K_{av})^{1/2}$ that was used to calculate the Stokes' radii of recombinant antibody and antibody/albumin complexes. Complex formation of Zag with HSA and MSA was analysed by incubating equimolar amounts of Zag and albumin (10 μM) in PBS1x at room temperature and subsequent analysis by size exclusion chromatography (SEC). SDS-PAGE analysis of collected samples was performed to evaluate albumin binding.

Circular dichroism measurements – CD spectra were obtained on a Jasco J-815 instrument (Jasco Co, Tokyo, Japan) using a 1 mm path length cuvette. Spectra were collected from 190 to 260 nm at 37ºC , with a scan speed of 50 nm/min. Samples were prepared in 50 mM Tris buffer with 100 mM NaCl, 5 mM $CaCl_2$, pH 7.5. HSA and Zag ABD spectra were measured at 4 μM and 20 μM respectively. The CD signal of Zag ABD protein was also recorded in the presence of albumin. Zag ABD protein was added to a HSA 4 μM solution at ratios from 1:0.25 to 1:1. All spectra were further corrected by subtracting the contribution of the appropriate blank.

Expression and purification of ^{13}C ^{15}N-labelled Zag ABD – The Zag expression protocol was performed has previously described by Marley and co-workers[23]. ^{13}C-glucose and $(^{15}NH_4)_2SO_4$, purchased from Cambridge Isotopes Laboratory (Cambridge, MA) were the only carbon and nitrogen sources, respectively, and the other reagents were purchased from Sigma-Aldrich (USA). The culture medium was supplemented with: 1g/L $(^{15}NH_4)_2SO_4$, 4 g/L 13C-glucose, 100mg/L thiamine, 1 ml 0,01 M $FeCl_3$ and MEM Vitamins 1x. Expression was induced by the addition of 1 mM isopropyl β-D-1-thiogalactopyranoside (IPTG) and growth during 16 h at 20 ºC. Cells were harvested by centrifugation (7000 rpm, 15 min at 4 ºC) and washed in M9 Salts medium 1x without any source of carbon and nitrogen. After another centrifugation step (10000 rpm, 10 min at 4 ºC) the cells were frozen at -20 ºC at least during 30 min. For protein purification, cells were re-suspended in 50 ml equilibration buffer (50 mM HEPES, 1 M NaCl, 5 mM $CaCl_2$, 30 mM imidazole, pH 7.5) supplemented with protease inhibitors (Roche, Germany). Cells were lysed by sonication. Centrifugation (9500 rpm for 30

min at 4 ºC) was used to remove cell debris, and the supernatant was filtered through a 0.2 µm syringe filter. The Zag protein was purified using AKTA FPLC System by nickel chelate affinity chromatography with HisTrap HP columns. After a washing step (50 mM HEPES, 1 M NaCl, 5 mM $CaCl_2$, 60 mM imidazole, pH 7.5) the Zag protein was eluted with a linear imidazole gradient from 60 to 300 mM in 50 mM HEPES, 1 M NaCl, 5 mM $CaCl_2$, pH 7.5. Protein fractions were pooled, then desalted and concentrated in 50 mM HEPES, 100 mM NaCl, 5 mM $CaCl_2$, pH 7.5 using Amicon 3K (Millipore, USA). Protein concentration was determined spectrophotometrically at 280 nm.

NMR spectroscopy – A 1 mM sample of ^{15}N and $^{15}N/^{13}C$ purified Zag protein in 10 mM Tris-HCl, 100 mM NaCl, 10% D_2O, pH 7.5 was used for structural characterization of backbone and side-chain assignments. NMR spectra were collected at 25 °C on a Bruker Avance II+ 400 MHz and 600 MHz both with a 5 mm x,y,z-shielded pulse field gradient triple-resonance probe (the 600 MHz is equipped with a cryoprobe) all supported by the National NMR Network (PTNMR) at the Chemistry Department, Faculdade de Ciências e Tecnologia, Universidade Nova de Lisboa. A series of three-dimensional spectra [CBCA(CO)NH, HNCACB, HNCO, CC(CO)NH, ^{15}N-TOCSY-HSQC, HCCH-COSY, ^{1}H-^{1}H-^{15}N-NOESY-HSQC, ^{1}H-^{1}H-^{13}C-NOESY-HSQC] and two-dimensional [^{1}H-^{15}N HSQC] were collected for complete assignment and NOE measurement (mixing time of 120 ms). The number of complex points and spectral width are summarised in Table 1. For Fourier transformation all dimensions were zero-filled twice and linear prediction and zero filling were equally employed. All NMR data were processed using NMRPipe[24] and analyzed using CCPN[25].
Structure calculations were performed with the programs ATNOS/CANDID[26,27] implemented in UNIO in combination with CYANA[28], using as input the amino sequence, the chemical shift lists, and the three ^{1}H, ^{1}H, NOE experiments: three-dimensional ^{13}C- and ^{15}N-resolved NOESY recorded at 600 MHz with a mixing time of 120 ms. The standard protocol with seven cycles of peak picking using ATNOS, NOE assignment with CANDID, and structure calculation with CYANA-2.1[28] was applied. ϕ and ψ dihedral angle constraints were derived from the chemical shift index[29] and TALOS analysis[30]. In each UNIO cycle, the angle constraints were combined with the updated NOE upper distance constraints in the input for the subsequent CYANA-2.1 structure calculation cycle. The 20 conformers with the lowest residual target function values and without violations of dihedral angle restraints or distance were subjected to restrained energy minimization in explicit water with Xplor-NIH[31,32]. The quality of the structures was evaluated using the programs PROCHECK-NMR[33] and

WHATIF[34]. The root mean square deviation to the mean structure for the structured region of the protein (residues 3–60) is 2.24 ± 0.55 Å for the backbone and 2.86 ± 0.50 Å for all heavy atoms. The Ramachandran plot for the ensemble of 20 structures determined with PROCHECK-NMR[33] had 90.2% of residues in core regions, 9.6% of residues in allowed regions and 0.2% of residues in disallowed regions. Summary WHAT IF statistics[34] are shown below. These statistics provide an overall summary of the quality of the structure as compared with current reliable structures. Structure Z-scores show a number of constraint-independent quality indicators. RMS Z-scores mostly give an impression of how well the model conforms to common refinement constraint values. The standard deviation shows variation over models in the ensemble, where appropriate.

Structure Z-scores: first-generation packing quality, -0.77±0.36; second-generation packing quality, -2.77 ± 0.48; Ramachandran plot appearance, -2.49 ± 0.46; χ^1/χ^2 rotamer normality, -2.46 ± 0.46; backbone conformation, 5.63 ± 0.66. RMS Z-scores: bond lengths, 0.68 ± 0.03; bond angles, 0.66 ± 0.04; ω angle restraints, 0.80 ± 0.08; side-chain planarity, 0.77 ± 0.20; improper dihedral distribution, 0.85 ± 0.07; inside/outside distribution, 1,17 ± 0.03.

RESULTS

Expression and purification of Zag

Zag ABD is composed by 52 aa and the DNA sequence published by Jonsson and co-workers (1995)[4] . In order to characterize the Zag ABD, the Zag gene was cloned into the pT7 vector with an hexahistidyl (His_6) in C-terminus (Fig. 1A). The ABD was expressed in *E. coli* BL21(DE3) and purified by IMAC. The observed expression yield per liter of shake-flask culture without optimization was relatively high for the Zag protein (8-10 mg/L) (Fig. 1B). SDS-PAGE and Western Blot results of the final purified samples of protein showed a single protein band for Zag under reducing (Fig. 1C and D).

Zag ABD thermal stability

The thermal stability of Zag ABD was calculated using the Protein Thermal Shift Kit and Protein Thermal Shift Software (Table 2). The results indicate a high thermal stability of the albumin-binding domain in a range of temperature of 67 to 75ºC.

Binding of Zag ABD to albumins

In order to evaluate the albumin-binding capacity of Zag ABD, ELISA assays were performed at neutral pH 7.4 and at pH 6.0, to simulate the acidic environment, existing in

endosomes, where neonatal Fc receptor (FcRn) mediates the recycling of albumin in order to maintain the long life of this plasma protein[35]. The human, rat and mouse serum albumin binding of Zag was similar in both pH conditions (Fig. 2A and 2B, Table 3). Binding of Zag to albumin at pH 6.0 was slightly increased ($EC_{50\ (HSA)}$ = 0.12 nM; $EC_{50\ (RSA)}$ = 0.11 nM) when compared with binding at pH 7.4 ($EC_{50\ (HSA)}$ = 0.36 nM; $EC_{50\ (RSA)}$ = 3.26 nM), except for MSA (EC_{50} = 0.21 nM at pH 6.0 *versus* EC_{50} = 0.13 nM at pH 7.4) that presented similar values.

Moreover, SEC analysis also shows the interaction between Zag and human and mouse serum albumin in solution (Fig. 3 and Table 3). Zag and albumins were incubated at 1:1, molar (corresponding to ~1:4, (w/w) Zag:HSA) in PBS1x at room temperature. Peak positions of marker proteins are indicated. Zag eluted as a monomer with an apparent molecular mass of 10.3 kDa (R_S 1.62 nm). HSA major peak (monomer) with an apparent molecular mass of 68.1 kDa (R_S 3.67 nm) and MSA monomer with an apparent mass of 64.3 kDa (R_S 3.60 nm) were shifted after incubation with Zag to 82.4 kDa (R_S 3.78 nm) and 89 kDa (R_S 3.87 nm), respectively.

Circular dichroism

CD spectroscopy allowed the study of Zag structure and possible conformational changes after HSA binding. HSA spectrum in buffer solution shows two negative bands near 208 and 222 nm and a positive band near 195 nm, typical of α-helical conformation (Fig. 4A)[36]. Zag protein spectrum presents also the negative bands typical of the helical conformation with the positive band less pronounced (Fig. 4B). The addition of Zag protein to a HSA solution revealed that the formed complex maintains a helical structure and also that adding increasing concentrations of Zag to HSA solution results in an increase in the helical content (Fig. 4C).

Zag NMR

A 2D ^{1}H-^{15}N HSQC spectrum is a reliable method to judge the suitability of a particular protein for structural determination by NMR spectroscopy. A well-folded protein would display a wide dispersion of amide proton chemical shifts in 2D ^{1}H-^{15}N HSQC spectrum, as seen on Fig. 5 for Zag protein. Such good dispersion of the cross-peaks in the spectrum is undoubtedly a sign of a correct folding. Towards the complete structure determination of Im7H3M3 by NMR spectroscopy, backbone and side-chain assignments are essential. Complete backbone resonance assignment of Im7H3M3 was achieved, excluding the His-tag tail in the N-terminus of the protein.

The chemical shift index (CSI) analysis on Zag has shown the presence of helix conformations between residues A9 to Q24 (helix 1), D29 to K37 (helix 2) and V41 to S53 (helix 3). The helical regions of the repeated protein G-related albumin-binding domains, known as GA modules, found in streptococci protein G (G148-GA3)[7] and *Peptostreptococcis magnus* protein PAB (ALB8-GA)[6] exhibit ~60% sequence identity and both fold to form three-helix bundle structures. In protein G ABD, helix I ranges from residues 7 or 8 to 20 or 21, helix II ranges from residues 26 to 35 or 36, and helix III ranges from 38 to 51[7]. Protein PAB ABD three-helix bundle starts in the first helix at Ala-17 or Asn-18 and ends with Lys-33. The second helix begins with Asp-38 and ends with Asn-45. The third helix spans Val-50 to Ala-62[6]. A three-alpha-helix bundle similar to these ABDs is also present in the Ig-binding domain (IgBD) from staphylococcal protein A[37,38]. However, a comparison of the amino acid sequences of ABDs with IgBD from protein A revealed no detectable significant sequence homology.

DISCUSSION

In the present study, we characterize the *Streptococcus zooepidemicus* Zag ABD albumin-binding properties and determine its three-dimensional structure. Our data shown that the Zag ABD was stably produced in *E. coli*, with high yields of protein of several milligrams per liter of culture (Fig. 1B). Our findings of Zag binding to serum albumin were in the range of nanomolar. For instance, at pH 6.0 Zag ABD binding to HSA, RSA and MSA was slightly increased with values of EC_{50} = 0.12 nM, 0.11 nM and 0.21 nM, respectively, compared with binding at pH 7.4 with EC_{50} values of 0.36 nM, 1.26 nM and 0.13 nM. Quite a few studies evaluated the binding capacities between different bacterial serum albumin-binding domains, showing different results usually with affinities in the range of nanomolar [4,16,21,39]. Jonsson and co-workers investigated the binding properties of ZAG surface proteins and discovered that protein ZAG bind serum albumin of human, horse, rat, mouse, and dog origin, but not pig, rabbit, sheep, cow, hen or goat origin. The interaction of ZAG cell surface protein with different ligands was also calculated by surface plasmon resonance and the K_{off} values of the interaction with HSA and α_2M were 8.3 x 10^7 and 1.4 x 10^8 M^{-1}, respectively[4].

The SEC results of Zag binding to human and mouse albumin also support the efficient binding of this ABD to serum albumin, showing the formation of complexes of Zag/albumin with the increase of the Stokes radius. Stork and colleagues also verified that a recombinant diabody fusion with ABD3 from protein G presented a slightly increased binding at pH 6.0

then pH 7.4 with K_D of 1.7 nM versus 0.9 nM, respectively[40]. Protein G optimal binding was confirmed at acidic pH and was lower at higher temperatures[41].

Moreover, our measured affinity of Zag in fusion with an anti-TNFα VHH[23] for HSA, RSA and MSA, were in the range of nanomolar affinity, with values of K_D = 4.57 nM, 0.42 nM and 40.6 nM (data not shown), respectively, showing similar results to those obtained in previous studies, reporting affinities in the same range for the streptococcal protein G ABD[16,39-41]. Furthermore, binding of VHH-Zag to human, rat and mouse albumin was not reduced at pH 6.0 (data not shown), demonstrating that VHH-Zag binding to albumin is stable at low pH e.g., found in endosomes. These findings and the formation of Zag/albumin complexes *in vitro*, support the fact that Zag ABD binds to albumin and can be triggered by FcRn-mediated recycling mechanism to achieve a long half-life, i.e. albumin has a half-life of ~19 days in humans[35].

Zag ABD also exhibit high thermal stability, presenting melting temperatures in the range of 67 to 75 ºC (Table 2). These data are consistent with our previous work were we fused the Zas ABD with an anti-TNF VHH single domain antibody[22].

Our CD studies support also the efficient formation of the Zag and HSA complex. Spectra of isolated HSA and Zag in buffer solution are typical of α-helical proteins (Fig. 4). The addition of increasing concentrations of Zag protein to a 4 μM HSA solution show that the formed complex maintains the helical structure. Moreover, the increase of the negative bands signal while increasing Zag concentration indicates higher helical content in the complex structure (Fig. 4C).

The NMR assignments are according with the CD measurements and revealed that Zag ABD exhibit a three-alpha-helix conformation (Fig. 6). These results are similar with the structure of the ABDs from proteins G and PAB, previously determined by NMR spectroscopy to be left-handed three-helix bundles[6,7]. The ABD from protein G human albumin binding site involves residues mainly in the second α-helix[16]. The crystal structure of HSA in complex with the GA module of protein PAB with a resolution 2.7 Å reveals a novel binding epitope located in domain II of the albumin molecule, in residues close to a cleft bounded by helices 2 and 3 in domain IIA, helices 7 and 8 in domain IIB, and the loop region before helix 7 in IB. In the GA module, residues from the second helix and the two loops surrounding it are involved in HSA binding[42]. Additionally, the presence of fatty acids bounded to HSA seems to influence HSA-GA complex formation, proposing that the PAB GA module is capable of binding to different conformations of HSA[43,44].

However, it will be necessary more structural data, using NMR or X-ray crystallography to determine the binding sites of Zag ABD in human serum albumin and to analyze the interactions of Zag/albumin.

The high degree of similarity between these ABDs with respect to sequence, structure and stability, and the observed differences in dynamics, binding affinity and binding specificity to different albumins suggest the emergence of an evolutionary pattern. Bacterial strains with GA modules and thereby HSA-binding activity are more virulent and protein PAB-expressing strains of *P. magnus* are resistant to the antibiotic tetracycline, suggesting that the transfer of these GA modules is probably the result of a selective pressure driven by broad spectrum antibiotics[43]. Previous studies also propose that plasma protein binding may contribute for the pathogenesis and virulence of these microorganisms, and the binding adds selective advantages to the bacteria by promoting their growth[19].

Our biodistribution results of an anti-TNFα VHH in fusion with Zag ABD to extend the circulation time and improve the pharmacokinetic properties of the single-domain antibody, show that the novel antibody molecule presents specific binding to serum albumin, compared with the parental antibody. Likewise, the fusion with this ABD can improve the *in vivo* performance of the nanobody, decreasing the blood clearance, renal retention and excretion. These findings demonstrate that the Zag fusion can be considered as a promising approach to improve the pharmacokinetics of therapeutic proteins. Characterization of binding properties and structural information of Zag ABD also reveal high similarities with other bacterial ABDs used as protein scaffolds in pharmaceutical industry currently, showing the potential of this domain to be further developed as a protein scaffold for therapeutic applications.

REFERENCES

1. Kontermann, R.E. (2009) Strategies to extend plasma half-lives of recombinant antibodies. *Biodrugs* **23**, 93-109

2. Dennis, M.S., Zhang, M., Meng, G., Kadkhodayan, M., Kirchofer, D., Combs, D., Damico, L.A. (2002) Albumin binding as a general strategy for improving the pharmacokinetics of proteins. *J. Biol. Chem.* **277**, 35035-35043

3. Kontermann, R.E. (2007) A novel tri-functional antibody fusion protein with improved pharmacokinetic properties generated by fusing a bispecific single-chain diabody with an albumin-binding domain from streptococcal protein G. *Protein Eng. Des. Sel.* **20**, 569-576

4. Jonsson, H., Lindmark, H., Guss, B. (1995) A Protein G-related cell surface protein in *Streptococcus zooepidemicus*. *Infect. Immun.* **63**, 2968-2975

5. de Chatêau, M., Björck, L. (1994) Protein PAB, a mosaic albumin-binding bacterial protein representing the first contemporary example of module shuffling. *J. Biol. Chem.* **269**, 12147-12151

6. Johansson, M., de Châteu, M., Björck, L., Forsén, S., Drakenberg, T., Wikström, M. (1995) The GA module, a mobile albumin-binding bacterial domain, adopts a three-helix-bundle structure. *FEBS Lett.* **374**, 257-261

7. Kraulis, P.J., Jonasson, P., Nygren, P.A., Uhlén, M., Jendeberg, L., Nilsson, B., Kördel, J. (1996) The serum albumin-binding domain of streptococcal protein G is a three-helical bundle: a heteronuclear NMR study. *FEBS Lett.* **378**, 190-194

8. Malm, M., Kronqvist, N., Lindberg, H., Gudmundsdotter, L., Bass, T., Frejd, F.Y., Höidén-Guthenberg, I., Varasteh, Z., Orlova, A., Tolmachev, V., Ståhl, S., Löfblom, J. (2013) Inhibiting HER3-Mediated Tumor Cell Growth with Affibody Molecules Engineered to Low Picomolar Affinity by Position-Directed Error-Prone PCR-Like Diversification. *PLoS One* **8**, e62791

9. Nivelbrant, J., Alm, T., Hober, S., Löfblom, J. (2011) Engineering bispecific into a single albumin-binding domain. *PLoS One* **6**, e25791

10. Ahmad, J.N., Li, J., Biedermannová, L., Kuchař, M., Sípová, H., Semerádtová, A., Cerný, J., Petroková, H., Mikulecký, P., Polínek, J., Staněk, O., Vondrášek, J., Homola, J., Malý, J., Osička, R., Sebo, P., Malý, P. (2011) Novel high-affinity binders of human interferon gamma derived from albumin-binding domain of protein G. *Proteins* **80**, 774-789

11. Magnusson, K., Sehlin, D., Syvänen, S., Svedberg, M.M., Philipson, O., Söderberg, L., Tegerstedt, K., Holmquist, M., Gellerfors, P., Tolmachev, V., Antoni, G., Lannfelt, L., Hall, H., Nilsson, L.N. (2013) Specific uptake of an amyloid-β protofibril-binding antibody-tracer in AβPP transgenic mouse brain. *J. Alzheimers Dis.* **37**, 29-40

12. Malm, M., Kronqvist, N., Lindberg, H., Gudmundsdotter, L., Bass, T., Frejd, F.Y., Höidén-Guthenberg, I., Varasteh, Z., Orlova, A., Tolmachev, V., Ståhl, S., Löfblom, J. (2013) Inhibiting HER3-mediated tumor cell growth with affibody molecules engineered to low picomolar affinity by position-directed error-prone PCR-like diversification. *PLoS One* **8**, e62791

13. Orlova, A., Jonsson, A., Rosik, D., Lundqvist, H., Lindborg, M., Abrahmsen, L., Ekblad, C., Frejd, F.Y., Tolmachev, V. (2013) Site-specific radiometal labeling and improved

biodistribution using ABY-027, a novel HER2-targeting affibody molecule-albumin-binding domain fusion protein. *J. Nucl. Med.* **54**, 961-968

14. Honarvar, H., Jokilaakso, N., Andersson, K., Malmberg, J., Rosik, D., Orlova, A., Karlström, A.E., Tolmachev, V., Järver, P. (2013) Evaluation of backbone-cyclized HER2-binding 2-helix affibody molecule for in vivo molecular imaging. *Nucl. Med. Biol*. **40**, 378-386

15. Frick, I.-M., Ákesson, P., Cooney, J., Sjöbring, U., Schmidt, K.-H., Gomi, H., Hattori, S., Tagawa, C., Kishimoto, F., Björck, L. (1994) Protein H – a surface protein of *Streptococcus pyogenes* with separate binding sites for IgG and albumin. *Mol. Microbiol.* **12**, 143-151

16. Sjöbring, U. (1992) Isolation and molecular characterization of a novel albumin-binding protein from group G streptococci. *Infect. Immun.* **60**, 3601-3608

17. Tashiro, M., Montelione, G.T. (1995) Structures of bacterial immunoglobulin-binding domains and their complexes with immunoglobulins. *Curr. Opin. Struct. Biol*. **5**, 471-481

18. Tashiro, M., Tejero, R., Zimmerman, D.E., Celda, B., Nilsson, B., Montelione, G.T. (1997) High-resolution solution NMR structure of the Z domain of staphylococcal protein A. *J. Mol. Biol*. **272**, 573-590

19. Johannson, M.U., Frick, I.-M., Nilsson, H., Kraulis, P.J., Hober, S., Jonasson, O., Linhult, M., Nygren, P.A., Uhlén, M., Björck, L. (2002) Structure, specificity, and mode of interaction for bacterial albumin-binding modules. *J. Biol. Chem.* **277**, 8114-8120

20. He, Y., Chen, Y., Rozak, D.A., Bryan, P.N., Orban, J. (2007) An artificially evolved albumin binding module facilitates chemical shift epitope mapping of GA domain interactions with phylogenetically diverse albumins. *Protein Sci.* **16**, 1490-1494

21. Nygren, P.-Å., Ljungquist, C., Trømborg, H., Nustad, K., Uhlén, M. (1990) Species-dependent binding of serum albumin binding domains of streptococcal protein G. *J. Mol. Recognit.* **1**, 69-74

22. Morais, M., Cantante, C., Gano, L., Santos, I., Lourenço, S., Santos, C., Fontes, C., Aires da Silva, F., Gonçalves, J., Correia, J.D. (2014) Biodistribution of a ^{67}Ga-labeled anti-TNF VHH single-domain antibody containing a bacterial albumin-binding domain (Zag). *Nucl. Med. Biol*. pii: S0969-8051(14)00012-22

23. Marley, J., Lu, M., Bracken, C. (2001) A method for efficient isotopic labeling of recombinant proteins. *J. Biomol. NMR* **20**, 71-75

24. Delaglio, F., Grzesiek, S., Vuister, G.W., Zhu, G., Pfeifer, J., Bax, A. (1995). NMRPipe: a multidimensional spectral processing system based on UNIX pipes. *J. Biomol. NMR* **6**, 277-293.

25. Vranken, W.F., Boucher, W., Stevens, T.J., Fogh, R.H., Pajon, A., Llinas, M., Ulrich, E.L., Markley, J.L., Ionides, J., Laue, E.D. (2005) The CCPN data model for NMR spectroscopy: development of a software pipeline. *Proteins* **59**, 687-696.

26. Herrmann, T., Guntert, P., Wuthrich, K. (2002) Protein NMR structure determination with automated NOE assignment using the new software CANDID and the torsion angle dynamics algorithm DYANA. *J. Mol. Biol.* **319**, 209-227

27. Herrmann, T., Guntert, P., Wuthrich, K. (2002) Protein NMR structure determination with automated NOE-identification in the NOESY spectra using the new software ATNOS. *J. Biomol. NMR* **24**, 171-189

28. Guntert, P. (2004) Automated NMR structure calculation with cyana. *Methods Mol. Biol.* **278**, 353-378

29. Wishart, D.S., Sykes, B.D. (1994) The 13C chemical-shift index: a simple method for the identification of protein secondary structure using 13C chemical-shift data. *J. Biomol. NMR* **4**, 171-180

30. Cornilescu, G., Delaglio, F., and Bax, A. (1999) Protein backbone angle restraints from searching a database for chemical shift and sequence homology. *J. Biomol. NMR* **13**, 289-302

31. Schwieters, C.D., Kuszewski, J.J., Tjandra, N., Clore, G.M. (2003). The Xplor-NIH NMR molecular structure determination package. *J. Magn. Reson.* **160**, 65-73

32. Schwieters, C.D., Kuszewski, J.J., Clore, G.M. (2006). Using Xplor-NIH for molecular structure determination. *Prog. Nucl. Magn. Reson. Spectrosc.* **48**, 47-62

33. Laskowski, R.A., Rullmann, J.A.C., MacArthur, M.W., Kaptein, R., Thornton, J.M. (1996). AQUA and PROCHECK-NMR: programs for checking the quality of protein structures solved by NMR. *J. Biomol. NMR* **8**, 477-486

34. Vriend, G. (1990) WHAT IF: a molecular modeling and drug design program. *J. Mol. Graph.* **8**, 52-56

35. Sleep, D., Cameron, J., Evans, L.R. (2013) Albumin as a versatile platform for drug half-life extension. *Biochim. Biophys. Acta* **1830**, 5526-5534

36. Kelly, S.M., Jess, T.J., Price, N.C. (2005) How to study proteins by circular dichroism. *Biochim. Biophys. Acta* **1751**, 119-139

37. Gouda, H., Torigoe, H., Saito, A., Sato, M., Arata, Y., Shimada, I. (1992) Three-dimensional solution structure of the B domain of staphylococcal protein A: comparisons of the solution and crystal structures. *Biochemistry* **31**, 9665-9672

38. Lyons, B.A., Tashiro, M., Cedergren, L., Nilsson, B., Montelione, G.T. (1993) An improved strategy for determining resonance assignments for isotopically enriched proteins and its application to an engineered domain of staphylococcal protein A. *Biochemistry* **32**, 7839-7845

39. Linhult, M., Binz, H.K., Uhlén, M., Hober, S. (2002) Mutational analysis of the interaction between albumin-binding domain from streptococcal protein G and human serum albumin. *Protein Sci*. **11**, 206-213

40. Stork, R., Müller, D., Kontermann, R.E. (2007) A novel tri-functional antibody fusion protein with improved pharmacokinetic properties generated by fusing a bispecific single-chain diabody with an albumin-binding domain from streptococcal protein G. *Protein Eng. Des. Sel.* **20**, 569-576

41. Stork, R., Campigna, E., Robert, B., Müller, D., Kontermann, R.E. (2009) Biodistribution of a bispecific single-chain diabody and its half-life extended derivatives. *J. Biol. Chem.* **284**, 25612-25619

42. Lejon, S., Frick, I.M., Björck, L., Wikström, M., Svensson, S. (2004) Crystal structure and biological implications of a bacterial albumin binding module in complex with human serum albumin. *J. Biol. Chem*. **279**, 42924-42928

43. de Château, M., Björck, L. (1996) Identification of interdomain sequences promoting the intronless evolution of a bacterial protein family. *Proc. Natl. Acad. Sci. USA*. **93**, 8490-8495

44. Lejon, S., Cramer, J.F., Nordberg, P. (2008) Structural basis for the binding of naproxen to human serum albumin in the presence of fatty acids and the GA module. *Acta Crystallogr. Sect. F Struct. Biol. Cryst. Commun*. **64**, 64-69

ABBREVIATIONS

ABD, albumin-binding domain; CD, circular dichroism; FcRn, neonatal Fc receptor; HSA, human serum albumin; IgG, immunoglobulin G; MSA, mouse serum albumin; NMR, nuclear magnetic resonance; RSA, rat serum albumin.

ACKNOWLEDGMENTS

C. Cantante and D. Gaspar acknowledge Fundação para a Ciência e a Tecnologia (FCT) for the fellowships SFRH/BD/48598/2008 and SFRH/BPD/73500/2010, respectively. The NMR work was possible due to generous funds from Fundação para a Ciência e a Tecnologia (project RECI/BBB-BQB/0230/2012 and CQFB Strategic Project PEst-C/EQB/LA0006/2011) and the Portuguese NMR Network (RNRMN).

FIGURE LEGENDS

Fig. 1: Construction and expression of Zag ABD. (A) Sequence of Zag albumin-binding domain (B) SDS-PAGE of the samples collected during IMAC purification, (C) SDS-PAGE and (D) Western Blot analysis of the Zag purified protein (3 µg/lane) under non-reducing conditions. Gel was stained with Coomassie brilliant blue (B and C) or immunobloted with an anti-His-tag antibody (D).

Fig. 2: Binding of Zag to human, rat and mouse albumin at pH 6.0 and 7.4. Binding of Zag ABD to serum albumin was evaluated in ELISA at neutral pH - pH 7.4 (A); and acidic pH - pH 6.0 (B). Bound proteins were detected using an HRP-conjugated anti-His-tag antibody.

Fig. 3: Size exclusion chromatography for Zag/albumin complexes analysis. Zag (A), HSA (B), Zag + HSA (C), MSA (D) and Zag + MSA (E). Zag ABD was incubated at equimolar concentrations with albumin in PBS1x at room temperature. Peak positions of marker proteins are indicated.

Fig. 4: CD studies of Zag and Zag/HSA binding. Far UV-CD spectra of HSA (A), Zag ABD in the absence (B) and presence of HSA (C). HSA was kept at 4 µM (A). Zag protein was measured at 20 µM (B) and added to a HSA solution at 1:0.25, 1:0.5, 1:0.75 and 1:1 ratios (C, black arrow).

Fig. 5: ^{1}H-^{15}N HSQC spectrum of Zag ABD. ^{1}H-^{15}N HSQC spectrum at 600 MHz of Zag in 10 mM Tris-HCl, 100 mM NaCl, 10% D_2O, pH 7.5 at 25 °C. The spectrum showed a good chemical shift dispersion for both nuclei (^{1}H and ^{15}N) as occurs in a folded protein.

Fig. 6: Three-dimensional structure of Zag ABD determined by NMR.

TABLES

Table 1: NMR experiments for Zag assignment.

	Complex points			Spectral width (Hz)			Scans
	^{1}H	^{13}C	^{15}N	^{1}H	^{13}C	^{15}N	
Backbone assignment							
CBCA(CO)NH	2048	40	128	7591	1905	11318	16
HNCACB	2048	40	128	7591	1905	11320	16
HNCO	2048	40	128	7591	1905	3333	16
Side-chain assignment							
CC(CO)NH	2048	40	128	9615	1905	11318	16
^{15}N-TOCSY-HSQC	2048	42	296 [a]	6356	1905	6403 [a]	8
HCCH-COSY	2048	64	144 [a]	4242	6667	4269 [a]	16
NOE measurement							
^{1}H-^{1}H-^{15}N-NOESY-HSQC	2048	40	256 [a]	7591	1905	7591 [a]	16
^{1}H-^{1}H-^{13}C-NOESY-HSQC	2048	64	256 [a]	7813	11318	7802 [a]	8

[a] The dimension should be read as ^{1}H

Table 2: Thermal stability of Zag ABD.

Protein	**Tm B - Mean (°C)**	**Tm B – Median (°C)**	**Tm D - Mean (°C)**	**Tm D - Median (°C)**
Zag	73.79 ± 3.15	75.39 ± 3.15	66.68 ± 6.64	68.97 ± 6.64

Tm B - Calculated Boltzamnn melting temperature; Tm D - Calculated Derivated melting temperature.

Table 3: Binding of Zag to HSA, RSA and MSA.

Protein	**EC_{50} for HSA (nM)**	**EC_{50} for RSA (nM)**	**EC_{50} for MSA (nM)**
Zag pH 6.0	0.12 ± 0.11	0.11 ± 0.06	0.21 ± 0.09
Zag pH 7.4	0.36 ± 0.11	1.26 ± 0.06	0.13 ± 0.06

Table 4: Zag ABD and Zag/albumin complexes molecular mass and hydrodynamic volume.

Protein or complex	Length	Calculated M_r[a]	SEC apparent M_r	Stokes' radius ($R_{S)}$
	aa	**kDa**	**kDa**	**nm**
Zag	67	7.7	10.3	1.62
HSA	585	66.5	68.1	3.67
MSA	584	65.9	64.3	3.60
Zag/HSA	-	74.2	82.4	3.78
Zag/MSA	-	73.6	89.0	3.87

Figure 1

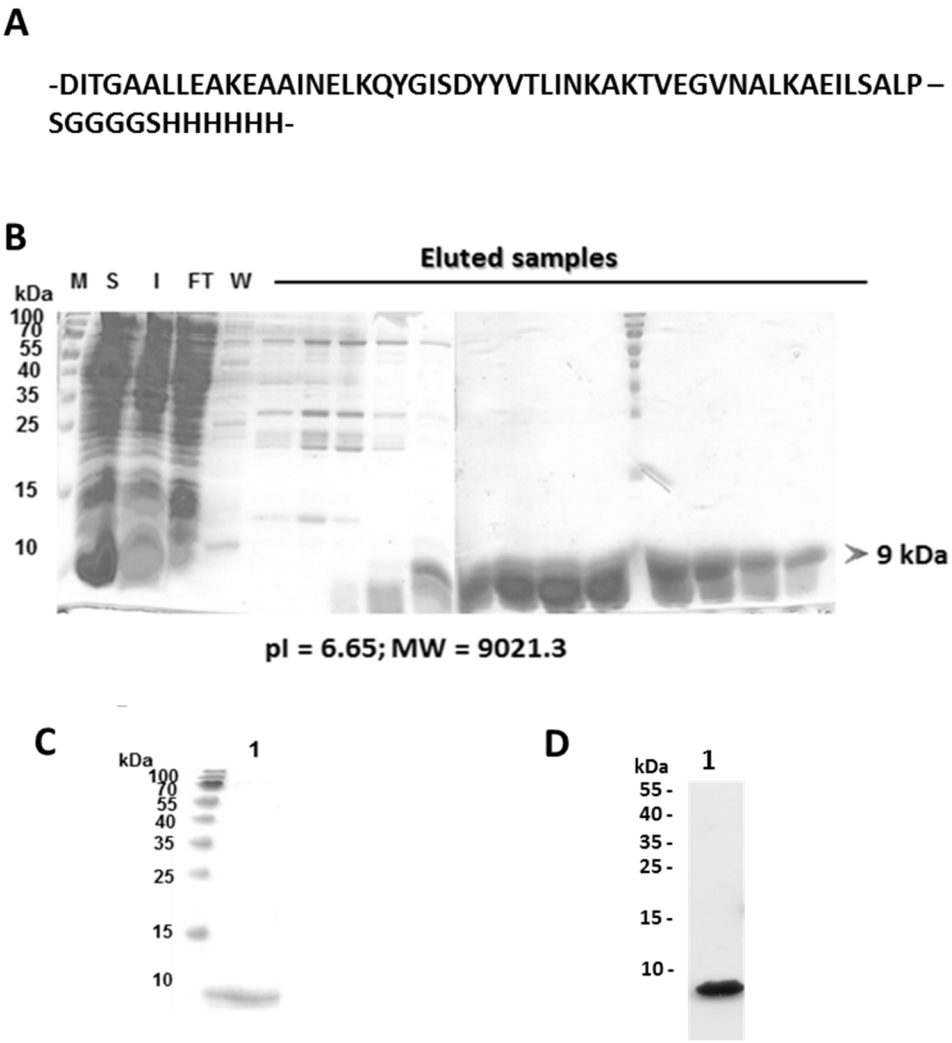
A
-DITGAALLEAKEAAINELKQYGISDYYVTLINKAKTVEGVNALKAEILSALP –
SGGGGSHHHHHH-
B
Eluted samples
M S I FT W
kDa
100
70
55
40
35
25
15
10
9 kDa
pI = 6.65; MW = 9021.3
C
kDa
1
100
70
55
40
35
25
15
10
D
kDa
1
55 -
40 -
35 -
25 -
15 -
10 -

Figure 2

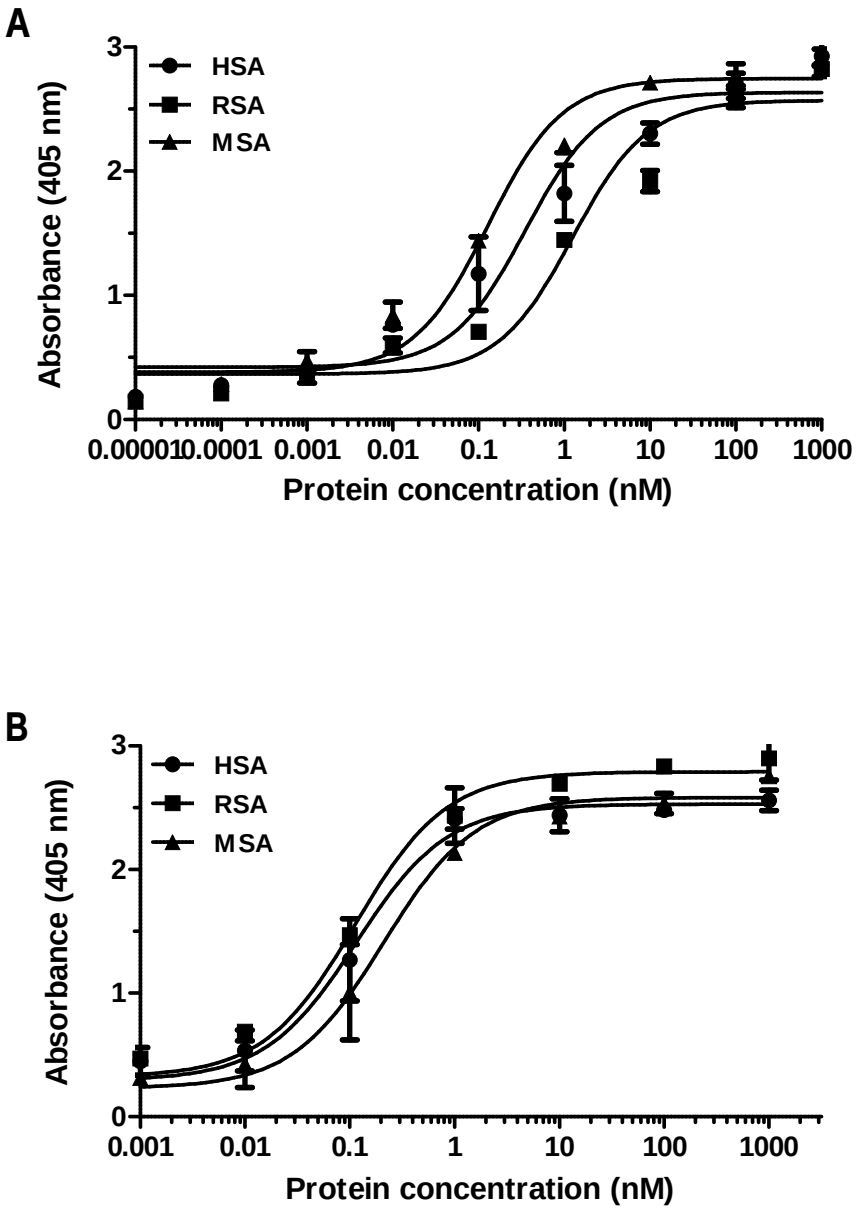
A
HSA
RSA
MSA
Absorbance (405 nm)
0
1
2
3
0.00001
0.0001
0.001
0.01
0.1
1
10
100
1000
Protein concentration (nM)
B
HSA
RSA
MSA
Absorbance (405 nm)
0
1
2
3
0.001
0.01
0.1
1
10
100
1000
Protein concentration (nM)

Figure 3

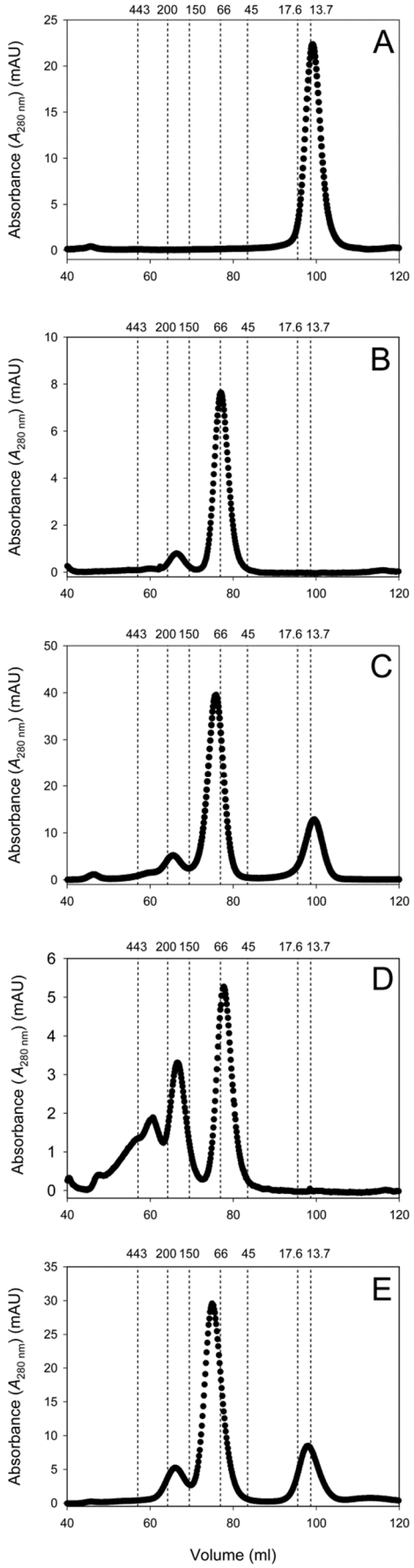
443 200 150 66 45 17.6 13.7
A
B
C
D
E
Absorbance ($A_{280\ nm}$) (mAU)
Volume (ml)

Figure 4

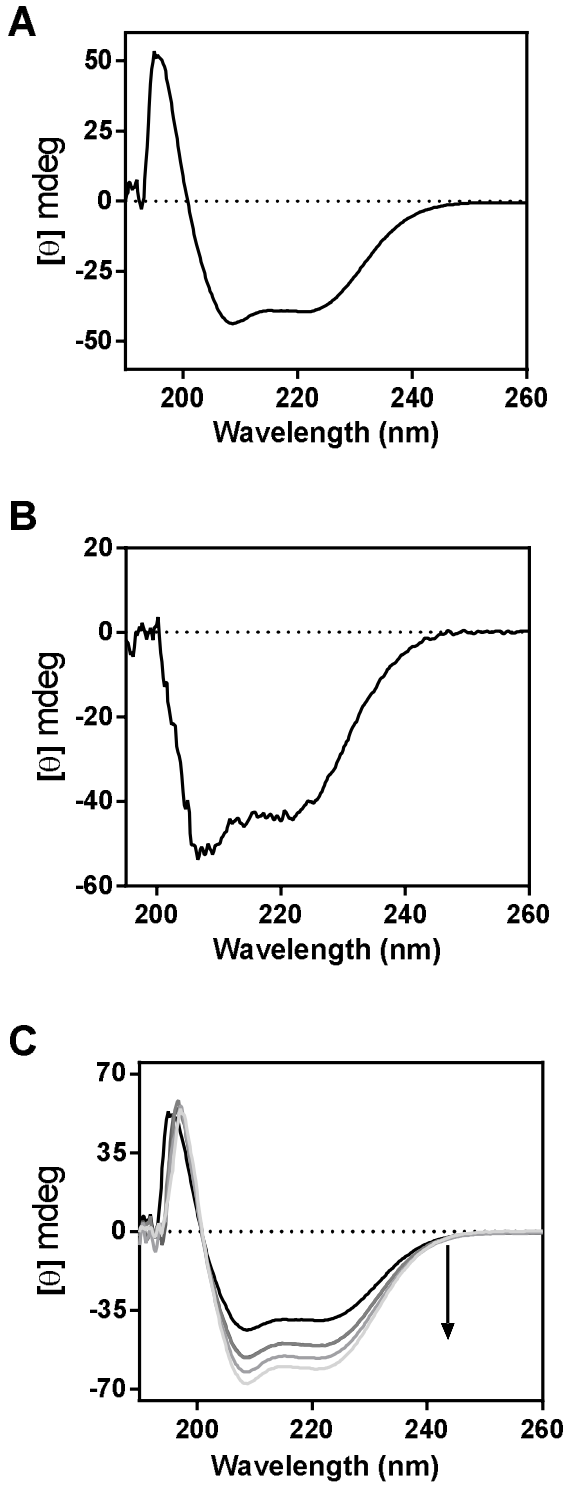
A
50
25
0
-25
-50
[θ] mdeg
200
220
240
260
Wavelength (nm)
B
20
0
-20
-40
-60
[θ] mdeg
200
220
240
260
Wavelength (nm)
C
70
35
0
-35
-70
[θ] mdeg
200
220
240
260
Wavelength (nm)

Figure 5

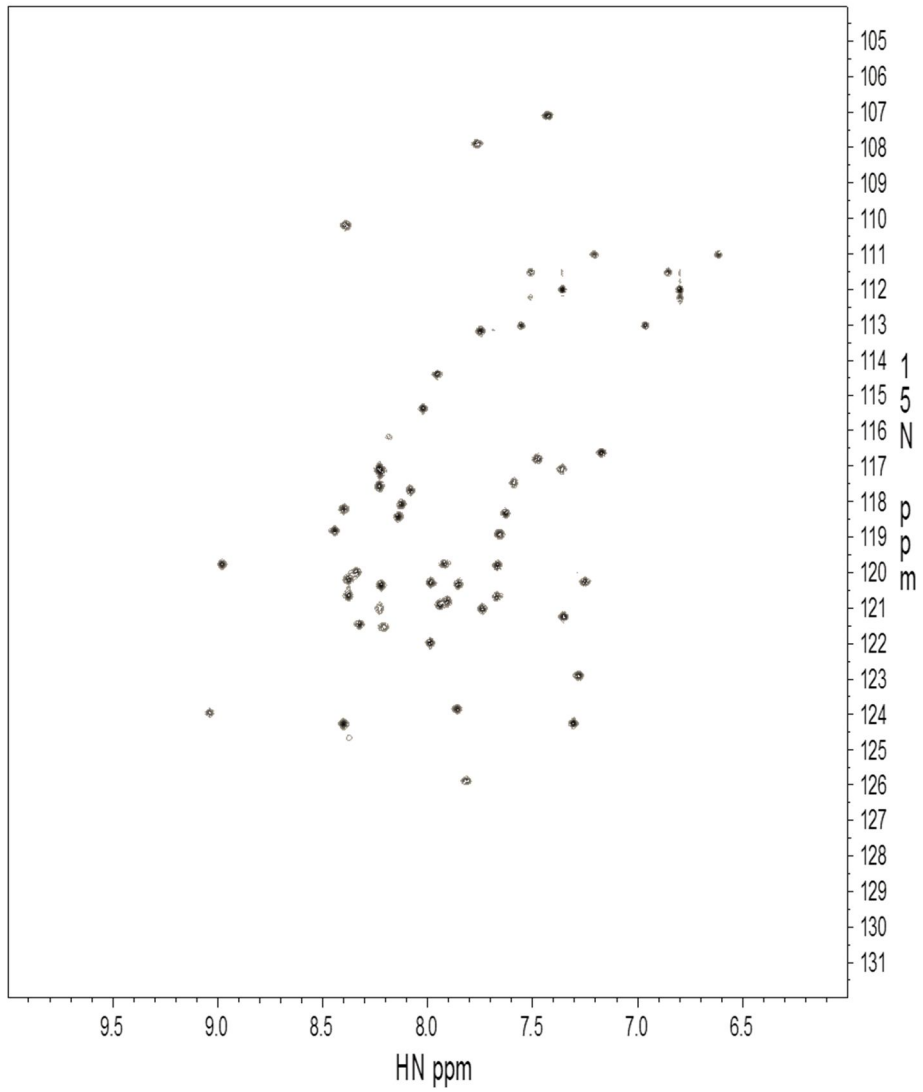
105
106
107
108
109
110
111
112
113
114
115
116
117
118
119
120
121
122
123
124
125
126
127
128
129
130
131
15N ppm
9.5
9.0
8.5
8.0
7.5
7.0
6.5
HN ppm

Figure 6

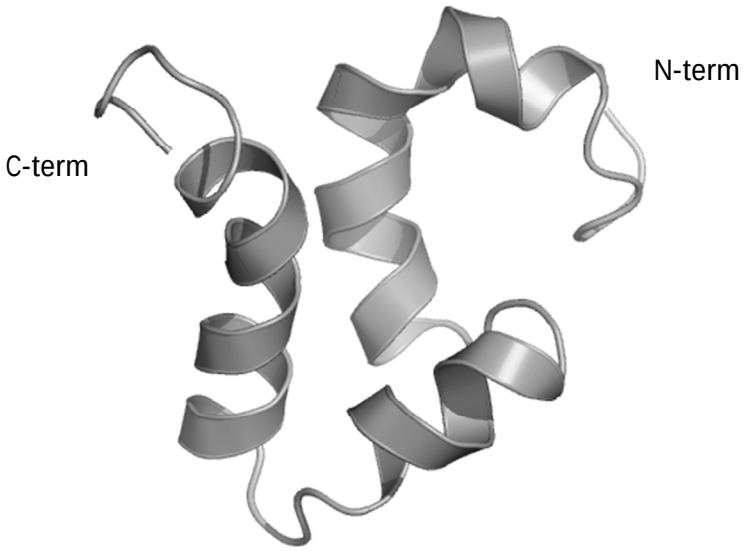

ALBUMIN-BINDING CHARACTERIZATION AND IN SILICO STRUCTURE PREDICTION OF PROTEIN H ABD FROM STREPTOCOCCUS PYOGENES

Brief Introduction

Streptococcal albumin-binding domains have been broadly investigated as fusion proteins to improve the pharmacokinetic properties of therapeutic proteins and as protein scaffolds for therapeutic applications (Kontermann, 2012).

Protein H is a cell-surface protein from *S. pyogenes*, with an Ig-binding region located in the N-terminus and an ABD in the C-terminus, composed by three C repeats with a high amino acid sequence homology between them (Frick *et al*., 1995).

In this research work we characterize the protein H ABD (ProtH) ability to bind albumin and predicted *in silico* the three-dimensional structure of this module. Firstly, we optimize the production of the ProtH ABD (C1C2C3) and C repeats (C1, C2, C3, C1C2 and C2C3) in *E.coli*, an easy way to obtain high amounts of protein with lower costs. Then we characterize the albumin binding and stability of the ProtH ABD and C repeats. Finally, we investigated the conformation of ProtH ABD (C1C2C3) in the presence and absence of human serum albumin and predicted *in silico* the three-dimensional structure of ProtH motif.

Albumin-binding characterization and *in silico* structure prediction of protein H ABD from *Streptococcus pyogenes*

Cátia Cantante[1,2], João Leandro[3], Diana Gaspar[2], Paula Leandro[3], Miguel Castanho[2], Frederico Aires-da-Silva[4,5] and João Gonçalves[1,2]

[1] CPM-URIA, Faculdade de Farmácia, Universidade de Lisboa, 1649-003 Lisbon, Portugal

[2] Instituto de Medicina Molecular, Faculdade de Medicina, Universidade de Lisboa,1649-028 Lisbon, Portugal

[3] iMed.UL, Faculdade de Farmácia, Universidade de Lisboa, 1649-003 Lisbon, Portugal

[4] Technophage, SA, 1649-028 Lisbon, Portugal

[5] Faculdade de Medicina Veterinária, Universidade de Lisboa, 1300-477 Lisbon, Portugal

Keywords: Protein H, streptococcal cell surface proteins, albumin-binding domain, serum albumin, scaffolds.

Background: Albumin-binding domains (ABD) have become extremely important as therapeutic scaffolds and as a promising strategy to extend the half-life of therapeutic proteins**.** Streptococcal ProtH albumin-binding domain (ABD) is a part of protein H cell surface protein.

Results: Streptococcal protein H ABD was stably produced in bacteria, presenting high binding activity to serum albumin (mouse, rat and human) and shown to have a predicted alpha-helix three dimensional conformation.

Conclusions: The protein H ABD domain has albumin-binding properties similar to other streptococcal ABDs, e.g. protein G ABD3 and can be useful as a therapeutic scaffold and as half-life extension approach.

Significance: This study establishes the ProtH ABD as a possible scaffold that can be further engineered for several therapeutic applications, such as the improvement of the pharmacokinetics of therapeutic proteins.

ABSTRACT

Protein H, a cell surface protein from *Streptococcus pyogenes*, presents a multiple domain structure comprising an albumin-binding domain (ABD) composed by three C repeats (C1C2C3), an immunoglobulin G (IgG)-binding region and a α_2-macroglobulin binding site. In this study, we characterize the albumin binding properties of ProtH ABD and their C repeats domains and also predict the three-dimensional conformation of this molecule by an *in silico* approach. Firstly, ProtH ABD (C1C2C3) and C repeats constructs were stably produced in bacteria and thermal stability was determined, showing a high thermal stability for ProtH ABD (58 to 63 ºC) and all constructs, specially observed for the C1 repeat (74 ºC). To characterize the albumin binding of ProtH ABD and C repeats, ELISA assays and size

exclusion chromatography (SEC) were performed. The ProtH ABD (C1C2C3) exhibit a high binding to human, rat and mouse serum albumin and, from all constructs, C1 repeat presented the highest binding to human albumin. Furthermore, ProtH/albumin complexes were isolated by SEC, confirming the albumin-binding of the ABD also seen by ELISA, and the presence of monomers of ProtH ABD alone and for the complexes ProtH/human serum albumin (HSA) and ProtH/mouse serum albumin (MSA). Furthermore, Far-UV circular dichroism analysis of the ProtH secondary structure indicates a high helical content and shows that when bound to HSA, the formed complex is also α-helical structured. Finally, structure prediction *in silico* also suggests that ProtH ABD has an α-helical three dimensional structure. These findings demonstrate the great potential of ProtH ABD as an application for half-life improvement of therapeutic proteins and peptides, and as a protein scaffold for therapeutic uses.

INTRODUCTION

Protein H, is a multidomain protein present on the cell surface of some strains of *Streptococcus pyogenes*[1]. This protein is found in clinical isolates of the M1 serotype[2] and has affinity for the constant (IgGFc) region of immunoglobulin (Ig) G and serum albumin[1]. The role for protein H and other immunoglobulin-binding proteins in *S. pyogenes* pathogenicity and virulence is unclear. The protein H, like protein G[3], presents different binding sites for albumin and immunoglobulin G (IgG). Protein H albumin-binding domain (ProtH ABD) is closer to the bacterial cell wall and was mapped to three repeats (C1-C3) in the C-terminal half of protein H[1], whereas IgG-binding domain is located towards the N-terminal. No homology was detected when the IgGFc-binding repeats were compared with the same regions of protein G, but the albumin-binding regions of protein G and H were shown to have evolved convergently[4]. In protein G, albumin-binding is in the N-terminal half and IgGFc binding in the C-terminus of the molecule[4]. Competitive binding experiments demonstrated that protein G and H bound to the same or closely located sites in albumin, which has previously been mapped for protein G to disulfide loops 6-8[5].

In the last 20 years, a broad class of bacterial albumin-binding domains have been investigated and described[6,7]. A previous study from de Château and Björck showed, for the first time, that peptostreptococcal protein PAB from *Finegoldia magna*, it is a mosaic albumin-binding bacterial protein, representing an example of a shuffled bacterial module[8]. Several structural studies with bacterial albumin-binding domains showed similar structural organization in these molecules, identifying a three-helix-bundle structure in protein G-related

albumin-binding (GA)[9-11] modules and immunoglobulin-binding domains (IgBD)[12,13]. The structures of GA modules from proteins PAB[7,8] and G[9] show a three-alpha-helix architecture, and recent studies used these molecules based-structure to develop new scaffolds for therapeutic applications in several diseases, e.g. cancer and inflammatory diseases[14-16]. For instance, affibody molecules are robust 3-helix protein scaffolds based on a modified B-domain of staphylococcal protein A, and represent a successful example of the therapeutic, diagnosis, and biotechnological applications of protein scaffolds derived from bacterial domains with affinity for plasma proteins[17,18]. Another successful application of these ABDs is the fusion with therapeutic proteins or peptides to improve the pharmacokinetic properties of these molecules. The bacterial ABDs properties have been extensively studied for this purpose, with promising results in the circulation time extension of short half-life molecules[19-23]. Within this context, ABD scaffolds have demonstrated particular promise in the therapeutic and diagnostic area and have been the subject of considerable interest by Academia and Industry. Therefore, in the present study, we characterize the albumin-binding properties of the bacterial ProtH ABD derived from *Streptococcus pyogenes* cell surface protein H and investigate the secondary structure and the predicted three dimensional structure of this ABD.

EXPERIMENTAL PROCEDURES

Materials – Human serum Albumin (HSA) (catalog no. A3782), rat serum albumin (RSA) (catalog no. A6272) and mouse serum albumin (MSA) (catalog no. A3139). Antibody HRP-conjugated anti-HA-tag, 2,2'-Azino-di-[3-ethylbenzthiazoline sulfonate (6)] diammonium salt (ABTS) and cOmplete EDTA-free protease inhibitors cocktail were acquired from Roche (Germany).

Cloning of ProtH and ProtH domains –All constructs were cloned in pT7-PL-VHH-HISHA, previous constructed by Morais and colleagues[19]. The DNA encoding the ProtH (C1C2C3) albumin-binding domain of *Streptococcus pyogenes* was generated by PCR. For amplification we used the primers H-SfiI-F (5'-GGG CCC AGG CGG CCA AGC AAA TCT CGG AAG CAA GCC G- 3') and H-SfiI-R (5'-CCT GGC CGG CCT GGC CTT CTT TCA GCG CCT TGG CCT CC-3'), by means of a plasmid synthesized by DNA 2.0 (pJ201:27789 – H peptide_opt) with the DNA sequence of the ProtH ABD as a template, adding SfiI restriction sites at the fragment 5' and 3' ends, respectively. The resulting PCR fragments were gel-purified, digested with the restriction enzymes and cloned into the appropriately cut

pT7-PL-VHH-HisHA vector. A short GS linker (SGGGGS) was used to link the ProtH ABD to the His and HA tags. For the construction of ProtH domains C1, C2, C3, C1C2 and C2C3, the procedure was repeated using the following primers for amplification: H-SfiI-F; H-SfiI-R 5'-CCT GGC CGG CCT GGC CCT CTT TCA ACT TCT GGT GCT CGG-3'; HC2-SfiI-F 5'-GGG CCC AGG CGG CCG ACA AGC AGA TTA GCG ACG CG-3'; HC2-SfiI-R 5'-CCT GGC CGG CCT GGC CTT CTT TCA GCT TCT GAT GTT CCG C-3'; HC3-SfiI-F 5'-GGG CCC AGG CGG CCG ATA AGC AAA TCT CCG ACG CCA-3' and H-SfiI-R. All constructs were verified by sequencing.

Expression and purification of ProtH – The ProtH ABD was expressed in *Escherichia coli* strain BL21(DE3). One liter of LB, containing 100 µg/ml ampicillin was inoculated with 10 ml of overnight culture of bacterial cells transformed with all the constructs and grown to exponential phase (A_{600} = 0.6-0.9) at 37 ºC. Expression was induced by the addition of 1 mM isopropyl β-D-1-thiogalactopyranoside (IPTG) and growth during 16 h at 18 ºC. Cells were harvested by centrifugation (4000 × *g* for 15 min at 4 ºC) and resuspended in 50 ml equilibration buffer (50 mM HEPES, 1 M NaCl, 5 mM $CaCl_2$, 30 mM imidazole, pH 7.5) supplemented with protease inhibitors. Cells were lysed by sonication. Centrifugation (9000 rpm for 30 min at 4 ºC) was used to remove cell debris, and the supernatant was filtered through a 0.2 µm syringe filter. Each protein was purified using AKTA FPLC System (GE Healthcare) by nickel chelate affinity chromatography with HisTrap HP columns (GE Healthcare). After a washing step (50 mM HEPES, 1 M NaCl, 5 mM $CaCl_2$, 60 mM imidazole, pH 7.5), all the constructs were eluted with a linear imidazole gradient from 60 to 300 mM in 50 mM HEPES, 1 M NaCl, 5 mM $CaCl_2$, pH 7.5. Protein fractions were pooled, then desalted and concentrated in 50 mM HEPES, 100 mM NaCl, 5 mM $CaCl_2$, pH 7.5 using Amicon 3K (Millipore). The samples fractions were pooled and protein purity was analyzed by SDS-PAGE. Protein concentration was determined spectrophotometrically at 280 nm at Nanodrop ND-1000.

Protein thermal stability - Melting temperature of the ProtH and ProtH C-repeats were determined using the Protein Thermal Shift Kit and 7500 Fast Real-Time PCR System (Applied Biosystems, USA) according manufacturer's instructions. Protein samples (5 µg/well) were tested in MicroAmp™ Fast Optical 96-well Reaction Plates and analyzed in triplicate using and diluted in 50 mM HEPES, 100 mM NaCl, 5 mM $CaCl_2$, pH 7.5, and Protein Thermal Shift™ Dye 1x. Collected data were analyzed with Protein Thermal Shift Software version 1.1.

ELISA – Albumin-binding of ProtH ABD was evaluated in 96-well coated with HSA, RSA, MSA (10 µg/well) overnight at 4 ºC. After 1 h blocking with 5% soya milk in PBS1×, purified ProtH constructs and serum samples were titrated in triplicate and incubated in PBS1×-soya milk 1% for 1 h, at room temperature. Detection was performed with HRP-conjugated anti-HA-tag antibody using ABTS substrate. Absorbance was measured at 405 nm in an ELISA reader. The blocker solution (PBS1×-soya milk 1%) was used as negative control. GraphPad Prism version 5 was utilized for data analysis.

Size Exclusion Chromatography – Molecular weight of ProtH ABD and formation of ProtH/albumin complexes was determined by FPLC–SEC on a HiLoad Superdex 200 HR column (GE Healthcare) with a flow rate of 0.7 ml/min and PBS as running buffer. The following standard proteins were used: apoferritin (443 kDa, R_S 6.1 nm), β-amylase (200 kDa, R_S 5.4 nm), alcohol dehydrogenase (150 kDa, R_S 4.55 nm), bovine serum albumin (67 kDa, R_S 3.55 nm), ovalbumin (45 kDa, R_S 3.05), myoglobin (17.6 kDa, R_S 1.91 nm), ribonuclease A (13.7 kDa, RS 1.64 nm) and cytochrome c (12.4 kDa, R_S 1.77 nm). Blue dextran and L-tyrosine were used to determine the void and total column volume, respectively. Elution volume of the protein standard was used to create a standard curve of Stokes' radius (R_S) *versus* $(-\log K_{av})^{1/2}$ that was used to calculate the Stokes' radii of ProtH and ProtH/albumin complexes. Complex formation of ProtH ABD with HSA and MSA was analyzed by incubating equimolar amounts of the ABD and albumin (10 µM) in PBS at room temperature and subsequent analysis by SEC. SDS-PAGE analysis of collected samples was performed to evaluate albumin binding.

Circular dichroism measurements – CD spectra were obtained on a Jasco J-815 instrument (Jasco Co, Tokyo, Japan) using a 1 mm path length cuvette. Spectra were collected from 190 to 260 nm at 37 ºC, with a scan speed of 50 nm/min. Samples were prepared in 50 mM Tris buffer with 100 mM NaCl, 5 mM $CaCl_2$, pH 7.5. HSA, ProtH ABD C1 and ProtH ABD spectra were measured at 4 µM, 50 µM and 20 µM respectively. The CD signal of ProtH ABD protein was also recorded in the presence of albumin. The protein was added to a HSA 4 µM solution at the ratios 1:0.25 and 1:1. All spectra were further corrected by subtracting the contribution of the appropriate blank.

Structure prediction of ProtH ABD – The three dimensional structure of ProtH ABD (UniProtKB/Swiss-Prot: P50470.1) was predicted *in silico* using the I-TASSER (as "Zhang-Server") server from the University of Michigan (http://zhanglab.ccmb.med.umich.edu/I-

TASSER/). I-TASSER server is an on-line platform for protein structure and function predictions. This server builds 3D models based on multiple-threading alignments by LOMETS (Local Meta-Threading-Server) and iterative template fragment assembly simulations. Function inslights are derived by matching the 3D models with BioLiP protein function database[24]. Protein Data Base format (pdb) files obtained with I-TASSER, were analyzed using USCF Chimera software version 1.9.

RESULTS

Expression and purification of ProtH ABD constructs

ProtH ABD is composed by 112 amino acid (aa) (Fig. 1A) and by three C-repeats denominated C1C2C3 with similar amino acid sequences[1] (Fig. 1B). In order to characterize the albumin binding of ProtH ABD and determine the region responsible for human serum albumin binding, several constructions of C repeats (C1C2C3, C1C2, C2C3, C1, C2 and C3) were cloned into the pT7 vector with a leader peptide in N-terminus and histidine (His_7) and HA tags in C-terminus (Fig. 1C).

The proteins were expressed in *E. coli* BL21(DE3), purified by IMAC and SDS-PAGE analysis of the purified proteins showed a single protein band for all the constructs under reducing conditions (Fig 1D). The observed expression yield per liter of shake-flask culture without optimization was relatively high for all constructs (10-15 mg). Similar quantities of purified protein were observed for C1, C2 or C3 domains (10-12 mg per liter) and C1C2, C2C3 and C1C2C3 constructs presented the higher protein yields after purification (~15mg per liter).

ProtH ABD thermal stability

Melting temperatures of ProtH ABD and ProtH ABD C repeats was determined using a Real-Time PCR System and the Protein Thermal Shift software version 1.1. The Protein Thermal Shift software calculates the melting temperatures (Tm) from each fluorescence profile (Boltzmann method) and also the T_m of the dFluorescence (derivative method). The derivative Tm values are taken from the top of the peak in the derivative plot, while the Boltzmann Tm values are taken from the inflection point of the fluorescence plot. The results obtained (Table 1) indicate that ProtH ABD has a high thermal stability in the range of 58 to 63 ºC. From C repeats, C1 possess the highest stability with a melting temperature of 74 ºC, comparing with C2, C3 and other combinations of these domains.

Binding of ProtH ABD to albumin

In order to evaluate the albumin-binding activity of ProtH ABD, ELISA assays were performed at neutral pH and acidic pH. These conditions were tested to reproduce the same pH conditions existing inside endosomes, during the recycling mechanism of albumin mediated by neonatal Fc receptor (FcRn), responsible for the long half-life of albumin[23,25]. The human, rat and mouse serum albumin binding of ProtH ABD was similar in both pH conditions (Fig. 2A and 2B). Binding of ProtH ABD to albumin at pH 6.0 presented EC_{50} values for HSA, RSA and MSA of 3.28 nM, 10.77 nM and 3.15 nM, respectively. At pH 7.4, EC_{50} for HSA and RSA were similar (EC_{50} = 9.77 nM and 10.92 nM, respectively), but EC_{50} for MSA was a slightly lower (0.13 nM). Since the ProtH ABD presents three C repeats responsible for albumin binding, all the C repeats alone or in combinations were tested to characterize the albumin-binding. As shown is Figure 3, the highest binding is observed for the ProtH ABD (C1C2C3), nevertheless both the C1C2 construct and the C1 repeat also presented also a high binding similar to the values shown by the C1C2C3 full domain. In contrast, the other C repeats combinations or alone presented a much lower binding to human albumin (Fig. 3).

To characterize the ProtH ABD:albumin interactions in more detail, SEC studies were also performed. As shown in Fig 4 and Table 2, SEC analysis also shows the interaction between ProtH ABD and human and mouse serum albumin in solution. ProtH ABD and albumins were incubated at 1:1, molar (corresponding to ~1:4, (w/w) ProtH:HSA) in PBS at room temperature. ProtH ABD eluted essentially as a monomer with an apparent molecular mass of 12.3 kDa (R_S 1.6 nm). HSA major peak (monomer) with an apparent molecular mass of 68.1 kDa (R_S 3.67 nm) and MSA monomer with an apparent mass of 64.3 kDa (R_S 3.60 nm) were shifted after incubation with ProtH ABD to 83.2 kDa (R_S 3.79 nm) and 89.2 kDa (R_S 3.88 nm), respectively.

CD analysis

Circular dichroism (CD) spectroscopy allowed the study of HSA, ProtH ABD and ProtH C1 structure and possible conformational changes after ProtH-HSA binding. HSA spectrum in buffer solution shows two negative bands near 208 and 222 nm and a positive band near 195 nm, typical of α-helical conformation (Fig. 5A)[26]. ProtH C1 and ProtH ABD spectra are also typical of the helical conformation revealing both negative bands at ~208 and 222 nm (Fig. 5B and C). The addition of ProtH ABD to a HSA protein solution revealed that the formed complex maintains the helical structure (Fig. 5D).

ProtH in silico predicted three-dimensional structures

The amino acid sequence of ProtH H ABD was submitted to the I-TASSER server for 3D protein structure prediction. The *in silico* prediction of the three dimensional structure using the I-TASSER server from the University of Michigan resulted in a 3D model with an alpha-helix conformation, represented by two pdb format pictures analyzed with Chimera software (Fig. 6A and B).

DISCUSSION

Streptococcal ABDs have been extensively studied and have become extremely important as therapeutic scaffolds and as promising approaches to extend the half-life of therapeutic proteins. In this study, we characterize the albumin-binding properties of ProtH ABD from protein H cell surface protein of *Streptococcus pyogenes* and evaluate the *in silico* prediction of ProtH domain conformation. Our data showed that ProtH ABD and ProtH ABD C repeats were stably expressed in *E. coli*, with high soluble yields of purified protein of several milligrams (10-15 mg) per liter of culture. Moreover, all the constructs exhibit high thermal stability, presenting melting temperatures of 58 to 63 ºC for the ProtH ABD (C1C2C3). From all C repeats constructs, C1 showed the highest stability with a melting temperature of 74 ºC, comparing with the lower melting temperatures of C2, C3 and the other combinations of these domains (Table 1).

Our results of ProtH ABD binding to serum albumin were in the range of nanomolar, according with previous studies from other groups[1,20-22]. Thus, binding of ProtH to HSA, RSA and MSA at pH 6.0 present EC_{50} values of 3.28 nM, 10.77 nM and 3.15 nM, respectively. At neutral pH 7.4 EC_{50} values were similar HSA and RSA (EC_{50} = 9.77 nM and 10.92 nM, respectively), but slightly lower for MSA (0.13 nM) of the value obtained at pH 6.0. Frick and colleagues investigated the separate binding sites of protein H for IgG and albumin, and discovered that protein H binds serum albumin and IgG in different binding domains. The affinity constant for the reaction between albumin and protein H, calculated by Scatchard plot was 7.8 x 10^9 M^{-1}, which was higher than the affinity for IgG (K_a = 1.6 x 10^9 M^{-1})[1]. Quite a few studies that evaluated the binding capacities between different bacterial ABDs are according to our data, showing results usually with affinities in the range of nanomolar [1,28,29]. Furthermore, we determine the albumin binding ability of each unit of the C repeats (C1, C2 and C3) and combinations of C repeats C1C2 and C2C3. Our results demonstrate that ProtH ABD containing the three C repeats (C1C2C3) has the highest binding to human albumin.

Moreover and importantly, these findings reveal that C1 repeat seems to perform a key role in the albumin binding of the ProtH ABD, showing a higher binding to albumin, similar to the values observed to the C1C2C3 and C1C2 domains. These cell wall-associated bacterial proteins usually contain tandemly repeated sequences, some with a single type of repeated motif, others with several distinct types of domains[29]. Hence, the C repeat units from the ABD of protein H have the same organization (C1C2C3) observed in the ABD from protein G[1]. The SEC results (Fig. 4) of ProtH ABD binding to human and mouse albumin also support the efficient binding of this ABD to serum albumin, showing the formation of complexes of ProtH/albumin with the increase in the of the Stokes radius.

The CD experiments performed in our studies show that both ProtH C1 and ProtH ABD have an α-helical structure in buffer solution (Fig. 5B and C). The addition of ProtH ABD to a HSA solution in a 1:1 ratio reveals that the formed complex maintains the initial secondary structure while the increase in the negative bands signal reveal a higher helical content (Fig. 5D), supporting efficient complex formation. A previous study presented similar results in the secondary structure analysis of protein H, using CD spectroscopy, and discovered that protein H is a predominantly α-helical protein at 4 ºC, with a α-helical content estimated to be 74%. In the presence of equimolar concentrations of albumin, the low-temperature conformation of protein H was stabilized, without affecting the α-helical conformation[30].

The ProtH ABD three dimensional *in silico* prediction is according with the CD experiments results, showing a possible α-helical structure conformation (Fig. 6). The server information also identifies ProtH ABD structural similarities in crystal structures of other bacterial proteins with anti-parallel coil-coil hairpin and helical-bundle conformations. Nilsson and co-workers analyzed the secondary structure of protein H and their results indicated that the extracellular part (sS, A, B and C regions) and part of the D region comprising amino acids 1-296 is predominantly (64%) α-helical. When the distribution of amino acids in the A, B and C domains of protein H and M1 protein, another M protein with C1C2C3 repeats, are analyzed, similarities with M proteins are evident and a high sequence similarity in both C repeats was observed. The analysis of M1 protein, reveals similar secondary structure profile, with the extracellular part of the molecule (amino-acids 1-404) consisting of 76% helical structure. The sequence of protein H was analyzed by a statistical method, showing a high probability for α-helical coiled-coil structure for almost the entire extracellular part (amino acids 49-302, including C repeats in amino acids 159-284). Furthermore, the evaluation of physicochemical properties of protein H determined that at a lower temperature (20 ºC) protein H is in a predominantly dimeric state, whereas at a higher

temperature (37 ºC) the molecule is found in a monomeric state. In both cases, the frictional ratio is indicative of a highly elongated structure. Interestingly, the frictional ratio representing the dimeric form is higher than the monomeric form, suggesting that the dimeric coil-coil state, observed at lower temperatures, is more elongated than the monomeric form and, at high temperatures conformation is considered to adopt a flexible conformation. Thus, at a physiological temperature protein H is considered to adopt a flexible conformation[30].

According with these findings and the 3D model structure predicted for ProtH ABD it will be expected that this ABD will adopt a flexible α-helical conformation. However, to evaluate this hypothesis it will be necessary more structural data, using NMR or X-ray crystallography to reach a three dimensional structure of ProtH ABD and to analyze the interactions of ProtH-albumin.

In summary, our albumin-binding studies and SEC results, confirm the formation of ProtH/albumin complexes *in vitro* and support the fact that surface protein H fusion with small therapeutic proteins can be an interesting strategy to improve the extension of the circulation time of these molecules, triggered by the FcRn-mediated recycling mechanism. Indeed, a comparative analysis of the half-life of an anti-TNFα nanobody in fusion with ProtH was currently performed in our laboratory, showing promising results of this ABD as a strategy for half-life extension of small-sized therapeutics. Moreover, the present study demonstrates that the C1 repeat alone presents a high binding to albumin, similar to full ProtH ABD, and this domain is also very stable. The advantage of a small size protein with the same features of albumin binding, that due to the small size, will be more stable and less immunogenic, and easier to engineer will be a promising approach to improve the half-life of therapeutic proteins and as a protein scaffold, for therapeutic applications. Exploring the physicochemical properties of this molecule and the ProtH-albumin interactions can also improve the properties of this ABD for therapeutic purposes.

REFERENCES

1. Frick, I.-M., Ákesson, P., Cooney, J., Sjöbring, U., Schmidt, K.-H., Gomi, H., Hattori, S., Tagawa, C., Kishimoto, F., Björck, L. (1994) Protein H – a surface protein of *Streptococcus pyogenes* with separate binding sites for IgG and albumin. *Mol. Microbiol.* **12**, 143-151

2. Podbielski, A. (1993) Three different types of organization of vir regulon in group A streptococci. *Mol. Gen. Genet.* **237**, 287-300

3. Björck, L., Kastern, W., Lindhal, G., Widebäck, K. (1987) Streptococcal protein G, expressed by streptococci or by *Escherichia coli*, has separate binding sites for human albumin and IgG. *Mol. Immunol*. **24**, 1113-1122

4. Åkerström, B., Nielsen, B., Björck, L. (1987) Definition of IgG- and albumin-binding regions of streptococcal protein G. *J. Bio.l Chem*. **262**, 13388-13391

5. Falkenberg, C., Björck, L., Ákesson, P. (1992) Localization of the binding site for streptococcal protein G on human serum albumin. Identification of a 5.5-kDa protein G binding albumin fragment. *Biochemistry*. **31**, 1451-1457

6. Kontermann, R.E. (2009) Strategies to extend plasma half-lives of recombinant antibodies. *Biodrugs* **23,** 93-109

7. Kontermann, R.E. (2011) Strategies for extended serum half-life of protein. *Curr. Opin. Biotechnol.* **22**, 1-9

8. de Chatêau, M., Björck, L. (1994) Protein PAB, a mosaic albumin-binding bacterial protein representing the first contemporary example of module shuffling. *J. Biol. Chem*. **269**, 12147-12151

9. Cramer, J.F., Nordberg, P.A., Hajdu, J., Lejon, S. (2007) Crystal structure of a bacterial albumin-binding domain at 1.4 Å resolution. *FEBS Lett*. **581**, 3178-3182

10. Johansson, M.U., de Château, M., Björk, L., Forsén, S., Drakenberg, T., Wikström, M. (1995) The GA module, a mobile albumin-binding bacterial domain, adopts a three-helix-bundle structure. *FEBS Lett*. **374**, 257-261

11. Kraulis, P.J., Jonasson, P., Nygren, P.A., Uhlén, M., Jendeberg, L., Nilsson, B., Kördel, J. (1996) The serum albumin-binding domain of streptococcal protein G is a three-helical bundle: a heteronuclear NMR study. *FEBS Lett*. **378**, 190-194

12. Tashiro, M., Montelione, G.T. (1995) Structures of bacterial immunoglobulin-binding domains and their complexes with immunoglobulins. *Curr. Opin. Struct. Biol*. **5**, 471-81

13. Tashiro, M., Tejero, R., Zimmerman, D.E., Celda, B., Nilsson, B., Montelione, G.T. (1997) High-resolution solution NMR structure of the Z domain of staphylococcal protein A. *J. Mol. Biol*. **272**, 573-90

14. Malm, M., Kronqvist, N., Lindberg, H., Gudmundsdotter, L., Bass, T., Frejd, F.Y., Höidén-Guthenberg, I., Varasteh, Z., Orlova, A., Tolmachev, V., Ståhl, S., Löfblom, J. (2013) Inhibiting HER3-Mediated Tumor Cell Growth with Affibody Molecules Engineered to Low Picomolar Affinity by Position-Directed Error-Prone PCR-Like Diversification. *PLoS One* **8**, e62791

15. Nivelbrant, J., Alm, T., Hober, S., Löfblom, J. (2011) Engineering bispecific into a single albumin-binding domain. *PLoS One* **6**, e25791

16. Ahmad, J.N., Li, J., Biedermannová, L., Kuchař, M., Sípová, H., Semerádtová, A., Cerný, J., Petroková, H., Mikulecký, P., Polínek, J., Staněk, O., Vondrášek, J., Homola, J., Malý, J., Osička, R., Sebo, P., Malý, P. (2011) Novel high-affinity binders of human interferon gamma derived from albumin-binding domain of protein G. *Proteins*. **80**, 774-789

17. Löfblom, J., Feldwisch, J., Tolmachev, V., Carlsson, J., Ståhl, S., Frejd, F.Y. (2010) Affibody molecules: engineering proteins for therapeutic, diagnostic and biotechnological applications. *FEB Lett*. **584**, 2670-2680

18. Tolmachev, V., Tran, T.A., Rosik, D., Sjöberg, A., Abrahmsén, L., Orlova, A. (2012) Tumor targeting using affibody molecules: interplay of affinity, target expression level, and binding site composition. *J. Nucl. Med.* **53**, 953-960

19. Morais, M., Cantante, C., Gano, L., Santos, I., Lourenço, S., Santos, C., Fontes, C., Aires da Silva, F., Gonçalves, J., Correia, J.D. (2014) Biodistribution of a ^{67}Ga-labeled anti-TNF VHH single-domain antibody containing a bacterial albumin-binding domain (Zag). *Nucl. Med. Biol.* pii: S0969-8051(14)00012-22

20. Kontermann, R.E. (2012) Half-life modulating strategies - an introduction. In Kontermann, R.E. (ed). Therapeutic proteins: strategies to modulate theirs half-lives, Wiley-Blackwell, 2012, **1**, 3-21

21. Frejd, F.Y. (2012) Half-life extension by binding to albumin through and albumin binding domain. In Kontermann, R.E. (ed). Therapeutic proteins: strategies to modulate theirs half-lives, Wiley-Blackwell, 2012, **14**, 269-283

22. Stork, R., Müller, D., Kontermann, R.E. (2007) A novel tri-functional antibody fusion protein with improved pharmacokinetic properties generated by fusing a bispecific single-chain diabody with an albumin-binding domain from streptococcal protein G. *Protein Eng Des Sel.* **20**, 569-576

23. Stork, R., Campigna, E., Robert, B., Müller, D., Kontermann, R.E. (2009) Biodistribution of a bispecific single-chain diabody and its half-life extended derivatives. *J. Biol. Chem.* **284**, 25612-25619

24. Roy, A., Kucukural, A., Zhang, Y. (2010) I-TASSER: a unified platform for automated protein structure and function prediction. *Nat. Protoc.* **5**, 725-738

25. Roopenian, D.C., Akilesh, S. (2007) FcRn: the neonatal Fc receptor comes of age. *Nat. Rev. Immunol.* **7**, 715-725

26. Kelly, S.M., Jess, T.J., Price, N.C. (2005) How to study proteins by circular dichroism. *Biochim. Biophys. Acta* **1751**, 119-139

27. Linhult, M., Binz, H.K., Uhlén, M., Hober, S. (2002) Mutational analysis of the interaction between albumin-binding domain from streptococcal protein G and human serum albumin. *Protein Sci*. **11**, 206-213

28. de Chatêau, M., Holst, E., Björck, L. (1996) Protein PAB, an albumin-binding bacterial surface promoting growth and virulence. *J. Biol. Chem*. **271**, 26609-26615

29. Johansson, M.U., de Château, M., Wikström, M., Forsén, S., Drakenberg, T., Björck, L. (1997) Solution structure of the albumin-binding GA module: a versatile bacterial protein domain. *J. Mol. Biol.* **266**, 859-865

30. Nilsson, B.H.K., Frick, I.-M., Åkesson, P., Forsén, S. Björck, L., Åkerström, B., Wikström, M. (1995) Structure and stability of protein H and the M1 protein from *Streptococcus pyogenes*. Implications for other surface proteins of Gram-positive bacteria. *Biochemistry* **34**, 13688-13698

ABBREVIATIONS

ABD, albumin-binding domain; FcRn, neonatal Fc receptor; HSA, human serum albumin; IgG, immunoglobulin G; MSA, mouse serum albumin; NMR, nuclear magnetic resonance, ProtH, protein H albumin-binding domain; RSA, rat serum albumin; SEC, size exclusion chromatography, TNFα, tumor necrosis factor α.

ACKNOWLEDGMENTS

C. Cantante and D. Gaspar acknowledge Fundação para a Ciência e a Tecnologia (FCT) for fellowships SFRH/BD/48598/2008 and SFRH/BPD/73500/2010, respectively.

FIGURE LEGENDS

Fig. 1: Construction and production of ProtH ABD and C repeats. (A) Sequence of ProtH albumin-binding domain. (B) Sequence alignment of ProtH ABD C1, C2 and C3 repeats. (C) Schematic representation of the different ProtH ABD constructs under investigation in this study. Each ABD domain has an N-terminal leader peptide (LP) a C-terminal histidine (His_7) and human influenza hemagglutinin protein tags (HA). (D) SDS-PAGE analysis of the ProtH ABD and ProtH ABD domains purified proteins (3 µg/lane) under reducing. Gel was stained with Coomassie brilliant blue.

Fig. 2: Binding of ProtH ABD to human, rat and mouse albumin. Binding of ProtH ABD to serum albumin was evaluated in ELISA at neutral pH - pH 7.4 (A); and acidic pH - pH 6.0 (B). Bound proteins were detected using an HRP-conjugated anti-HA tag antibody.

Fig. 3: Binding of ProtH domains to human serum albumin. Binding of ProtH ABD C1-C3 repeats to HSA were evaluated by ELISA at 1000 nM and 100 nM concentrations. Control (-) PBS1x-soya milk 1%. Bound proteins were detected using an HRP-conjugated anti-HA tag antibody.

Fig. 4: Size exclusion chromatography for ProtH/albumin complexes analysis. ProtH ABD (C1C2C3) (A), HSA (B), ProtH ABD + HSA (C), MSA (D) and ProtH ABD + MSA (E). ProtH ABD was incubated at equimolar concentrations with albumin in PBS at room temperature. Peak positions of marker proteins are indicated.

Fig. 5: CD studies of ProtH and ProtH/HSA binding. Far UV-CD spectra of HSA (A), ProtH C1 and ProtH in the absence (C) and presence (D) of HSA. HSA was kept at 4 µM (A) and ProtH C1 at 50 µM (B). ProtH protein was measured at 20 µM (C) and added to a HSA solution at 1:0.25, and 1:1 ratios (D, black curve, HSA; grey curve HSA:ProtH 1:0.25; grey dotted curve, HSA:ProtH 1:1).

Fig. 6: *In silico* prediction of ProtH ABD (C1C2C3) structure. Three-dimensional structure models of ProtH ABD were predicted *in silico* prediction using the I-TASSER server. ProtH ABD predicted structure is represented in two PDB pictures (A and B) with the C1 repeat represented in orange and red, C2 repeat represented in green and C3 repeat coloured in blue.

TABLES

Table 1: Thermal stability of ProtH and ProtH C repeats.

Protein	Tm B - Mean ±SD (°C)	Tm B – Median ±SD (°C)	Tm D - Mean ±SD (°C)	Tm D - Median ±SD (°C)
ProtH (C1C2C3)	58.28 ± 0.68	57.69 ± 0.68	62.91 ± 0.24	63.06 ± 0.24
C1	74.00 ± 3.39	74.00 ± 3.39	74.09 ± 3.36	74.09 ± 3.36
C2	58.58 ± 0.90	58.39 ± 0.90	57.10 ± 2.11	55.24 ± 2.11
C3	58.87 ± 1.19	59.47 ± 1.19	58.86 ± 4.67	54.95 ± 4.67
C1C2	54.89 ± 0.54	55.15 ± 0.54	55.05 ± 3.68	51.59 ± 3.68
C2C3	59.57 ± 0.47	59.50 ± 0.47	45.64 ± 9.49	45.75 ± 9.49

Tm B - Calculated Boltzamnn melting temperature; Tm D - Calculated Derivated melting temperature.

Table 2: ProtH ABD/albumin complexes.

Protein or complex	Length	Calculated M_r[a]	SEC apparent M_r	Stokes' radius ($R_{S)}$
	aa	**kDa**	**kDa**	**nm**
ProtH	148	16.7	12.3	1.6
HSA	585	66.5	68.1	3.67
MSA	584	65.9	64.3	3.60
ProtH/HSA	-	83.2	83.2	3.79
ProtH/MSA	-	82.6	89.2	3.88

[a]Calculated based on the amino acid sequence.

Table 3: Binding of ProtH to HSA, RSA and MSA.

Protein	EC_{50} for HSA (nM)	EC_{50} for RSA (nM)	EC_{50} for MSA (nM)
ProtH pH 6.0	3.28 ± 0.03	10.77 ± 0.03	3.15 ± 0.02
ProtH pH 7.4	9.77 ± 0.03	10.92 ± 0.02	0.13 ± 0.03

Figure 1

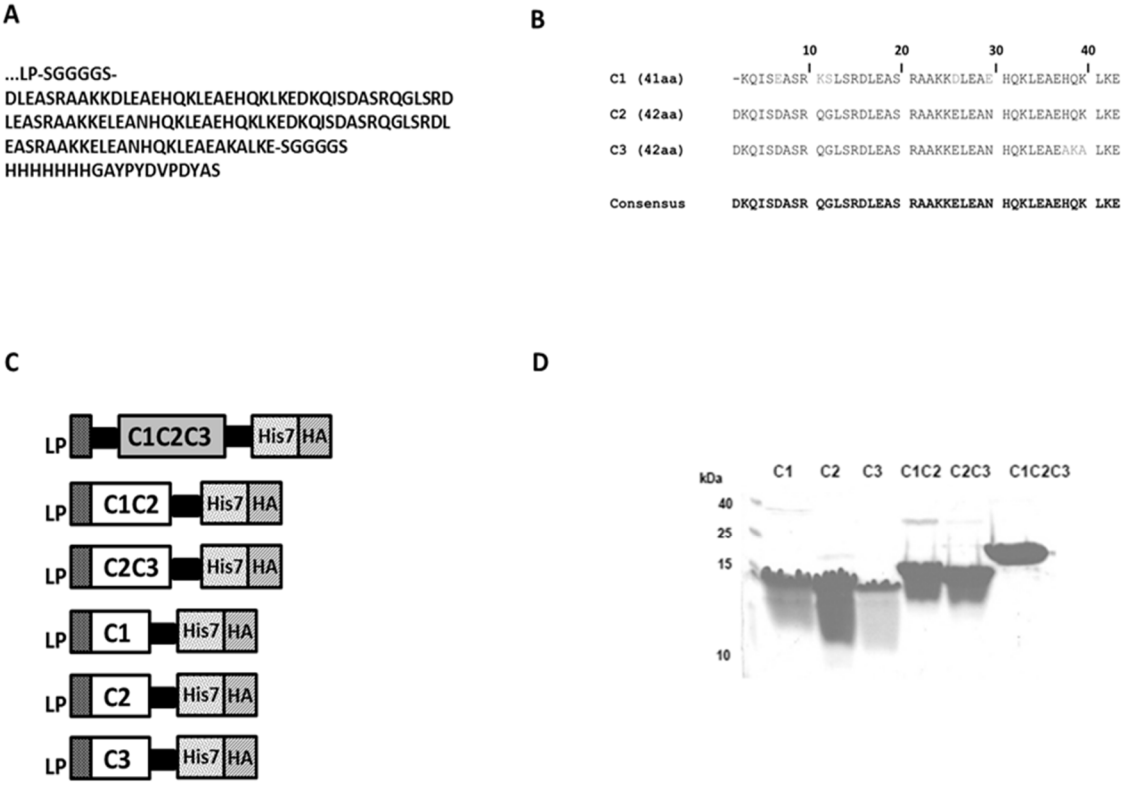
A
...LP-SGGGGS-
DLEASRAAKKDLEAEHQKLEAEHQKLKEDKQISDASRQGLSRD
LEASRAAKKELEANHQKLEAEHQKLKEDKQISDASRQGLSRDL
EASRAAKKELEANHQKLEAEAKALKE-SGGGGS
HHHHHHHGAYPYDVPDYAS
B
10
20
30
40
C1 (41aa) -KQISEASR KSLSRDLEAS RAAKKDLEAE HQKLEAEHQK LKE
C2 (42aa) DKQISDASR QGLSRDLEAS RAAKKELEAN HQKLEAEHQK LKE
C3 (42aa) DKQISDASR QGLSRDLEAS RAAKKELEAN HQKLEAEAKA LKE
Consensus DKQISDASR QGLSRDLEAS RAAKKELEAN HQKLEAEHQK LKE
C
LP C1C2C3 His7 HA
LP C1C2 His7 HA
LP C2C3 His7 HA
LP C1 His7 HA
LP C2 His7 HA
LP C3 His7 HA
D
kDa
C1 C2 C3 C1C2 C2C3 C1C2C3
40
25
15
10

Figure 2

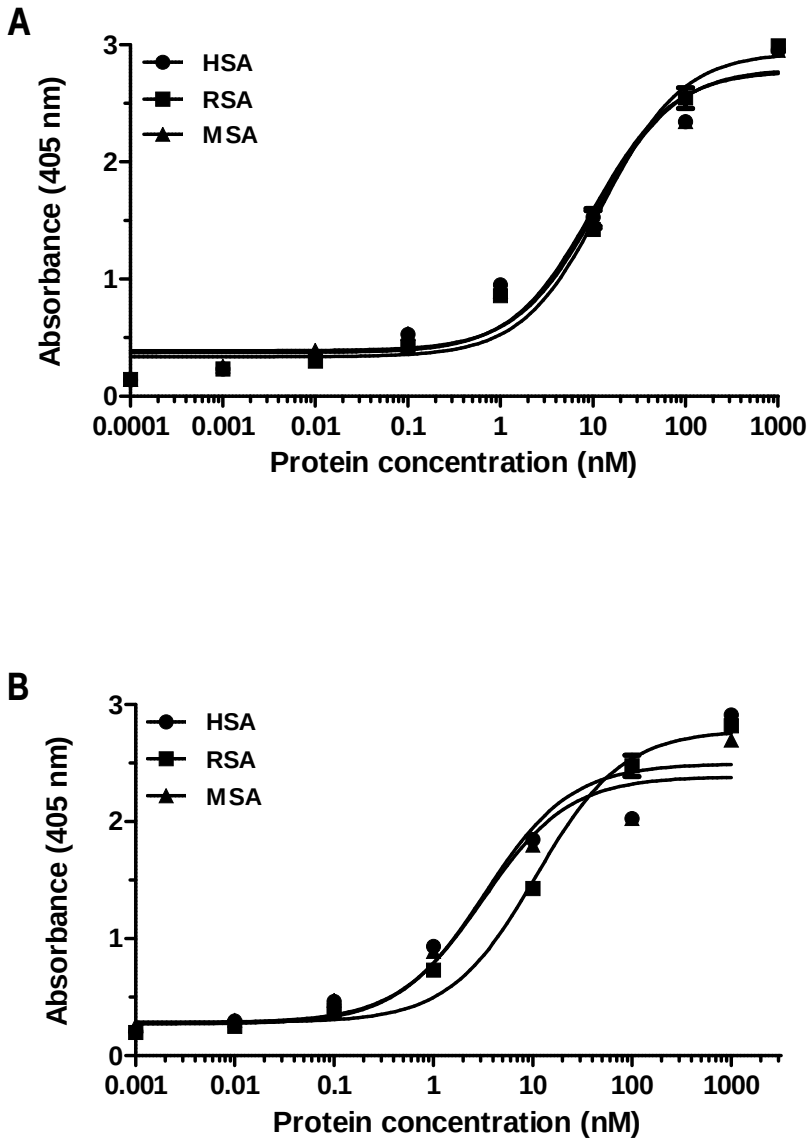
A
HSA
RSA
MSA
Absorbance (405 nm)
0
1
2
3
0.0001
0.001
0.01
0.1
1
10
100
1000
Protein concentration (nM)
B
HSA
RSA
MSA
Absorbance (405 nm)
0
1
2
3
0.001
0.01
0.1
1
10
100
1000
Protein concentration (nM)

Figure 3

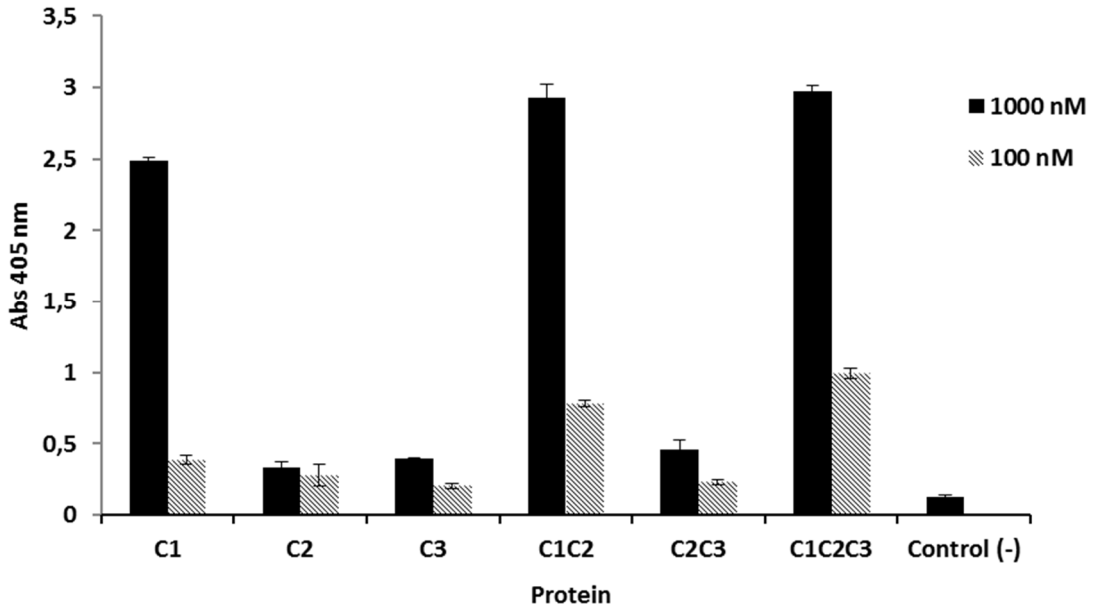
3,5
3
2,5
2
1,5
1
0,5
0
Abs 405 nm
1000 nM
100 nM
C1
C2
C3
C1C2
C2C3
C1C2C3
Control (-)
Protein

Figure 4

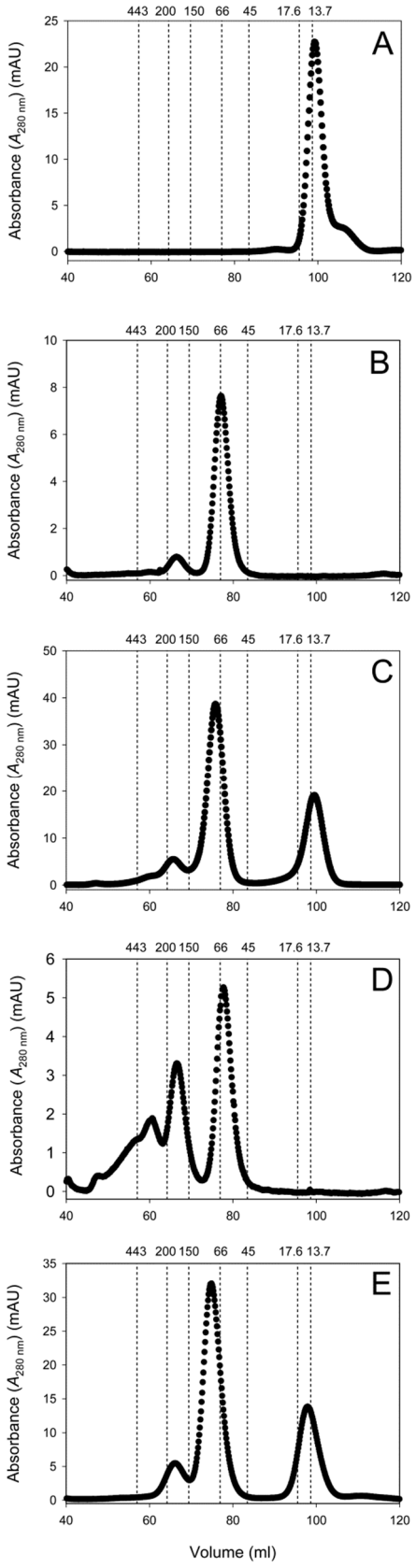
443 200 150 66 45 17.6 13.7
A
B
C
D
E
Absorbance ($A_{280\ nm}$) (mAU)
Volume (ml)

Figure 5

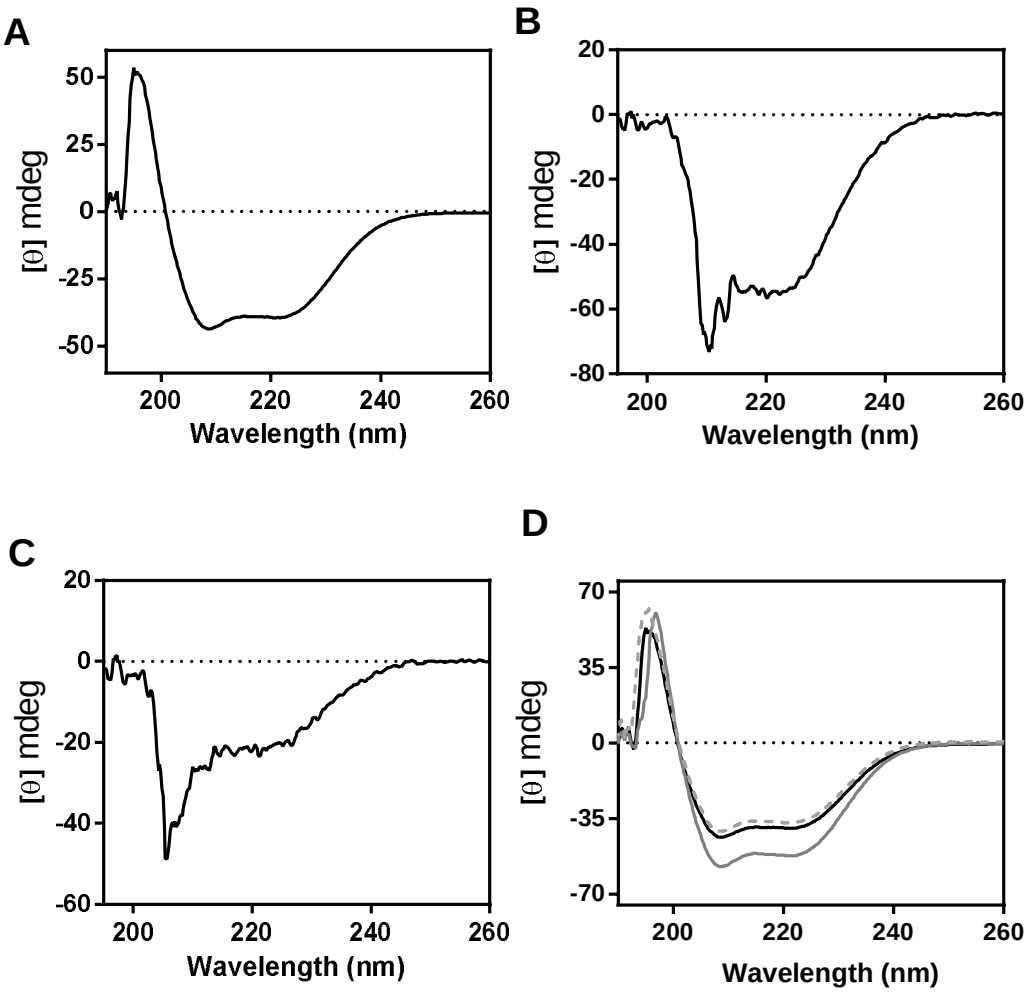
A
B
C
D
[θ] mdeg
Wavelength (nm)
50
25
0
-25
-50
20
-20
-40
-60
-80
35
-35
-70
200
220
240
260

Figure 6

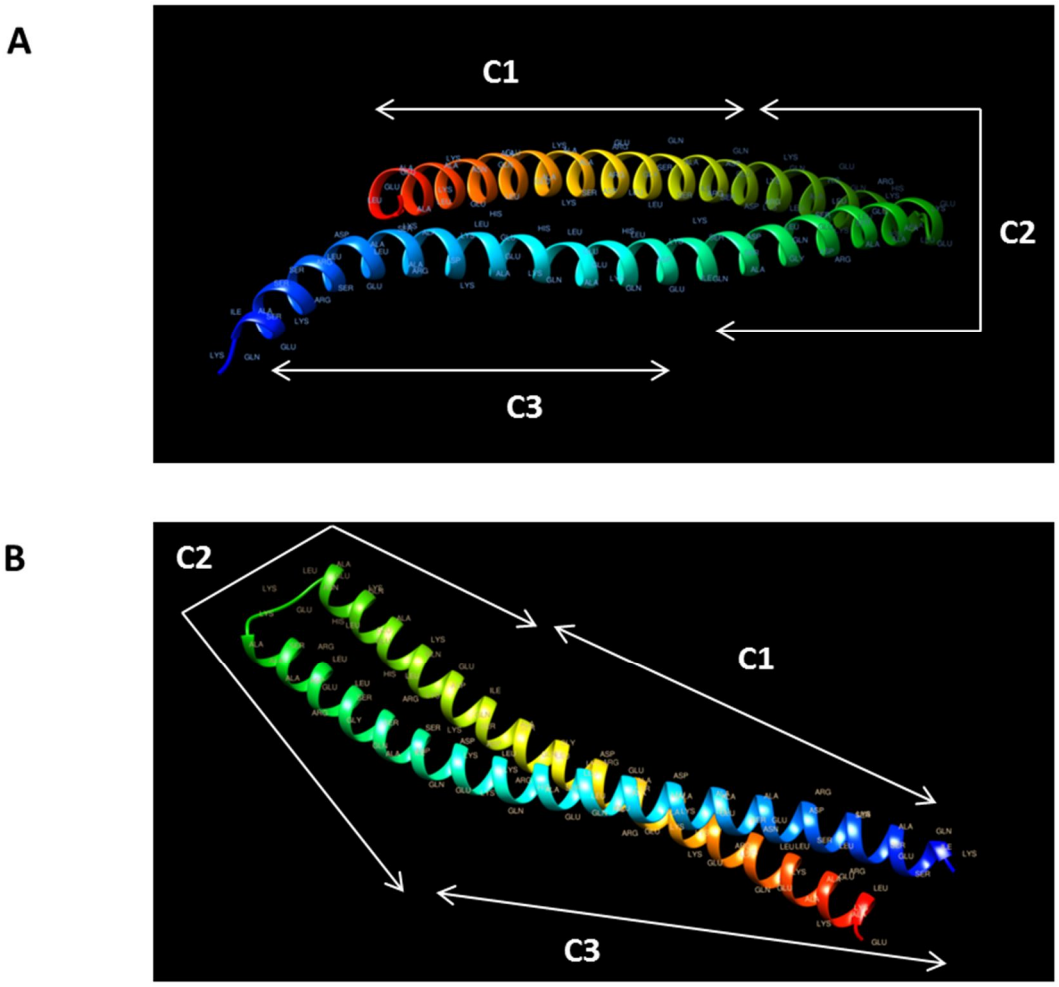

CONCLUDING REMARKS AND FUTURE PERSPECTIVES

The discovery and application of albumin-binding domains to improve the pharmacokinetics of small-sized therapeutics and as therapeutic protein scaffolds have demonstrated a great potential in biomedical research in the last years and opened new insights for biotechnological research, therapeutic and diagnosis applications. The enormous potential of these proteins has been explored by several pharmaceutical and biotechnological companies, but there is still an urgent need in the art of new strategies to improve circulation half-life. New efforts need to be made to develop new small molecules or protein scaffolds that can be explored and engineering for therapeutic applications. Current strategies for half-life extension of therapeutic proteins used by pharmaceutical industry are focused in PEGylation or in the chemical conjugation of other recombinant PEG mimetics. However, "PEGylation" technology has several drawbacks, e.g. clinical grade PEG derivates are expensive and their covalent coupling to a recombinant protein requires additional downstream process and purification steps, thus lowering yield and raising the costs. Moreover, PEG is not biodegradable, which can cause side effects such as vacuolation of kidney epithelium upon continuous treatment, and the chemical coupling step can lead to reduced binding and activity of the PEGylated protein (Gaberc-Porekar *et al*., 2008; Knop *et al*., 2010). Albumin-binding moieties are a good alternative to increase the circulation time of biodrugs. Current approaches using bacterial albumin-binding domains are based in the ABDs from proteins G and PAB, and the Ig-binding domain Z from staphylococcal protein A used as scaffold for the optimization of Affibody molecules. All these bacterial proteins have in common a three-α-helix structure and the natural binding to plasma proteins, which has been described to be involved in the escape of immune system surveillance, adding selective advantages to bacteria as a virulence factor. This Thesis study was developed to explore the potential of two new streptococcal albumin-binding domains, the Zag ABD from *S. zooepidemicus* ZAG protein and the ProtH ABD from *S. pyogenes* protein H, as strategies to improve pharmacokinetic properties of therapeutic proteins. To validate our ABDs half-life strategy and as a proof-of-concept, the Zag and ProtH domains were fused with an anti-TNFα VHH single-domain antibody. We aim to investigate the albumin-binding properties for half-life extension or targeting, stability, and three-dimensional structures of these domains for future applications as fusion partners and protein scaffolds. Both albumin-binding proteins were described for the first time in the 90's and there were not developed for therapeutic research. Therefore, this project represents a new challenge in protein-based drugs development and also provides an easy, fast, low cost, and reliable methodology to improve half-life of several therapeutic proteins, with special interest in the treatment of rheumatoid

arthritis and cancer, due to accumulation of albumin in tumours and arthritic joints. Moreover, with further investigation, these ABDs will be promising approaches for half-life extension of several therapeutic molecules and proteins, for the treatment of a wide number of diseases.

All the Zag and ProtH constructions were successfully engineered and optimized for bacterial expression and IMAC purification with high yields of purified soluble protein, high degree of purity, without using several complicated and costly steps of purification. These protocols allow an inexpensive and easy protein production, using simple protein purification technology and, also allow a simple scale up process. After production, VHH-Zag and VHH-ProtH fusion proteins showed a high thermal stability and a high affinity for human, rat and mouse in the range of nanomolar, which was described as well for other recombinant antibodies in fusion with ABD from protein G (Stork *et al*., 2007; Stork *et al*., 2009; Hopp *et al*., 2010). Binding to albumin was not reduced at low pH (pH 6.0), suggesting that the presence of ABD does not interfere with the pH-dependent binding of HSA to FcRn *in vitro*.

The size exclusion chromatography results also confirm the HSA and MSA binding in solution, but with different stoichiometry for the Zag and ProtH fusion proteins. For instance, VHH-Zag presented a monomeric form alone and in complex with mouse and human albumins. However, VHH-ProtH alone in solution forms dimers and trimers, and the same stoichiometry is observed in complex with human albumin, but the VHH-ProtH/MSA complexes have an apparent monomeric form. One possible explanation for these results is that protein H could form temperature-dependent dimers with higher affinity for human albumin and IgG than the monomer (Åkerström *et al*., 1992; Frick *et al*., 1995). Nilson and colleagues findings showed that at lower temperature protein H is in a predominantly dimeric state, whereas at higher temperatures this protein is found in monomeric state (Nilsson *et al*., 1995).

ABDs have been successfully fused to a number of proteins, retaining the functional activity both of the albumin binding part and the fused part. VHH-ProtH and VHH-Zag fusion proteins maintained the TNFα binding (in the range of nanomolar) in the presence of albumin, and the blockade effect of the interaction of TNFα/TNFR from the therapeutic TNFα-neutralizing VHH from Ablynx, for the treatment of rheumatoid arthritis. VHH, VHH-Zag and VHH-ProtH presented high serum stability, maintaining the antigen binding properties without suffer degradation in human serum during 24 days and in mouse serum until 4 days. Importantly, both Zag and ProtH substantially improved the circulation time of VHH *in vivo*, in approximately 39-fold for VHH-Zag (terminal half-life of 30.55 h) and in 26-fold for VHH-ProtH (terminal half-life of 20.54 h), respectively. As a half-life extension strategy,

fusion to Zag ABD resulted in a higher improvement of the circulation time of the VHH nanobody.

In the past decades, the growth of nuclear medicine has been due mainly to the availability of technetium-99m (^{99m}Tc) radiopharmaceuticals. This isotope is a metastable nuclear isomer with a half-life of 6 h and is used in over 80% of all diagnostic procedures (Kratz and Elsadek, 2012). The organ biodistribution profiles of ^{99m}Tc-VHH-Zag and ^{99m}Tc-VHH-ProtH presented very different results in blood, kidneys and liver. The ^{99m}Tc-VHH-Zag exhibited a slow elimination from blood and an accumulation in irrigated organs such as liver. ^{99m}Tc-VHH was rapidly cleared from the blood and presented a high accumulation in kidneys. Comparing with ^{99m}Tc-VHH-Zag, ^{99m}Tc-VHH-ProtH exhibited higher retention in kidneys and a reduced presence in blood, showing a distribution profile similar to ^{99m}Tc-VHH. However, the biodistribution profile of ^{99m}Tc-VHH-ProtH do not interfere with the long half-life of the molecule, improved in 26-fold compared with the unmodified nanobody.

Coppieters and collegues biodistribution studies with bispecific VHH against TNFα in fusion with a VHH targeting albumin (TR2-TR2-AR1), as a strategy for half-life improvement, showed similar results with a substantially extended half-life for the TR2-TR2-AR1 of 2.2 days in BALB/c mice (*versus* 35 min and 54 min, for the monomeric and dimeric forms, respectively). The ^{99m}Tc-radiolabelled nanobodies, tested with a CIA preclinical model, also demonstrated an accumulation of radioactivity in the inflamed paws. The radioactivity was superior in the albumin targeting fusion proteins due to the accumulation of albumin in inflammation sites, with higher concentrations exhibited after 24 h after injection, and a higher uptake correlated with the higher clinical scores for the corresponding limbs (Coppieters *et al*., 2006).

Furthermore, VHH and VHH-Zag recombinant antibodies biodistribution was evaluated in mice, using gallium 67 (^{67}Ga)-citrate. ^{67}Ga is a useful radiopharmaceutical for diagnostic in tumour detection, especially for patients with Hodgkin and non-Hodgkin lymphoma, lung cancer, malignant melanoma, breast carcinoma and Ewing's sarcoma (Kratz and Elsadek, 2012), and presents a decay half-life of 3.26 days. Since mouse serum presents a half-life of ~1-2 days, we purposed to compare the biodistribution profile of the VHH and VHH-Zag proteins using a radionuclide with a decay half-life higher than MSA, with previous radiolabelling with ^{99m}Tc (decay half-life of approximately 6 h). Our results showed that the conjugation with p-SCN-Bn-NOTA and the radiolabelling with the radionuclide ^{67}Ga (^{67}GA-NOTA) did not affect the albumin and TNFα binding. The profiles of biodistribution were similar with the study of biodistribution with ^{99m}Tc-VHH and ^{99m}Tc-VHH-Zag. Thus, ^{67}Ga-

NOTA-VHH-Zag uptake in blood and kidneys was superior, comparing with the ^{67}Ga-NOTA-VHH that also presented highest kidney retention and almost a total excretion at 24 h. The biodistribution profile of ^{67}Ga-NOTA-VHH exhibited a rapid clearance from blood and most tissues. Instead, ^{67}Ga-NOTA-VHH-Zag presented a slow washout from blood, muscle and bone, and an accumulation in highly irrigated organs such as liver, spleen and lung.

This increased half-life most likely correlates with the half-life of serum albumin, which are 1.07-1.6 days for murine serum albumin and ~19 days for human serum albumin (Andersson *et al.*, 1991; Peters, 1996; Stevens *et al.*, 1992; Schmidt *et al.*, 2013).

Even though Zag and ProtH ABDs have shown substantial improvements in pharmacokinetic properties of the nanobody, concerns with the immunogenicity of these molecules for therapeutic applications may occur due to their bacterial origins. For instance, immunogenicity of the albumin-binding domain of protein G, in the amino acid sequence 254-299, was detected in mice strains (Sjölander *et al.*, 1997). For therapeutic purposes, particularly in small proteins that require administration by repeated injections, it will be necessary reduce or ideally eliminate the immunogenicity. There are several de-immunization strategies that can be applied in future, to reduce the immunogenicity of these molecules (de Groot *et al.*, 2005; Baker and Jones, 2007; Nagata and Pastan, 2009). Currently, we have already de-immunization studies ongoing for the Zag ABD. We have already identified and removed potential immunogenic epitopes by an *in silico* approach. After de-immunization, the Zag ABD maintained the albumin-binding ability and half-life extension properties when fused with therapeutic proteins.

In a future perspective it will be necessary to identify the immunogenic amino acids or regions in the sequence of the ProtH ABD and engineer the protein to eliminate the immunogenic epitopes.

The Zag and ProtH ABDs fusion to the VHH, showed promising results for the improvement of pharmacokinetic properties of the therapeutic molecules without affecting the efficacy of the biodrug against the therapeutic target. After these findings, we proposed to characterize the albumin-binding properties of these ABDs and also study the structural conformations of both domains, in order to investigate their three-dimensional structures and understand the dynamic between ABD/albumin.

Our data demonstrated that both unfused ABDs can be stably produced in *E. coli* and have albumin-binding in nanomolar range, according what is described in other studies (Frick *et al.*, 1995, Linhult *et al.*, 2002; Hopp *et al.*, 2010; Kontermann, 2011, Kontermann, 2012). Though, Zag ABD is a G-related protein or GA module, with an amino acid sequence very

different from the ProtH ABD sequence. The Zag ABD is composed by 52 amino acids in one domain, and ProtH ABD exhibit a three C repeat organization (C1C2C3) with high homology between the three units. Like the GA modules, the C repeats comprise about 40 amino acid residues, but these HSA-binding units show no sequence homology with GA motifs (Frick *et al.*, 1995). With a view to determine the albumin-binding of these units, several constructs were stably produced in bacteria, showing that the C1 repeat alone exhibit a high similar binding to the observed for the three repeats together (C1C2C3). These observations prove that C1 domain is the major responsible for the albumin binding of ProtH.

It is generally observed that proteins with high sequence identities have similar three-dimensional structures. It therefore appears likely that various GA modules, e.g. in protein G, will be found to have similar three-dimensional structures, due to the high sequence identities (around 60%) (Johansson *et al.*, 1995). According with these observations, the NMR assignment shows a three-alpha helix structure in the Zag ABD. The *in silico* prediction of three-dimensional structure of ProtH also exhibited a helical conformation. Another interesting finding, demonstrated by CD measurements it is that the conformation of both ABDs is maintained in the presence of human albumin. However, it will be necessary more structural data, using NMR or X-ray crystallography to reach a three-dimensional structure of ProtH ABD and to analyze the interactions of ProtH/albumin. Currently, X-ray crystallography studies of Zag/HSA complexes are being developed to determine the binding sites of Zag to albumin, and to evaluate in more detail the ABD/albumin interactions.

With more structural data to identify the region of albumin binding in both Zag and ProtH, and the binding site in albumin as well, it will be possible engineering these domains to improve their affinity to the target and stability. It will interesting to investigate if a higher affinity of these domains will increase the circulation time of fused therapeutic molecules.

To investigate the impact of very high affinity binding to albumin, an affinity matured variant of ABD has been developed by Jonsson and co-workers (Jonsson *et al.*, 2008). ABD3 was used as a starting point to construct a library of domain variants. Fifteen of the 46 amino acids in the protein were subject to constrained randomization and displayed on bacteriophage for selection. A first set of binders showed improved binding affinities with K_D in the low picomolar affinity range. Sequence features of individual variants were combined to create a second generation set of seven binders. One of the resulting binders, denoted ABD035, had relatively high Tm, excellent thermal refolding properties and an increased affinity for albumin. Initial SPR experiments suggested a very high affinity for human serum albumin with K_D between 50–500 fM (Jonsson *et al.*, 2008). The affinity was later measured in

solution, and a K_D of 120 fM was obtained. The affinity was improved also for albumin of other species including rat, mouse and cynomolgus monkeys. When used as fusion partner for scDb constructs, the affinity matured binder increased the affinity of the trispecific fusion protein for HSA with a factor of 80 and for MSA with a factor of 12 (Fredj, 2012).

Even if we improve the affinity of these motifs for half-life extension, with our data it will not be possible to realize what happen in the albumin when the nanobody reaches the therapeutic target is plasma circulation. In order to answer this question, it will be also important to investigate the albumin allosteric modifications the Zag and ProtH fusion proteins induce when the therapeutic protein is bound to albumin and catch up the therapeutic target in circulation. In a future perspective, it will be interesting to perform structural studies with VHH-Zag and VHH-ProtH in the presence of albumin and TNFα, using NMR or X-ray crystallography to study the dynamic of these protein-protein interactions.

Furthermore, the C1 repeat from ProtH ABD alone demonstrated a high binding to serum albumin, very similar with the binding of the full ABD. Due to C1 repeat smaller size (41 aa and 4.7 kDa) it will be more stable and less immunogenic, and easier to engineering as a fusion partner in order to improve pharmacokinetics of therapeutic proteins. In the future, it will be interesting to compare the C1 ability of binding to albumin, and pharmacokinetic parameters, including organ biodistribution, using the same anti-TNFα VHH as proof-of-concept.

Another interesting approach it will be to use both Zag and ProtH ABDs as protein scaffolds for therapeutic purposes. Therefore, it will be interesting engineering these domains against clinical relevant therapeutic targets or as one therapeutic molecule targeting an antigen or receptor and albumin, for circulation time extension. For example, Nilvebrant and colleagues created a single-domain bispecific affinity protein targeting TNFα and serum albumin (Nilvebrant *et al.*, 2011). For this purpose they have chosen an alkali-stabilized form of an ABD from protein G (Alm *et al.*, 2010) as a scaffold, and selected by phage-display, mutations on helix one and three, that are not involved in HSA interaction. This strategy proposes to combine the advantages of a small size protein (e.g. efficient production in a bacterial host or by chemical synthesis, and specificity to the therapeutic target) with an intrinsic extended half-life, that may reduce the blood clearance with an increase in the circulation time typical for antibodies (Nilvebrant *et al.*, 2011; Nilvebrant and Hober, 2013).

Due to the accumulation of albumin in arthritic joints and tumours, the natural albumin-binding ability of these ABDs will be an advantage for engineering the molecules as protein scaffolds for the treatment of cancer and rheumatoid arthritis. Affibody biotechnology

company is developing scaffolds, named affibody technology (Feldwisch and Tolmachev, 2012; Löfblom *et al.*, 2010). These scaffolds have characteristics and structural organization very similar with the Zag ABD, showing successful results in diagnostics and therapeutics of several diseases. Other biotechnology companies like Molecular Partners AG, which makes use of the DARPin technology (Boersma and Plückthun, 2011; Gebauer and Skerra, 2009; Stumpp *et al.*, 2008), also explore and engineering α-helical scaffolds for therapeutic purposes with great results.

Several protein therapeutics such as antibodies, often suffer from low efficacy, costly development, and sometimes toxic side effects. This means that these molecules perform at only a fraction of their potential, and are therefore not fulfilling their promise. Protein scaffolds can be selected to bind to any given target molecule, with unmatched affinity and specificity. These characteristics make them ideal agonistic, antagonistic or inhibitory drug candidates. Furthermore, these proteins can be rapidly developed and engineered candidates to include further enhancement of pharmacokinetic properties and adaptation to carry various effector functions, or multiple binding specificities can be combined enabling completely new drug formats. These formats are also advantageous because can be manufactured in low cost and high yield bacterial fermentation, and are easily formulated.

In conclusion, in this project it was possible to achieve our goals, showing that both Zag and ProtH ABDs are promising strategies to improve the pharmacokinetics of therapeutic proteins, and also that both domains can be further engineered as therapeutic scaffolds.

REFERENCES

Agreda-Vásquez, G.P., Espinosa-Poblano, I., Sánchez-Guerrero, S.A., Crespo-Solís, E., Cabrera-Vásquez, S., López-Salmorán, J., Barajas, J., Peñaloza-Ramírez, P., Tirado-Cárdenas, N., Velázquez, A. (2008) Starch and albumin mixture as replacement fluid in therapeutic plasma exchange is safe and effective. *J. Clin. Apher*. **23**, 163-167

Aires da Silva, F., Corte-Real, S., Gonçalves, J. (2008) Recombinant antibodies as therapeutic agents. *Biodrugs* **22**, 1-15

Akerström, B., Nielsen, E., Björck L. (1987) Definition of the IgG- and albumin-binding regions of streptococcal protein G. *Biol. Chem*. **262**, 13388-13391

Akerström, B., Björck L. (1989) Protein L: an immunoglobulin light chain-binding bacterial protein. Characterization of binding and physicochemical properties. *J. Biol. Chem*. **264**, 19740-19746

Akesson, P., Cooney, J., Kishimoto, F., Björck, L. (1990) Protein H – a novel IgG binding bacterial protein. *Mol. Immunol*. **27**, 523-531

Akesson, P., Schmidt, K.-H., Cooney, J., Björck, L. (1994) M1 protein and protein H: IgGFc- and albumin-binding streptococcal surface proteins encoded by adjacent genes. *Biochemistry*. **300**, 877-886

Alm, T., Yderland, L., Nilvebrant, J., Halldin, A., Hober, S. (2010) A small bispecific protein selected for orthogonal affinity purification. *J. Nucl. Med.* **51**, 1131-1138

Andersen, J.T., Dee Qian, J., Sandlie, I. (2006) The conserved histidine 166 residue of the human neonatal Fc receptor heavy chain is critical for the pH-dependent binding to albumin. *Eur. J. Immunol.* **36**, 3044-3051

Andersen, J.T., Pehrson, R., Tolmachev, V., Daba Bekele, M., Abrahmsén, L., Sandie, I., Ekblad, C. (2011) Extending half-life by indirect targeting of the neonatal Fc receptor (FcRn) using minimal albumin binding domain (ABD). *J. Biol. Chem*. **286**, 5234-5241

Anderson, C.L., Chaudhury, C., Kim, J., Bronson, C.L., Wani, M.A., Mohanty, S. (2006) Perspective - FcRn transports albumin: relevance to immunology and medicine. *Trends Immunol*. **27**, 343-348

Andersson, C.E., Lonnroth, I.C., Gelin, L.J., Moldawer, L.L., Lundholm, K.G. (1991) Pretranslational regulation of albumin synthesis in tumor-bearing mice: the role of anorexia and undernutrition. *Gastroenterology*. **100**, 938-945

Arend, W.P., Dayer, J.M. (1990) Cytokines and cytokine inhibitors or antagonists in rheumatoid arthritis. *Arthritis Rheum*. **33**, 305-315

Arnett, F.C., Edworthy, S.M., Bloch, D.A., McShane, D.J., Fries, J.F., Cooper, N.S., Healey, L.A., Kaplan, S.R., Liang, M.H., Luthra, H.S., Medsger, T.A. Jr, Mitchell, D.M., Neustadt, D.H., Pinals, R.S., Schaller, J.G., Sharp, J.T., Wilder, R.L., Hunder G.G. (1988) The American Rheumatism Association 1987 revised criteria for the classification of rheumatoid arthritis. *Arthritis Rheum*. **31**, 315-324

Arndt, M.A., Kraus, J., Rybak, S.M. (2004) Antigen binding and stability properties of non-covalently linked CD22 single-chain Fv dimers. *FEBS Lett*. **578**, 257-261

Atzeni, F., Benucci, M., Sallì, S., Bongiovanni, S., Boccassini, L., Sarzi-Puttini, P. (2013) Different effects of biological drugs in rheumatoid arthritis. *Autoimmun. Rev*. **12**, 575-579

Babson, A.L., Winnick, T. (1954) Protein transfer in tumor-bearing rats. *Cancer Res*. **14**, 606-611

Baker, M.P., Jones, T.D. (2007) Identification and removal of immunogenicity in therapeutic proteins. *Curr. Opin. Drug. Discov. Devel.* **10**, 219-227

Ballantyne, F.C., Fleck, A., Dick, W.C. (1971) Albumin metabolism in rheumatoid arthritis. *Ann. Rheum. Dis.* **30**, 265-270

Ballmer, P.E., Ochsenbein, A.F., Shütz-Hofmann, S. (1994) Transcapillary escape rate of albumin positively correlates with plasma albumin concentration in acute but not in chronic inflammatory disease. *Metabolism.* **43**, 697-705

Barber, M.D., Ross, J.A., Fearon, K.C. (1999) Changes in nutritional, functional, and inflammatory markers in advanced pancreatic cancer. *Nutr. Cancer.* **35**, 106-110

Batra, S.K., Jain, M., Wittel, U.A., Chauhan, S.C., Colvher, D. (2002) Pharmacokinetics and biodistribution of genetically engineered antibodies. *Curr. Opin. Biotechnol.* **13**, 603-608

Baum, R.P., Prasad, V., Müller, D., Schuchardt, C., Orlova, A., Wennborg, A., Tolmachev, V., Felwisch, J. (2010) Molecular imaging of HER2-expressing malignat tumors in breast cancer patients using synthetic 111In- or 68Ga-labeled affibody molecules. *J. Nucl. Med.* **51**, 892-897

Beckman, R.A., Weiner, L.M., Davis, H.M. (2007) Antibody constructs in cancer therapy: protein engineering strategies to improve exposure in solid tumors. *Cancer.* **109**, 170-179

Beeken, W.L., Volwiler, W., Goldsworthy, P.D., Garby, L.E., Reynolds, W.E., Stogsdill, R., Stemler, R.S. (1962) Studies of I-131-albumin catabolism and distribution in normal young male adults. *J. Clin. Invest.* **41**, 1312-1333

Bendele, A.M., Chlipala, E.S., Scherrer, J., Frazier, J., Sennello, G., Rich, W.J., Edwards, C.K. 3rd. (2000) Combination benefit of treatment with the cytokine inhibitors interleukin-1 receptor antagonist and PEGylated soluble tumor necrosis factor receptor type I in animal models of rheumatoid arthritis. *Arthritis Rheum.* 43, 2648-2659

Berge, A., Kihlberg, B.M., Sjöholm, A.G., Björck, L. (1997) Streptococcal protein H forms soluble complement-activating complexes with IgG, but inhibits complement activation by IgG-coated targets. *J. Biol. Chem.* **272**, 20774-20781

Beste, G., Schmidt, F.S., Stibora, T., Skerra, A. (1999) Small antibody-like proteins with prescribed ligand specificities derived from the lipocalin fold. *Proc. Natl. Acad. Sci. USA.* **96**, 1898-1903

Bhattacharya, A.A., Grüne, T., Curry, S. (2000) Crystallographic analysis reveals common modes of binding of medium and long-chain fatty acids to human serum albumin. *J. Mol. Biol.* **303**, 721-732

Binz, H.K., Amstutz, P., Kohl, A., Stumpp, M.T,, Briand, C., Forrer, P., Grütter, M.G., Plückthun, A. (2004) High-affinity binders selected from designed ankyrin repeat protein libraries. *Nat. Biotechnol.* **22**, 575-582

Björck, L. Kastern, W., Lindahl, G., Widebäck, K. (1987) Streptococcal protein G, expressed by streptococci or by *Escherichia coli*, has separate binding sites for human albumin and IgG. *Mol. Immunol.* **24**, 1113-1122

Boersma, Y.L., Plückthun, A. (2011) DARPins and other repeat protein scaffolds: advances in engineering and applications. *Curr. Opin. Biotechnol.* **22**, 849-857

Borghouts, C., Kunz, C., Groner, B. (2005) Peptide aptamers: recent developments for cancer therapy. *Expert. Opin. Biol. Ther.* **5**, 783-797

Brecher, M.E., Owen, H.G., Bandarenko, N. (1997) Alternatives to albumin: starch replacement for plasma exchange. *J. Clin. Apher*. **12**, 146-153

Brennan, F.M., Chantry, D., Jackson, A., Maini, R., Feldmann, M. (1989) Inhibitory effect of TNF alpha antibodies on synovial cell interleukin-1 production in rheumatoid arthritis. *Lancet*. **2**, 244-247

Butler, D.M., Malfait, A.M., Mason, L.J., Warden, P.J., Kollias, G., Maini, R.N., Feldmann, M., Brennan, F.M. (1997) DBA/1 mice expressing the human TNF-alpha transgene develop a severe, erosive arthritis: characterization of the cytokine cascade and cellular composition. *J. Immunol*. **159**, 2867-2876

Caporali, R., Pallavicini, F.B., Filippini, M., Gorla, R., Marchesoni, A., Favalli, E.G., Sarzi-Puttini, P., Atzeni, F., Montecucco, C. (2009) Treatment of rheumatoid arthritis with anti-TNF-alpha agents: a reappraisal. *Autoimmun. Rev*. **8**, 274-280

Chaudhury, C., Brooks, C.L., Carter, D.C., Robinson, J.M., Anderson, C.L. (2006) Albumin binding to FcRn: distinct from the FcRn-IgG interaction. *Biochemistry*. **45**, 4983-4990

Chen W., Zhu Z., Feng Y., Xiao X., Dimitrov D.S. (2008) Construction of a large phage displayed human antibody domain library with a scaffold based on a newly identified highly soluble, stable heavy chain variable domain. *J. Mol. Biol*. **382**, 779-789

Chen, W., Zhu, Z., Xiao, X., Dimitrov, D.S. (2009) Construction of a human antibody domain (VH) library. *Methods Mol. Biol*. **525**, 81-99

Chen, W., Zhu, Z., Feng, Y., Dimitrov, D.S. (2010) A large human domain antibody library combining heavy and light chain CDR3 diversity. *Mol. Immunol*. **47**, 912-921

Choy, E.H., Panayi, G.S. (2001) Cytokine pathways and joint inflammation in rheumatoid arthritis. *N. Engl. J. Med*. **344**, 907-916

Coppieters, K., Dreier, T., Silence, K., de Haard, H., Lauwereys, M., Casteels, P., Beirnaert, E., Jonckheere, H., Van de Wiele, C., Staelens, L., Hostens, J., Revets, H., Remaut, E., Elewaut, D., Rottiers, P. (2006) Formatted anti-tumor necrosis factor alpha VHH proteins derived from camelids show superior potency and targeting to inflamed joints in a murine model of collagen-induced arthritis. *Arthritis Rheum.* **54**, 1856-1866

Constantinou, A., Epenetos, A.A., Hreczuk-Hirst, D., Jain, S., Deonarain, M.P. (2008) Modulation of antibody pharmacokinetics by chemical polysialylation. *Bioconjug. Chem*. **19**, 643-650

Constantinou, A., Chen, C., Deonarain, M.P. (2010) Modulating the pharmacokinetics of therapeutic antibodies. *Biotechnol. Lett*. **32**, 609-622

Cortez-Retamozo, V., Lauwereys, M., Hassanzadeh Gh, G., Gobert, M., Conrath, K., Muyldermans, S., De Baetselier, P., Revets, H. (2002) Efficient tumor targeting by single-domain antibody fragments of camels. *Int. J. Cancer.* **98**, 456-462

Cortez-Retamozo, V., Backmann, N., Senter, P.D., Wernery, U., De Baetselier, P., Muyldermans, S., Revets, H. (2004) Efficient cancer therapy with a nanobody-based conjugate. *Cancer Res*. **64**, 2853-2857

Cramer, J.F., Nordberg, P.A., Hajdu, J., Lejon, S. (2007) Crystal structure of a bacterial-binding domain at 1.4 Å resolution. *FEB Letters*. **581**, 3178-3182

Cunningham, M.W. (2000) Pathogenesis of group A streptococcal infections. *Clin. Microbiol. Rev*. **13**, 470-511

de Château, M., Björck, L. (1994) Protein PAB, a mosaic albumin-binding bacterial protein representing the first contemporary example of module shuffling. *J. Biol. Chem*. **269,** 12147-12151

de Château, M., Björck, L. (1996) Identification of interdomain sequences promoting the intronless evolution of a bacterial protein family. *Proc. Natl. Acad. Sci. USA*. **93**, 8490-8495

de Château, M., Holst, E., Björck, L. (1996) Protein PAB, an albumin-binding bacterial surface protein promoting growth and virulence. *J. Biol. Chem*. **271**, 26609-26615

de Groot, A.S., Knopp, P.M., Martin, W. (2005) De-immunization of therapeutic proteins by T-cell epitope modification. *Dev. Biol.* **122**, 171-194

Deisenhofer, J. (1981) Crystallographic refinement and atomic models of a human Fc fragment and its complex with fragment B of protein A from *Staphylococcus aureus* at 2.9- and 2.8-A resolution. *Biochemistry* **20**, 2361-2370

Dennis, M.S., Lazarus, R.A. (1994) Kunitz domain inhibitors of tissue factor-factor VIIa. I. Potent inhibitors selected from libraries by phage display. *J. Biol. Chem*. **269**, 22129-22136

Dennis, M.S., Zhang, M., Meng, Y.G., Kadkhodayan, M., Kirchhofer, D., Combs, D., Damico L.A. (2002) Albumin binding as a general strategy for improving the pharmacokinetics of proteins. *J. Biol. Chem*. **277**, 35035-35043

Dennis, M.S., Jin, H., Dugger, D., Yang, R., McFarland, L., Ogasawara, A., Williams, S., Cole, M.J., Ross, S., Schwall, R. (2007) Imaging tumors with an albumin-binding Fab, a novel tumor-targeting agent. *Cancer Res.* **67**, 254-261

Derrick, J.P., Wigley, D.B. (1994) The third IgG-binding domain from streptococcal protein G. An analysis by X-ray crystallography of the structure alone and in a complex with Fab. *J. Mol. Biol*. **243**, 906-918

Dimitrov, D.S. (2009) Engineered CH2 domais (nanoantibodies). *mAbs*. **1**, 26-28

Dimitrov, D.S., Marks, J.D. (2009) Therapeutic antibodies: current state and future trends - is a paradigm change coming soon? *Methods Mol. Biol*. **525**, 1-27

Dumelin, C.E., Trüssel, S., Buller, F., Trachsel, E., Bootz, F., Zhang, Y., Mannocci, L., Beck, S.C., Drumea-Mirancea, M., Seeliger, M.W., Baltes, C., Müggler, T., Kranz, F., Rudin, M., Melkko, S., Scheuermann, J., Neri, D. (2008) A portable albumin binder from DNA-encoded chemical library. *Angew Chem. Int. Ed. Engl*. **47**, 3196-3201

Duncan, R. (2006) Polymer conjugates as anticancer nanomedicines. *Nat. Rev. Cancer*. **6**, 688-701

Elsadek, B., Kratz, F. (2012) Impact of albumin on drug delivery – new applications on the horizon. *J. Control Release*. **157**, 4-28

Falkenberg, C., Björck, L., Åkerström, B. (1992) Localization of the binding site for streptococcal protein G on human serum albumin. Identification of a 5.5-kilodalton protein G binding albumin fragment. *Biochemistry*. **31**, 1451-1457

Fanali, G., di Masi, A., Trezza, V., Marino, M., Fasano, M., Ascenzi, P. (2012) Human serum albumin: from bench to bedside. *Mol. Aspects Med.* **33**, 209-290

Fasano, M., Curry, S., Terreno, E., Galliano, M., Fanali, G., Narciso, P., Notari, S., Ascenzi, P. (2005) The extraordinary ligand binding properties of human serum albumin. *IUBMB Life*. **57**, 787-796

Feldmann, M. (2002) Development of anti-TNF therapy for rheumatoid arthritis. *Nat. Rev. Immunol*. **2**, 364-371

Feldwisch, J., Tolmachev, V. (2012) Engineering of affibody molecules for therapy and diagnostics. *Methods Mol. Biol*. **899**, 103-126

Ferrer, M., Maiolo, J., Kratz, P., Jackowski, J.L., Murphy, D.J., Delagrave, S., Inglese, J. (2005) Directed evolution of PDZ variants to generate high-affinity detection reagents. *Protein Eng. Des. Sel.* **18**, 165-173

Fishburn, C.S. (2008) The pharmacology of PEGylation: balancing PD with PK to generate novel therapeutics. *J. Pharm. Sci*. **97**, 4167-4183

Fischetti, V.A. (1989) Streptococcal M protein: molecular design and biological behavior. *Clin. Microbio. Rev*. **2**, 285-314

Flessner, M.F., Lofthouse, J., Zakaria, R. (1997) *In vivo* diffusion of immunoglobulin G in muscle: effects of binding, solute exclusion, and lymphatic removal. *Am. J. Physiol*. **273**, H2783-H2793

Frejd, F.Y. (2012) Half-life extension by binding to albumin through and albumin binding domain. In Kontermann, R.E. (ed). Therapeutic proteins: strategies to modulate theirs half-lives, Wiley-Blackwell, 2012, **14**, 269-283

Frenken, L.G., Hessing, J.G., Van den Hondel, C.A., Verrips, C.T. (1998) Recent advances in the large-scale production of antibody fragments using lower eukaryotic microorganisms. *Res. Immunol.* **149**, 589-599

Frenken, L.G., van der Linden, R.H., Hermans, P.W., Bos, J.W., Ruuls, R.C., de Geus, B., Verrips, C.T. (2000) Isolation of antigen specific llama VHH antibody fragments and their high level secretion by *Saccharomyces cerevisiae*. *J. Biotechnol*. **78**, 11-21

Frick, I.-M., ´kesson, P., Cooney, J., Sjöbring, U., Schmidt, K.-H., Gomi, H., Hattori, S., Tagawa, C., Kishimoto, F., Björck, L. (1994) Protein H – a surface protein of *Streptococcus pyogenes* with separate binding sites for IgG and albumin. *Mol. Microbiol*. **12**, 143-151

Frick, I.-M., Crossin, K.L., Edelman, G.M., Björck, L. (1995) Protein H – a bacterial surface protein with affinity for both immunoglobulin and fibronectin type III domains. *EMBO J.* **14**, 1674-1679

Frick, I.-M., Mörgelin, M., Björck, L. (2000) Virulent aggregates of *Streptococcus pyogenes* are generated by homophilic protein-protein interactions. *Mol. Microbiol.* **37**, 1232-1247

Frick, I.-M., ´kesson, P., Rasmussen, M., Schmidtchen, A., Björck, L. (2003) SIC, a secreted protein of *Streptococcus pyogenes* that inactivates antibacterial peptides. *J. Biol. Chem*. **278**, 16561-16566

Gaberc-Porekar, V., Zore, I., Podobnik, B., Menart, V. (2008) Obstacles and pitfalls in the PEGylation of therapeutic proteins. *Curr. Opin. Drug Discov. Devel*. **11**, 242-250

Gebauer, M., Skerra, A. (2009). Engineered protein scaffolds as next-generation antibody therapeutics. *Curr. Opin. Chem. Biol*. **13**, 245-255

Ghuman, J., Zunszain, P.A., Petitpas, I., Bhattacharya, A.A., Otagiri, M., Curry, S. (2005) Structural basis of the drug-binding specificity of human serum albumin. *J. Mol. Biol*. **353**, 38-52

Graille, M., Stura, E.A., Corper, A.L., Sutton, B.J., Taussig, M.J., Charbonnier, J.B., Silverman, G.J. (2000) Crystal structure of a *Staphylococcus aureus* protein A domain complexed with the Fab fragment of a human IgM antibody: structural basis for recognition of B-cell receptors and superantigen activity. *Proc. Natl. Acad. Sci. USA*. **97**, 5399-5404

Graille, M., Harrison, S., Crump, M.P., Findlow, S.C., Housden, N.G., Muller, B.H., Battail-Poirot, N., Sibaï, G., Sutton, B.J., Taussig, M.J., Jolivet-Reynaud, C., Gore, M.G., Stura, E.A. (2002) Evidence for plasticity and structural mimicry at the immunoglobulin light chain-protein L interface. *J. Biol. Chem*. **277**, 47500-47506

Gregoriadis, G., Fernandes, A., Mital, M., McCormack, B. (2000) Polysialic acids: potential in improving the stability and pharmacokinetics of proteins and other therapeutics. *Cell. Mol. Life Sci*. **57**, 1964-1969

Gregoriadis, G., Jain, S., Papaioannou, I., Laing, P. (2005) Improving the therapeutic efficacy of peptides and proteins: a role for polysialic acids. *Int. J. Pharm*. **300**, 125-130

Grönwall, C., Ståhl, S. (2009) Engineered affinity proteins - generation and applications. *J. Biotechnol*. **140**, 254-269

Gülich, S., Linhult, M., Nygren, P.Å. Uhlén, M, Hober, S. (2000) Stability towards alkaline conditions can be engineered into a protein ligand. *J. Biotechnol*. **80**, 169-178

Gupta, D., Lis, C.G. (2010) Pretreatment serum albumin as a predictor of cancer survival: a systematic review of the epidemiological literature. *Nutr. J*. **9**, 69-85

Guss, B., Eliasson, M., Olsson, A. Uhlén, M., Frej, A.-K., Jörnvall, H., Flock, J.-I., Lindberg, M. (1986) Structure of the IgG-binding regions of streptococcal protein G. *EMBO J*. **5**, 1567-1575

Hamidi, M., Azadi, A., Rafiei, P. (2006) Pharmacokinetic consequences of pegylation. *Drug Deliv*. **13**, 399-409

Haraldsoon, B., Sörensson, J. (2004) Why do we not all have proteinuria? An update of our current understanding of the glomerular barrier. *News Physiol. Sci*. **19**, 7-10

Harris, J.M., Chess, R.B. (2003) Effect of PEGylation on pharmaceuticals. *Nat. Rev. Drug Discov*. **2**, 214-221

Hartung, A., Bendas, G. (2012) Half-life extension with pharmaceutical formulations: liposomes. In Kontermann, R.E. (ed). Therapeutic proteins: strategies to modulate theirs half-lives, Wiley-Blackwell, 2012, **16**, 299-314

Hey, T., Knoller, H., Vorstheim, P. (2012) Half-life estension through HESylation. In Kontermann, R.E. (ed). Therapeutic proteins: strategies to modulate theirs half-lives, Wiley-Blackwell, 2012, **7**, 117-140

Högbom, M., Eklund, M., Nygren, P.A., Nordlund, P. (2003) Structural basis for recognition by an in vitro evolved affibody. *Proc. Natl. Acad. Sci. USA*. **100**, 3191-3196

Holliger, P., Hudson, P.J. (2005) Engineering antibody fragments and the rise of single domains. *Nat. Biotechnol*. **23**, 1126-1136

Holt, L.J., Herring, C., Jerpers, L.S., Woolven, B.P., Tomlinson, I.M. (2003) Domain antibodies: proteins for therapy. *Trends Biotechnol*. **21**, 484-490

Holt, L.J., Basran, A., Jones, K., Chorlton, J., Jespers, L.S., Brewis, N.D., Tomlinson, I.M. (2008) Anti-serum albumin domain antibodies for extending the half-lives of short lived drugs. *Protein Eng. Des. Sel*. **21**, 283-288

Honegger, A. (2008) Engineering antibodies for stability and efficient folding. In Chernajovsky Y, Nissim A (eds).Therapeutic Antibodies. Handbook of Experimental Pharmacology, Springer-Verlag Berlin Heidelberg, 2008, **181**, 47-68

Hopp, J., Hornig, N., Zettlitz, K.A., Schwarz, A., Fuss, N., Müller, D., Kontermann, R.E. (2010) The effects of affinity and valency of an albumin-binding domain (ABD) on the half-life of a single-chain diabody-ABD fusion protein. *Protein Eng. Des. Sel.* **23**, 827-834

Hudson, P.J., Souriau, C. (2003) Engineered antibodies. *Nat. Medicine*. **9**, 129-134

Hutt, M., Färber-Schwarz, A., Unverdorben, F., Richter, F., Kontermann, R.E. (2011) Plasma half-life extension of small recombinant antibodies by fusion to immunoglobulin-binding domains. *J. Biol. Chem.* **287**, 4462-4469

Jefferis, R. (2005) Glycosylation of recombinant antibody therapeutics. *Biotechnol. Prog*. **21**, 11-16

Jevsevar, S., Kunstelj, M., Porekar, V.G. (2010) PEGylation of therapeutic proteins. *Biotechnol. J.* **5**, 113-128

Ji, Y., Carlson, B., Kondagunta, A., Cleary, P., (1997) Intranasal immunization with C5a peptidase prevents nasopharyngeal colonization of mice by the group A Streptococcus. *Infect. Immun*. **65**, 2080-2087

Johannson, M.U., de Château, M., Björck, L., Forsén, S., Drakenberg, T., Wikström, M. (1995) The GA module, a mobile albumin-binding bacterial domain, adopts a three-helix-bundle structure. *FEBS Letters*. **374**, 257-261

Johannson, M.U., de Château, M., Wikström, M., Forsén, S., Drakenberg, T., Björck, L. (1997) Solution structure of the albumin-binding GA module: a versatile bacterial protein domain. *J. Mol. Biol.* **266**, 859-865

Johannson, M.U., Frick, I.-M., Nilsson, H., Kraulis, P.J., Hober, S., Jonasson, O., Linhult, M., Nygren, P.A., Uhlén, M., Björck, L. (2002) Structure, specificity, and mode of interaction for bacterial albumin-binding modules. *J. Biol. Chem*. **277**, 8114-8120

Jonsson, H., Frykerg, L., Rantamäki, L., Guss, B. (1994) MAG, a novel plasma protein receptor from *Streptococcus dysgalactiae*. *Gene*. **143**, 85-89

Jonsson, H., Müller, H.-P. (1994) The type III Fc receptor from *Streptococcus dysgalactiae* is also an α_2-macroglobulin receptor. *Eur. J. Biochem*. **220**, 819-826

Jonsson, H., Burtsoff-Asp, C., Guss, B^a. (1995) Streptococcal protein MAG – a protein with broad albumin binding specificity. *Biochim. Biophys. Acta* **1249**, 65-71

Jonsson, H., Lindmark, H., Guss, B^b. (1995) A Protein G-related cell surface protein in *Streptococcus zooepidemicus*. *Infect. Immun.* **63**, 2968-2975

Jonsson, A., Dogan, J., Herne, N., Abrahmsén, L., Nygren, P.A. (2008) Engineering of a femtomolar affinity binding protein to human serum albumin. *Protein Eng. Des. Sel*. **21**, 515-527

Jonsson, A., Wållberg, H., Herne, N., Ståhl, S., Frejd, F.Y. (2009) Generation of tumour-necrosis-factor-alpha-specific affibody molecules capable of blocking receptor binding in vitro. *Biotechnol. Appl. Biochem*. **54**, 93-103

Kenanova, V., Olafsen, T., Crow, D.M., Sundaresan, G., Subbarayan, M., Carter, N.H., Ikle, D.N., Yazaki, P.J., Chatziioannou, A.F., Gambir, S.S., Williams, L.E., Shively, J.E., Colcher, D., Raubitschek, A.A., Wu, A.M. (2005) Tailoring the pharmacokinetics and positron emission tomography imaging properties of anti-carcinoembryonic antigen single-chain Fv-Fc antibody fragments. *Cancer Res.* **65**, 622-631

Kihlberg, B.M., Collin, M., Olsén, A., Björck, L. (1999) Protein H, an antiphagocytic surface protein in *Streptococcus pyogenes*. *Infect. Immun*. **67**, 1708-1714

Kim, J. (2012) The biology of the neonatal Fc receptor (FcRn). In Kontermann, R.E. (ed). Therapeutic proteins: strategies to modulate theirs half-lives, Wiley-Blackwell, 2012, **8**, 143-155

Klareskog, L., McDevitt, H. (1999) Rheumatoid arthritis and its animal models: the role of TNF-alpha and the possible absence of specific immune reactions. *Curr. Opin. Immunol*. **11**, 657-662

Klooster, R., Maassen, B.T.H., Stam, J.C., Hermans, P.W., ten Haaft, M.R., Detmers, F.J.M., de Haard, H.J., Post, J.A., Verrips, C.T. (2007) Improved anti-IgG and HSA affinity ligans: clinical application of VHH antibody technology. *J. Immunol. Methods*. **324**, 1-12

Knight, D.M., Trinh, H., Le, J., Siegel, S., Shealy, D., McDonough, M., Scallon, B., Moore, M.A., Vilcek, J., Daddona, P.,Ghrayed, J. (1993) Construction and initial characterization of a mouse-human chimeric anti-TNF antibody. *Mol. Immunol*. **30**, 1443-1453

Knop, K., Hoogenboom, R., Fischer, D., Schubert, U.S. (2010) Poly(ethylene glycol) in drug delivery: pros and cons as well as potential alternatives. *Angew. Chem. Int. Ed. Engl*. **49**, 6288-6308

Koide, A., Bailey, C.W., Huang, X., Koide, S. (1998) The fibronectin type III domain as a scaffold for novel binding proteins. *J. Mol. Biol*. **284**, 1141-1151

Kolmar, H., Skerra, A. (2008) Alternative binding proteins get mature: rivalling antibodies. *FEBS J*. **275**, 2667

König, T., Skerra, A. (1998) Use of an albumin-binding domain for the selective immobilization of recombinant capture antibody fragments on ELISA plates. *J. Immunol. Methods*. **218**, 73-83

Kontermann, R.E. (2009) Strategies to extend plasma half-lives of recombinant antibodies. *Biodrugs*. **23**, 93-109

Kontermann, R.E. (2011) Strategies to extended serum half-lives of protein therapeutic. *Curr. Opin. Biotechnol*. **22**, 868-876

Kontermann, R.E. (2012) Half-life modulating strategies – an introduction. In Kontermann, R.E. (ed). Therapeutic proteins: strategies to modulate theirs half-lives, Wiley-Blackwell, 2012, **1**, 3-21

Kragh-Hansen, U., Chuang, V.T.G., Otagiri, M. (2002) Pratical Aspects of the ligand-binding and enzymatic properties of human serum albumin. *Biol. Pharm. Bull*. **25**, 695-704

Kratz, F. (2008) Albumin as a drug carrier: design of prodrugs, drug conjugates and nanoparticules. *J. Control Release*. **132**, 171-183

Kratz, F., Elsadek, B. (2012) Clinical impact of serum proteins on drug delivery. *J. Control Release*. **61**, 429-445

Kraulis, P.J., Jonasson, P., Nygren, P.A., Uhlén, M., Jendeberg, L., Nilsson, B., Kördel, J. (1996) The serum albumin-binding domain of streptococcal protein G is a three-helix bundle: a heteronuclear NMR study. *FEBS Lett*. **378**, 190-194

Kronvall, G., Simmons, A., Myhre, E.B., Jonsson, S. (1979) Specific absorption of human serum albumin, immunoglobulin A, and immunoglobulin G with selected strains of group A and G streptococci. *Infect. Immun*. **25**, 1-10

Landfester, K., Musyanovych, A., Mailänder, V. (2012) Half-life extension with pharmaceutical formulations: nanoparticles by the miniemulsion process. In Kontermann, R.E. (ed). Therapeutic proteins: strategies to modulate theirs half-lives, Wiley-Blackwell, 2012, **17**, 315-339

Larson, R.A., Boogaerts, M., Estey, E., Karanes, C., Stadtmauer, E.A., Sievers, E.L., Mineur, P., Bennett, J.M., Berger, M.S., Eten, C.B., Munteanu, M., Loken, M.R., Van Dongen, J.J., Bernstein, I.D., Appelbaum, F.R. (2002) Antibody-targeted chemotherapy of older patients with acute myeloid leukemia in first relapse using Mylotarg (gemtuzumab ozogamicin). *Leukemia*. **16**, 1627-1636

Lejon, S., Frick, I.-M., Björck, L., Wikström, M., Svensson, S. (2004) Crystal structure and biological implications of a bacterial albumin binding module in complex with human serum albumin. *J. Biol. Chem*. **279**, 42924-42928

Lejon, S., Cramer, J.F., Nordberg, P. (2008) Structural basis for the binding of naproxen to human serum albumin in the presence of fatty acids and the GA module. *Acta Crystallogr. Sect. F Struct. Biol. Cryst. Commun*. **64**, 64-69

Lencer, W.I., Blumberg, R.S. (2005) A passionate kiss, then run: exocytosis and recycling of IgG by FcRn. *Trends Cell Biol*. **15**, 5-9

Li, H., d'Anjou, M. (2009) Pharmacological significance of glycosylation in therapeutic proteins. *Curr. Opin. Biotechnol*. **20**, 678-684

Linhult, M., Binz, H.K., Uhlén, M., Hober, S. (2002) Mutational analysis of the interaction between albumin-binding domain from streptococcal protein G and human serum albumin. *Protein Sci*. **11**, 206-213

Lobo, E.D., Hansen, R.J., Balthasar, J.P. (2004) Antibody pharmacokinetics and pharmacodynamics. *J. Pharm. Sci*. **93**, 2645-2668

Löfblom, J., Feldwisch, J., Tolmachev, V., Carlsson, J., Ståhl, S., Frejd, F.Y. (2010) Affibody molecules: engineered proteins for therapeutic, diagnostic and biotechnological applications. *FEBS Lett*. **584**, 2670-2680

Lundberg, E., Höidén-Guthenberg, I., Larsson, B., Uhlén, M., Gräslund, T. (2007). Site-specifically conjugated anti-HER2 Affibody molecules as one-step reagents for target expression analyses on cells and xenograft samples. *J. Immunol. Methods*. **319**, 53–63

Macklis, R.M. (2006) Iodine-131 tositumomab (Bexxar) in a radiation oncology environment. *Int. J. Radiat. Oncol. Biol. Phys*. **66**, S30-34

Mahmood, I., Green, M.D. (2005) Pharmacokinetic considerations in the development of therapeutic proteins. *Clin. Pharmacokinet*. **44**, 331-347

Mahmood, I. (2009) Methods to determine pharmacokinetic profiles of therapeutic proteins. *DDTEC*. **209**, e1-e5

Mamo, W., Fröman, G., Sundäs, A., Wadström, T. (1987) Binding of fibronectin, fibrinogen and Type II collagen to streptococci isolated from bovine mastitis. *Microb. Pathog*. **2**, 417-424

Mamo, W., Jonsson, P., Flock, J.-I., Lindberg, M., Müller, H.-P., Wadström, T., Nelson, L. (1994) Vaccination against *Staphylococcus aureus* mastitis: immunological response of mice vaccinated with fibronectin-binding proten (FnBP-A) to challenge with *S. aureus*. *Vaccine*. **12**, 988-992

Martin, W.L., West, A.P. Jr, Gan, L., Bjorkman, P.J. (2001) Crystal structure of 2.8 ´ of an FcRn/heterodimeric Fc complex: mechanism of pH-dependent binding. *Mol. Cell*. **7**, 867-877

Mazor, Y., Noy, R., Wels, W.S., Benhar, I. (2007) chFRP5-ZZ-PE38, a large IgG-toxin immunoconjugate outperforms the corresponding smaller FRP5(Fv)-ETA immunotoxin in eradicating ErbB2-expressing tumor xenografts. *Cancer Lett*. **257**, 124-135

McMillan, D.C., Watson, W.S., O'Gorman, P., Preston, T., Scott, H.R., McArdle, C.S. (2001) Albumin concentrations are primarily determined by the body cell mass and the systemic inflammatory response in cancer patients with weight loss. *Nutr. Cancer*. **39**, 210-213

Meibohm, B. (2012) Pharmacokinetics and half-life of protein therapeutics. In Kontermann, R.E. (ed). Therapeutic proteins: strategies to modulate theirs half-lives, Wiley-Blackwell, 2012, **2**, 23-38

Melmed, G.Y., Targan, S.R., Yasothan, U., Hanicq, D., Kirkpatrick, P. (2008) Certolizumab pegol. *Nat. Rev. Drug Discov*. **7**, 641-642

Müller, D., Karle, A., Meissburger, B., Höfig, I., Stork, R., Kontermann, R.E. (2007) Improved pharmacokinetics of recombinant bispecific antibody molecules by fusion to human serum albumin. *J. Biol. Chem*. **282**, 12650-12660

Müller, D., Kontermann, R.E. (2007) Recombinant bispecific antibodies for cellular cancer immunotherapy. *Curr. Opin. Mol. Ther*. **9**, 319-326

Müller, H.-P., Blobel, H. (1985) Binding of human alpha-2-macroglobulin to streptococci of group A, B, C and G. In Kimura Y., Kotami S., Shiokawa S. (ed.), Recent advances in streptococci and streptococcal diseases. Reedbooks, Chertsey, England, 1985, 96-97

Müssener, A., Litton, M.J., Lindroos, E., Klareskog, L. (1997) Cytokine production in synovial tissue of mice with collagen-induced arthritis (CIA). *Clin. Exp. Immunol*. **107**, 485-493

Murphy, J.P., Duggleby, C.J., Atkinson, M.A., Trowern, A.R., Atkinson, T., Goward, C.R. (1994) The functional units of a peptostreptococcal protein L. *Mol Microbiol*. **12**, 911-920

Muyldermans, S. (2013) Nanobodies: natural single-domain antibodies. *Annu. Rev. Biochem*. **82**, 775-797

Myhre, E.B., Kronvall, G. (1980) Demonstration of a new type of immunoglobulin G receptor in *Streptococcus zooepidemicus* strains. *Infect. Immun*. **27**, 808-816

Nagata, S., Pastan, I. (2009) Removal of B cell epitopes as a practical approach for reducing the immunogenicity of foreign protein-based therapeutics. *Adv. Drug. Deliv. Rev*. **61**, 977-985

Nilsson, J., Ståhl, S., Lundeberg, J., Uhlén, M, Nygren, P.Å. (1997) Affinity fusion strategies for detection, purification, and immobilization of recombinant proteins. *Protein Expr. Purif*. **11**, 1-16

Nilsson, F.Y, Tolmachev, V. (2007) Affibody molecules: new protein domains for molecular imaging and targeted tumor therapy. *Curr. Opin. Drug Discov. Develop.* **10**, 167-175

Nilsson, M., Wasylik, S., Mörgelin, M., Olin, A.I., Meijers, J.C.M., Derksen, R.H., Groot, P.G., Herwald, H. (2008) The antibacterial activity of peptides derived from human beta-2 glycoprotein I is inhibited by protein H and M1 protein from *Streptococcus pyogenes*. *Mol. Microbiol*. **67**, 482-492

Nilvebrant, J., Alm, T., Hober, S., Löfblom, J. (2011) Engineering bispecific into a single albumin binding domain. *PLoS One* **6**, e25791

Nilvebrant, J., Hober, S. (2013) The albumin-binding domain as a scaffold for protein engineering. *Comput. Struct. Biotechnol. J.* **6**, e201303009

Niwa, Y., Iio, A., Niwa, G., Sakane, T., Tsunematsu, T., Kanoh, T. (1990) Serum albumin metabolism in rheumatic diseases: relationship to corticosteroids and peptic ulcer. *J. Clin. Lab. Immunol*. **31**, 11-16

Nord, K., Gunneriusson, E., Ringdahl, J., Ståhl, S., Uhlén, M., Nygren, P.Å. (1997) Binding proteins selected from combinatorial libraries of an alpha-helical bacterial receptor domain. *Nat. Biotechnol*. **15**, 772-777

Nord, K., Nord, O., Uhlén, M., Kelley, B., Ljungqvist, C., Nygren, P.Å. (2001) Recombinant human factor VIII-specific affinity ligands selected from phage-displayed combinatorial libraries of protein A. *Eur. J. Biochem.* **268**, 1-10

Nygren, P.Å., Eliasson, M., Abrahmsén, L., Uhlén, M., Palmcrantz, E. (1988) Analysis and use of the serum albumin binding domains of streptococcal protein G. *J. Mol. Recognit*. **1**, 69-74

Nygren, P.Å., Ljungquist, C., Trømborg, H., Nustad, K., Uhlén, M. (1990) Species-dependent binding of serum albumin binding domains of streptococcal protein G. *Eur. J. Biochem.* **193**, 143-148

Nygren, P.Å., Uhlén, M., Flodby, P., Andersson, R., Wigzell, H. (1991) *In vivo* stabilization of human recombinant CD4 derivate by fusion to a serum-albumin-binding receptor. In Vaccines 91 (Chanock, R. M., Ginsberg, H. S., Brown, F., Lerner, R. A. eds) Cold Spring Harbor Laboratory Press, Cold Spring Harbor, NY, Laboratory Press, Cold Spring Harbor, NY, 63-368

O'Dell, J. (2004) Therapeutic strategies for rheumatoid arthritis. *N. Engl. J. Med*. **350**, 2591-2602

Olsson, A., Eliasson, M., Guss, B., Nilsson B., Hellman U., Lindberg M., Uhlén M. (1990) Structure and evolution of the repetitive gene encoding streptococcal protein G. *Eur. J. Biochem*. **168**, 319-324

Orlova, A., Magnusson, M., Eriksson, T.L., Nilsson, M., Larsson, B., Höidén-Guthenberg, I., Widström, C., Carlsson, J., Tolmachev, V., Ståhl, S., Nilsson, F.Y. (2006) Tumor imaging using a picomolar affinity HER2 binding affibody molecule. *Cancer Res.* **66**, 4339-4348

Patti, J.M., Bremell, T., Krajewska-Pietrasik, D., Abdelnour, A., Tarkowski, A., Rydén, C., Höök, M. (1994) The *Staphylococcus aureus* collagen adhesion is a virulence determinant in experimental septic arthritis. *Infect. Immun*. **62**, 152-161

Peer, D., Karp, J.M., Hong, S., Farokhzad, O.C., Margalit, R., Langer, R. (2007) Nanocarriers as an emerging platform for cancer therapy. *Nat. Nanotechnol*. **2**, 751-760

Peters, T. Jr. (1985) Serum albumin. *Adv. Protein Chem*. **37**, 161-245

Peters, T. Jr (1996) All about albumin, biochemistry, genetics, and medical applications. Academic Press, California, 432pp

Pisal, D.S., Kosloski, M.P., Balu-Iyer, S.V. (2010) Delivery of therapeutic proteins. *J. Pharm. Sci*. **99**, 2557-2575

Podbielski, A. (1993) Three different types of organization of vir regulon in group A streptococci. *Mol. Gen. Genet*. **237**, 287-300

Reddy, S.T., Berk, D.A., Jain, R.K., Swarts, M.A. (2006) A sensitive *in vivo* model for quantifying interstitial convective transport to injected macromolecules and nanoparticules. *J. Appl. Physiol*. **101**, 1162-1169

Renberg, B., Nordin, J., Merca, A., Uhlén, M., Feldwisch, J., Nygren, P.-A. Karlström, A.E- (2007) Affibody molecules in protein capture microarrays: evaluation of multidomain ligands and different detection formats. *J. Proteome Res*. **6**, 171-179

Retnoningrum, D.S., Cleary, P.P. (1994) M12 protein from *Streptococcus pyogenes* is a receptor for immunoglobulin G3 and human albumin. *Infect. Immun*. **62**, 2387-2394

Robinson, M.K., Doss, M., Shaller, C., Narayanan, D., Marks, J.D., Adler, L.P., González Trotter, D.E., Adams, G.P. (2005) Quantitative immuno-positron emission tomography imaging of HER2-positive tumor xenografts with an iodine-124 labeled anti-HER2 diabody. *Cancer Res*. **65**, 1471-1478

Rodewald, R., Karnovsky, M.J. (1974) Porous structures of the glomerular slit diaphragm in the rat and mouse. *J. Cell Biol*. **60**, 423-433

Roopenian D.C., Akilesh S. (2007) FcRn: the neonatal Fc receptor comes of age. *Nat. Rev. Immunol*. **7**, 715-725

Roovers R.C., Laeremans T., Huang L., De Taeye S., Verkleij A.J., Revets H., de Haard H.J., van Bergen en Henegouven P.M. (2007) Efficient inhibition of EGFR signalling and of tumor growth by antagonistic anti –EFGR Nanobodies. *Cancer Immunol. Immuther*. **56**, 303-317

Ropes, M.W., Bennett, G.A., Cobb, S., Jacox, R., Jessar, R.A. (1959) 1958 revision of diagnostic criteria for rheumatoid arthritis. *Arthritis Rheum*. **2**, 16-20

Rutgeerts P., Schreiber S., Feagan B., Keininger D.L., O'Neil L., Fedorak R.N. (2008) Certolizumab pegol, a monthly subcutaneously administered Fc-free anti-TNFα, improves health-related quality of life in patients with moderate to severe Crohn's disease. *Int. J. Colorectal Dis*. **23**, 289-296

Saerens, D., Ghassabeh, G.H., Muyldermans, S. (2008) Single-domain antibodies as building blocks for novel therapeutics. *Curr. Opin. Pharmacol*. **8**, 600-608

Sánchez, L.M., Penny, D.M., Bjorkman, P.J. (1999) Stoichiometry of the interaction between the major histocompatibility complex-related Fc receptor and its Fc ligand. *Biochemistry*. **38**, 9471-9476

Sandin, C., Carlsson, F., Lindahl, G. (2006) Binding of human plasma proteins to *Streptococcus pyogenes* M protein determines the location of opsonic and non-opsonic epitopes. *Mol. Microbiol*. **59**, 20-30

Saxne, T., Palladino, M.A. Jr, Heinegård, D., Talal, N., Wollheim, F.A. (1988) Detection of tumor necrosis factor alpha but not tumor necrosis factor beta in rheumatoid arthritis synovial fluid and serum. *Arthritis Rheum*. **31**, 1041-1045

Schellenberger, V., Wang, C.-W., Geething, N.C., Spink, B.J., Campbell, A., To, W., Scholle, M.D., Yin, Y., Yao, Y., Bogin, O., Cleland, J.L., Silverman, J., Stemmer, W.P. (2009) A recombinant polypeptide extends the in vivo half-life of peptides and proteins in a tunable manner. *Nat. Biotechnol*. **27**, 1186-1190

Schlapschy, M., Thoebald, I., Mack, H., Schottelius, M., Wester, H.J., Skerra, A. (2007) Fusion of a recombinant antibody fragment with a homo-amino-acid polymer: effects on biophysical properties and prolonged plasma half-life. *Protein Eng. Des. Sel*. **20**, 273-284

Schmidt, M.M., Townson, S.A., Andreucci, A.J., King, B.M., Schirmer, E.B., Murillo, A.J., Dombrowski, C., Tisdale, A.W., Lowden, P.A., Masci, A.L., Kovalchin, J.T., Erbe, D.V., Wittrup, K.D., Furfine, E.S., Barnes, T.M. (2013) Crystal structure of an HSA/FcRn complex reveals recycling by competitive mimicry of HSA ligands at a pH-dependent hydrophobic interface. *Structure*. **21**, 1966-1978

Schneider, S., Buchert, M., Georgiev, O., Catimel, B., Halford, M., Stacker, S.A., Baechi, T., Moelling, K., Hovens, C.M. (1999) Mutagenesis and selection of PDZ domains that bind new protein targets. *Nat. Biotechnol*. **17**, 170-175

Schotellius, A.G.J., Moldawer, L.L., Dinarello, C.A., Asadullah, K., Sterry, W., Edwards, C.K. (2004) Biology of tumor necrosis factor-alpha implications for psoriasis. *Exp. Dermatol*. **13**, 193-222

Schulte, S. (2009) Half-life extension through albumin fusion technologies. *Thromb. Res*. **124 Suppl 2**, S6-8

Scott, D.L., Kingsley, G.H. (2006) Tumor necrosis factor inhibitors for rheumatoid arthritis. *N. Engl. J. Med*. **355**, 704-712

Scott, D.L., Wolfe, F., Huizinga, T.W. (2010) Rheumatoid arthritis. *Lancet*. **376**, 1094-1108

Silence, K. Lauwereys, M., Hans de, H. (2007) Single-domain antibodies directed against tumor necrosis factor-alpha and uses therefore. United States Patent Application Publication, US 2007/0077249 A1, 101pp

Silverman, J., Liu, Q., Bakker, A., To, W., Duguay, A., Alba, B.M., Smith, R., Rivas, A., Li, P., Le, H., Whitehorn, E., Moore, K.W., Swimmer, C., Perlroth, V., Vogt, M., Kolkman, J., Stemmer, W.P. (2005) Multivalent avimer proteins evolved by exon shuffling of a family of human receptor domains. *Nat. Biotechnol*. **23**, 1556-1561

Sinclair, A.M., Elliott, S. (2005) Glycoengineering; the effect of glycosylation on the properties of therapeutic proteins. *J. Pharm. Sci*. **94**, 1626-1635

Sjöbring, U., Falkenberg, C., Nielsen, E., Åkerström, B., Björck, L. (1988) Isolation of a 14-kDa albumin-binding fragment of streptococcal protein G. *J. Immunol*. **140**, 1595-1599

Sjöbring, U., Björck, L., Kastern, W. (1989) Protein G genes: structure and distribution of IgG-binding and albumin-binding domains. *Mol. Microbiol*. **3**, 319-327

Sjöbring, U., Björck, L., Kastern, W. (1991) Streptococcal protein G. Gene Structure and protein binding properties. *J. Biol. Chem*. **266**, 399-405

Sjöbring, U. (1992) Isolation and molecular characterization of a novel albumin-binding protein from group G streptococci. *Infect. Immun*. **60**, 3601-3608

Sjölander, A., Nygren, P.-Å., Ståhl, S., Berzins, K., Uhlén, M., Perlmann, P., Andersson, R. (1997) The serum albumin-binding region of streptococcal protein G: a bacterial fusion partner with carrier-related properties. *J. Immunol. Methods*. **201**, 115-123

Skerra, A. (2007) Alternative non-antibody scaffolds for molecular recognition. *Curr. Opin. Biotechnol.* **18**, 295-304

Sleep, D., Cameron, J. Evans, L.R. (2013) Albumin as a versatile platform for drug half-life extension. *Biochim. Biophys. Acta.* **1830**, 5526-5534

Smith, T.C., Sledjeski, D.D., Boyle, M.D. (2003) *Streptococcus pyogenes* infection in mouse skin leads to a time-dependent up-regulation of protein H expression. *Infect. Immun.* **71**, 6079-6082

Solá R.J., Griebenow K. (2010) Glycosylation of therapeutic proteins: an effective strategy to optimize efficacy. *BioDrugs.* **24**, 9-21

Stevens, D.K., Eyre, R.J., Bull, R.J. (1992) Adduction of hemoglobin and albumin *in vivo* by metabolites of trichloroethylene, trichloroacetate, and dichloroacetate in rats and mice. *Fundam. Appl. Toxicol.* **19**, 336-342

Storey, G.O., Comer, M., Scoot, D.L. (1994) Chronic arthritis before 1876: early British cases suggesting rheumatoid arthritis. *Ann. Rheum. Dis.* **53**, 557-560

Stork, R., Zettlitz, K.A., Müller, D., Rether, M., Hanisch, F.G., Kontermann, R.E. (2008) N-glycosylation as novel strategy to improve pharmacokinetic properties of bispecific single-chain diabodies. *J. Biol. Chem.* **283**, 7804-7812

Stork, R., Campigna, E., Robert, B., Müller, D., Kontermann, R.E. (2009) Biodistribution of a bispecific single-chain diabody and its half-life extended derivates. *J. Biol. Chem.* **284**, 25612-25619

Stretsov, V., Nuttal, S. (2005) Do sharks have a new antibody lineage? *Immunol. Lett.* **97**, 159-160

Stumpp, M.T., Binz, H.K., Amstutz, P. (2008) DARPins: a new generation of protein therapeutics. *Drug Discov. Today.* **13**, 695-701

Sun, L.C., Chu, K.S., Cheng, S.C., Lu, C.Y., Kuo, C.H., Hsieh, J.S., Shih, Y.L,, Chang, S.J., Wang, J.Y. (2009) Preoperative serum carcinoembryonic antigen, albumin and age are supplementary to UICC staging systems in predicting survival for colorectal cancer patients undergoing surgical treatment. *BMC Cancer.* **9**, 288

Sugio, S., Kashima. A., Mochizuki, S., Noda, M., Kobayashi, K. (1999) Crystal structure of human serum albumin at 2.5 A resolution. *Protein Eng.* **12**, 439-446

Talay, S.R., Grammel, M.P., Chhatwal, G.S. (1996) Structure of a group C streptococcal protein that binds to fibrinogen, albumin and immunoglobulin G via overlapping modules. *Biochem. J.* **315**, 577-582

Tang, L., Persky, A.M., Hochhaus, G., Meibohm, B. (2004) Pharmacokinetic aspects of biotechnology products. *J. Pharm. Sci.* **93**, 2184-2204

Tashiro, M., Montelione, G. (1995) Structures of bacterial immunoglobulin-binding domains and their complexes with immunoglobulins. *Curr. Biol.* **5**, 471-481

Ternant, D., Paintaud, G. (2005) Pharmacokinetics and concentration-effect relationships for therapeutic monoclonal antibodies and fusion proteins. *Expert Opin. Biol. Ther.* **5 Suppl. 1**, S37-47

Tijink, B.M., Laeremans, T., Budde, M., Stigter-van Walsun, M., Dreier, T., de Haard, H.J., Leemans, C.R., van Dongen, G.A. (2008) Improved tumor targeting of anti-epidermal growth factor receptor Nanobodies through albumin binding: taking advantage of modular Nanobody technology. *Mol. Cancer Ther.* **7**, 2288-2297

Tolmachev, V., Orlova, A., Pehrson, R., Galli, J., Baastrup, B., Andersson, K., Sandström, M., Rosik, D., Carlsson, J., Lundqvist, H., Wennborg, A., Nilsson, F.Y. (2007) Radionuclide therapy of HER2-positive microxenografts using a 177Lu-labeled HER2-specific Affibody molecule. *Cancer Res.* **67**, 2773-2782

Tracey, D., Klareskog, L., Sasso, E.H., Salfeld, J.G., Tak, P.P. (2008) Tumor necrosis factor antagonist mechanisms of action: a comprehensive review. *Pharmacol. Ther.* **117**, 244-279

Tryggvason, K., Wartiovaara, J. (2005) How does the kidney filter plasma? *Physiology*. **20**, 96-101

Unverdorben, F., Färber-Schwarz, A., Richter, F., Hutt, M., Kontermann, R.E. (2012) Half-life extension of a single-chain diabody by fusion to domain B of staphylococcal protein A. *Protein Eng. Des. Sel.* **25**, 81-88

Valentin-Weigand, P., Traore, M.Y., Blobel, H., Chhatwal, G.S. (1990) Role of α_2-macroglobulin in phagocytosis of group A and C streptococci. *FEMS Microbiol. Lett.* **70**, 321-324

van de Weert, M., Jorgensen, L., Moeller, E.H., Frokjaer, S. (2005) Factors of importance for successful delivery system for proteins. *Expert Opin. Drug Deliv*. **2**, 1029-1037

Veronese, F.M., Mero, A. (2008) The impact of PEGylation on biological therapies. *Biodrugs.* **22**, 315-329

Vose, J.M., Bierman, P.J., Loberiza Jr., F.J., Bociek, R.G., Matso, D., Armitage, J.O. (2007) Phase I trial of (90)Y-ibritumomab tiuxetan in patients with relapsed B-cell non-Hodgkin's lymphoma following high-dose chemotherapy and autologous stem cell transplantation. *Leuk. Lymphoma*. **48**, 683-690

Walker, A., Dunlevy, G., Rycroft, D., Topley, P., Holt, L.J., Herbert, T., Davies, M., Cook, F., Holmes, S., Jespers, L., Herring, C. (2010) Anti-serum albumin domain antibodies in the development of highly potent, efficacious and long-acting interferon. *Protein Eng. Des. Sel*. **23**, 271-278

Walsh, G. (2005) Biopharmaceuticals: recent approvals and likely directions. *Trends Biotechnol*. **23**, 553-558

Walsh, G. (2010) Biopharmaceutical benchmarks 2010. *Nat. Biotechnol.* **28**, 917-924

Wartiovaara, J., Ofverstedt, L.G., Khoshnoodi, J., Zhang, J., Mäkelä, E., Sandin, S., Ruotsalainen, V., Cheng, R.H., Jalanko, H., Skoglund, U., Tryggvason, K. (2004) Nephrin strands contribute to a porous slit diaphragm scaffold as revealed by electron tomography. *J. Clin. Invest.* **114**, 1475-1483

Weidle, U.H., Auer, J., Brinkmann, U., Georges, G., Tiefenthaler, G. (2013) The emerging role of new protein scaffold-based agents for treatment of cancer. *Cancer Genomics Proteomics*. **10**, 155-168

Weir, N., Athwal, D., Brown, D., Foulkes, R., Kollias, G., Nesbitt, A., Popplewell, A., Spitali, M., Stephens, S. (2006) A new generation of high-affinity humanized PEGylated Fab´ fragment anti-tumor necrosis factor-α monoclonal antibodies. *Therapy*, **3**, 535-545

Wesolowski, J., Alzogaray, V., Reyelt, J., Unger, M., Juarez, K., Urrutia, M., Cauerhff, A., Danquah, W., Rissiek, B., Scheuplein, F., Schwarz, N., Adriouch, S., Boyer, O., Seman, M., Licea, A., Serreze, D.V., Goldbaum, F.A., Haag, F., Koch-Nolte, F. (2009) Single domain antibodies: promising experimental and therapeutic tools in infection and immunity. *Med. Microbiol. Immunol.* **198**, 157-174

Widebäck, K., Havliceck, J., Kronvall, G. (1983) Demonstration of a receptor for mouse and human serum albumin in Streptococcus pyogenes. *Acta Pathol. Microbiol. Immunol. Scand. Sect. B.* **91**, 373-382

Wilkinson, P., Jeremy, R., Brooks, F.P., Hollander, J.L. (1965) The mechanism of hypoalbuminemia in rheumatoid arthritis. *Ann. Intern. Med.* **63**, 109-114

Williams, A., Baird, L.G. (2003) DX-88 and HAE: a developmental perspective. *Transfus. Apher. Sci.* **29**, 255-258

Wunder, A., Müller-Ladner, U., Stelzer, E.H., Funk, J., Neumann, E., Stehle, G., Pap, T., Sinn, H., Gay, S., Fiehn, C. (2003) Albumin-based drug delivery as novel therapeutic approach for rheumatoid arthritis. *J. Immunol.* **170**, 4793-4801

Xu, L., Aha, P., Gu, K., Kuimelis, R.G., Kurz, M., Lam, T., Lim, A.C., Liu, H., Lohse, P.A., Sun, L., Weng, S., Wagner, R.W., Lipovsek, D. (2002) Directed evolution of high-affinity antibody mimics using mRNA display. *Chem. Biol.* **9**, 933-942

Yeun, J.Y., Kaysen, G.A. (1998) Factors influencing serum albumin in dialysis patients. *Am. J. Kidney Dis.* **32**, S118-S125

Zito, S.W. (1997) Pharmaceutical biotechnology: programmed text. Technomic Pub. Co., Lancaster, PA, 177pp

Zwerina, J., Hayer, S., Tohidast-Akrad, M., Bergmeister, H., Redlich, K., Feige, U., Dunstan, C., Kollias, G., Steiner, G., Smolen, J., Schett, G. (2004) Single and combined inhibition of tumor necrosis factor, interleukin-1, and RANKL pathways in tumor necrosis factor-induced arthritis: effects on synovial inflammation, bone erosion, and cartilage destruction. *Arthritis Rheum.* **50**, 277-290